ACCSCIENCE PUBLISHING

Microbes & Immunity

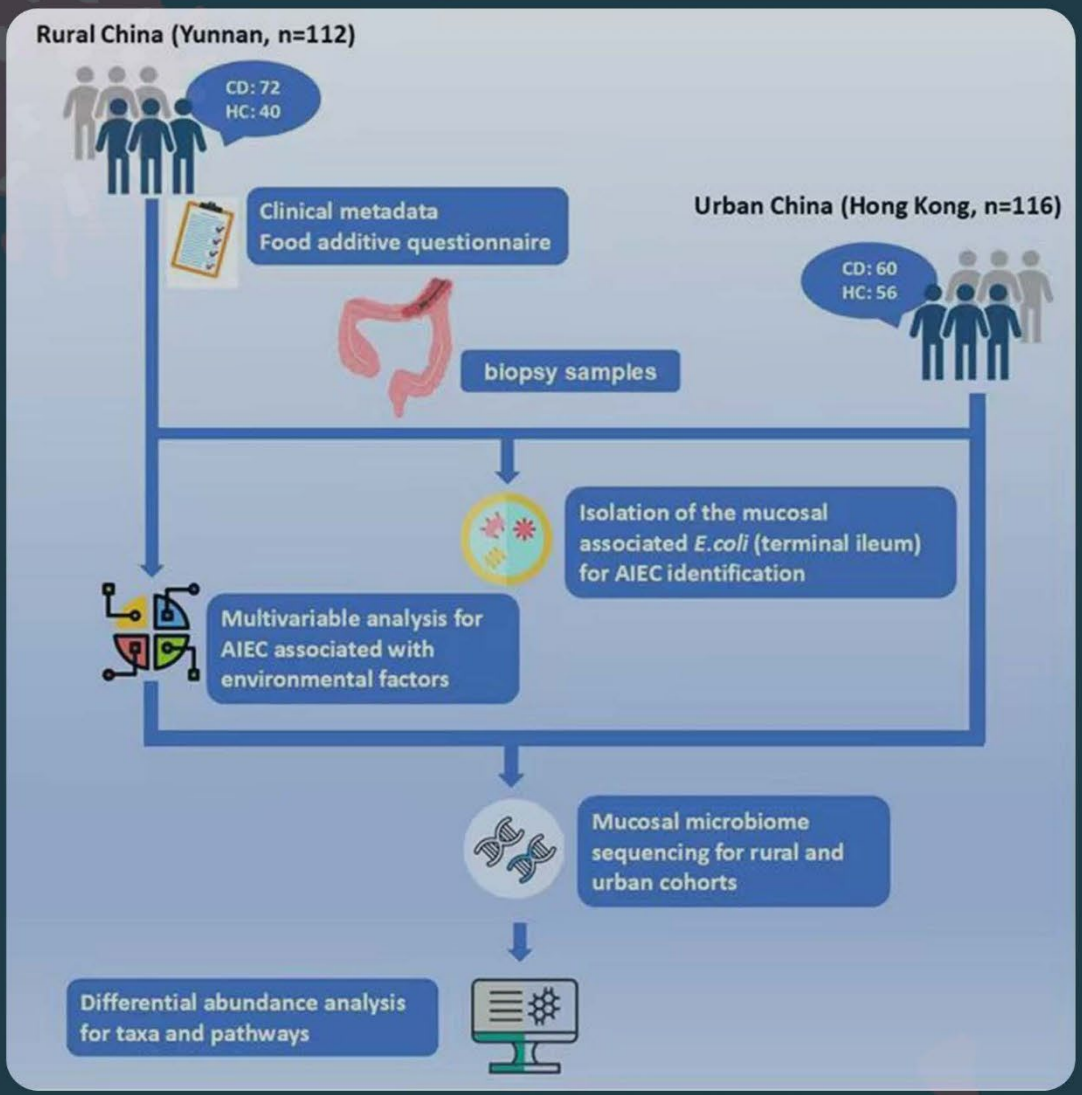

Adherent-invasive Escherichia coli (AIEC) in Crohn's disease acrooss urban and rural China

ISSN: 3041-0886 (Print)
ISSN: 3029-2883 (Online)
Volume 2 · Issue 4
October 2025

ACCSCIENCE PUBLISHING

Microbes & Immunity

Print ISSN: 3041-0886
Online ISSN: 3029-2883

Microbes & Immunity is a multidisciplinary peer-reviewed journal dedicated to advancing the understanding of the interactions between microbes and the immune system. The journal provides an open access publishing platform for researchers, clinicians, and scientists to disseminate their original research, reviews, and perspectives related to various aspects of microbes and immunity. The journal aims to foster collaboration and knowledge exchange in the fields of microbiology, immunology, infectious diseases, and related disciplines.

About the Publisher

AccScience Publishing is a publishing company based in Singapore. We publish a range of high-quality, open-access, peer-reviewed journals and books from a broad spectrum of disciplines.

Contact Us

Managing Editor
mi.office@accscience.sg

AccScience Publishing
9 Raffles Place, Republic Plaza 1 #06-00 Singapore 048619.

Volume 2 • Issue 4 • October 2025
ISSN 3041-0886 (print) ISSN 3029-2883 (online)

MICROBES & IMMUNITY

ACCSCIENCE PUBLISHING

Access Science Without Barriers

MICROBES & IMMUNITY

ISSN: 3041-0886 (print)
ISSN: 3029-2883 (online)

Editorial and Production Credits

Publisher: AccScience Publishing
Managing Editor: Jane Xu
Production Editor: Sharmila Velapasamy
Article Layout and Typeset: Sinjore Technologies (India)

For all advertising queries, contact mi.office@accscience.sg.

Supplementary file

Supplementary files of articles can be obtained at https://accscience.com/journal/MI/2/4.

Disclaimer

AccScience Publishing is not liable to the statements, perspectives, and opinions contained in the publications. The appearance of advertisements in the journal shall not be construed as a warranty, endorsement, or approval of the products or services advertised and/or the safety thereof. AccScience Publishing disclaims responsibility for any injury to persons or property resulting from any ideas or products referred to in the publications or advertisements. AccScience Publishing remains neutral with regard to jurisdictional claims in published maps and institutional affiliations.

Microbes & Immunity

Editorial Board

*Youth Editorial Board Members**

*Editorial Board Members as of October 16, 2025

ACCSCIENCE PUBLISHING

Volume 2 | Issue 4 | October 2025 | Page 1 – 160 |

Microbes & Immunity

https://accscience.com/journal/MI

CONTENTS

COMMUNICATION

ACCSCIENCE PUBLISHING

Microbes & Immunity

REVIEW ARTICLE

Staphylococcus aureus capsule: Production, function, and regulation

Yifan Rao[1], Zuwen Guo[2], Huagang Peng[2], Xiancai Rao[2]*, and Guixue Wang[1,3]*

[1]Key Laboratory of Biorheological and Technology of the Ministry of Education, State and Local Joint Engineering Laboratory for Vascular Implants, Modern Life Science Experiment Teaching Center at Bioengineering College of Chongqing University, Chongqing, China

[2]Department of Microbiology, College of Basic Medical Sciences, Key Laboratory of Microbial Engineering under the Educational Committee in Chongqing, Army Medical University (Third Military Medical University), Chongqing, China

[3]Jinfeng Laboratory, Chongqing, China

Abstract

Staphylococcus aureus is a major opportunistic pathogen that causes a wide spectrum of human and animal diseases. Capsule is one of the key virulence factors of *S. aureus*. Approximately 90% of *S. aureus* isolates produce capsular polysaccharides (CPs) that envelop the entire bacterial cells. CPs can suppress the phagocytosis of *S. aureus* by innate immune cells, promote intracellular survival, and reduce the killing efficacy of antimicrobial agents. As a result, CPs are versatile candidates for vaccine development. The synthesis of *S. aureus* CPs is controlled by the *cap* operon, which contains 16 genes encoding functional enzymes involved in the biosynthesis and transport of CPs. During *S. aureus* growth, *cap* operon expression is strictly regulated. The control region of the *cap* operon is characterized by two promoters: a housekeeping sigma factor A (SigA)-dependent promoter and a stress-responsive sigma factor B-dependent promoter. Many transcription factors, including both positive and negative regulatory molecules, are timely involved in the regulatory network of *S. aureus* capsule synthesis. Moreover, environmental conditions such as medium composition and carbon dioxide levels further modulate CP production. In this review, the structure and function of *S. aureus* CPs are introduced, and the biosynthesis of *S. aureus* CPs is discussed. Moreover, the regulation of *S. aureus* CP production is summarized, the factors affecting CP production are outlined, and the preparation of *S. aureus* CPs is reviewed. The advanced information presented here may provide useful references for further research on the production and function of *S. aureus* CPs.

Keywords: *Staphylococcus aureus*; Capsular polysaccharides; Immune evasion; Cap operon; Virulence factors; Capsule purification

***Corresponding authors:**
Xiancai Rao
(xcrao@tmmu.edu.cn)
Guixue Wang
(wanggx@cqu.edu.cn)

Citation: Rao Y, Guo Z, Peng H, Rao X, Wang G. *Staphylococcus aureus* capsule: Production, function, and regulation. *Microbes & Immunity*. 2025;2(4):1-16. doi: 10.36922/mi.8392

Received: January 3, 2025

Revised: April 9, 2025

Accepted: April 15, 2025

Published online: May 2, 2025

1. Introduction

Staphylococcus aureus is a Gram-positive opportunistic pathogen that commonly colonizes the skin, nasopharynx, and mucosal surfaces of healthy individuals.[1] Under conditions of immune suppression or epithelial barrier disruption, *S. aureus* can

cause not only skin and soft tissue infection, bronchitis, pneumonia, endocarditis, and brain abscess but also lead to food poisoning, exfoliative dermatitis, and toxin-mediated diseases.[2-4] In the United States, mortality due to *S. aureus* infections exceeds that of acquired immunodeficiency syndrome and viral hepatitis.[5] In China, *S. aureus* remains the most frequently isolated Gram-positive bacterial pathogen in clinical settings. According to the 2023 CHINET surveillance report (http://www.chinets.com), *S. aureus* accounted for 9.23% of all clinical isolates, ranking as the third most prevalent bacteria after the Gram-negative *Escherichia coli* (18.11%) and *Klebsiella pneumoniae* (14.22%).

Virulence factors are the weapons by which a bacterium causes disease. *S. aureus* can produce a variety of virulence factors,[6] such as hemolysins, enterotoxins, exfoliative toxins, and toxic shock syndrome toxins.[5,7] Capsule is also an important virulence factor of *S. aureus*.[8] In 1931, Gilbert first reported that the capsule plays a vital role in the pathogenesis of *S. aureus*,[9] and accumulated data have revealed that more than 90% of clinical *S. aureus* isolates produce capsules.[10] Although the structure, biosynthesis, function, and regulation of *S. aureus* capsular polysaccharides (CPs) have been reviewed,[11-14] significant progress has been made in recent years. For instance, the known functions of *S. aureus* capsule have expanded to include protection against phagocytosis,[15] inhibition of neutrophil chemotaxis,[16] promotion of bacterial adhesion and colonization, resistance to phage adsorption,[17] and stimulation of antibody production.[18]

Based on immunological specificity, monosaccharide composition, and glycosidic linkage of CPs, *S. aureus* capsules are classified into 13 serotypes (CP1 – CP13).[14,19-21] Notably, epidemiological investigations have revealed that more than 80% of clinically significant *S. aureus* strains carry CP5 or CP8.[16] This review comprehensively examines *S. aureus* capsule biology, covering: (i) structural and functional characteristics, (ii) biosynthetic pathways, mainly for CP5 and CP8, (iii) genetic and environmental regulation, and (iv) CP preparation methods. The integrated information provides a valuable resource for future research on capsule-mediated pathogenesis and potential therapeutic targets.

2. Structure and function of *S. aureus* capsule

The *S. aureus* capsule is a linear polysaccharide structurally composed of amino-hexuronic acid and oligosaccharide repeat units.[11] In general, the glycosidic linkages of monosaccharides and the number of repeating oligosaccharide units vary among *S. aureus* strains, resulting in complex and diverse CP structures, with molecular weight ranging from 100 to 2,000 kDa.[22] Among the 13 *S. aureus* CP serotypes, only five types (CP1, CP2, CP4, CP5, and CP8) have been structurally characterized (Figure 1A). *S. aureus* CPs are primarily composed of rare monosaccharide units. In 1974, Liau *et al.* identified three key components in CP1 strain M: Taurine, 2-acetamido-2-deoxy-α-D-galactopyranosyluronic acid, and N-acetyl-D-fucosamine (D-FucNAc).[23] The complete CP1 structure was elucidated in 1983 by Murthy *et al.*, who determined its repeating unit, with taurine covalently linked through amide bonds to every fourth GalNAcA residue.[24] Notably, a CP1 variant (strain D), identified in 1982, shares the same polysaccharide backbone but lacks taurine modifications.[25] The full structure of *S. aureus* CP2 was determined in 1964.[26] This capsular polymer contains equimolar amounts of 2-acetamido-2-deoxy-D-glucuronic acid (D-GlcNAcA) and 2-(N-acetylalanylamino)-2-deoxy-D-glucuronic acid units, linked through β-(1→4) glycosidic bonds. *S. aureus* CP4 consists of a repeating disaccharide unit of 2-acetamido-2-deoxy-D-mannopyranuronic acid (D-ManNAcA) and D-FucNAc with a β-(1→3) glycosidic linkage.[11] The overall structure of CP5 was first characterized in 1990 as a repeating trisaccharide unit and revised in 2005 to the corrected structure: →4)-β-D-ManNAcA-(1→4)-α-L-FucNAc(3-OAc)-(1→3)-β-D-FucNAc-(1→.[20] In contrast, the revised chemical structure of CP8 was established by Jones (2005), who described a repeating trisaccharide unit in *S. aureus* strain Becker: →3)-β-D-ManNAc(4-OAc)-(1→3)-α-L-FucNAc-(1→3)-α-D-FucNAc-(1→.[11,20]

Morphologically, colonies of *S. aureus* with CP1 and CP2 are mucoid, indicating rich capsule production. In contrast, the colonies formed by CP3–CP13 *S. aureus* isolates are non-mucoid, and their capsules are not readily observed.[27] To date, the precise chemical structures of additional *S. aureus* CP types remain uncharacterized due to their rare clinical isolation.

The majority of clinical *S. aureus* isolates carry CP5 or CP8.[16] In Mexico, 262 clinical methicillin-resistant *S. aureus* (MRSA) strains were isolated, of which 93.5% were characterized as CP5 and the remainder as CP8.[16] Mohamed *et al.* analyzed 506 clinical *S. aureus* isolates and found that 72% strains carried CP5 and 28% possessed CP8.[28] Similarly, Shi *et al.*[29] reported that in dairy goats across China, CP5 accounted for 52.5% and CP8 for 47.5% of *S. aureus* isolates strains. The reason for the higher prevalence of CP5 over CP8 in clinical settings remains unclear. Bardiau *et al.*[30] revealed that CP8-positive *S. aureus* strains exhibited a lower invasion rate than CP5-positive strains. Structurally, the main difference between

A

CP type	Strain	Repeating unit
CP1	M	→4)-α-D-GalNAcA-(1→4)-α-D-GalNAcA-(1→3)-α-D-FucNAc(1→
CP2	K-93M	→4)-α-D-GlcNAcA β-(1→4)-2-(Nacetylalanylamino)-2-deoxy-D-GlcA(1→
CP4	T	→3)-β-D-ManNAcA-(1→3)-D-FucNAc(1→
CP5	Reynolds	→4)-β-D-ManNAcA-(1→4)-α-L-FucNAc(3-OAc)-(1→3)-β-D-FucNAc(1→
CP8	Becker	→3)-β-D-ManNAcA(4-OAc)-(1→3)-α-L-FucNAc-(1→3)-α-D-FucNAc(1→

B

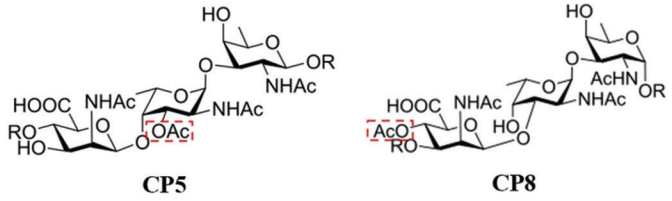

CP5 CP8

Figure 1. Repeating units and structure of *Staphylococcus aureus* CPs. (A) Oligosaccharide repeating units of five characterized *S. aureus* CP types. CP1 strain M has a taurine modification, which is covalently linked through amide bonds to every fourth GalNAcA residue. CP2 contains GlcNAcA and 2-(N-acetylalanylamino)-2-deoxy-D-GlcA linked by β-(1→4) linkages. CP4 strain T contains the repeating disaccharide unit of D-ManNAcA and D-FucNAc with a β-(1→3) glycosidic linkage. CP5 and CP8 carry OAc modifications. (B) Chemical structure of CP5 and CP8 units. The dashed red boxes show the OAc linking in CP5 and CP8. Figure created using PowerPoint software.

Abbreviations: CP: Capsular polysaccharide; GalNAcA: N-acetyl-pyranogalactosylic acid; FucNAc: N-acetyl-fucopyranosyl; GlcNAcA: N-acetyl-glucuronic acid; GlcA: Glucuronic acid; ManNAcA: N-acetyl-mannopyranosyl uronic acid; NHAc: Acetamido; OAc: O-acetylation.

CP5 and CP8 lies in their glycosidic linkages and the sites of O-acetylation (Figure 1B).[10,14,17,31] However, the isolation rate of each *S. aureus* serotype varies by region. Further accumulation of epidemiological data is needed to determine the dominant capsular types in specific areas.

Functionally, the bacterial capsule plays an important role in *S. aureus* pathogenicity. Following infection, the capsule enhances the survival of *S. aureus* in the host.[32,33] Using a mouse peritoneal infection model, Thakker *et al.*[34] showed that a CP5-expressing *S. aureus* strain had a higher survival rate than an acapsular strain, with similar results observed in bacteremia,[35] septic arthritis,[36] abscess,[15] and surgical wound infection models.[37] The capsule can suppress phagocytosis of *S. aureus* by innate immune cells, serving as a versatile barrier for immune evasion.[38] Studies have shown that CPs effectively mask surface molecules of *S. aureus*, such as opsonins, peptidoglycan, and teichoic acids, thereby blocking recognition by phagocytes.[39] Kuipers *et al.*[38] incubated GFP-labeled CP5 *S. aureus* strain Reynolds and its CP-negative mutant with freshly isolated human neutrophils, finding that the encapsulated strain resisted phagocytosis, while the unencapsulated strain was efficiently taken up. Alvarez *et al.*[40] reported that pre-treatment of *S. aureus* strains Reynolds and Newman with salicylic acid, a major aspirin metabolite, enhanced internalization into MAC-T cells compared with untreated control. In an NMRI mouse bloodstream infection model, inoculation with 7×10^6 colony-forming unit of CP5 *S. aureus* strain Reynolds resulted in 55% mortality, significantly higher than the 18% mortality observed in the group challenged with CP-deficient mutants.[36] These results suggest that the immune-evasive role of CPs contributes to the virulence of *S. aureus* isolates.

CPs may promote the intracellular survival of *S. aureus*. Nilsson *et al.*[36] evaluated the contribution of the capsule to staphylococcal survival within neutrophils and found that once phagocytized, CP5-positive *S. aureus* cells were less effectively killed compared to CP-deficient bacteria. This phenomenon has also been observed in other encapsulated bacteria such as *Streptococcus pneumoniae.*[41] Moreover, *S. aureus* CPs can prevent phage adsorption to the bacterial surface. A phage-mediated transfer of tetracycline resistance plasmid failed when an encapsulated staphylococcal strain was used.[42] Homogeneous CP expression can interfere with wall teichoic acid (WTA)-dependent phage binding.[43] Collectively, CPs protect *S. aureus* from both intracellular killing and phage lysis, although the precise molecular mechanisms remain largely unknown.

Antimicrobial resistance of *S. aureus* poses a great challenge to infection control.[44] While no association has been reported between biofilm formation and CP type,[45] the capsule can reduce the efficacy of antimicrobial agents. Matthes *et al.*[46] revealed that capsule-producing *S. aureus* isolates were more tolerant to treatment with cold atmospheric pressure argon plasma, which exerts a broad antimicrobial effect. Jansen *et al.*[47] reported that vancomycin-intermediate *S. aureus* (VISA) isolate SA137/93A and its spontaneous-mutant SA137/93G produced higher levels of

CP compared to vancomycin-susceptible *S. aureus* (VSSA) controls. Correspondingly, expression of *cap5E*, a key gene for CP biosynthesis, was significantly elevated in the VISA strains SA137/93A, SA137/93G, and Mu50, compared to the VSSA strains SA1450/94, Reynolds, and Newman. However, the mechanism by which the capsule contributes to antimicrobial resistance requires further investigation.

As extracellular cell wall components composed of polysaccharide chains, CPs are good candidates for vaccine development. Most vaccine candidates have focused on CP5 and CP8.[48] Berti *et al.*[49] highlighted the critical role of O-acetylation in the functional immune response. Both CP5 and CP8 of *S. aureus* possess O-acetylation, but at distinct sites: C3 of L-FucNAc for CP5 and C4 of D-ManNAcA for CP8 (Figure 1B). Scully *et al.*[50] demonstrated that O-acetylation is essential for CPS-CRM197 conjugates to elicit effective antibody responses against *S. aureus* both *in vivo* (mouse model) and *in vitro*. Although robust antibody responses were observed following primary vaccination, the StaphVAX-Nabi vaccine – comprising CP5 and CP8 conjugated to *Pseudomonas aeruginosa* exotoxin A – failed in Phase III clinical trials.[51] One possible explanation for this failure is abnormal O-acylation modifications in the vaccine antigen. A four-antigen *S. aureus* vaccine (CP5/CP8/rmClfA/rMntC) demonstrated a good safety profile, high tolerability, and strong immunogenicity in Phase I clinical testing.[52]

Chemical synthesis of a single repeating trisaccharide often fails to generate sufficient antigenic activity. The presence of rare monosaccharides, cis-glycosidic linkages, and O-acetylation poses significant challenges in the synthetic production of CP5 and CP8 fragments. Østerlid *et al.*[53] reported the stereoselective assembly of complex CP8 fragments – including trimer, hexamer, nonamer, and dodecamer units – and demonstrated through immunization studies that a minimum of three repeating units is required to elicit an adequate immune response. Sorieul *et al.*[54] developed a multiepitope vaccine by conjugating *S. aureus* CP8 with a chimeric protein containing Hla (an *S. aureus* cytotoxin) and PcrV (a *P. aeruginosa* cytotoxin). This vaccine successfully induced antibodies against all three antigens and conferred functional protection, demonstrating its potential as a proof-of-concept for multivalent vaccines targeting polymicrobial infections.

Collectively, CPs contribute to multiple aspects of *S. aureus* pathogenicity; however, the effect of CPs on virulence may be strain-specific due to variability in CP expression among clinical isolates. Advances in glycoconjugate vaccine development – leveraging bacterial carbohydrates as key antigens – hold promise for improved strategies to control *S. aureus* infections.

3. Biosynthesis of *S. aureus* capsule

The genes encoding the enzymes responsible for capsule synthesis in *S. aureus* are clustered in a *cap* operon comprising 16 genes, designated *capA* to *capP*.[31] The capsule serotypes are commonly used to distinguish gene clusters from different *cap* operons, such as *cap5A–cap5P* and *cap8A–cap8P* for CP5 and CP8, respectively.[38] Amino acid sequence comparisons revealed that 12 out of the 16 Cap proteins encoded CP5 and CP8 operons are highly conserved, exhibiting more than 97% sequence identity (Figure 2). In contrast, the remaining four proteins – CapH, CapI, CapJ, and CapK – share <43% sequence identity and are considered serotype-specific enzymes, playing key roles in determining CP5 and CP8 serotypes.[55]

The biosynthesis of *S. aureus* CPs is a complex and orderly process. Rausch *et al.*[31] proposed a biosynthetic pathway for CP production in *S. aureus* (Figure 3). Successful capsule formation requires the coordinated activity of all *cap* operon-encoded enzymes. The process begins with the formation of a tyrosine kinase complex by CapA and CapB. This complex regulates the activity of several downstream enzymes through phosphorylation and controls the use of metabolic precursors for CP synthesis. CapC acts as a negative regulator by inhibiting CapB kinase activity, thereby reducing target protein phosphorylation.

UDP-D-*N*-acetylglucosamine (UDP-D-GlcNAc) serves as a primary precursor for CP synthesis. CapD and CapN enzymes catalyze its conversion into soluble UDP-N-acetyl-D-fucosamine (UDP-D-FucNAc). CapM then transfers the phosphosugar moiety of UDP-D-FucNAc to the membrane-anchored lipid carrier undecaprenyl-phosphate ($C_{55}P$), generating the intermediate lipid I_{cap}. In parallel, enzymes CapE, CapF, and CapG convert UDP-D-GlcNAc to soluble UDP-N-acetyl-L-fucosamine (UDP-L-FucNAc).[56] This is subsequently linked to lipid I_{cap} by the transferase CapL, forming lipid II_{cap}. CapP and CapO catalyze the formation of UDP-N-acetyl-D-mannosaminuronic acid (UDP-D-ManNAcA) from UDP-D-GlcNAc. This nucleotide-activated monosaccharide is added to lipid II_{cap} by the transmembrane protein CapI, yielding the final capsule precursor lipid III_{cap}. The resulting undecaprenyl-phosphate-linked trisaccharide is further modified by the acetyltransferase CapH, which catalyzes the O-acetylation of L-FucNAc at the C3 position in CP5 strains.[20,57] Finally, the completed and modified precursor is translocated to the cell surface by CapK and CapJ, resulting in capsule formation.

Understanding this putative biosynthetic pathway provides crucial insights into the regulatory mechanisms

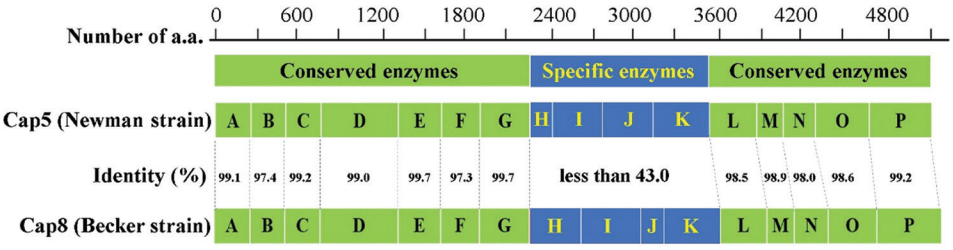

Figure 2. Amino acid (a.a.) homology comparison of enzymes involved in the biosynthesis of CP5 and CP8 in *Staphylococcus aureus*. A total of 16 enzymes encoded by the *cap* operon were compared. The approximate number of a.a. for each protein is indicated on the top scale. The percentage of a.a. identity between CP5 and CP8 is displayed. The comparison revealed that 12 out of 16 enzymes are highly conserved between CP5 and CP8, sharing more than 97% of amino acid identity. The remaining enzymes (CapH, CapI, CapJ, and CapK) exhibit <43% homology. Figure created using PowerPoint software.

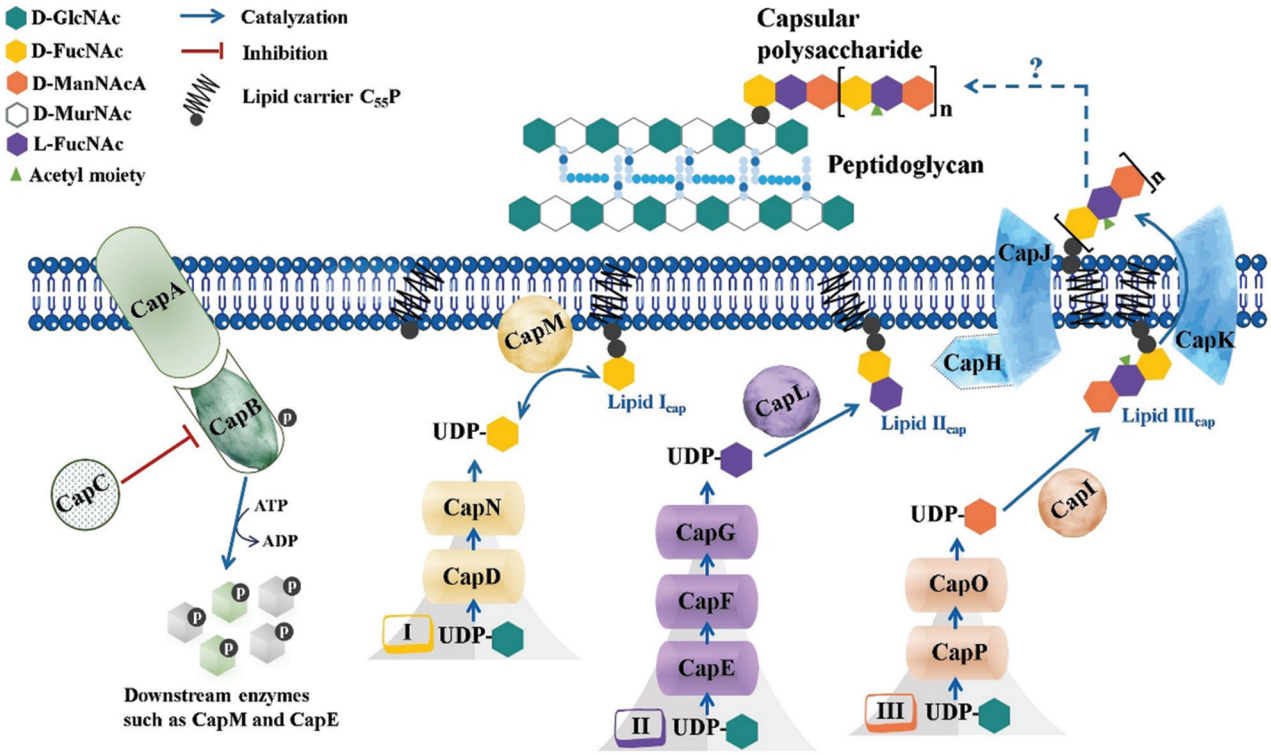

Figure 3. Schematic model for the CP biosynthesis and its regulation in *Staphylococcus aureus*. CapA, CapB, and CapC regulate precursor consumption for CP synthesis by controlling the activity of downstream enzymes through phosphorylation. CP biosynthesis begins in the cytoplasm with three enzymatic cascades that convert the universal precursor UDP-D-GlcNAc into three distinct nucleotide-activated sugars: UDP-D-FucNAc, UDP-L-FucNAc, and UDP-D-ManNAcA. First, CapD catalyzes the formation of UDP-2-acetamido-2,6-dideoxy-D-xylo−4-hexulose, which is reduced by the membrane-associated reductase CapN to yield UDP-D-FucNAc. CapM subsequently transfers the D-FucNAc moiety to undecaprenyl-phosphate ($C_{55}P$), generating lipid I_{cap}. Second, CapE, CapF, and CapG convert UDP-D-GlcNAc to UDP-L-FucNAc, which is then attached to lipid I_{cap} by the transferase CapL, forming lipid II_{cap}. Finally, CapP (epimerase) and CapO (dehydrogenase) collaboratively convert UDP-D-GlcNAc to UDP-D-ManNAcA, which is transferred to lipid II_{cap} by the transmembrane protein CapI, completing the assembly of lipid III_{cap}. Post-synthetic modifications involve the putative acetyltransferase CapH, which mediates C3-O-acetylation of L-FucNAc residues in lipid III_{cap}. The mature precursor is translocated across the membrane through the putative flippase CapK, followed by extracellular polymerization catalyzed by CapJ. However, the mechanism of CP attachment to peptidoglycan remains obscure. Figure created using PowerPoint software.
Abbreviations: CP: Capsular polysaccharides; GlcNAc: N-acetyl-glucosamine; FucNAc: N-acetyl-fucosamine; ManNAc: N-acetyl-mannosamine; ManNAcA: N-acetyl-mannosaminuronic acid; C55P: Undecaprenyl-phosphate.

of capsule synthesis and its role in *S. aureus* pathogenesis. However, the enzymatic roles of CapL (transferase), CapH (acetyltransferase), CapK (flippase), and CapJ (polymerase) still require experimental validation. Moreover, the mechanisms by which capsule precursors are attached to the N-acetylmuramic acid moiety of *S. aureus* peptidoglycan, and how the lipid carrier $C_{55}P$ is recycled for new biosynthetic cycles, remain unclear.

Rausch *et al.*[31] suggested that CapA may participate in the cleavage of pyrophosphate linkages in lipid-bound capsule precursors, facilitating the release of C55P. This lipid carrier is essential for synthesizing other cell envelope components, including capsule, peptidoglycan, and WTAs.[14] Compared to CPs, WTAs play more diverse roles in *S. aureus* pathogenesis. Since both CP and WTA biosynthetic pathways rely on shared precursors such as UDP-GlcNAc, a metabolic trade-off may exist. Overproduction of WTAs could potentially reduce capsule synthesis, leading to an inverse correlation between WTA abundance and capsule density.[12] Overall, the spatiotemporal regulation of cell envelope component biosynthesis is crucial for *S. aureus* viability.

4. Expressional regulation of *S. aureus cap* genes

The *cap* operon of *S. aureus* encodes a variety of enzymes involved in capsule polymer biosynthesis, acetylation, and transport.[31] However, most studies on *cap* gene regulation have focused on CP5 and CP8. The promoter regions of the *cap* operon for CP5 and CP8 (P_{cap}) are highly conserved, suggesting similar regulatory mechanisms for the expression of capsule synthesis genes in both serotypes.[58] Notably, the P_{cap} contains sigma factor B (SigB)-dependent (P_{SigB}) and SigA-dependent (P_{SigA}) promoters, with P_{SigB} acting as the primary promoter and P_{SigA} serving a secondary role in *cap* gene expression.[59] Several transcription factors form a regulatory network that modulates the activity of these two promoters.

The P_{SigA} core promoter is positioned 135 bp upstream of the *capA* start codon and includes the −35 (TTCACA) and −10 (TAATTA) elements. In contrast, P_{SigB} lies 56 bp upstream of the *capA* start codon, with −35 (GTTTAA) and −10 (ATGTAA) sequences.[22] The inhibitory transcription factors such as CodY, SaeR, and Rot bind near P_{SigA}, indirectly suppressing P_{SigB} activity. Conversely, positive regulators including SpoVG, RbsR, and MgrA enhance capsule synthesis by activating P_{SigB}.[60-62] Studies have demonstrated that MsaB/CspA promotes SigB activity and stabilizes *cap* transcripts, thereby enhancing capsule synthesis. However, other studies reported that the MsaB/CspA acts indirectly, possibly through regulators such as SpoVG, RbsR, or MgrA.[63] The exact mechanism underlying MsaB/CspA-mediated regulation of capsule synthesis remains to be elucidated. Moreover, SaeR binds to the inter-promoter region between P_{SigB} and P_{SigA}, inhibiting both promoters.[18] A broader range of transcription factors – such as AgrA,[64,65] SarA,[66,67] ArlRS,[68] CcpA,[69] RpiR,[70,71] ClpC,[68,72] RsaA,[73] SbcDC,[68,74] and SpdC[75] – also modulate capsule biosynthesis, often indirectly. These regulators may orchestrate a regulatory network controlling *cap* gene expression.

Phenotypic analyses of mutants are typically used to assess the roles of these transcription factors. As shown in Figure 4, phosphorylated SpoVG directly binds downstream of P_{SigB}, promoting CP synthesis,[60,76] while *spoVG* expression itself is positively regulated by SigB. SbcDC reduces capsule production by downregulating *arlRS* and *mgrA*.[74] MgrA, a global regulator, promotes CP

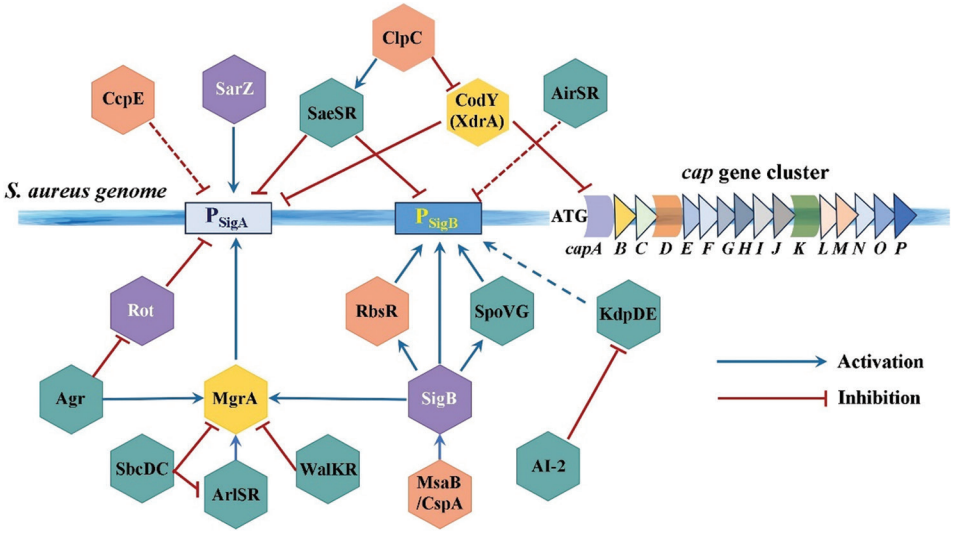

Figure 4. Schematic diagram of the regulatory network governing *cap* gene expression in *Staphylococcus aureus*. The *cap* promoter region contains a factor sigma B (SigB)-dependent promoter (P_{SigB}) and SigA-dependent promoter (P_{SigA}). Regulatory factors known to directly or indirectly impact *cap* expression primarily act by modulating the activity of P_{SigB} or P_{SigA}. Blue arrows indicate activation, while red arrows represent inhibition of the target activity. Dashed arrows indicate functions that require further experimental verification. Figure created using PowerPoint software.

synthesis by activating P_{SigA} rather than P_{SigB} and mediates the regulatory effects of ArlSR and Agr on capsule production.[62] ArlRS promotes capsule gene expression through MgrA-dependent pathways.[68] The Agr quorum sensing system influences capsule production both by activating *cap* gene expression through MgrA and by inhibiting Rot.[65] AI-2 quorum sensing molecules suppress capsule production through the KdpDE two-component system, although its impact on P_{SigB} remains unclear.[77]

CcpE, a positive regulator of the tricarboxylic acid cycle, has shown contradictory effects on capsule production, likely due to variations in strain backgrounds or sampling time points.[12] CodY bind at two sites within P_{cap} – upstream of P_{SigA} and downstream of P_{SigB}, extending into the coding region of the *capA* gene.[22] Under nutrient-rich conditions, CodY represses *cap* expression by preventing other positive regulators from binding. When nutrients are limited, CodY affinity decreases, allowing factors like RbsR to bind and promote capsule production.[78] This mechanism partially explains the observed temporal regulation: capsule synthesis is inhibited during early and mid-log phases but activated during late growth stages.

Beyond transcriptional control, post-transcriptional mechanisms also modulate CP biosynthesis.[12] The CapAB tyrosine kinase complex dynamically regulates enzymatic checkpoints through reversible phosphorylation, helping balance precursor allocation between CP synthesis and competing pathways such as WTA and peptidoglycan biosynthesis.[31] Moreover, the Ser/Thr kinase PknB, which is activated by sensing lipid II levels, inhibits CapAB activity and the glycosyltransferase function of CapM, leading to decreased CP production.[79] Such inhibition is likely a protective strategy to preserve essential precursors for cell growth.

Overall, the production of CPs in *S. aureus* is controlled by diverse regulatory factors and post-transcriptional regulatory mechanisms. This complexity highlights the tight control of capsule biosynthesis, underscoring its importance in the survival and pathogenicity of *S. aureus*.

5. Main factors affecting capsule production

Capsule production in *S. aureus* is temporally regulated and varies throughout the bacterial growth cycle. During lag and logarithmic growth phases, *cap* gene expression is inhibited, with significant upregulation occurring in the late logarithmic stage.[65] This timing correlates with the activation of the key positive regulator SigB, which is itself inhibited by Rot and CodY in the earlier stages of growth.[22] Studies have shown that SigB is often activated and expressed in the late logarithmic phase.[80-85] This sequential activation pattern supports the hypothesis that delayed capsule production is a strategic adaptation by *S. aureus* to optimize energy use: prioritizing the synthesis of colonization-related factors (e.g., adhesins and surface proteins) during early growth, while deferring energy-intensive virulence factors – such as capsules, secreted proteases, toxins, and hemolysins – until later stages.[86] This temporal regulation enables *S. aureus* to adapt efficiently to changing environmental conditions and host defenses.

Apart from genetic regulation, CP production is strongly influenced by environmental factors, including nutrient availability and carbon dioxide (CO_2) concentration. Thakker *et al.*[34] found that CP5-type *S. aureus* strain Reynolds produced robust capsules when cultured on solid media, conferring resistance to neutrophil phagocytosis, though this ability was lost in broth culture. Further quantitative testing showed that capsule production on solid media was 100-fold higher than in the broth culture. Further studies using a CP5 *S. aureus* strain isolated from a dairy cow mastitis sample evaluated capsule production across different media – brain–heart infusion (BHI), Columbia, and mod 110 – each prepared in solid and liquid forms, with or without the addition of lactose or glucose. The results showed that mod 110 medium produced the highest capsule yield, followed by Columbia, and BHI. Across all media types, solid cultures presented higher capsule production than liquid culture, and the addition of lactose increased the capsule yield of the CP5 strain.[87] Similar trends were observed for CP8 strains, where solid Columbia medium produced a higher capsule amount than its liquid counterpart. In contrast, the addition of glucose promoted capsular production in a human-derived CP5 *S. aureus* isolate.[88]

In addition to the medium and nutrients, gas compositions such as CO_2 concentration also significantly affect CP synthesis. Under normal air conditions (0.03% CO_2), the capsule synthesis is inhibited. However, elevated CO_2 levels (1–5%) markedly increase capsule production.[58] This phenomenon was evidenced in *in vivo* models, including cystic fibrosis patients and rat granuloma pouch models, where only 1 – 5% of *S. aureus* cells expressed CPs.[89] However, when cultured aerobically *in vitro*, 70 – 90% of these isolates re-expressed CPs. These data demonstrate that CO_2 levels in host environments serve as a key environmental regulator of capsule production.

Capsule production is enhanced by the addition of sodium chloride or under iron-deficient conditions.[65,90] In contrast, it is decreased when *S. aureus* is cultured in the media containing yeast extract, under alkaline growth conditions, or in low-oxygen environments.[65,91,92] These findings underscore the substantial impact of culture

medium composition, nutrient content, and gaseous environment on capsule production. Despite these insights, the molecular mechanisms by which environmental cues regulate capsule synthesis remain incompletely understood. Nonetheless, these findings offer valuable guidance for optimizing capsule production in research and potential therapeutic applications.

6. Preparation and detection of *S. aureus* capsule

The capsule of *S. aureus* is a protective structure on the surface of bacterial cell walls. Methods such as pyrolysis, ultrasonication, and lysozyme treatment are commonly used to extract and prepare *S. aureus* CPs.[93-96] Pyrolysis is typically performed under high temperature and pressure conditions (121°C, 15 psi), which disrupt the bacterial cell envelope and release CPs.[93] Following pyrolysis, centrifugation is used to remove cellular debris and isolate crude CP extracts. Ultrasonication employs acoustic cavitation to generate negative pressure waves that rupture the bacterial cell wall, effectively releasing CPs.[97] Compared to pyrolysis, ultrasonication is highly efficient, energy-efficient, and time-saving approach. However, prolonged ultrasonication may alter the spatial structure of CPs, making this method unsuitable for structure analysis of CPs. In contrast, enzymatic methods such as treatment with lysostaphin offer a gentler approach that preserves CP structural integrity.[95] Because *S. aureus* CPs are alkaline macromolecules, they are sensitive to acidic environments, where glycosidic bonds can be hydrolyzed.[98] Thus, parameters such as solution pH, solvent polarity, and ionic strength must be carefully optimized during CP preparation to maintain stability and yield.

The crude CP extracts often contain DNA, RNA, proteins, teichoic acids, monosaccharides, and oligosaccharides; the removal of these impurities to obtain pure CPs is challenging.[99,100] During the process of purification, bio-enzymes can be used to improve CP yield and purity: DNase I removes genomic DNA, RNase I removes RNA, and lysostaphin eliminates residual *S. aureus* cellular fragments.[101] Protein can be removed by enzymatic hydrolysis or Sevag method.[102] Enzymatic hydrolysis not only reduces the cost of the purification process but also minimizes the use of harmful reagents, ensuring greater biosafety. For the removal of monosaccharides and oligosaccharides, dialysis is effective. Among the most persistent impurities is teichoic acid, which shares structural similarities with CPs and can interfere with purification. However, teichoic acids contain ortho-hydroxyl groups that are absent in CPs. This subtle difference can be exploited for selective removal: weak oxidizing agent like sodium metaperiodate ($NaIO_4$) oxidize teichoic acid-specific ortho-hydroxyl groups, enabling their separation from CPs by DEAE-cellulose ion-exchange chromatography.[101]

After common impurity removal, membrane separation technologies such as ultrafiltration and microfiltration are used to further purify CP. These pressure-driven filtration techniques utilize membranes with selective permeability, enabling the purification, separation, and concentration of CPs from residual polysaccharide impurities.[103,104] CP purification exploits differences in composition between target capsular material and contaminant polysaccharides. Common methods include DEAE-Sephacel gel filtration, ion-exchange chromatography, agarose column chromatography, and high-performance liquid chromatography (HPLC).[105,106] For HPLC analysis, the use of polysaccharide-specific columns is recommended, as conventional C18 or NH_2 columns can result in significant inaccuracies. After purification, Residual impurities in the final CP product must be quantified and assessed against established thresholds. Optical density at 260 nm, measured using a spectrophotometer, is used to determine RNA and DNA contents, while protein content is commonly determined using the Lowry method.[99] According to the quality requirements of the World Health Organization, purified CPs should contain <1% protein and nucleic acid contentamination.[107]

The quantification of *S. aureus* CPs is critical, given the limited yield obtained from labor-intensive purification procedures. CP-antibody-based enzyme-linked immunosorbent assay (ELISA) is a classical quantitative strategy for *S. aureus* CPs.[108,109] However, the availability of specific antibodies targeting all CP types of *S. aureus*, especially CP5 and CP8, remains limited. To overcome these limitations, several alternative methods, such as chemical assays, infrared spectroscopy, capillary electrophoresis, and chromatography, have been developed to indirectly measure CP content by determining the total carbohydrate concentration.[110] Chemical strategies such as anthrone-sulfuric acid and phenol-sulfuric acid assays are simple and stable for bacterial capsule quantification.[111,112] A standard curve using glucose standards as a reference is typically employed to estimate CP concentrations. In the phenol-sulfuric acid method, sulfuric acid hydrolyzes CPs into monosaccharides, which are rapidly dehydrated to produce glycolaldehyde compounds. These intermediates then react with phenol to generate stable orange-yellow compounds with a maximum absorbance at 490 nm, which remains stable for over 160 min, allowing accurate quantification.[113] To improve the accuracy of these assays, residual-free monosaccharides and oligosaccharides should be removed before analysis. Although more sophisticated techniques such as infrared spectroscopy,

capillary electrophoresis, and chromatography offer higher sensitivity and resolution, they require specialized equipment and are not routinely used in all laboratories. Ultimately, the choice of quantification method should align with laboratory capabilities and experimental objectives.

7. *S. aureus* without capsule

Capsule is the key virulence factor of many pathogenic bacteria; encapsulated bacteria can use capsules to cause invasive diseases.[114] In contrast, acapsular bacteria show hypersusceptible to C3 complement deposition and often present avirulence in animal models.[115] Although CP5 and CP8 are the predominant capsule types in human *S. aureus* isolates, the majority of bovine mastitis-associated strains in Argentina lack capsule production.[116] Grunert *et al*.[117] characterized two persistent *S. aureus* subtypes (HP/ST9 and LP/ST504) from dairy cattle and found that both strains exhibited phenotypic traits of lacking CP expression, low cytotoxicity, and high biofilm production. During infection, host factors may drive the emergence of regulatory phenotypes of *S. aureus* for better adaption to the infection site. Suligoy *et al*. revealed that *S. aureus* can switch CP expression on or off *in vivo*, and stable non-encapsulated *S. aureus* mutants can regain production of CP and staphyloxanthin for bloodstream survival.[96]

The mechanisms of acapsular *S. aureus* formation are varied. Fischer *et al*. assessed CP and *agr* expression in 195 *S. aureus* strains from infected patients at a German university hospital and found that loss of *agr* function was frequently associated with an acapsular phenotype.[118] Inactivation of AgrC by IS256 insertion resulted in stable acapsular phenotype in *S. aureus* strain HU-14.[96] Similarly, deletions of *sigB* or *rbsR* significantly decreased CP expression in *S. aureus* isolates.[61] MgrA is a strong activator for capsule production, and a Becker mutant with the *mgrA* deletion presented an acapsular phenotype.[119] In addition, oxacillin treatment has been shown to suppress the expression of *cap* operon, resulting in an acapsular phenotype.[120] Collectively, these findings demonstrate that an array of factors can affect CP expression in *S. aureus* isolates and their modulation may result in acapsular variants with altered pathogenic potential.

8. Conclusion and perspectives

S. aureus capsule facilitates bacterial immune evasion through anti-phagocytic effects. The synthesis of *S. aureus* CPs is mediated by enzymes encoded within the *cap* gene cluster,[22,121] whose expression is tightly regulated during bacterial growth by over 10 identified regulatory factors.[122] Although the regulatory mechanisms underlying *cap* gene expression remain incompletely understood, ongoing research continues to identify novel regulatory molecules. Most regulators modulate capsule biosynthesis by directly or indirectly affecting P_{SigB} activity in the *cap* promoter region, while a few molecules like SaeSR execute their regulatory roles through P_{SigA} suppression.[123] Elucidating the CP regulatory network is critical for understanding key pathogenic processes, including bacterial colonization, infection dissemination, and persistence of *S. aureus*.

The production of *S. aureus* capsules typically increases during the late-log growth phase, though the molecular mechanisms governing this transition remain unclear. While constitutive SigB expression has been shown to induce premature capsule production,[22] strategies for enhancing capsule yield require further investigation. This knowledge gap highlights the need for comprehensive studies to clarify the temporal regulation of capsule synthesis and its clinical implications.

External factors, including growth medium composition, culture format (solid vs. liquid), CO_2 levels, and nutrient availability, significantly influence *S. aureus* capsule synthesis.[34,87] These stimuli likely exert their effects through bacterial signaling pathways or metabolic regulators, though the mechanistic interplay between environmental cues and capsule production remains poorly characterized.

Standardized methods for capsule isolation and quantification are critical for advancing research. Immunoassays such as ELISA with CP-type specific antibodies are the gold standard when validated reagents are available. When specific antibodies are unavailable, alternative approaches like the phenol-sulfuric acid method may be performed; however, standard protocols would be beneficial for the research community.

In conclusion, capsules play important roles in the pathogenicity of *S. aureus*, and capsule production may be driven by strain-specific traits, culture conditions, and growth phase dynamics. Further investigation of the molecular convergence between exogenous triggers and endogenous regulatory networks for *S. aureus* capsule production represents a vital research frontier with implications for therapeutic development and infection control strategies.

Acknowledgments

We thank Drs. Weilong Shang and Yi Yang from Army Medical University for providing critical insights for the manuscript.

Funding

The study was supported by the National Natural Science Foundation of China (Grant no. 82272341 for Xiancai Rao; Grant no. 82472301 for Yifan Rao) and Category II Academic Excellence Program of Xinqiao Hospital of Army Medical University (Grant no. 2023XKRC019 for Yifan Rao). The funders had no role in study design, data collection, interpretation, or the decision to submit the work for publication.

Conflict of interest

Xiancai Rao is an Editorial Board Member of this journal but was not in any way involved in the editorial and peer-review process conducted for this paper, directly or indirectly. Separately, other authors declared that they have no known competing financial interests or personal relationships that could have influenced the work reported in this paper.

Author contributions

Conceptualization: Xiancai Rao, Guixue Wang
Visualization: Yifan Rao, Huagang Peng
Writing–original draft: Yifan Rao, Zuwen Guo, Huagang Peng
Writing–review & editing: Yifan Rao, Xiancai Rao, Guixue Wang

Ethics approval and consent to participate

Not applicable.

Consent for publication

Not applicable.

Availability of data

Not applicable.

References

1. Eltabeeb MA, Hamed RR, El-Nabarawi MA, *et al*. Nanocomposite alginate hydrogel loaded with propranolol hydrochloride kolliphor-based cerosomes as a repurposed platform for methicillin-resistant *Staphylococcus aureus*-(MRSA)-induced skin infection; *in-vitro*, *ex-vivo*, *in-silico*, and *in-vivo* evaluation. *Drug Deliv Transl Res*. 2025;15(2):556-576.

   doi: 10.1007/s13346-024-01611-z

2. Li L, Koirala B, Hernandez Y, *et al*. Identification of structurally diverse menaquinone-binding antibiotics with *in vivo* activity against multidrug-resistant pathogens. *Nat Microbiol*. 2022;7(1):120-131.

   doi: 10.1038/s41564-021-01013-8

3. Chen XW, Chen HQ, Wu JH, *et al*. Isoniazid potentiates tigecycline to kill methicillin-resistant *Staphylococcus aureus*. *Emerg Microbes Infect*. 2025;14(1):2434587.

   doi: 10.1080/22221751.2024.2434587

4. Dang X, Han S, Du Y, Fei Y, Guo B, Wang X. Engineered environment-friendly multifunctional food packaging with superior nonleachability, polymer miscibility and antimicrobial activity. *Food Chem*. 2025;466:142192.

   doi: 10.1016/j.foodchem.2024.142192

5. DeLeo FR, Chambers HF. Reemergence of antibiotic-resistant *Staphylococcus aureus* in the genomics era. *J Clin Invest*. 2009;119(9):2464-2474.

   doi: 10.1172/JCI38226

6. Gordon RJ, Lowy FD. Pathogenesis of methicillin-resistant *Staphylococcus aureus* infection. *Clin Infect Dis*. 2008;46(Suppl 5):S350-S359.

   doi: 10.1086/533591

7. Nguyen TH, Cheung G, Rigby KM, *et al*. Rapid pathogen-specific recruitment of immune effector cells in the skin by secreted toxins. *Nat Microbiol*. 2022;7(1):62-72.

   doi: 10.1038/s41564-021-01012-9

8. Chakraborty T, Polley S, Ray Chaudhuri N, *et al*. A staphylococcal capsule-producing enzyme that unfolds via multiple intermediates predominantly exists as the trimers at low concentrations. *J Biomol Struct Dyn*. 2024;1-15.

   doi: 10.1080/07391102.2024.2438364

9. Gilbert I. Dissociation in an encapsulated *Staphylococcus*. *J Bacteriol*. 1931;21(3):157-160.

   doi: 10.1128/jb.21.3.157-160.1931

10. Sompolinsky D, Samra Z, Karakawa WW, Vann WF, Schneerson R, Malik Z. Encapsulation and capsular types in isolates of *Staphylococcus aureus* from different sources and relationship to phage types. *J Clin Microbiol*. 1985;22(5):828-834.

    doi: 10.1128/jcm.22.5.828-834.1985

11. Visansirikul S, Kolodziej SA, Demchenko AV. *Staphylococcus aureus* capsular polysaccharides: A structural and synthetic perspective. *Org Biomol Chem*. 2020;18(5):783-798.

    doi: 10.1039/c9ob02546d

12. Keinhörster D, George SE, Weidenmaier C, Wolz C. Function and regulation of *Staphylococcus aureus* wall teichoic acids and capsular polysaccharides. *Int J Med Microbiol*. 2019;309(6):151333.

    doi: 10.1016/j.ijmm.2019.151333

13. Tuchscherr L, Löffler B, Buzzola FR, Sordelli DO. *Staphylococcus aureus* adaptation to the host and persistence: Role of loss of capsular polysaccharide expression. *Future Microbiol*. 2010;5(12):1823-1832.

doi: 10.2217/fmb.10.147

14. O'Riordan K, Lee JC, Chan KH, Lee JC. *Staphylococcus aureus* capsular polysaccharides. *Clin Microbiol Rev*. 2004;17(1):218-234.

doi: 10.1128/CMR.17.1.218-234.2004

15. Portolés M, Kiser K, Bhasin N, *et al*. *Staphylococcus aureus* Cap5O has UDP-mannac dehydrogenase activity and is essential for capsule expression. *Infect Immun*. 2001;2(69):917-923.

doi: 10.1128/IAI.69.2.917-923.2001

16. Echaniz-Aviles G, Velazquez-Meza ME, Rodriguez-Arvizu B, *et al*. Detection of capsular genotypes of methicillin-resistant *Staphylococcus aureus* and clonal distribution of the cap5 and cap8 genes in clinical isolates. *Arch Microbiol*. 2022;204(3):186.

doi: 10.1007/s00203-022-02793-1

17. Wilkinson BJ, Holmes KM. *Staphylococcus aureus* cell surface: Capsule as a barrier to bacteriophage adsorption. *Infect Immun*. 1979;23(2):549-552.

doi: 10.1128/iai.23.2.549-552.1979

18. Behera A, Rai D, Kulkarni SS. Total syntheses of conjugation-ready trisaccharide repeating units of *Pseudomonas aeruginosa* O11 and *Staphylococcus aureus* type 5 capsular polysaccharide for vaccine development. *J Am Chem Soc*. 2020;142(1):456-467.

doi: 10.1021/jacs.9b11309

19. Von Eiff C, Taylor KL, Mellmann A, *et al*. Distribution of capsular and surface polysaccharide serotypes of *Staphylococcus aureus*. *Diagn Microbiol Infect Dis*. 2007;58(3):297-302.

doi: 10.1016/j.diagmicrobio.2007.01.016

20. Jones C. Revised structures for the capsular polysaccharides from *Staphylococcus aureus* types 5 and 8, components of novel glycoconjugate vaccines. *Carbohydr Res*. 2005;340(6):1097-1106.

doi: 10.1016/j.carres.2005.02.001

21. Østerlid KE, Cergano R, Overkleeft HS, Van der Marel GA, Codée JD. Synthesis of a set of *Staphylococcus aureus* capsular polysaccharide type 1 oligosaccharides carrying taurine esters. *Chemistry*. 2025;0:e202500132.

doi: 10.1002/chem.202500132

22. Keinhörster D, Salzer A, Duque Jaramillo A, *et al*. Revisiting the regulation of the capsular polysaccharide biosynthesis gene cluster in *Staphylococcus aureus*. *Mol Microbiol*. 2019;112(4):1083-1099.

doi: 10.1111/mmi.14347

23. Liau DF, Melly MA, Hash JH. Surface polysaccharide from *Staphylococcus aureus* M that contains taurine, D-aminogalacturonic acid, and D-fucosamine. *J Bacteriol*. 1974;119(3):913-922.

doi: 10.1128/jb.119.3.913-922.1974

24. Murthy SV, Melly MA, Harris TM, Hellerqvist CG, Hash JH. The repeating sequence of the capsular polysaccharide of *Staphylococcus aureus* M. *Carbohydr Res*. 1983;117:113-123.

doi: 10.1016/0008-6215(83)88080-x

25. Karakawa WW, Young DA, Kane JA. Structural analysis of the cellular constituents of a fresh clinical isolate of *Staphylococcus aureus*, and their role in the interaction between the organisms and polymorphonuclear leukocytes in the presence of serum factors. *Infect Immun*. 1978;21(2):496-505.

doi: 10.1128/iai.21.2.496-505.1978

26. Lu SR, Lai YH, Chen JH, Liu CY, Mong KK. Dimethylformamide: An unusual glycosylation modulator. *Angew Chem Int Ed Engl*. 2011;50(32):7315-7320.

doi: 10.1002/anie.201100076

27. Lee JC, Liu MJ, Parsonnet J, Arbeit RD. Expression of type 8 capsular polysaccharide and production of toxic shock syndrome toxin 1 are associated among vaginal isolates of *Staphylococcus aureus*. *J Clin Microbiol*. 1990;28(12):2612-2615.

doi: 10.1128/jcm.28.12.2612-2615.1990

28. Mohamed N, Timofeyeva Y, Jamrozy D, *et al*. Molecular epidemiology and expression of capsular polysaccharides in *Staphylococcus aureus* clinical isolates in the United States. *PLoS One*. 2019;14(1):e0208356.

doi: 10.1371/journal.pone.0208356

29. Shi H, Wang L, Li G, *et al*. Characteristic profiles of molecular types, antibiotic resistance, antibiotic resistance genes, and virulence genes of *Staphylococcus aureus* isolates from caprine mastitis in China. *Front Cell Infect Microbiol*. 2025;15:1533844.

doi: 10.3389/fcimb.2025.1533844

30. Bardiau M, Caplin J, Detilleux J, *et al*. Existence of two groups of *Staphylococcus aureus* strains isolated from bovine mastitis based on biofilm formation, intracellular survival, capsular profile and agr-typing. *Vet Microbiol*. 2016;185:1-6.

doi: 10.1016/j.vetmic.2016.01.003

31. Rausch M, Deisinger JP, Ulm H, *et al*. Coordination of capsule assembly and cell wall biosynthesis in *Staphylococcus aureus*. *Nat Commun*. 2019;10(1):1404.

doi: 10.1038/s41467-019-09356-x

32. Karakawa WW, Sutton A, Schneerson R, Karpas A, Vann WF. Capsular antibodies induce type-specific phagocytosis of capsulated *Staphylococcus aureus* by human polymorphonuclear leukocytes. *Infect Immun*. 1988;56(5):1090-1095.

doi: 10.1128/iai.56.5.1090-1095.1988

33. Nanra JS, Buitrago SM, Crawford S, *et al*. Capsular polysaccharides are an important immune evasion mechanism for *Staphylococcus aureus*. *Hum Vaccin Immunother*. 2013;9(3):480-487.

doi: 10.4161/hv.23223

34. Thakker M, Park J, Carey V, Lee JC. *Staphylococcus aureus* serotype 5 capsular polysaccharide is antiphagocytic and enhances bacterial virulence in a murine bacteremia model. *Infect Immun*. 1998;11(66):5183-5189.

doi: 10.1128/IAI.66.11.5183-5189.1998

35. Watts A, Ke D, Wang Q, *et al*. *Staphylococcus aureus* strains that express serotype 5 or serotype 8 capsular polysaccharides differ in virulence. *Infect Immun*. 2005;73(6):3502-3511.

doi: 10.1128/IAI.73.6.3502-3511.2005

36. Nilsson IM, Lee JC, Bremell T, Rydén C, Tarkowski A. The role of staphylococcal polysaccharide microcapsule expression in septicemia and septic arthritis. *Infect Immun*. 1997;65(10):4216-4221.

doi: 10.1128/iai.65.10.4216-4221.1997

37. McLoughlin RM, Solinga RM, Rich J, *et al*. CD4+ T cells and CXC chemokines modulate the pathogenesis of *Staphylococcus aureus* wound infections. *Proc Natl Acad Sci USA*. 2006;103(27):10408-10413.

doi: 10.1073/pnas.0508961103

38. Kuipers A, Stapels DAC, Weerwind LT, *et al*. The *Staphylococcus aureus* polysaccharide capsule and Efb-dependent fibrinogen shield act in concert to protect against phagocytosis. *Microbiology (Reading)*. 2016;162(7):1185-1194.

doi: 10.1099/mic.0.000293

39. Sutra L, Rainard P, Poutrel B. Phagocytosis of mastitis isolates of *Staphylococcus aureus* and expression of type 5 capsular polysaccharide are influenced by growth in the presence of milk. *J Clin Microbiol*. 1990;28(10):2253-2258.

doi: 10.1128/jcm.28.10.2253-2258.1990

40. Alvarez LP, Barbagelata MS, Gordiola M, Cheung AL, Sordelli DO, Buzzola FR. Salicylic acid diminishes *Staphylococcus aureus* capsular polysaccharide type 5 expression. *Infect Immun*. 2010;78(3):1339-1344.

doi: 10.1128/IAI.00245-09

41. Brissac T, Martínez E, Kruckow KL, *et al*. Capsule promotes intracellular survival and vascular endothelial cell translocation during invasive pneumococcal disease. *mBio*. 2021;12(5):e0251621.

doi: 10.1128/mBio.02516-21

42. Witte W. Transfer of drug-resistance-plasmids in mixed cultures of Staphylococci. *Zentralbl Bakteriol Orig A*. 1977;237(2-3):147-159.

43. Lehmann E, Van Dalen R, Gritsch L, *et al*. The capsular polysaccharide obstructs wall teichoic acid functions in *Staphylococcus aureus*. *J Infect Dis*. 2024;230(5):1253-1261.

doi: 10.1093/infdis/jiae188

44. Kaku N, Ishige M, Yasutake G, *et al*. Long-term impact of molecular epidemiology shifts of methicillin-resistant *Staphylococcus aureus* on severity and mortality of bloodstream infection. *Emerg Microbes Infect*. 2025;14(1):2449085.

doi: 10.1080/22221751.2024.2449085

45. Babra C, Tiwari J, Costantino P, *et al*. Human methicillin-sensitive *Staphylococcus aureus* biofilms: Potential associations with antibiotic resistance persistence and surface polysaccharide antigens. *J Basic Microbiol*. 2014;54(7):721-728.

doi: 10.1002/jobm.201200557

46. Matthes R, Lührman A, Holtfreter S, *et al*. Antibacterial activity of cold atmospheric pressure argon plasma against 78 genetically different (mecA, luk-P, agr or capsular polysaccharide type) *Staphylococcus aureus* strains. *Skin Pharmacol Physiol*. 2016;29(2):83-91.

doi: 10.1159/000443210

47. Jansen A, Szekat C, Schröder W, *et al*. Production of capsular polysaccharide does not influence *Staphylococcus aureus* vancomycin susceptibility. *BMC Microbiol*. 2013;13:65.

doi: 10.1186/1471-2180-13-65

48. Berni F, Enotarpi J, Voskuilen T, *et al*. Synthetic carbohydrate-based cell wall components from *Staphylococcus aureus*. *Drug Discov Today Technol*. 2020;38:35-43.

doi: 10.1016/j.ddtec.2021.01.003

49. Berti F, De Ricco R, Rappuoli R. Role of O-acetylation in the immunogenicity of bacterial polysaccharide vaccines. *Molecules*. 2018;23(6):1340.

doi: 10.3390/molecules23061340

50. Scully IL, Pavliak V, Timofeyeva Y, Liu Y, Singer C, Anderson AS. O-Acetylation is essential for functional antibody generation against *Staphylococcus aureus* capsular polysaccharide. *Hum Vaccin Immunother*. 2018;14(1):81-84.

doi: 10.1080/21645515.2017.1386360

51. Fattom AI, Horwith G, Fuller S, Propst M, Naso R. Development of StaphVAX, a polysaccharide conjugate vaccine against *S. aureus* infection: From the lab bench to phase III clinical trials. *Vaccine*. 2004;22(7):880-887.

doi: 10.1016/j.vaccine.2003.11.034

52. Begier E, Seiden DJ, Patton M, *et al*. SA4Ag, a 4-antigen *Staphylococcus aureus* vaccine, rapidly induces high levels of bacteria-killing antibodies. *Vaccine*. 2017;35(8):1132-1139.

doi: 10.1016/j.vaccine.2017.01.024

53. Østerlid KE, Sorieul C, Unione L, *et al*. Long, synthetic *Staphylococcus aureus* type 8 capsular oligosaccharides reveal structural epitopes for effective immune recognition. *J Am Chem Soc*. 2025;147(3):2829-2840.

doi: 10.1021/jacs.4c16118

54. Sorieul C, Mikladal B, Wu DY, *et al*. Multimeric, multivalent fusion carrier proteins for site-selective glycoconjugate vaccines simultaneously targeting *Staphylococcus aureus* and *Pseudomonas aeruginosa*. *Chem Sci*. 2025;16(13):5688-5700.

doi: 10.1039/d4sc08622h

55. Sau S, Bhasin N, Wann ER, Lee JC, Foster TJ, Lee CY. The *Staphylococcus aureus* allelic genetic loci for serotype 5 and 8 capsule expression contain the type-specific genes flanked by common genes. *Microbiology (Reading)*. 1997;143(7):2395-2405.

doi: 10.1099/00221287-143-7-2395

56. Kneidinger B, O'Riordan K, Li J, Brisson JR, Lee JC, Lam JS. Three highly conserved proteins catalyze the conversion of UDP-N-acetyl-D-glucosamine to precursors for the biosynthesis of O antigen in *Pseudomonas aeruginosa* O11 and capsule in *Staphylococcus aureus* type 5. Implications for the UDP-N-acetyl-L-fucosamine biosynthetic pathway. *J Biol Chem*. 2003;278(6):3615-3627.

doi: 10.1074/jbc.M203867200

57. Bhasin N, Albus A, Michon F, Livolsi PJ, Park JS, Lee JC. Identification of a gene essential for O-acetylation of the *Staphylococcus aureus* type 5 capsular polysaccharide. *Mol Microbiol*. 1998;27(1):9-21.

doi: 10.1046/j.1365-2958.1998.00646.x

58. Herbert S, Newell SW, Lee C, *et al*. Regulation of *Staphylococcus aureus* type 5 and type 8 capsular polysaccharides by CO_2. *J Bacteriol*. 2001;183(15):4609-4613.

doi: 10.1128/JB.183.15.4609–4613.2001

59. Ouyang S, Sau S, Lee CY. Promoter analysis of the cap8 operon, involved in type 8 capsular polysaccharide production in *Staphylococcus aureus*. *J Bacteriol*. 1999;181(8):2492-2500.

doi: 10.1128/JB.181.8.2492-2500.1999

60. Jutras BL, Chenail AM, Rowland CL, *et al*. Eubacterial SpoVG homologs constitute a new family of site-specific DNA-binding proteins. *PLos One*. 2013;8(6):e66683.

doi: 10.1371/journal.pone.0066683

61. Lei MG, Lee CY. RbsR activates capsule but represses the rbsUDK operon in *Staphylococcus aureus*. *J Bacteriol*. 2015;197(23):3666-3675.

doi: 10.1128/JB.00640-15

62. Lei MG, Lee CY. MgrA activates staphylococcal capsule via SigA-dependent promoter. *J Bacteriol*. 2020;203(2):e00495-20.

doi: 10.1128/JB.00495-20

63. Batte JL, Samanta D, Elasri MO. MsaB activates capsule production at the transcription level in *Staphylococcus aureus*. *Microbiology (Reading)*. 2016;162(3):575-589.

doi: 10.1099/mic.0.000243

64. Dassy B, Hogan T, Foster TJ, Fournier JM. Involvement of the accessory gene regulator (agr) in expression of type 5 capsular polysaccharide by *Staphylococcus aureus*. *J Gen Microbiol*. 1993;139(6):1301-1306.

doi: 10.1099/00221287-139-6-1301

65. George SE, Nguyen T, Geiger T, *et al*. Phenotypic heterogeneity and temporal expression of the capsular polysaccharide in *Staphylococcus aureus*. *Mol Microbiol*. 2015;98(6):1073-1088.

doi: 10.1111/mmi.13174

66. Van Wamel W, Xiong YQ, Bayer AS, Yeaman MR, Nast CC, Cheung AL. Regulation of *Staphylococcus aureus* type 5 capsular polysaccharides by agr and sarA in vitro and in an experimental endocarditis model. *Microb Pathog*. 2002;33(2):73-79.

doi: 10.1006/mpat.2002.0513

67. Luong T, Sau S, Gomez M, Lee JC, Lee YC. Regulation of *Staphylococcus aureus* capsular polysaccharide expression by agr and sarA. *Infect Immun*. 2002;70(2):444-450.

doi: 10.1128/IAI.70.2.444-450.2002

68. Luong TT, Lee CY. The arl locus positively regulates *Staphylococcus aureus* type 5 capsule via an mgrA-dependent pathway. *Microbiology (Reading)*. 2006;152(10):3123-3131.

doi: 10.1099/mic.0.29177-0

69. Seidl K, Muller S, Francois P, *et al*. Effect of a glucose impulse on the CcpA regulon in *Staphylococcus aureus*. *BMC Microbiol*. 2009;18(9):95.

doi: 10.1186/1471-2180-9-95

70. Zhu Y, Nandakumar R, Sadykov MR, *et al*. RpiR homologues may link *Staphylococcus aureus* RNAIII synthesis and pentose phosphate pathway regulation. *J Bacteriol*. 2011;193(22):6187-6196.

doi: 10.1128/JB.05930-11

71. Gaupp R, Wirf J, Wonnenberg B, *et al*. RpiRc is a pleiotropic effector of virulence determinant synthesis and attenuates pathogenicity in *Staphylococcus aureus*. *Infect Immun*. 2016;84(7):2031-2041.

doi: 10.1128/IAI.00285-16

72. Graham JW, Lei MG, Lee CY. Trapping and identification of cellular substrates of the *Staphylococcus aureus* ClpC chaperone. *J Bacteriol*. 2013;195(19):4506-4516.

doi: 10.1128/JB.00758-13

73. Romilly C, Lays C, Tomasini A, *et al*. A non-coding RNA promotes bacterial persistence and decreases virulence by regulating a regulator in *Staphylococcus aureus*. *PLoS Pathog*.

2014;10(3):e1003979.

doi: 10.1371/journal.ppat.1003979

74. Chen Z, Luong TT, Lee CY. The sbcDC locus mediates repression of type 5 capsule production as part of the SOS response in *Staphylococcus aureus*. *J Bacteriol*. 2007;189(20):7343-7350.

doi: 10.1128/JB.01079-07

75. Poupel O, Proux C, Jagla B, Msadek T, Dubrac S. SpdC, a novel virulence factor, controls histidine kinase activity in *Staphylococcus aureus*. *PLoS Pathog*. 2018;14(3):e1006917.

doi: 10.1371/journal.ppat.1006917

76. Bischoff M, Brelle S, Minatelli S, Molle V. Stk1-mediated phosphorylation stimulates the DNA-binding properties of the *Staphylococcus aureus* SpoVG transcriptional factor. *Biochem Biophys Res Commun*. 2016;473(4):1223-1228.

doi: 10.1016/j.bbrc.2016.04.044

77. Zhao L, Xue T, Shang F, Sun H, Sun B. *Staphylococcus aureus* AI-2 quorum sensing associates with the KdpDE two-component system to regulate capsular polysaccharide synthesis and virulence. *Infect Immun*. 2010;78(8):3506-3515.

doi: 10.1128/IAI.00131-10

78. Batte JL, Sahukhal GS, Elasri MO. MsaB and CodY interact to regulate *Staphylococcus aureus* capsule in a nutrient-dependent manner. *J Bacteriol*. 2018;200(17):e00294-18.

doi: 10.1128/JB.00294-18

79. Hardt P, Engels I, Rausch M, *et al*. The cell wall precursor lipid II acts as a molecular signal for the Ser/Thr kinase PknB of *Staphylococcus aureus*. *Int J Med Microbiol*. 2017;307(1):1-10.

doi: 10.1016/j.ijmm.2016.12.001

80. Li X, Busch LM, Piersma S, *et al*. Functional and proteomic dissection of the contributions of CodY, SigB and the hibernation promoting factor HPF to interactions of *Staphylococcus aureus* USA300 with human lung epithelial cells. *J Proteome Res*. 2024;23(10):4742-4760.

doi: 10.1021/acs.jproteome.4c00724

81. Bischoff M, Entenza JM, Giachino P. Influence of a functional sigB operon on the global regulators SAR and AGR in *Staphylococcus aureus*. *J Bacteriol*. 2001;183(17):5171-5179.

doi: 10.1128/JB.183.17.5171-5179.2001

82. Bischoff M, Dunman P, Kormanec J, *et al*. Microarray-based analysis of the *Staphylococcus aureus* σB regulon. *J Bacteriol*. 2004;186(13):4085-4099.

doi: 10.1128/JB.186.13.4085-4099.2004

83. Pane-Farre J, Jonas B, Forstner K, Engelmann S, Hecker M. The σB regulon in *Staphylococcus aureus* and its regulation. *Int J Med Microbiol*. 2006;296(4-5):237-258.

doi: 10.1016/j.ijmm.2005.11.011

84. Mader U, Nicolas P, Depke M, *et al*. *Staphylococcus aureus* transcriptome architecture: From laboratory to infection-mimicking conditions. *PLoS Genet*. 2016;12(4):e1005962.

doi: 10.1371/journal.pgen.1005962

85. Li J, Zhu K, Li C, *et al*. Alkaline shock protein 23 (Asp23)-controlled cell wall imbalance promotes membrane vesicle biogenesis in *Staphylococcus aureus*. *J Extracell Vesicles*. 2024;13(9):e12501.

doi: 10.1002/jev2.12501

86. Cheung AL, Bayer AS, Zhang G, *et al*. Regulation of virulence determinants *in vitro* and *in vivo* in *Staphylococcus aureus*. *FEMS Immunol Med Microbiol*. 2004;40(1):1-9.

doi: 10.1016/S0928-8244(03)00309-2

87. Yang Z, Zhang N, Liu Q, *et al*. The effect of culture condition on Type 5 capsular polysaccharide production of *Staphylococcus aureus* from diary cattle. *Agri Sci Tech*. 2008;9(1):85-88.

doi: 10.16175/j.crki.1009-4009.2008.01.030

88. Poutrel B, Gilbert FB, Lebrun M. Effects of culture conditions on production of type 5 capsular polysaccharide by human and bovine *Staphylococcus aureus* strains. *Clin Diagn Lab Immunol*. 1995;2(2):166-171.

doi: 10.1128/cdli.2.2.166-171.1995

89. Herbert S, Worlitzsch D, Dassy B, *et al*. Regulation of *Staphylococcus aureus* capsular polysaccharide type 5: *In vitro* and *in vivo* inhibition by CO_2. *Pneumologie*. 1997;51(11):1043-1050.

90. Pohlmann-Dietze P, Ulrich M, Kiser KB, *et al*. Adherence of *Staphylococcus aureus* to endothelial cells: Influence of capsular polysaccharide, global regulator agr, and bacterial growth phase. *Infect Immun*. 2000;68(9):4865-4871.

doi: 10.1128/IAI.68.9.4865-4871.2000

91. Dassy B, Stringfellow WT, Lieb M, Fournier JM. Production of type 5 capsular polysaccharide by *Staphylococcus aureus* grown in a semi-synthetic medium. *J Gen Microbiol*. 1991;137(5):1155-1162.

doi: 10.1099/00221287-137-5-1155

92. Stringfellow WT, Dassy B, Lieb M, Fournier JM. *Staphylococcus aureus* growth and type 5 capsular polysaccharide production in synthetic media. *Appl Environ Microbiol*. 1991;57(2):618-621.

doi: 10.1128/aem.57.2.618-621.1991

93. Fournier JM, Vann WF, Karakawa WW. Purification and characterization of *Staphylococcus aureus* type 8 capsular polysaccharide. *Infect Immun*. 1984;45(1):87-93.

doi: 10.1128/iai.45.1.87-93.1984

94. O'Brien CN, Guidry AJ, Fattom A, Shepherd S, Douglass LW, Westhoff DC. Production of antibodies to *Staphylococcus*

aureus serotypes 5, 8, and 336 using poly (DL-lactide-co-glycolide) microspheres. *J Dairy Sci*. 2000;83(8):1758-1766.

doi: 10.3168/jds.S0022-0302(00)75046-6

95. Havaei SA, Hancock IC. The capsular turnover product of Staphylococcus aureus strain Smith. *Fems Microbiol Lett*. 1994;118(1-2):37-43.

doi: 10.1111/j.1574-6968.1994.tb06800.x

96. Suligoy CM, Díaz RE, Gehrke AK, *et al*. Acapsular Staphylococcus aureus with a non-functional agr regains capsule expression after passage through the bloodstream in a bacteremia mouse model. *Sci Rep*. 2020;10(1):14108.

doi: 10.1038/s41598-020-70671-1

97. Ashkenazi I, Longwell M, Byers B, *et al*. Nanoparticle ultrasonication: A promising approach for reducing bacterial biofilm in total joint infection-an *in vivo* rat model investigation. *Arthroplasty*. 2024;6(1):57.

doi: 10.1186/s42836-024-00279-7

98. Bei J, Wu J, Liu J. Re-N-acetylation of group B Streptococcus type ia capsular polysaccharide improves the immunogenicity of glycoconjugate vaccines. *Carbohydr Polym*. 2024;330:121848.

doi: 10.1016/j.carbpol.2024.121848

99. Gaikwad WK, Jana SK, Dhere RM, Ravenscroft N, Kodam KM. Purification of capsular polysaccharides isolated from *S. pneumoniae* serotype 2 by hydrogen peroxide and endonuclease. *Carbohydr Polym*. 2022;294:119783.

doi: 10.1016/j.carbpol.2022.119783

100. Reddy GP, Hayat U, Bush CA, Morris JG Jr. Capsular polysaccharide structure of a clinical isolate of *Vibrio vulnificus* strain BO62316 determined by heteronuclear NMR spectroscopy and high-performance anion-exchange chromatography. *Anal Biochem*. 1993;214(1):106-115.

doi: 10.1006/abio.1993.1463

101. Wu J, Yang X, Wang Z. Isolation, purification and reactingogenicity of *Staphylococcus aureus* type 8 capsular polysaccharide. *Chin Vet Sci*. 2010;40(12):1214-1217.

doi: 10.16656/j.issn.1673-4696.2010.12.002

102. Wang L, Wang L, Shi Q, *et al.* Purification and molecular weight distribution of a key exopolysaccharide component of *Bacillus megaterium* TF10. *J Environ Sci (China)*. 2018;63:9-15.

doi: 10.1016/j.jes.2016.12.006

103. Goncalves VM, Takagi M, Lima RB, Massaldi H, Giordano RC, Tanizaki MM. Purification of capsular polysaccharide from *Streptococcus pneumoniae* serotype 23F by a procedure suitable for scale-up. *Biotechnol Appl Biochem*. 2003;37(3):283-287.

doi: 10.1042/BA20020075

104. Li S, Zhao S, Pei J, *et al*. Stimuli-responsive lysozyme nanocapsule engineered microfiltration membranes with a dual-function of anti-adhesion and antibacteria for biofouling mitigation. *ACS Appl Mater Interfaces*. 2021;13(27):32205-32216.

doi: 10.1021/acsami.1c07445

105. He Y, Hou W, Thompson M, Holovics H, Hobson T, Jones MT. Size exclusion chromatography of polysaccharides with reverse phase liquid chromatography. *J Chromatogr A*. 2014;1323:97-103.

doi: 10.1016/j.chroma.2013.11.010

106. Ahmadi K, Aslani MM, Pouladfar G, *et al*. Preparation and preclinical evaluation of two novel *Staphylococcus aureus* capsular polysaccharide 5 and 8-fusion protein (Hla-MntC-SACOL0723) immunoconjugates. *Iubmb Life*. 2020;72(2):226-236.

doi: 10.1002/iub.2159

107. Pato TP, Barbosa AP, Da SJJ. Purification of capsular polysaccharide from *Neisseria meningitidis* serogroup C by liquid chromatography. *J Chromatogr B Analyt Technol Biomed Life Sci*. 2006;832(2):262-267.

doi: 10.1016/j.jchromb.2006.01.008

108. Ahmadi K, Hasaniazad M, Kalani M, *et al*. Comparative study of the immune responses to the HMS-based fusion protein and capsule-based conjugated molecules as vaccine candidates in a mouse model of *Staphylococcus aureus* systemic infection. *Microb Pathog*. 2021;150:104656.

doi: 10.1016/j.micpath.2020.104656

109. Tollersrud T, Kenny K, Reitz AJ Jr., Lee, JC. Genetic and serologic evaluation of capsule production by bovine mammary isolates of *Staphylococcus aureus* and other *Staphylococcus* spp. from Europe and the United States. *J Clin Microbiol*. 2000;38(8):2998-3003.

doi: 10.1128/JCM.38.8.2998-3003.2000

110. Mechref Y, Hu Y, Desantos-Garcia JL, Hussein A, Tang H. Quantitative glycomics strategies. *Mol Cell Proteomics*. 2013;12(4):874-884.

doi: 10.1074/mcp.R112.026310

111. Che D, Huang Z, He F. Comparison between sulfuric acid-phenol and sulfuric acid-anthrone methods used for determination of polysaccharides in shoots of *Aralia elata* (Miq.) seem. *Agri Biotech*. 2018;3(7):170-173.

112. Cuesta G, Suarez N, Bessio MI, *et al*. Quantitative determination of pneumococcal capsular polysaccharide serotype 14 using a modification of phenol-sulfuric acid method. *J Microbiol Methods*. 2003;52(1):69-73.

doi: 10.1016/s0167-7012(02)00151-3

113. Masuko T, Minami A, Iwasaki N, Majima T, Nishimura S, Lee YC. Carbohydrate analysis by a phenol-sulfuric acid method in microplate format. *Anal Biochem*. 2005;339(1):69-72.

doi: 10.1016/j.ab.2004.12.001

114. An H, Qian C, Huang Y, *et al*. Functional vulnerability of liver macrophages to capsules defines virulence of blood-borne bacteria. *J Exp Med*. 2022;219(4):e20212032.

doi: 10.1084/jem.20212032

115. Shainheit MG, Valentino MD, Gilmore MS, Camilli A. Mutations in pneumococcal cpsE generated via *in vitro* serial passaging reveal a potential mechanism of reduced encapsulation utilized by a conjunctival isolate. *J Bacteriol*. 2015;197(10):1781-1791.

doi: 10.1128/JB.02602-14

116. Tuchscherr LP, Buzzola FR, Alvarez LP, Caccuri RL, Lee JC, Sordelli DO. Capsule-negative S*taphylococcus aureus* induces chronic experimental mastitis in mice. *Infect Immun*. 2005;73(12):7932-7937.

doi: 10.1128/IAI.73.12.7932-7937.2005

117. Grunert T, Stessl B, Wolf F, Sordelli DO, Buzzola FR, Ehling-Schulz M. Distinct phenotypic traits of *Staphylococcus aureus* are associated with persistent, contagious bovine intramammary infections. *Sci Rep.* 2018;8(1):15968.

doi: 10.1038/s41598-018-34371-1

118. Fischer J, Lee JC, Peters G, Kahl BC. Acapsular clinical *Staphylococcus aureus* isolates lack agr function. *Clin Microbiol Infect*. 2014;20(7):O414-O417.

doi: 10.1111/1469-0691.12429

119. Lei MG, Gudeta DD, Luong TT, Lee CY. MgrA negatively impacts *Staphylococcus aureus* invasion by regulating capsule and FnbA. *Infect Immun*. 2019;87(12):e00590-19.

doi: 10.1128/IAI.00590-19

120. Lei MG, Lee CY. Repression of capsule production by XdrA and CodY in *Staphylococcus aureus*. *J Bacteriol*. 2018;200(18):e00203-18.

doi: 10.1128/JB.00203-18

121. Rai D, Kulkarni SS. Total synthesis of trisaccharide repeating unit of *Staphylococcus aureus* type 8 (CP8) capsular polysaccharide. *Org Lett*. 2023;25(9):1509-1513.

doi: 10.1021/acs.orglett.3c00290

122. Lei MG, Lee CY. Regulation of staphylococcal capsule by SarZ is SigA-dependent. *J Bacteriol*. 2022;204(8):e0015222.

doi: 10.1128/jb.00152-22.

123. Gao S, Jin W, Quan Y, *et al*. Bacterial capsules: Occurrence, mechanism, and function. *NPJ Biofilms Microbiomes*. 2024;10(1):21.

doi: 10.1038/s41522-024-00497-6

ACCSCIENCE PUBLISHING

Microbes & Immunity

REVIEW ARTICLE

A conceptual model of the role of infectious agents in autoimmune diseases

Konstantinos L. Katsifarakis*

Department of Civil Engineering, Hydraulics and Environmental Engineering Division, Faculty of Engineering, Aristotle University of Thessaloniki, Thessaloniki, Central Macedonia, Greece

Abstract

The correlation between microbes and autoimmunity is well established, but many underlying mechanisms remain obscure. Thus, this paper attempts to elucidate the role of infectious agents (bacteria, viruses, etc.) in autoimmune diseases. To offer a concise framework for many relevant research findings, the following general conceptual model is proposed and discussed: autoimmune diseases arise from alterations in cells, tissues, or organs, caused by infectious agents. These alterations evolve with time, beginning as subtle, often undetectable changes. As the alterations become more severe, they can be identified by the immune system, which may subsequently attack the infected cells. This process allows for new explanations of relationships between triggers of autoimmunity and infectious agents, the time lag between infection and autoimmune response, the progressive nature of autoimmune diseases, and the role of virus persistence. It can also offer a new point of view on molecular mimicry and epitope spreading. The roles of genetic predisposition, sex, stress, dietary habits, the "hygiene hypothesis," and the healing effects of β-interferon also fit into this framework. In addition, the side effects of malignancy treatments using immune checkpoint inhibitors can also be explained. Adhering to the framework, it is concluded that treatments should aim to eliminate the cause of these evolving alterations, namely, the infectious agents. Presumably, they could be based on antibiotics and antiviral drugs. Future research directions are suggested for evaluating the proposed conceptual model.

Keywords: Autoimmune diseases; Infectious agents; Molecular mimicry; Epitope spreading; Hygiene hypothesis; Virus persistence; Immune checkpoint inhibitors; Resilience

***Corresponding author:**
Konstantinos L. Katsifarakis (klkats@civil.auth.gr)

Citation: Katsifarakis KL. A conceptual model of the role of infectious agents in autoimmune diseases. *Microbes & Immunity*. 2025;2(4):17-26. doi: 10.36922/MI025100017

Received: March 3, 2025

Revised: March 25, 2025

Accepted: April 1, 2025

Published online: May 5, 2025

1. Introduction

Autoimmune diseases tend to evolve into a scourge, particularly in developed countries. At present, 80 – 120 diseases have been identified as autoimmune,[1] depending on the classification criteria.[2] A common feature of autoimmune diseases is the immune system's aberrant attack on the body's own cells, tissues, or organs, treating them as foreign. Despite this shared characteristic, different triggers and evolution courses have been identified, as described by Theofilopoulos *et al.*[3]

At a fundamental level, autoimmune diseases have been linked to various dysfunctions of the immune system, such as impaired tolerance,[4-6] hormonal dysregulation,[7] or

misdirection by infectious agents (bacteria, viruses, etc.), often in conjunction with environmental factors. Current mainstream treatments aimed at relieving symptoms are mainly based on immunosuppressive or immunomodulatory drugs.[8] Despite these advances, the precise mechanism and etiology of autoimmune diseases remain unclear.[9]

This paper is focused on the mechanism that underlies the autoimmune response. A general conceptual model and evidence supporting its plausibility are outlined and discussed. Moreover, several new explanations of autoimmune response features that can be derived from the model are presented and briefly discussed. Finally, research directions aimed at the development of new treatments for autoimmune diseases are proposed.

2. The proposed conceptual model

An outline of the proposed mechanism of autoimmune response is as follows: autoimmune diseases are due to alterations of the cells, tissues, or organs that are subsequently attacked by the immune system. These alterations are caused by infectious agents (bacteria, viruses, etc.) and evolve with time. Initially, they are small and often undetectable by the immune system. However, when they exceed a certain threshold, the affected cells are targeted and subsequently attacked by the immune system. It can be hypothesized that the targeted cells have a recognizable "imprint" of the pathogen. Autoimmune disease symptoms typically emerge when cumulative cell damage leads to detectable dysfunction, the nature of which depends on the specific disease. This time-dependent process is schematically presented in Figures 1 and 2, both of which depict time on the x-axis.

In Figure 1, the alteration degree is shown on the y-axis, the dark blue line represents the evolution of cell alteration with time, and the broken red line indicates the alteration's detection threshold. Similarly, in Figure 2, the cumulative tissue damage is shown on the y-axis, the dark blue line represents the evolution of damage with time, and the broken red line marks the onset of autoimmune disease symptoms.

2.1. Previous research correlating autoimmune diseases with infectious agents

The proposed model aligns with observations of many researchers, who have correlated autoimmune diseases with infectious agents, such as bacteria or viruses.[10-12] For example, Coxsackie enterovirus has been associated with type 1 diabetes[13] and Epstein–Barr virus with Guillain–Barré syndrome, multiple sclerosis, systemic lupus erythematosus (SLE), rheumatoid arthritis, and

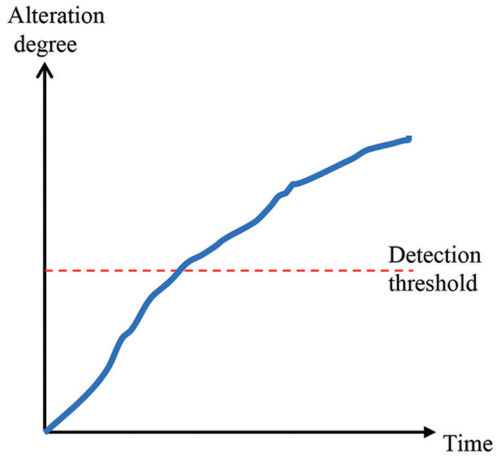

Figure 1. Evolution of cell alteration with time

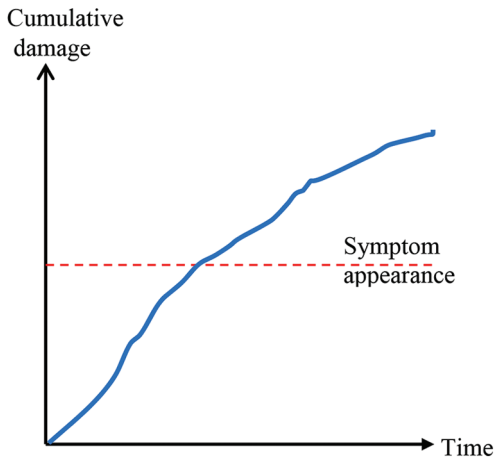

Figure 2. Evolution of cumulative tissue damage with time

other autoimmune diseases.[14] The severe acute respiratory syndrome coronavirus 2 virus has recently been considered a triggering factor of autoimmune diseases.[15] Moreover, vaccines have also been suspected of triggering such diseases.[16-18]

Regarding correlation with bacteria, a prominent, undisputable example is Sydenham chorea.[19] The attack of immune cells on the basal ganglia is triggered by infection with hemolytic streptococci. When diagnosed early, this disease can be successfully treated with a high dose of antibiotics, such as penicillin, to completely eliminate *Streptococcus*. This is followed by a lower long-term prophylaxis dose.[20] Recovery - and eventually cure - is manifested by the gradual elimination of movement disorders.

Another example is the pediatric autoimmune neuropsychiatric disorders associated with streptococcal infections. They are different from Sydenham chorea,[21]

and, as their name denotes, they are directly related to infections by gram-positive or spherical bacteria.

Moreover, inflammatory bowel diseases, comprising Crohn's disease and ulcerative colitis, have been related to gastrointestinal pathogens, such as *Campylobacter* species, *Salmonella* species, enterohepatic *Helicobacter* species, *Mycobacterium avium paratuberculosis*, *Clostridioides difficile*, and *Listeria monocytogenes*.[22] Notably, several gastrointestinal microbes and intestinal helminths have been inversely associated with the risk of inflammatory bowel diseases.[23]

Similarly, autoimmune thyroid diseases, namely, Graves's and Hashimoto's diseases, have been correlated with many types of infectious agents, such as hepatitis C virus, Coxsackie virus, *Yersinia enterocolitica*, *Borrelia burgdorferi*, *Helicobacter pylori*, and retroviruses.[24]

Other autoimmune diseases could also be induced or exacerbated by many different microbial infections, as summarized by Von Herrath *et al.*[25] Multiple sclerosis, for instance, has been related to viruses of the herpes[26] and the human endogenous retrovirus families, as well as protozoa and bacteria.[27] At the same time, Guillain-Barré syndrome has been associated mainly with *Campylobacter jejuni*, cytomegalovirus, Epstein-Barr virus, influenza A virus, *Mycoplasma pneumoniae*, and *Haemophilus influenzae*.[28] In addition, primary Sjögren's syndrome has been related to infections by viruses, such as Epstein–Barr[29] and hepatitis C.[30]

The correlations between common autoimmune diseases and specific pathogens are summarized in Table 1. The content should be considered as indicative, as a comprehensive review of all research relating autoimmune diseases to microbial infections is beyond the scope of this paper.

The role of Vitamin D in alleviating symptoms of inflammatory bowel diseases through "restoration" of intestinal microbiota and, eventually, of the gut barrier function,[31] is also indicative of the complex relationship between microbes and autoimmune diseases.

Moreover, another important correlation between pathogens and autoimmunity is found in the mechanism of bystander activation.[10,32,33] This phenomenon refers to the activation of T cells without antigen recognition, which is indirectly caused by the inflammatory environment generated during immune responses to pathogens. Bystander activation plays an important role in triggering or aggravating autoimmune diseases, such as multiple sclerosis, rheumatoid arthritis, type 1 diabetes, and autoimmune encephalomyelitis.

Autoimmunity has also been related to virus persistence.[33,34] The persistence of infectious agents plays a key role in the proposed conceptual model of autoimmune diseases, as it takes time for cellular alterations to accumulate to a detectable or recognizable extent.

Table 1. Correlations between common autoimmune diseases and specific pathogens

Autoimmune disease	Pathogens
Crohn's disease	*Campylobacter* species, *Salmonella* species, enterohepatic *Helicobacter* species, *Mycobacterium avium paratuberculosis, Clostridioides difficile*, and *Listeria monocytogenes*
Graves's disease	Hepatitis C virus, Coxsackie virus, *Yersinia enterocolitica, Borrelia burgdorferi, Helicobacter pylori,* and retroviruses
Guillain-Barré syndrome	*Campylobacter jejuni*, cytomegalovirus, Epstein-Barr virus, influenza A virus, *Mycoplasma pneumoniae*, and *Haemophilus influenzae*
Hashimoto's disease	Hepatitis C virus, Coxsackie virus, *Yersinia enterocolitica, Borrelia burgdorferi, Helicobacter pylori,* and retroviruses
Multiple sclerosis	Herpes, viruses of the human endogenous retrovirus family, protozoa, and bacteria
PANDAS	Gram-positive or spherical bacteria.
Rheumatoid arthritis	Epstein-Barr virus
Sjogren's syndrome	Epstein-Barr virus and hepatitis C virus
Sydenham chorea	Hemolytic streptococcus
Systemic lupus erythematosus	Epstein-Barr virus
Type 1 diabetes	Coxsackie enterovirus
Ulcerative colitis	*Campylobacter* species, *Salmonella* species, enterohepatic *Helicobacter* species, *Mycobacterium avium paratuberculosis, Clostridioides difficile*, and *Listeria monocytogenes*

Abbreviation: PANDAS: Pediatric autoimmune neuropsychiatric disorders associated with streptococcal infections.

3. Contribution of the proposed model to the understanding of autoimmunity

While the correlation of autoimmunity with infectious agents is well established, the mechanisms involved are not completely understood, and many relevant issues remain obscure.[35] The conceptual model proposed in this paper allows for new explanations of some important features of autoimmune diseases, which are outlined in the following paragraphs.

Progressive forms of autoimmune diseases can be explained in the following way: The patient's immune system targets specific cells (e.g., myelin in multiple

sclerosis) that already carry the pathogen's "imprint." Meanwhile, viruses or bacteria, which have not been eliminated, alter previously unaffected cells, which then become targets of the immune system.

Relapsing-remitting forms of autoimmune diseases in the proposed conceptual model can be understood as follows: the end of a relapsing phase occurs when the number of cells bearing a detectable pathogen's "imprint" falls below a threshold, which varies depending on the specific disease. The cessation of the inflammatory phase provides relief for the patients. Moreover, it may be accompanied by a certain degree of recovery, which depends on the resilience of the affected tissues, organs, or systems, particularly their regenerative capacity.

Nevertheless, the infectious agents have not been completely eliminated, and the "imprinting" process persists. During the remitting phase, this process remains undetected, while its rate might be lower than repair/regeneration. Symptoms reemerge when cumulative cellular damage, due to the attack of the immune system on altered cells, exceeds a certain threshold. New infections by pathogens may facilitate the onset of the subsequent relapsing phase by accelerating the "imprinting" process and/or by reactivating the patients' immune system.

Autoimmune diseases with good prognosis are considered cured when the immune system (naturally or with the support of antiviral drugs or antibiotics, as in Sydenham chorea) successfully eliminates the infectious agents, halting further cellular alteration. The degree of residual damage depends on the resilience of the affected system.

Notably, the role of resilience in general can be distinguished according to three types:

(i) Degree of damage from a given stress. In resilient systems, the damage does not completely inhibit the functioning of the stressed system.
(ii) Speed of recovery from damage that has occurred
(iii) The ability to substitute damaged parts with others that undertake the function of the damaged ones. This is particularly important in network structures, either biological or artificial. In most cases, a system that has recovered functionally is less resilient than before the damage.

Regarding the autoimmunity challenges discussed in this paper, the first and third types of resilience may contribute to the time lag between infection and detection of autoimmune response. Moreover, the second and third types contribute to patients' temporal recovery or permanent cure, in remitting-relapsing and good-prognosis autoimmune diseases, respectively.

Moreover, the role of molecular mimicry, which is considered "one of the leading mechanisms by which infectious or chemical agents may induce autoimmunity," as stated by Rojas *et al*.,[12(p100)] can be seen from a different point of view, in the framework of the proposed conceptual model. The basic idea is that autoimmune cells mistake self-cells as foreign, due to similarities between the host's protein structures and those of invading bacteria or viruses.[36] For instance, *Bacteroides fragilis*, a member of the normal human gut microbiota, encodes a protein similar to human ubiquitin and could trigger an autoimmune response.[37] There is an increase in evidence on the ability of bacteria to mimic human proteins and contribute to the onset of autoimmune diseases and their related clinical implications.[38] However, molecular mimicry may also have the "opposite" effect, allowing pathogens to evade the host's immune response.[39,40] This effect could be regarded as more predictable. The model, discussed in this paper, might offer the "missing link" between the two possible effects of molecular mimicry. During the first stage, the "invaders" avoid attacks by the immune system and can cause alterations to the host's cells. Subsequently, when the immune system can recognize them, it targets the "invaders" along with the cells with the pathogens' "imprint." This two-stage process can explain the time lag between infection and autoimmune response, as it takes some time for the infectious agents to affect a substantial number of cells to a degree detectable by the immune system. In the same framework, time-lag differences from disease to disease (and even from case to case for the same disease) can also be explained, as different infectious agents may be involved.

Another important issue, related to many autoimmune diseases, is epitope spreading.[41,42] As summarized by Cornaby *et al*.,[43] epitope spreading can be triggered by assorted viruses, bacterial infections, and stress. The occurrence can be justified in the conceptual model framework presented in this paper. As the alteration of infected cells evolves over time, it is reasonable to expect that the autoimmune response may target different epitopes within the same antigen, a phenomenon known as epitope spreading.

Finally, the role of the persistence of infectious agents is adequately explained, as their continued existence is essential for the continuation of the "imprinting" process.

4. The proposed model and other factors related to autoimmune responses

The roles of genetic predisposition, sex, dietary habits, stress, and lifestyle in developing autoimmune responses are well documented. These roles, together with the

"hygiene hypothesis" and the healing effects of interferon-β (IFN-β), fit well into the framework of the new approach to the mechanism of autoimmune diseases, as explained in the following paragraphs.

4.1. Genetic predisposition

The role of genetic factors in autoimmune diseases is indisputable.[5,44-46] Genetic predisposition to autoimmune diseases in general has been reported by Criswell *et al.*[47] and Li *et al.*[48] Criswell *et al.*[47] studied 265 multiplex families and found that at least two "core" autoimmune diseases were present in each of these families. Li *et al.*[48] analyzed the relationship between the polymorphisms of a particular gene and susceptibility to autoimmune diseases. In addition, the genetic susceptibility of specific organs to autoimmune diseases has been reported by Owen *et al.*[49]

The findings, which relate autoimmune diseases to genetic factors, fit well in the framework of the proposed model. If the problem lies with the attacked organ, it could be linked to its susceptibility to certain microbes, the "imprint" of which renders it a target of the immune system. This explains the existence of many autoimmune diseases, each affecting different systems of the patients. Moreover, the presence of more than one disease in multiplex families can be due to their members' infection by the same virus, resulting in different autoimmune diseases. Even if genetic predisposition is linked to features of the immune system, these features could relate to increased ability to recognize pathogens' imprints.

4.2. Sex

Women are generally more susceptible than men to many autoimmune diseases (such as SLE, thyroiditis, and rheumatoid arthritis), while they are more resistant to infections.[5,50] A similar difference is exhibited in vaccine responses: women generally develop higher antibody responses and may experience more adverse events than men.[51]

The link between resistance to infections and susceptibility to autoimmune diseases can be explained by the proposed model of the occurrence of autoimmune diseases. Women have a more efficient immune system, which eventually protects them better from infections. However, this efficacy makes it easier for the immune system to detect pathogens' imprints and, thus, attack self-cells, leading to more frequent occurrences of autoimmune responses. This explanation does not contradict findings relating sex-dependent differences with hormones (such as estrogens and progestins), genes on the X chromosome, or environmental factors. The only difference is that, in the framework of the proposed conceptual model, these factors can be considered as causes of differences between women and men, in terms of immune system efficiency (besides boosting or suppressing it directly).

It has been observed that during pregnancy, women are less susceptible to infections. As a result, fetuses are better protected. This reduction of susceptibility could be reasonably related to increased alertness of the immune system, which, in turn, could favor the appearance or exacerbation of autoimmune diseases. Nevertheless, this is not always the case. For instance, remission of rheumatoid arthritis during pregnancy has been extensively reported.[52] However, the causes are still unclear, and the proposed conceptual model does not offer an explanation, either.

4.3. Dietary habits

The correlation of diet with certain autoimmune diseases is statistically sound. Several explanations have been proposed in the literature, such as industrial food processing and food additive consumption. According to Lerner and Matthias,[53(p479)] "additives increase intestinal permeability by breaching the integrity of tight junction paracellular transfer. In fact, tight junction dysfunction is common in multiple autoimmune diseases." Moreover, micronutrient deficiency, such as Vitamin D hypovitaminosis, has been related to the onset and progression of autoimmune diseases[54] through impaired gut barrier function, due to deficient intestinal microbiota.[31] Diet has also been related to the onset of autoimmune diseases through molecular mimicry.[55]

Such observations fit very well in the framework of the proposed model: unhealthy or unbalanced diet habits render certain tissues more susceptible to infectious agents and facilitate their alteration, making them targets of the immune system.

4.4. Hygiene hypothesis

It is well-established that autoimmune diseases are much more widespread in developed countries than in developing ones.[56] The well-known "hygiene hypothesis"[57] directly correlates the decreasing incidence of infections in developed countries with the increase of autoimmune (and allergic) diseases.

This correlation, which is still an open research issue,[58] can be explained in the framework of the proposed mechanism of autoimmune diseases in the following way: in regions with poor hygienic conditions and limited access to medical treatment, many individuals succumb to diseases that rarely cause deaths in developed countries. However, in developed countries, some affected individuals, despite receiving treatment, are not completely cured. The infectious agents may not be completely eradicated and continue to leave their "imprint" on cells, organs, or systems, rendering them immune system targets.

4.5. Stress

It has been known for many years that stress (mainly chronic stress) can cause immunosuppression.[59] It may also increase the risk or exacerbation of autoimmune diseases,[7,59-62] which entail increased immune system activity. This apparent contradiction can be resolved in the framework of the proposed mechanism: in the first stage, stress-induced weakness of the immune system facilitates cell "imprinting" by pathogens. During the later stage, the immune system recognizes mounting alterations of the affected cells and attacks them. This two-stage process allows for a time lag between stress periods and exacerbations of autoimmune diseases.

4.6. Treatment of multiple sclerosis with IFNβ

IFNβ is mildly effective in treating the relapsing-remitting form of multiple sclerosis. However, the precise mechanisms through which IFNβ achieves its therapeutic effects are not fully understood.[63,64]

IFNs are known to stimulate cells infected by viruses to produce proteins that prevent virus replication within them, eventually hindering infections. The complex IFN contribution to combating cancer-associated viruses remains an active area of ongoing research.[65]

Given the undisputed antiviral properties of IFNs, irrespective of the exact mechanism, the therapeutic effect of IFNβ on multiple sclerosis can be reasonably related to its infection-stemming properties. This fits perfectly in the framework of the proposed model, which attributes the evolution of autoimmune diseases to residual infectious agents. As the disease has been related to different infectious agents, variations in the efficiency of their treatment with IFNβ could be attributed, at least partially, to the virus involved in each case.

5. Drug-induced autoimmunity

Some drugs have been linked to triggers of autoimmune diseases, such as SLE and rheumatoid arthritis.[5,66] The exact mechanism of drug-induced autoimmunity is still unknown. A case, which could reasonably be explained in the framework of the proposed conceptual model, is discussed in the following paragraph.

5.1. Treatment of malignancy

Some new treatments for malignancy have been related to autoimmunity. These treatments use immune checkpoint inhibitors (CPIs) to facilitate the patient's immune system to attack cancer cells. Side effects include a range of immune-related adverse events (IRAEs), from neurological effects[67,68] to rheumatological effects.[69] CPIs play an essential role in regulating immune responses.[70] Therefore, the appearance of such IRAEs could be expected, at least in the form of exacerbation of pre-existing autoimmune diseases. However, seemingly unrelated cells (tissues or organs) are also affected in certain instances. A possible explanation, closely related to the proposed model of autoimmune diseases, is that a similar, but distinct, process takes place in the second case. The underlying similarity is that the affected cells are not completely healthy. In the first case, the attacked cells bear the "imprint" of the pathogen, linked to a prior infection. In contrast, in the second case, they bear a slight cancerous alteration, which cannot be detected with current diagnostic means. The "boosted" immune system, on detecting alterations, even slight ones, attacks the affected cells, irrespective of the alteration's cause.

6. Conclusion

The proposed conceptual model, which attributes autoimmune diseases to progressive alteration of host cells caused by infectious agents, can explain many aspects of these diseases. If this model proves valid, halting the progression or even curing autoimmune diseases may be possible by developing new antibiotics or antiviral drugs. These drugs should aim to completely eliminate the infectious agents that cause cell alterations, rendering them immune system targets.

Halting the progress of an autoimmune disease does not result in the spontaneous restoration of damaged tissues. As mentioned in Section 3, the degree of residual damage depends on the resilience of each affected system. For this reason, it seems reasonable to combine antibiotics or antiviral therapies with immunomodulatory agents to reduce progressive damage until the underlying infectious cause is eliminated. Once the infectious agents are fully eradicated, continued use of immunomodulatory drugs may become unnecessary, or, at the very least, redundant.

7. Directions for further research

The following research directions would be very helpful to validate (or partially validate) the proposed conceptual model of the mechanism underlying autoimmune diseases, and to establish new treatment protocols, to the extent that the model proves accurate:

(i) Further statistical studies on the temporal correlation between the first manifestation or seizures of autoimmune diseases and infections from viruses or bacteria.
(ii) Clinical trials of existing and new antibiotics or antiviral drugs to stop the further progression of autoimmune diseases and eventually cure them.

(iii) Identify previously unknown infectious agents affecting organs or tissues commonly affected in autoimmune diseases.
(iv) Statistical studies on possible correlations between new malignancy treatments, eventually aiming at facilitating immune system response, and the appearance of IRAEs. In particular, if a relationship between cells (tissues or organs) affected by IRAEs and metastatic cancer expansions is detected, it could help understand the mechanism of this apparent disorientation of the immune system.

Research in this area could be pursued in parallel with research on the function of the immune system and the particular features of each autoimmune disease.

Acknowledgments

The author would like to thank Dr. V. Aroniadou-Anderjaska for specific comments and overall help. Moreover, the author would like to dedicate this paper to the memory of Kostas Vassiliou, a close relative, who passed away in his early forties, after suffering many years from multiple sclerosis.

Funding

None.

Conflict of interest

The author declares that he has no competing interests.

Author contributions

This is a single-authored article.

Ethics approval and consent to participate

Not applicable.

Consent for publication

Not applicable.

Availability of data

Not applicable.

Further disclosure

The paper has been deposited (a slightly shorter version, with a slightly different title) in Preprints.org (http://www.preprints.org) (doi: 10.20944/preprints202501.0893.v1).

References

1. Rose N, Mackay I, editors. *The Autoimmune Diseases*. United States: Elsevier Academic Press; 2020.
2. Rose NR, Bona C. Defining criteria for autoimmune diseases (Witebsky's postulates revisited). *Immunol Today*. 1993;14:426-430.
   doi: 10.1016/0167-5699(93)90244-F
3. Theofilopoulos A, Kono D, Baccala R. The multiple pathways to autoimmunity. *Nat Immunol*. 2017;18:716-24.
   doi: 10.1038/ni.3731.
4. Meffre E, O'Connor KC. Impaired B-cell tolerance checkpoints promote the development of autoimmune diseases and pathogenic autoantibodies. *Immunol Rev*. 2019;292:90-101.
   doi: 10.1111/imr.12821
5. Pisetsky DS. Pathogenesis of autoimmune disease. *Nat Rev Nephrol*. 2023;19:509-524.
   doi: 10.1038/s41581-023-00720-1
6. Rosenblum MD, Remedios KA, Abbas AK. Mechanisms of human autoimmunity. *J Clin Invest*. 2015;125(6):216-228.
   doi: 10.1172/JCI78088.
7. Stojanovich, L. Stress and autoimmunity. *Autoimmun Rev*. 2010;9(5):A271-A276.
   doi: 10.1016/j.autrev.2009.11.014
8. Bluestone JA, Anderson M. Tolerance in the age of immunotherapy. *N Engl J Med*. 2020;383:1156-1166.
   doi: 10.1056/NEJMra1911109
9. Rałowska-Gmoch W, Koszewicz M, Łabuz-Roszak B, Budrewicz S, Dziadkowiak E. Diagnostic criteria and therapeutic implications of rapid-onset demyelinating polyneuropathies. *Exp Mol Pathol*. 2024;140:04942.
   doi: 10.1016/j.yexmp.2024.104942
10. Ercolini AM, Miller SD. The role of infections in autoimmune disease. *Clin Exp Immunol*. 2009;155(1):1-15.
    doi: 10.1111/j.1365-2249.2008.03834.x
11. Fairweather D, Kaya Z, Shellam GR, Lawson CM, Rose NR. From infection to autoimmunity. *J Autoimmun*. 2001;16(3):175-186.
    doi: 10.1006/jaut.2000.0492
12. Rojas M, Restrepo-Jiménez P, Monsalve DM, *et al*. Molecular mimicry and autoimmunity. *J Autoimmun*. 2018;95:100-123.
    doi: 10.1016/j.jaut.2018.10.012
13. Dotta F, Censini S, Van Halteren AG, *et al*. Coxsackie B4 virus infection of beta cells and natural killer cell insulitis in recent-onset type 1 diabetic patients. *Proc Natl Acad Sci U S A*. 2007;104:5115-5120.
    doi: 10.1073/pnas.0700442104
14. Lossius A, Johansen JN, Torkildsen Ø, Vartdal F, Holmøy T. Epstein-barr virus in systemic lupus erythematosus, rheumatoid arthritis and multiple sclerosis-association and

causation. *Viruses*. 2012;4(12):3701-3730.

doi: 10.3390/v4123701

15. Sher EK, Ćosović A, Džidić-Krivić A, Farhat EK, Pinjić E, Sher F. Covid-19 a triggering factor of autoimmune and multi-inflammatory diseases. *Life Sci*. 2023;319:121531.

doi: 10.1016/j.lfs.2023.121531

16. Vellozzi C, Iqbal S, Broder K. Guillain-Barre syndrome, influenza, and influenza vaccination: The epidemiologic evidence. *Clin Infect Dis*. 2014;58:1149-1155.

doi: 10.1093/cid/ciu005

17. Polykretis P, Donzelli A, Lindsay JC, *et al*. Autoimmune inflammatory reactions triggered by the COVID-19 genetic vaccines in terminally differentiated tissues. *Autoimmunity*. 2023;56(1):2259123.

doi: 10.1080/08916934.2023.2259123

18. Rojas M, Herrán M, Ramírez-Santana C, *et al*. Molecular mimicry and autoimmunity in the time of COVID-19. *J Autoimmun*. 2023;139:103070.

doi: 10.1016/j.jaut.2023.103070

19. Cardoso F. Sydenham's chorea. *Curr Treat Options Neurol*. 2008;10:230-5.

doi: 10.1007/s11940-008-0025-x

20. Bonthius DJ, Karacay B. Sydenham's chorea: Not gone and not forgotten. *Semin Pediatr Neurol*. 2003;10:11-19.

doi: 10.1016/S1071-9091(02)00004-9

21. Van Toorn R, Weyers HH, Schoeman JF. Distinguishing PANDAS from Sydenham's chorea: Case report and review of the literature. *Eur J Paediatr Neurol*. 2004;8:211-216.

doi: 10.1016/j.ejpn.2004.03.005

22. Axelrad JE, Cadwell KH, Colombel JF, Shah SC. The role of gastrointestinal pathogens in inflammatory bowel disease: A systematic review. *Ther Adv Gastroenter*. 2021;14:17562848211004493.

doi: 10.1177/17562848211004493

23. Wang M, Wu L, Weng R, Zheng W, Wu Z, Lv Z. Therapeutic potential of helminths in autoimmune diseases: Helminth-derived immune-regulators and immune balance. *Parasitol Res*. 2017;116:2065-2074.

doi: 10.1007/s00436-017-5544-5

24. Shukla SK, Govind Singh G, Ahmad S, Pant P. Infections, genetic and environmental factors in pathogenesis of autoimmune thyroid diseases. *Microb Pathog*. 2018;116:279-288.

doi: 10.1016/j.micpath.2018.01.004

25. Von Herrath M, Fujinami R, Whitton J. Microorganisms and autoimmunity: Making the barren field fertile? *Nat Rev Microbiol*. 2003;1:151-157.

doi: 10.1038/nrmicro754

26. Domingues TD, Malato J, Grabowska AD, *et al*. Association analysis between symptomology and herpesvirus IgG antibody concentrations in myalgic encephalomyelitis/chronic fatigue syndrome (ME/CFS) and multiple sclerosis. *Heliyon*. 2023;9(7):e18250.

doi: 10.1016/j.heliyon.2023.e18250

27. Libbey JE, Cusick MF, Fujinami RS. Role of pathogens in multiple sclerosis. *Int Rev Immunol*. 2014;33:266-283.

doi: 10.3109/08830185.2013.823422

28. Willison HJ, Jacobs BC, Van Doorn PA. Guillain-Barré syndrome. *Lancet*. 2016;388(10045):717-727.

doi: 10.1016/S0140-6736(16)00339-1

29. Maślińska M. The role of Epstein-Barr virus infection in primary Sjögren's syndrome. *Curr Opin Rheumatol*. 2019;31(5):475-483.

doi: 10.1097/BOR.0000000000000622

30. Wang Y, Dou H, Liu G, *et al*. Hepatitis C virus infection and the risk of Sjögren or sicca syndrome: A meta-analysis. *Microbiol Immunol*. 2014;58:675-687.

doi: 10.1111/1348-0421.12202

31. Battistini C, Ballan R, Herkenhoff ME, Saad SM, Sun J. Vitamin D modulates intestinal microbiota in inflammatory bowel diseases. *Int J Mol Sci*. 2021;22(1):362.

doi: 10.3390/ijms22010362

32. Shim CH, Cho S, Shin YM, Choi JM. Emerging role of bystander T cell activation in autoimmune diseases. *BMB Rep*. 2022;55(2):57-64.

doi: 10.5483/BMBRep.2022.55.2.183

33. Fujinami RS, Von Herrath MG, Christen U, Whitton JL. Molecular mimicry, bystander activation, or viral persistence: Infections and autoimmune disease. *Clin Microbiol Rev*. 2006;19(1):80-94.

doi: 10.1128/cmr.19.1.80-94.2006

34. Frazer IH. Autoimmunity and persistent viral infection: Two sides of the same coin? *J Autoimmun*. 2008;31(3):216-218.

doi: 10.1016/j.jaut.2008.04.014

35. Smatti MK, Cyprian FS, Nasrallah GK, Al Thani AA, Almishal RO, Yassine HM. Viruses and autoimmunity: A review on the potential interaction and molecular mechanisms. *Viruses*. 2019;11(8):762.

doi: 10.3390/v11080762

36. Oldstone MBA. Molecular mimicry, microbial infection, and autoimmune disease: Evolution of the concept, in molecular mimicry: Infection-inducing autoimmune disease. In: Oldstone, MBA, editor. *Current Topics in Microbiology and Immunology*. Berlin, Heidelberg: Springer; 2005. p. 296.

doi: 10.1007/3-540-30791-5_1

37. Stewart L, Edgar JDM, Blakely G, Patric S. Antigenic mimicry of ubiquitin by the gut bacterium *Bacteroides fragilis*: A potential link with autoimmune disease. *Clin Exp Immunol*. 2018;194(2):153-165.

doi: 10.1111/cei.13195

38. Suliman BA. Potential clinical implications of molecular mimicry-induced autoimmunity. *Immun Inflamm Dis*. 2024;12:e1178.

doi: 10.1002/iid3.1178

39. Maguire C, Wang C, Ramasamy A, *et al*. Molecular mimicry as a mechanism of viral immune evasion and autoimmunity. *Nat Commun*. 2024;15:9403.

doi: 10.1038/s41467-024-53658-8

40. Würzner, R. Evasion of pathogens by avoiding recognition or eradication by complement, in part via molecular mimicry. *Mol Immunol*. 1999;36(4-5):249-260.

doi: 10.1016/S0161-5890(99)00049-8

41. Vanderlugt CJ, Miller SD. Epitope spreading. *Curr Opin Immunol*. 1996;8:831-836.

doi: 10.1016/S0952-7915(96)80012-4

42. Venkatesha SH, Durai M, Moudgil KD. Epitope spreading in autoimmune diseases. In: Mahroum N, Watad A, Shoenfeld Y, editors. *Infection and Autoimmunity*. 3rd ed., Ch. 5. Academic Press; 2024. p61-89.

doi: 10.1016/B978-0-323-99130-8.00038-6

43. Cornaby C, Gibbons L, Mayhew V, Sloan CS, Welling A, Poole BD. B cell epitope spreading: Mechanisms and contribution to autoimmune diseases. *Immunol Lett*. 2015;163(1):56-68.

doi: 10.1016/j.imlet.2014.11.001

44. Long H, Yin H, Wang L, Gershwin ME, Lu Q. The critical role of epigenetics in systemic lupus erythematosus and autoimmunity. *J Autoimmun*. 2016;74:118-138.

doi: 10.1016/j.jaut.2016.06.020

45. Kahaly GJ, Hansen MP. Type 1 diabetes associated autoimmunity. *Autoimmun Rev*. 2016;15:644-648.

doi: 10.1016/j.autrev.2016.02.017

46. Ma WT, Chang CH, Gershwin ME, Lian ZX. Development of autoantibodies precedes clinical manifestations of autoimmune diseases: A comprehensive review. *J Autoimmun*. 2017;83:95-112.

doi: 10.1016/j.jaut.2017.07.003

47. Criswell LA, Pfeiffer KA, Lum RF, *et al*. Analysis of families in the multiple autoimmune disease genetics consortium (MADGC) collection: The PTPN22 620W allele associates with multiple autoimmune phenotypes. *Am J Hum Genet*. 2005;76(4):561-571.

doi: 10.1086/429096

48. Li J, Lin SY, Lv YB, Tang HM, Peng F. Association study of MMP-9 -1562C/T gene polymorphism with susceptibility to multiple autoimmune diseases: A meta-analysis. *Arch Med Res*. 2017;48(1):105-112.

doi: 10.1016/j.arcmed.2017.01.001

49. Owen KA, Price A, Ainsworth H, *et al*. Analysis of trans-ancestral SLE risk loci identifies unique biologic networks and drug targets in African and European ancestries. *Am J Hum Genet*. 2020;107(5):864-881.

doi: 10.1016/j.ajhg.2020.09.007

50. Fairweather D, Beeler DJ, McCabe EJ, Lieberman SM. Mechanisms underlying sex differences in autoimmunity. *J Clin Invest*. 2024;134(18):e180076.

doi: 10.1172/JCI180076

51. Fischinger S, Boudreau CM, Butler AL, Streeck H, Alter G. Sex differences in vaccine-induced humoral immunity. *Semin Immunopathol*. 2019;41:239-249.

doi: 10.1007/s00281-018-0726-5

52. Raine C, Austin K, Giles I. Mechanisms determining the amelioration of rheumatoid arthritis in pregnancy: A systematic review. *Semin Arthritis Rheum*. 2020;50(6):1357-1369.

doi: 10.1016/j.semarthrit.2020.03.006

53. Lerner A, Matthias T. Changes in intestinal tight junction permeability associated with industrial food additives explain the rising incidence of autoimmune disease. *Autoimmun Rev*. 2015;14:479-489.

doi: 10.1016/j.autrev.2015.01.009

54. Murdaca G, Tonacci A, Negrini S, *et al*. Emerging role of vitamin D in autoimmune diseases: An update on evidence and therapeutic implications. *Autoimmun Rev*. 2019;18(9):102350.

doi: 10.1016/j.autrev.2019.102350

55. Guggenmos J, Schubart AS, Ogg S, *et al*. Antibody cross-reactivity between myelin oligodendrocyte glycoprotein and the milk protein butyrophilin in multiple sclerosis. *J Immunol*. 2004;172:661-668.

doi: 10.4049/jimmunol.172.1.661

56. Armelagos GJ, Brown PJ, Turner B. Evolutionary, historical and political economic perspectives on health and disease. *Soc Sci Med*. 2005;61(4):755-765.

doi: 10.1016/j.socscimed.2004.08.066

57. Okada H, Kuhn C, Feillet H, Bach JF. The 'hygiene hypothesis' for autoimmune and allergic diseases: An update. *Clin Exp Immunol*. 2010;160(1):1-9.

doi: 10.1111/j.1365-2249.2010.04139.x

58. Murdaca G, Greco M, Borro M, Gangemi S. Hygiene

hypothesis and autoimmune diseases: A narrative review of clinical evidences and mechanisms. *Autoimmun Rev*. 2021;20(7):102845.

doi: 10.1016/j.autrev.2021.102845

59. Pruett SB. Stress and the immune system. *Pathophysiology*. 2003;9(3):133-153.

doi: 10.1016/S0928-4680(03)00003-8

60. Jacobs R, Pawlak CR, Mikeska E, *et al*. Systemic lupus erythematosus and rheumatoid arthritis patients differ from healthy controls in their cytokine pattern after stress exposure. *Rheumatology*. 2001;40(8):868-875.

doi: 10.1093/rheumatology/40.8.868

61. Mitsonis CI, Potagas C, Zervas I, Sfagos K. The effects of stressful life events on the course of multiple sclerosis: A review. *Int J Neurosci*. 2009;119(3):315-335.

doi: 10.1080/00207450802480192

62. Song H, Fang F, Tomasson G, *et al*. Association of stress-related disorders with subsequent autoimmune disease. *JAMA*. 2018;319(23):2388-2400.

doi: 10.1001/jama.2018.7028

63. Dhib-Jalbut S, Marks S. Interferon-beta mechanisms of action in multiple sclerosis. *Neurology*. 2010;74(1 Suppl):S17-S24.

doi: 10.1212/WNL.0b013e3181c97d99

64. Hojati Z, Kay M, Dehghanian F. Mechanism of action of interferon beta in treatment of multiple sclerosis. In: Minagar A, editor. Multiple Sclerosis. Ch. 15. United States: Academic Press; 2016. p. 365-392.

doi: 10.1016/B978-0-12-800763-1.00015-4

65. Zhu YX, Li ZY, Yu ZL, *et al*. The underlying mechanism and therapeutic potential of IFNs in viral-associated cancers. *Life Sci*. 2025;361:123301.

doi: 10.1016/j.lfs.2024.123301

66. Xiao X, Chang C. Diagnosis and classification of drug-induced autoimmunity (DIA). *J Autoimmun*. 2014;48-49:66-72.

doi: 10.1016/j.jaut.2014.01.005

67. Graus F, Dalmau J. Paraneoplastic neurological syndromes in the era of immune-checkpoint inhibitors. *Nat Rev Clin Oncol*. 2019;16:535-548.

doi: 10.1038/s41571-019-0194-4

68. Möhn N, Beutel G, Gutzmer R, *et al*. Neurological immune related adverse events associated with nivolumab, ipilimumab, and pembrolizumab therapy-review of the literature and future outlook. *J Clin Med*. 2019;8(11):1777.

doi: 10.3390/jcm8111777

69. Cano-Cruz LG, Barrera-Vargas A, Mateos-Soria A, Soto-Perez-de-Celis E, Merayo-Chalico J. Rheumatological adverse events of cancer therapy with immune checkpoint inhibitors. *Arch Med Res*. 2022;53(2):113-121.

doi: 10.1016/j.arcmed.2021.09.004

70. Zhai Y, Moosavi R, Chen M. Immune checkpoints, a novel class of therapeutic targets for autoimmune diseases. *Front Immunol*. 2021;12:645699.

doi: 10.3389/fimmu.2021.645699

ACCSCIENCE PUBLISHING

Microbes & Immunity

REVIEW ARTICLE

Innovative perspectives on pulmonary immune responses: Pathogens versus protectors

Saeid Besharati*, Zohreh Nazari Yazdi, Marjan Sistani, and Shirin Esmaili Dolabinezhad

Nursing Research Center of Respiratory Diseases, National Research Institute of Tuberculosis and Lung Diseases, Shahid Beheshti University of Medicine Sciences, Tehran, Iran

(This article belongs to the *Special Issue: Immune Responses to Pulmonary Infections*)

Abstract

The pulmonary immune system serves as a critical frontline in the host's defense against invading pathogens. Understanding the dynamic interplay between invading pathogens and the host's immune defenses is essential for the development of innovative therapeutic strategies. This review explores the complex mechanisms underlying pulmonary immune responses, with a focus on the balance between pathogen virulence and host immunity. Relevant publications – including peer-reviewed articles, clinical studies, and technological advancements published between 2020 and 2025 – were identified through searches of electronic databases such as Google Scholar, PubMed, Scopus, and Web of Science. The findings reveal that pathogens employ sophisticated strategies to evade immune detection, such as modulation of host cell signaling pathways and the secretion of virulence factors. Conversely, the host mounts protective immune responses characterized by rapid activation of innate immunity, cytokine-mediated signaling, and the development of adaptive immune memory. Notably, recent studies have reported several novel biomarkers associated with enhanced pathogen clearance and tissue repair, highlighting their potential as therapeutic targets. This review provides new insights into pulmonary immune responses, highlighting the delicate balance between pathogen evasion and host defense mechanisms. By identifying key immune regulators and pathogen-specific vulnerabilities, it highlights potential targets for innovative treatments to enhance pulmonary immunity. These findings underscore the importance of interdisciplinary approaches in advancing knowledge of respiratory infections and immune defense.

Keywords: Host defense; Immune regulation; Pathogen evasion; Respiratory infections; Pulmonary immunity; Therapeutic targets

***Corresponding author:**
Saeid Besharati
(saeid.besharati@sbmu.ac.ir)

Citation: Besharati S, Yazdi ZN, Sistani M, Dolabinezhad SE. Innovative perspectives on pulmonary immune responses: Pathogens versus protectors. *Microbes & Immunity.* 2025;2(4):27-39.
doi: 10.36922/MI025100019

Received: March 6, 2025

Revised: April 23, 2025

Accepted: May 8, 2025

Published online: June 3, 2025

1. Introduction

The respiratory system serves as the host's crucial frontline against the external environment, constantly exposed to a myriad of pathogens, including bacteria, viruses, and fungi, as well as environmental pollutants and allergens. The lungs are particularly vulnerable to these challenges due to their large surface area and constant exposure to airborne particles.[1-3] To counter these threats, the pulmonary immune system has

evolved to detect and neutralize harmful agents while minimizing collateral damage to delicate lung tissues. Despite ongoing exposure, the lungs are equipped with a highly advanced immune defense network that maintains homeostasis and protects against infection and injury.[4-6] However, many pathogens have developed sophisticated mechanisms to evade or manipulate host immune defenses, leading to persistent infections, chronic inflammation, and respiratory disease. This review explores recent advancements in understanding the pulmonary immune responses, focusing on the complex interplay between evading pathogens and host immune defenses, and how innovative research is reshaping approaches to respiratory health.

The balance between pathogen invasion and immune protection is delicate, and its disruption can lead to severe lung diseases – such as pneumonia, tuberculosis, chronic obstructive pulmonary disease (COPD), and asthma. While these conditions are often linked to microbiome alterations, environmental pollutants, and allergens, pathogens still play a significant role. The recent emergence of novel pathogens, such as SARS-CoV-2, has further highlighted the urgent need to deepen our understanding of pulmonary immunity and to develop innovative strategies that strengthen protective responses while minimizing harmful inflammation.

This review explores the dynamic interplay between invading pathogens and the host's pulmonary immune defenses, highlighting cutting-edge research into the molecular and cellular mechanisms underlying pulmonary immunity. It emphasizes the dual role of immune cells and mediators as both protectors and potential contributors to tissue damage. By examining emerging therapeutic approaches – including immunomodulation, microbiome engineering, and advanced vaccine technologies – this review offers a comprehensive overview of current trends and future directions. A deeper understanding of these immune responses may lead to more effective interventions for respiratory infections and chronic lung diseases, ultimately improving global health outcomes.

2. Methods

This review article employs a systematic approach to synthesize current literature on pulmonary immune responses, focusing on the dynamic interplay between pathogens and host defense mechanisms. It incorporates a comprehensive analysis of both experimental and clinical studies to provide a holistic understanding of pulmonary immune responses. By incorporating diverse study types, the review ensures a robust exploration of innovative perspectives in this field.

2.1. Inclusion criteria

Studies included in this review met the following criteria:

(i) Focused on pulmonary immunity, including pathogen–host interactions, immune evasion strategies, and protective immune responses
(ii) Published in peer-reviewed journals between 2020 and January 2025, ensuring relevance to current scientific knowledge
(iii) Were available as full-text articles in English
(iv) Employed *in vitro*, *in vivo*, or clinical models to investigate pulmonary immune responses.

2.2. Exclusion criteria

Studies were excluded if they:

(i) Did not clearly focus on pulmonary immunity or lacked relevance to pathogen–host interactions
(ii) Were published only as abstracts, conference proceedings, or in non-peer-reviewed articles
(iii) Contained redundant or overlapping data without providing novel insights
(iv) Focused exclusively on non-respiratory systems or addressed only non-immunological aspects of pulmonary diseases.

2.3. Search strategy

A systematic search was conducted across major databases – including Google scholar, PubMed, Scopus, and Web of Science – using a combination of relevant keywords, including "pulmonary immunity," "pathogen–host interactions," "immune evasion," "lung protection," and "innovative therapies." Boolean operators (e.g., AND, OR) were used to refine the search strategy. Additional articles were identified through manual screening of reference lists from relevant articles. Only articles published in English between 2020 and January 2025 were considered. The initial search yielded 540 articles. After applying the exclusion criteria, 519 articles were removed. Following relevance screening, quality assessment, and evaluation of their focus on innovative perspectives in pulmonary immune responses, 21 articles met the inclusion criteria (Figure 1 and Table 1).

2.4. Study selection

The initial search yielded a broad range of articles, which were first screened based on titles and abstracts. Subsequently, full-text articles were assessed for eligibility according to the predefined inclusion and exclusion criteria. One independent reviewer conducted the screening process, and any discrepancies were resolved through discussion or consultation with a second reviewer.

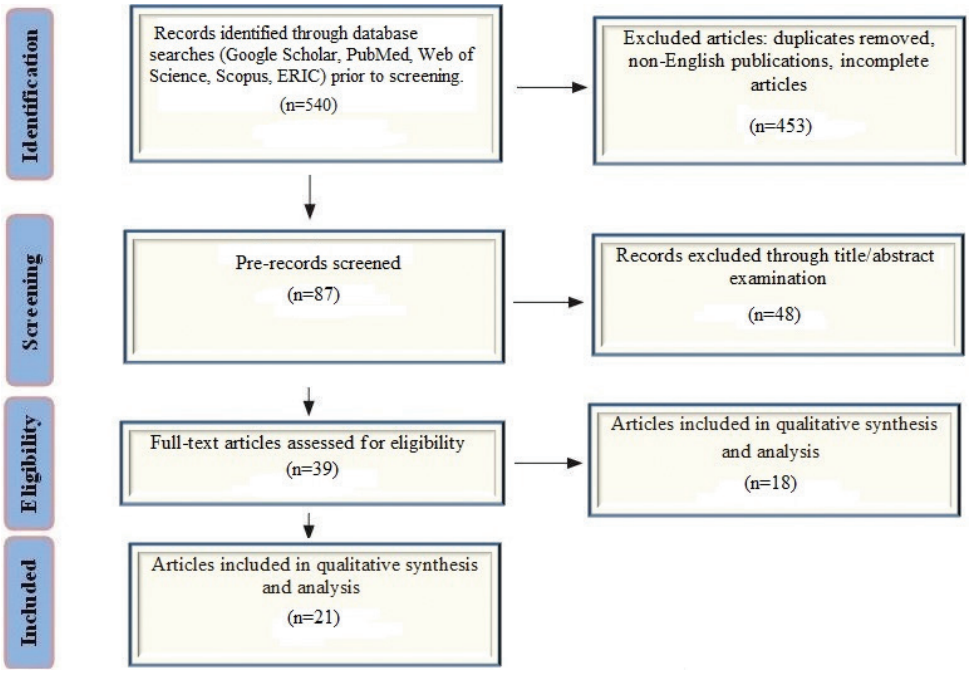

Figure 1. Flow chart of article screening
Abbreviation: ERIC: Education Resources Information Center.

Table 1. Key indicators used in the present review to evaluate core competencies in pulmonary immune responses

Results	Categories	Items	Example quotes	References
Enhanced understanding of immune mechanisms	Immune response pathways	Cytokine signaling, macrophage activation, and T-cell differentiation.	"Cytokine storms play a pivotal role in severe pulmonary infections."	43-45
Identification of novel biomarkers	Biomarker discovery	Protein markers, genetic signatures, and metabolic indicators.	"Elevated levels of protein X correlate with disease severity in patients."	46-48
Development of targeted therapies	Therapeutic innovations	Monoclonal antibodies, immunomodulators, and gene therapies.	"Monoclonal antibody Y shows promise in reducing viral load in preclinical models."	49-51
Role of microbiota in immunity	Microbiome-immune interactions	Gut–lung axis, microbial diversity, and probiotic interventions.	"The gut–lung axis modulates immune responses to respiratory pathogens."	52-54
Pathogens' immune evasion strategies	Pathogen adaptations	Antigenic variation, immune suppression, and biofilm formation.	"Pathogen X evades detection by altering surface proteins."	28,55,56
Protective host factors	Host defense mechanisms	Innate and adaptive immunity, and epithelial barrier function.	"Epithelial cells act as the first line of defense against invading pathogens."	57,58
Impact of environmental factors	Environmental influences	Air pollution, climate change, and occupational exposures.	"Exposure to particulate matter exacerbates pulmonary inflammation."	59,60
Advances in diagnostic tools	Diagnostic technologies	Artificial intelligence-based diagnostics, rapid testing, and imaging techniques.	"Artificial intelligence algorithms improve early detection of pulmonary infections."	61,62
Vaccine development progress	Vaccination strategies	mRNA vaccines, adjuvants, and mucosal vaccines.	"mRNA vaccines induce robust immune responses in the respiratory tract."	63,64
Cross-species immune comparisons	Comparative immunology	Animal models, evolutionary adaptations, and zoonotic infections.	"Comparative studies reveal conserved immune pathways across species."	65,66

2.5. Descriptive themes

The findings were organized into descriptive themes to highlight key insights:

(i) Pathogen strategies: Mechanisms employed by pathogens to evade or suppress pulmonary immune responses
(ii) Host defense mechanisms: Innate and adaptive immune responses that protect the lungs from infection
(iii) Innovative therapies: Emerging therapeutic approaches aimed at modulating pulmonary immune responses, including the use of immunomodulators and vaccines
(iv) Microbiome influence: The role of the lung microbiome in shaping immune responses.

3. Results

3.1. The pulmonary immune system

The pulmonary immune system is a complex and dynamic network that maintains a delicate balance between defending against pathogens and preventing excessive inflammation that could harm lung tissue. As a primary interface with the external environment, the lungs are constantly exposed to airborne pathogens, allergens, and environmental pollutants. This constant exposure necessitates a highly specialized and efficient immune response to provide protection while preserving respiratory function. This section explores the key components of the pulmonary immune system, emphasizing the interplay between pathogens and immune defense, and highlighting recent advances in research and emerging therapeutic strategies.

3.1.1. The pulmonary barrier: First line of defense

The respiratory epithelium, lined with ciliated cells and mucus-producing goblet cells, serves as the first physical and biochemical barrier against airborne pathogens. This epithelial layer is reinforced by antimicrobial peptides (AMPs), surfactant proteins, and secreted immunoglobulins that neutralize invaders before infection can be established. Recent studies have highlighted the crucial role of the epithelial barrier in shaping immune responses through the release of cytokines and chemokines, which recruit and activate immune cells.[7,8]

3.1.2. Innate immunity: Rapid and non-specific

The innate immune system in the lungs is characterized by its rapid response to invading pathogens. Alveolar macrophages – the most abundant immune cells in the airways – play a crucial role in phagocytosing pathogens and clearing apoptotic cells, thereby maintaining tissue homeostasis. In addition, dendritic cells act as immune sentinels, capturing antigens and migrating to lymph nodes to initiate adaptive immune responses. Neutrophils, while typically associated with acute inflammation, are also essential for combating bacterial and fungal infections. Recent research has highlighted the role of innate lymphoid cells (ILCs) in regulating mucosal immunity and tissue repair, offering new insights into their potential as therapeutic targets.[9]

3.1.3. Adaptive immunity: Precision and memory

The adaptive immune system provides a targeted and long-lasting defense against invading pathogens. T lymphocytes – including helper T cells such as Th1, Th2, and Th17, as well as regulatory T (Treg) cells – coordinate immune responses that are specifically tailored to distinct pathogens. On the other hand, B lymphocytes produce antigen-specific antibodies that neutralize pathogens and facilitate their clearance. Recent studies in single-cell sequencing have revealed significant heterogeneity within pulmonary T and B-cell populations, providing new insights into their roles in chronic lung diseases and vaccine-induced immunity.[10]

3.1.4. The microbiome: A double-edged sword

Once considered sterile, the lung microbiome is now recognized as a critical modulator of pulmonary immune responses. Commensal microbes contribute to immune homeostasis by competing with pathogens and modulating the immune system. However, dysbiosis – disruptions in the microbial community – has been linked to chronic inflammatory lung diseases such as asthma, COPD, and pulmonary fibrosis. Innovative therapeutic approaches – including probiotics and microbiome transplantation – are being explored to restore microbial balance and enhance pulmonary immunity.[11,12]

3.1.5. Immunopathology: When protection turns harmful

While the immune system is essential for protection, dysregulated responses can lead to immunopathology. Excessive inflammation – as observed in conditions such as acute respiratory distress syndrome or severe COVID-19 – can cause tissue damage and impair gas exchange. Conversely, inadequate immune responses, such as those in immunocompromised individuals, may lead to persistent infections. Understanding the mechanisms underlying these immune imbalances is crucial for developing targeted therapies that effectively modulate immune responses without compromising host defense.[13,14]

3.1.6. Innovative perspectives: Modulating the immune system

Recent advancements in immunology have laid the foundation for innovative strategies to enhance pulmonary immunity. These include:

(i) Immunotherapies: Monoclonal antibodies and immune checkpoint inhibitors are increasingly used to treat lung cancer and chronic respiratory infections
(ii) Vaccines: Advances in mRNA vaccine technology, highlighted by the success of COVID-19 vaccines, offer promising potential for preventing respiratory infections
(iii) Gene Editing: Clustered regularly interspaced short palindromic repeats (CRISPR)-based techniques are being explored to correct genetic defects in immune cells or enhance their protective functions within the lungs.
(iv) Nanotechnology: Engineered nanoparticles enable targeted delivery of drugs or vaccines directly to lung tissues, improving therapeutic efficacy while minimizing side effects.

a. *In vitro* models of lung epithelial cells

In vitro models of lung epithelial cells have become essential tools for investigating the early stages of pathogen invasion and the subsequent immune response. These models, typically derived from primary human bronchial or alveolar epithelial cells, closely replicate the structural and functional characteristics of the lung epithelium. By exposing these cells to pathogens – such as *Mycobacterium tuberculosis*,[15,16] influenza virus, or *Pseudomonas aeruginosa* – researchers can monitor real-time cellular responses, including the release of pro-inflammatory cytokines, disruption of the epithelial barrier, and activation of innate immune signaling pathways. In addition, these models facilitate high-throughput screening of potential therapeutics, offering a controlled platform to evaluate drug efficacy and toxicity before evaluation in more complex systems.

b. *In vivo* murine infection studies

While *in vitro* models of lung epithelial cells provide valuable insights into the early stages of pathogen invasion and the subsequent immune response, they cannot fully capture the complex interactions among immune cells, tissue architecture, and systemic responses present in a living organism. *In vivo* murine infection studies address this limitation by allowing researchers to examine pulmonary immune responses within the context of a whole organism. Mice – with their well-characterized immune systems and genetic manipulability – serve as ideal models for investigating host–pathogen interactions. For instance, studies using murine models have highlighted the role of alveolar macrophages in clearing bacterial infections and the contribution of T-cell subsets in controlling viral replication. In addition, transgenic and knockout mouse models have been pivotal in identifying key immune signaling pathways – such as the nucleotide oligomerization domain-like receptor protein 3 inflammasome and type I interferon (IFN) responses – that influence the outcomes of pulmonary infections.[17,18]

c. Advanced computational simulations

Alongside experimental approaches, advanced computational simulations have transformed the study of pulmonary immune responses. By integrating data from both *in vitro* and *in vivo* studies, these simulations can model complex immune networks and predict outcomes across various scenarios. For example, agent-based models simulate the interactions of individual immune cells and pathogens within the pulmonary microenvironment, providing valuable insights into spatial and temporal dynamics that are difficult to capture experimentally. Similarly, systems biology approaches utilize large-scale omics datasets to construct predictive models of immune signaling pathways, aiding the identification of potential therapeutic targets. Together, these computational tools not only enhance our understanding of pulmonary immunity but also facilitate the development of personalized treatment strategies

d. Innovative perspectives on pulmonary immune responses

The human respiratory system is a continuous battleground where pathogens and the immune system engage in a complex interplay of attack and defense. Recent advances in computational biology have transformed our understanding of these pulmonary immune responses, offering innovative insights into how the body defends itself against invading microorganisms. Advanced computational simulations have become powerful tools for dissecting and analyzing immune responses with unprecedented detail. By utilizing high-performance computing and machine learning algorithms, researchers can now model the dynamic interactions between pathogens and immune cells within the lung microenvironment. These simulations provide valuable insights into the spatial and temporal dynamics of immune responses, revealing how factors such as cytokine signaling, cellular migration, and pathogen evasion strategies influence infection outcomes. For instance, computational models have simulated the behavior of alveolar macrophages – the lung's first line of defense – and their interactions with bacterial or viral invaders. Such models can predict how variations in immune cell activity or pathogen virulence may shift the balance between effective clearance and chronic infection.[19,20]

In addition, advanced computational approaches facilitate the integration of multi-omics data – including genomics, transcriptomics, and proteomics – to construct comprehensive models of pulmonary immunity. These models help identify key molecular pathways and

biomarkers that influence the progression of respiratory diseases such as influenza, tuberculosis, or COVID-19. For example, simulations have highlighted the critical role of IFN responses in controlling viral replication, as well as the detrimental effects of excessive inflammation in severe pneumonia cases. One of the most promising applications of these computational simulations is accelerating novel therapeutic development. By virtually screening thousands of drug candidates and their effects on immune–pathogen interactions, researchers can prioritize the most effective interventions for experimental validation. This approach not only reduces the time and cost of traditional drug discovery but also opens new avenues for personalized medicine, enabling treatments tailored to an individual's unique immune profile.

e. Microbiome influence

Once considered sterile, the human lung is now recognized as a dynamic ecosystem rich in microbial life. The pulmonary microbiome – a complex community of bacteria, viruses, fungi, and other microorganisms – plays a pivotal role in shaping immune responses within the respiratory system. This dynamic interplay between the lung microbiome and the immune system can influence whether these microorganisms act as harmful pathogens or beneficial protectors in the ongoing pulmonary immune response.

Recent research highlights the dual nature of the lung microbiome. A balanced and diverse microbial community contributes to immune homeostasis by training the immune system to distinguish between harmless invaders and genuine threats. For example, commensal bacteria can stimulate the production of anti-inflammatory cytokines and promote the development of Treg cells, which help suppress excessive immune responses and prevent chronic inflammation. This protective role is essential for maintaining lung health and resilience against infections.[21] Conversely, dysbiosis – an imbalance in the microbial community – can shift the balance toward pathogenicity. When harmful microbes dominate, they disrupt the epithelial barrier, trigger hyperactive immune responses, and exacerbate conditions such as asthma, COPD, and pulmonary fibrosis. Pathogens such as *P. aeruginosa* and *Streptococcus pneumoniae* exploit these imbalances, leading to persistent infections and chronic inflammation. Moreover, the interaction between the microbiome and viral infections, such as influenza or SARS-CoV-2, further complicates the immune response, as dysbiosis may impair the lung's ability to mount an effective antiviral defense.

Innovative perspectives are emerging to enhance the microbiome's protective potential while minimizing its pathogenic risks. Therapeutic strategies – such as probiotic therapies, targeted antimicrobial treatments, and microbiome transplantation – are being developed to restore microbial balance and enhance pulmonary immunity. Advances in metagenomic sequencing and machine learning are enabling researchers to explore the complex interactions between microbial communities and immune cells, creating opportunities for personalized interventions.[22] In pulmonary immune responses, the microbiome acts as both foe and ally. Understanding its influence is crucial for the development of novel therapeutic approaches that shift the balance toward protection, offering new hope to millions of individuals affected by respiratory diseases. As research on the lung microbiome progresses, one thing remains clear: these microscopic inhabitants hold the key to shaping the future of pulmonary medicine.

f. The balance between protection and pathology

The pulmonary immune system must maintain a delicate balance between eliminating pathogens and preventing excessive inflammation. Disruption of this balance can lead to chronic inflammatory diseases such as asthma, COPD, and pulmonary fibrosis. For instance, an overactive Th2 response characterizes allergic asthma, while excessive neutrophil activity is associated with tissue damage in COPD. However, this delicate balance between protection and pathology often acts as a double-edged sword. While robust immune responses are essential for eliminating harmful pathogens, excessive or dysregulated immunity can lead to tissue damage, chronic inflammation, and pathological conditions such as fibrosis or autoimmune disorders. Understanding this balance is critical for developing innovative therapeutic strategies that enhance protective immunity without shifting the balance toward pathology.

g. Protective immunity: The first line of defense

The lungs are constantly exposed to environmental pathogens, allergens, and pollutants, necessitating a rapid and efficient immune response. Innate immune systems – such as alveolar macrophages, dendritic cells, and epithelial barriers – play a pivotal role in detecting and neutralizing threats. These cells recognize pathogen-associated molecular patterns and damage-associated molecular patterns through pattern recognition receptors, initiating a cascade of pro-inflammatory signals. Neutrophils, natural killer cells, and AMPs further contribute to pathogen clearance, while adaptive immunity – mediated by T and B cells – provides long-lasting protection through memory responses.[23]

However, the effectiveness of these responses depends on precise regulation. For instance, alveolar macrophages exhibit a unique ability to switch between pro- and anti-inflammatory phenotypes, ensuring inflammation resolves once the threat is eliminated. Similarly, Treg cells play a

crucial role in suppressing excessive immune activation and preventing collateral tissue damage.

4. Pathology: When protection goes awry

Despite these regulatory mechanisms, the pulmonary immune system is not infallible. Dysregulation can occur at multiple levels, leading to pathological outcomes. For example, excessive neutrophil recruitment and activation – while effective against bacteria – can release reactive oxygen species and proteases that damage lung tissue, contributing to conditions such as acute respiratory distress syndrome or COPD. Similarly, an overactive Th2 response to harmless allergens may trigger asthma, characterized by airway hyperresponsiveness and remodeling.[24] Chronic infections caused by pathogens such as *M. tuberculosis* or *P. aeruginosa* further disrupt this balance. These pathogens evade immune detection and persist in the lungs, driving sustained inflammation and tissue destruction. In some cases, the immune response itself becomes the primary driver of pathology, as seen in idiopathic pulmonary fibrosis, where aberrant wound healing and fibroblast activation lead to progressive scarring and loss of lung function.

5. Innovative perspectives: Restoring the delicate balance of pulmonary immune responses

Recent advances in immunology and biotechnology provide new insights into restoring the delicate balance between protection and pathology. Targeting specific immune pathways, such as cytokine signaling (e.g., interleukin [IL]-1β, IL-6, tumor necrosis factor α), shows promising potential in modulating excessive inflammation without compromising host defense. For instance, biologics like anti-IL-5 therapies have transformed the treatment of eosinophilic asthma by selectively suppressing harmful immune responses. Another innovative approach involves utilizing the power of the microbiome.

Once considered sterile, the lung microbiome is now recognized as a key player in immune regulation. Dysbiosis, or microbial imbalance, has been linked to chronic lung diseases, suggesting that restoring microbial diversity may help rebalance immune responses. Probiotics and prebiotics are being explored as potential therapies to achieve this balance. Furthermore, advances in gene editing technologies, such as CRISPR-Cas9, hold promising potential for correcting genetic defects that contribute to immune dysregulation. Similarly, personalized medicine approaches – guided by biomarkers and genetic profiling – aim to tailor therapies to individual patients, minimizing side effects and maximizing efficacy.

6. Pathogen evasion strategies: Evading the pulmonary immune defense

The respiratory system serves as the pathogen's primary target due to its constant exposure to the external environment. To successfully establish infection, pathogens have developed sophisticated strategies to evade the host's immune defenses. This review explores the complex mechanisms employed by pathogens to evade the pulmonary immune system, highlighting the ongoing battle between microbial invaders and host defenses.

6.1. Pathogen disguise and antigenic variation

Pathogens evade immune detection by altering their surface antigens, a strategy known as antigenic variation. For instance, influenza viruses frequently mutate their hemagglutinin and neuraminidase proteins, thereby enabling them to avoid recognition by pre-existing antibodies. Similarly, *M. tuberculosis* modifies its cell wall composition to avoid detection by pattern recognition receptors such as Toll-like receptors. This molecular mimicry allows pathogens to disguise themselves within the host environment, delaying immune recognition and response.

6.2. Inhibition of immune signaling

The pulmonary immune system is a complex network of cells, cytokines, and signaling pathways designed to protect the lungs against invading pathogens. However, many pathogens have developed sophisticated strategies to evade or inhibit immune signaling, shifting the balance in their favor. Conversely, excessive or dysregulated immune signaling can lead to chronic inflammation and tissue damage, highlighting the delicate interplay between protection and pathology. This section explores the mechanisms used by pathogens to inhibit immune signaling and the therapeutic potential of targeted immune modulation in pulmonary diseases.

6.2.1. Pathogen-mediated inhibition of immune signaling

Pathogens – including bacteria, viruses, and fungi – have developed diverse strategies to evade host immune defenses. For instance, *M. tuberculosis* inhibits macrophage activation and antigen presentation through multiple mechanisms. It secretes proteins – such as protein tyrosine phosphatase A and protein tyrosine phosphatase B – which dephosphorylate key host signaling molecules, including those in the mitogen-activated protein kinase and nuclear factor kappa B pathways, thereby suppressing pro-inflammatory cytokine production.

Similarly, respiratory viruses such as influenza A and SARS-CoV-2 encode proteins that disrupt IFN signaling.

The non-structural protein 1 of influenza A inhibits type I IFN production, while the open reading frame 6 protein of SARS-CoV-2 blocks the nuclear translocation of signal transducer and activator of transcription 1, a critical transcription factor for IFN-stimulated genes.[25-27] Fungal pathogens such as *Aspergillus fumigatus* also employ immune evasion strategies. They produce secondary metabolites like gliotoxin, which inhibits nuclear factor kappa B activation and induces apoptosis in immune cells. These pathogen-mediated disruptions of immune signaling not only facilitate microbial survival but also contribute to the progression of chronic pulmonary infections.[28]

6.2.2. Host-mediated inhibition of immune signaling: A protective mechanism?

While pathogen-mediated modulation of immune signaling is often detrimental, the host also downregulates immune responses to prevent excessive inflammation. Treg cells and anti-inflammatory cytokines – such as IL-10 and transforming growth factor β – play crucial roles in maintaining immune homeostasis. However, in chronic pulmonary diseases – such as asthma, COPD, and idiopathic pulmonary fibrosis – dysregulated immune signaling can lead to persistent inflammation and tissue remodeling. Therefore, targeted inhibition of specific immune signaling pathways has emerged as a promising therapeutic approach. For example, Janus kinase inhibitors have shown efficacy in suppressing cytokine storms in severe COVID-19 and autoimmune lung diseases.[29,30] Similarly, monoclonal antibodies targeting IL-4, IL-5, and IL-13 have transformed the treatment of eosinophilic asthma by selectively inhibiting Th2-mediated inflammation. However, the key challenge remains: suppressing harmful immune responses without compromising protective immunity.

a. Innovative therapeutic approaches

Recent advances in immunomodulatory therapies have introduced new strategies for targeting immune signaling in pulmonary diseases. Approaches such as small molecule inhibitors, biologics, and gene-editing technologies like CRISPR-Cas9 offer precise tools to modulate immune pathways. For instance, inhaled nanoparticles delivering small interfering RNA against pro-inflammatory cytokines can suppress inflammation locally, reducing the risk of systemic side effects. In addition, microbiome-based therapies are being explored to restore immune homeostasis in the lungs by modulating the gut–lung axis.[31]

b. The role of impaired mucociliary clearance (MCC) on the pulmonary microbiome and pathogen persistence

The MCC system is a critical defense mechanism in the respiratory tract, responsible for trapping and removing inhaled pathogens, pollutants, and cellular debris. When MCC is impaired – due to chronic respiratory diseases (e.g., COPD), cystic fibrosis, or primary ciliary dyskinesia – the lung microenvironment undergoes significant changes that disrupt the balance of the pulmonary microbiome and facilitate the persistence of harmful pathogens. Under normal conditions, MCC helps maintain a dynamic equilibrium in the lung microbiome by continuously eliminating microbes before they can colonize. However, impaired MCC leads to mucus accumulation, creating stagnant niches where bacteria can thrive.[32,33] Impaired MCC is not only unable to eliminate pathogens but also exacerbates inflammation. The resulting immune response further damages the airway epithelium, worsening MCC dysfunction in a vicious cycle. Prolonged inflammation alters the lung microenvironment, favoring pathogen adaptation and resistance.

6.3. Resistance to AMPs and phagocytosis

The pulmonary immune system relies heavily on AMPs and phagocytic cells such as macrophages and neutrophils to eliminate pathogens. However, pathogens such as *S. pneumoniae* and *Haemophilus influenzae* have developed resistance mechanisms to AMPs by modifying their cell membranes or secreting proteases that degrade these peptides. Furthermore, *Legionella pneumophila* and *M. tuberculosis* manipulate phagocytic cells, enabling them to survive and replicate within macrophages by inhibiting phagosome–lysosome fusion or resisting oxidative burst mechanisms.[31]

6.4. Biofilm formation

Biofilms are structured communities of microorganisms encased in a self-produced protective extracellular matrix. In the respiratory tract, pathogens such as *P. aeruginosa* and *S. aureus* form biofilms to shield themselves from immune cells and antibiotics. The biofilm matrix not only acts as a physical barrier but also modulates immune responses by trapping and neutralizing antimicrobial agents, thereby complicating treatment and contributing to chronic infections.[34,35] Biofilm formation begins with the attachment of planktonic (free-floating) microorganisms to the pulmonary epithelium or medical devices, such as endotracheal tubes. This attachment is facilitated by adhesins and other surface proteins that recognize host cell receptors or synthetic materials. Following attachment, the pathogens proliferate and secrete extracellular polymeric substances – including polysaccharides, proteins, and extracellular DNA – forming the biofilm matrix. This matrix not only provides structural integrity but also acts as a barrier against the host immune system – such as phagocytosis – and reduces the penetration of antibiotics.[36]

Within the biofilm, microorganisms undergo significant phenotypic changes, including altered metabolic activity and gene expression, which contribute to their increased resistance to antimicrobial agents.[37] This phenotypic shift is further exacerbated by the presence of persister cells – dormant subpopulations exhibiting high tolerance to antibiotics. In addition, biofilms facilitate horizontal gene transfer, promoting the spread of antibiotic resistance genes among microbial communities. The host immune system faces significant challenges in combating biofilm-associated infections. Neutrophils – the primary immune cells recruited to infection sites – often struggle to penetrate the biofilm matrix and instead release reactive oxygen species and proteolytic enzymes that can damage surrounding host tissues, contributing to chronic inflammation and tissue remodeling. Moreover, biofilms can modulate the host immune response by releasing virulence factors that disrupt signaling pathways and promote immune evasion.

6.5. Exploitation of immune checkpoints

Some pathogens exploit the host's immune regulatory mechanisms for their own advantage. For instance, *M. tuberculosis* upregulates immune checkpoint molecules such as programmed cell death protein 1 (PD-1) on T cells, thereby inducing T cell exhaustion and impairing adaptive immunity. By exploiting these regulatory pathways, pathogens effectively suppress immune responses, allowing them to persist in the host.

6.6. Exploitation of immune checkpoints in pulmonary immune responses

The immune checkpoint pathway, a critical regulator of immune homeostasis, plays both protective and detrimental roles in pulmonary immunity. While these checkpoints are essential for maintaining self-tolerance and preventing excessive immune activation, pathogens and tumors have developed sophisticated strategies to exploit them, enabling evasion of immune surveillance. In the lungs – a site of continuous exposure to environmental and microbial stimuli – this exploitation poses a major barrier to effective immunity and carries significant implications for respiratory health.[38] Immune checkpoints – such as PD-1/programmed death-ligand 1 (PD-L1) and cytotoxic T lymphocyte-associated protein 4 – are pivotal in modulating T-cell responses. Under normal conditions, these pathways ensure that immune reactions remain proportionate and targeted, thereby preventing collateral damage to delicate lung tissues. However, pathogens – including viruses such as influenza and SARS-CoV-2, as well as bacteria such as *M. tuberculosis* – have been shown to upregulate checkpoint molecules to suppress host immunity. For instance, during chronic viral infections or tuberculosis, the constant antigen exposure induces T-cell exhaustion, characterized by the upregulation of PD-1 on T cells and PD-L1 on infected cells or antigen-presenting cells. This interaction effectively dampens the immune response, allowing pathogens to establish chronic infections.[39]

The exploitation of immune checkpoints extends beyond infectious diseases. In lung cancer, tumor cells frequently manipulate these pathways to establish an immunosuppressive microenvironment. By expressing high levels of PD-L1, tumor cells engage PD-1 on cytotoxic T cells, leading to their functional exhaustion and impairing the anti-tumor immune response. This immune suppression has been a major focus of cancer immunotherapy, with checkpoint inhibitors such as anti-PD-1 and anti-cytotoxic T lymphocyte-associated protein 4 antibodies showing remarkable success in restoring T cell activity and improving patient outcomes. However, therapeutic targeting of immune checkpoints poses significant challenges. In the context of pulmonary infections, checkpoint inhibitors can trigger immune-mediated tissue damage, as seen in immune-related adverse events such as pneumonitis. Achieving a balance between restoring immune function and preventing immune hyperactivation remains a critical consideration in the development of immunotherapies for pulmonary diseases. Moreover, the interplay between immune checkpoints and the lung microbiome introduces additional complexity. Although it harbors a lower microbial density than the gut microbiome, the lung microbiome plays a crucial role in modulating local immune responses. Dysbiosis, or microbial imbalance, may influence checkpoint expression and function, potentially enhancing pathogen immune evasion or contributing to chronic inflammatory conditions such as asthma and COPD.

6.7. Modulation of host cell death pathways in pulmonary immune responses

Pathogens often manipulate host cell death pathways to evade recognition and elimination. For example, influenza viruses inhibit apoptosis in infected cells to prolong viral replication. Conversely, *M. tuberculosis* induces necrosis in macrophages, promoting bacterial dissemination while evading immune surveillance. By modulating cell death mechanisms, pathogens ensure their survival and propagation within the host.

The interplay between pathogens and the host's pulmonary immune system represents a complex and dynamic battle, in which modulation of host cell death pathways plays a pivotal role. Cell death mechanisms – including apoptosis, necrosis, pyroptosis, and necroptosis

– serve as critical defense strategies to eliminate infected cells and limit pathogen spread. However, pathogens have evolved sophisticated strategies to manipulate these pathways to their advantage, creating a delicate balance between protection and pathology.[40]

7. Innovative perspectives on pulmonary immune responses

Recent advances in immunology provide new insights into novel mechanisms and therapeutic targets in pulmonary immunity. ILCs – which mirror the functions of T-cell subsets but lack antigen-specific receptors – have emerged as key players. ILCs contribute to both protective and pathological immune responses in the lungs, offering new avenues for intervention.[41] In addition, the respiratory tract microbiome is now recognized as a critical modulator of pulmonary immunity. Commensal microbes influence immune cell development and function, while dysbiosis is linked to various respiratory diseases. Manipulating the microbiome through probiotics or targeted therapies holds promise for modulating immune responses.[42] Innovative technologies such as single-cell RNA sequencing and spatial transcriptomics provide unprecedented insights into the cellular and molecular dynamics of pulmonary immunity. These tools enable researchers to analyze the heterogeneity of immune cells within the lung and identify novel biomarkers and therapeutic targets.

8. Challenges and future directions

Despite these advancements, several challenges remain––including the heterogeneity of pulmonary diseases, the complexity of host–pathogen interactions, and the risk of immune-mediated damage. Therefore, future research should focus on:

(i) Identifying biomarkers for early disease detection and personalized therapy
(ii) Developing universal vaccines against highly mutable viruses such as influenza
(iii) Exploring the role of the lung–brain axis and systemic immune responses in pulmonary health.

9. Conclusion

The battle between pathogens and the pulmonary immune system is a dynamic and evolving struggle. Advances in understanding immune mechanisms and pathogen strategies are paving the way for innovative therapies that enhance protection while minimizing harm. Through the application of cutting-edge technologies and interdisciplinary approaches, the balance may be shifted in favor of host defense, promoting healthier lungs and improved quality of life for patients worldwide.

Acknowledgments

We are especially thankful to the nurses and advisors of the Nursing Research Center of Respiratory Diseases at Masih Daneshvari Hospital, who collaborated in this research.

Funding

None.

Conflict of interest

The authors declare no conflicts of interest.

Author contributions

Conceptualization: Saeid Besharati
Writing-original draft: Zohreh Nazari Yazdi, Marjan Sistani, Shirin Esmaili Dolabinezhad
Writing-review & editing: Saeid Besharati, Shirin Esmaili Dolabinezhad

Ethics approval and consent to participate

Not applicable.

Consent for publication

Not applicable.

Availability of data

Not applicable.

References

1. Dondi A, Carbone C, Manieri E, *et al*. Outdoor air pollution and childhood respiratory disease: The role of oxidative stress. *Int J Mol Sci*. 2023;24(5):4345.
doi: 10.3390/ijms24054345

2. Besharati S. The expanding antibiotic resistance: The requirement of new therapeutic strategy for the development of new anti-infective. In: *Innate Immunity - New Perspectives and Therapeutic Opportunities*. London: IntechOpen; 2025. p. 49.
doi: 10.5772/intechopen.1006935

3. Besharati S, Kalaleh AR. Personalized nursing and precision nursing: A concept of the future of the health model. *J Prev Diagn Treat Strategies Med*. 2024;3(4):227-234.
doi: 10.4103/jpdtsm.jpdtsm_48_24

4. Block H, Zarbock A. A fragile balance: Does neutrophil extracellular trap formation drive pulmonary disease progression? *Cells*. 2021;10(8):1932.
doi: 10.3390/cells10081932

5. Besharati S. The expanding antibiotic resistance: The requirement of new therapeutic strategy for the development

of new anti-infective. In: *Innate Immunity - New Perspectives and Therapeutic Opportunities*. London: IntechOpen; 2024.

doi: 10.5772/intechopen.1006935

6. Mojahed M, Besharati S, Farzanegan B, *et al*. Identification of operational errors in the stages of the hemovigilance program with the guidance of the Global Trigger Tool and comparing it with the reported errors. *Sci J Iran Blood Transfus Organ*. 2024;21(4):320-332.

7. Li R, Li J, Zhou X. Lung microbiome: New insights into the pathogenesis of respiratory diseases. *Signal Transduct Target Ther*. 2024;9(1):19.

doi: 10.1038/s41392-023-01722-y

8. Fröhlich E. Non-cellular layers of the respiratory tract: Protection against pathogens and target for drug delivery. *Pharmaceutics*. 2022;14(5):992.

doi: 10.3390/pharmaceutics14050992

9. Zhang H, He F, Li P, Hardwidge PR, Li N, Peng Y. The role of innate immunity in pulmonary infections. *BioMed Res Int*. 2021;2021(1):6646071.

doi: 10.1155/2021/6646071

10. Bizimana Rukundo T. Cross-reactivity in adaptive immunity: An overview. *Appl Sci (NIJBAS)*. 2024;5(3):39-43.

doi: 10.59298/NIJBAS/2024/5.3.394311

11. Whiteside SA, McGinniss JE, Collman RG. The lung microbiome: Progress and promise. *J Clin Investig*. 2021;131(15):e150473.

doi: 10.1172/JCI150473

12. Gillissen A, Paparoupa M. Inflammation and infections in asthma. *Clin Respir J*. 2015;9(3):257-269.

doi: 10.1111/crj.12135

13. Muyayalo KP, Gong GS, Kiyonga Aimeé K, Liao AH. Impaired immune response against SARS-CoV-2 infection is the major factor indirectly altering reproductive function in COVID-19 patients: A narrative review. *Hum Fertil* (*Camb*). 2023;26(4):778-796.

doi: 10.1080/14647273.2023.2262757

14. Saeid AB, De Rubis G, Williams KA, *et al*. Revolutionising lung health: Exploring the latest breakthroughs and future prospects of synbiotic nanostructures in lung diseases. *Chem Biol Interact*. 2024;395:111009.

doi: 10.1016/j.cbi.2024.111009

15. FarniaTP, Ghanavi J, Besharati S, Farnia P, Velayati AA. The pili at genomic level. *Pili in Mycobacterium Tuberculosis: Structure, Function, and Therapeutic Advances*. Netherlands: Elsevier; 2024. p. 161.

16. Fouladi MD, Besharati S, Farnia P, Khosravi A. A concise review of the effect of efflux pump on biofilm intensity in bacteria with a special view to mycobacterium. *J Prev Diagn Treat Strategies Med*. 2024;3(1):1-5.

doi: 10.4103/jpdtsm.jpdtsm_119_23

17. Mu P, Zhou S, Lv T, *et al*. Newly developed 3D *in vitro* models to study tumor-immune interaction. *J Exp Clin Cancer Res*. 2023;42(1):81.

doi: 10.1186/s13046-023-02653-w

18. Zong Y, Li H, Liao P, *et al*. Mitochondrial dysfunction: Mechanisms and advances in therapy. *Signal Transduct Target Ther*. 2024;9(1):124.

doi: 10.1038/s41392-024-01839-8

19. Zhou X, Wu Y, Zhu Z, *et al*. Mucosal immune response in biology, disease prevention and treatment. *Signal Transduct Target Ther*. 2025;10(1):7.

doi.org/10.1038/s41392-024-02043-4

20. Mochan E, Sego T. Mathematical modeling of the lethal synergism of coinfecting pathogens in respiratory viral infections: A review. *Microorganisms*. 2023;11(12):2974.

doi: 10.3390/microorganisms11122974

21. Qadri H, Shah AH, Almilaibary A, Mir MA. Microbiota, natural products, and human health: Exploring interactions for therapeutic insights. *Front Cell Infect Microbiol*. 2024;14:1371312.

doi: 10.1038/s41392-024-02043-4

22. Chiu CW, Tsai PJ, Lee CC, Ko WC, Hung YP. Application of microbiome management in therapy for Clostridioides difficile Infections: From fecal microbiota transplantation to probiotics to microbiota-preserving antimicrobial agents. *Pathogens*. 2021;10(6):649.

23. Land WG. The DAMP-driven host immune defense program against pathogens. In: *Damage-Associated Molecular Patterns in Human Diseases: Antigen-Related Disorders*. Vol. 3. Germany: Springer; 2023. p. 203-284.

doi: 10.1007/978-3-031-21776-0_4

24. Meng X, Layhadi JA, Keane ST, Cartwright NJ, Durham SR, Shamji MH. Immunological mechanisms of tolerance: Central, peripheral and the role of T and B cells. *Asia Pac Allergy*. 2023;13(4):175-186.

doi: 10.5415/apallergy.0000000000000128

25. Besharati S, Aghajani J, Farnia P, *et al*. Association between the Vitamin D Receptor Gene (FokI, BsmI, ApaI, and TaqI) polymorphism in health-care workers and susceptibility to COVID-19. *Biomed Biotechnol Res J (BBRJ)*. 2023;7(3):404-410.

doi: 10.4103/bbrj.bbrj_133_23

26. Farnia P, Besharati S, Farina P, *et al*. The role of efflux pumps transporter in multi-drug resistant tuberculosis: Mycobacterial memberane protein (MmpL5). *Int J Mycobacteriol*. 2024;13(1):7-14.

doi: 10.4103/ijmy.ijmy_37_24

27. Farnia P, Farnia P, Ghanavi J, Ayoubi S, Besharati S, Velayati AA. Comparison of proline-glutamate-proline-glutamate-polymorphic GC-rich sequences family protein Wag22 (Rv1759c), PE_PGRS31 (Rv1768), PE_PGRS32 (Rv1803), and *PE_PGRS33* gene (Rv1818c) in exponential state and under *in vitro* model of latency in same clinical isolates of *Mycobacterium tuberculosis*: Frameshift mutation in extensively drug-resistant and totally drug-resistant *Tuberculosis bacilli*. *Biomed Biotechnol Res J (BBRJ)*. 2023;7(4):621-632.

doi: 10.4103/bbrj.bbrj_271_23

28. Wang Y, Pruitt RN, Nürnberger T, Wang Y. Evasion of plant immunity by microbial pathogens. *Nat Rev Microbiol*. 2022;20(8):449-464.

doi: 10.1038/s41579-022-00710-3

29. Tanaka Y, Luo Y, O'Shea JJ, Nakayamada S. Janus kinase-targeting therapies in rheumatology: A mechanisms-based approach. *Nat Rev Rheumatol*. 2022;18(3):133-145.

doi: 10.1038/s41584-021-00726-8

30. Varahram M, Besharati S, Farnia P, *et al*. Correlation of single-nucleotide polymorphism at interferon-gamma R1 (at position- 56) in positive purified protein derivative health workers with COVID-19 infection. *Int J Mycobacteriol*. 2022;11(3):318-322.

doi: 10.4103/ijmy.ijmy_133_22

31. Lei L, Pan W, Shou X, *et al*. Nanomaterials-assisted gene editing and synthetic biology for optimizing the treatment of pulmonary diseases. *J Nanobiotechnol*. 2024;22(1):343.

doi: 10.1186/s12951-024-02627-w

32. Adivitiya, Kaushik MS, Chakraborty S, Veleri S, Kateriya S. Mucociliary respiratory epithelium integrity in molecular defense and susceptibility to pulmonary viral infections. *Biology* (*Basel*). 2021;10(2):95.

doi: 10.3390/biology10020095

33. Dransfield M, Rowe S, Vogelmeier CF, *et al*. Cystic fibrosis transmembrane conductance regulator: Roles in chronic obstructive pulmonary disease. *Am J Respir Crit Care Med*. 2022;205(6):631-640.

doi: 10.1164/rccm.202109-2064TR

34. Besharati S, Owlia P. Evaluation of biofilm production capacity in *Salmonella* isolated from chicken meat in Tehran municipally daily fruit and vegetable markets. *Daneshvar Med*. 2020;28(1):62-72.

35. Besharati S, Farnia P, Farnia P, Ghanavi J, Velayati AA. Investigation of the hypothesis of biofilm formation in coronavirus (COVID-19). *Biomed Biotechnol Res J (BBRJ)*. 2020;4(Suppl 1):S99-S100.

doi: 10.4103/bbrj.bbrj_126_20

36. Besharati S, Soleimani N, Rahbar M. Evaluation of the prevalence of Integron 1, 2 and biofilm formation in clinical isolates of *Pseudomonas aeruginosa* in Tehran, 2024. *J Isfahan Med Sch*. 2025;43:125-134.

doi: 10.48305/jims.v43.i805.0125

37. Besharati S, Owlia P, Sadeghi A, *et al*. Frequency, antibiotic resistance and serogroups of *Salmonella* among chicken meat specimens in Tehran, Iran. *Daneshvar Med*. 2020;27(4):1-10.

doi: 10.1007/s11032-023-01398-w

38. Yang R, Fu D, Liao A. The role of complement in tumor immune tolerance and drug resistance: A double-edged sword. *Front Immunol*. 2025;16:1529184.

doi: 10.3389/fimmu.2025.1529184

39. Chow A, Perica K, Klebanoff CA, Wolchok JD. Clinical implications of T cell exhaustion for cancer immunotherapy. *Nat Rev Clin Oncol*. 2022;19(12):775-790.

doi: 10.1038/s41571-022-00689-z

40. Zhang G, Wang J, Zhao Z, *et al*. Regulated necrosis, a proinflammatory cell death, potentially counteracts pathogenic infections. *Cell Death Dis*. 2022;13(7):637.

doi: 10.1038/s41419-022-05066-3

41. Gao D, Gao W, Zhai Z, Zhu W. Immune mechanisms and novel therapies for idiopathic pulmonary fibrosis. *Pharm Sci Adv*. 2024;2:100030.

doi: 10.1016/j.pscia.2023.100030

42. Ahmed R, Zaman T, Chowdhury F, *et al*. Single-cell RNA sequencing with spatial transcriptomics of cancer tissues. *Int J Mol Sci*. 2022;23(6):3042.

doi: 10.3390/ijms23063042

43. Pelaia C, Tinello C, Vatrella A, De Sarro G, Pelaia G. Lung under attack by COVID-19-induced cytokine storm: Pathogenic mechanisms and therapeutic implications. *Ther Adv Respir Dis*. 2020;14:1-9.

doi: 10.1177/1753466620933508

44. Hsu RJ, Yu WC, Peng GR, *et al*. The role of cytokines and chemokines in severe acute respiratory syndrome coronavirus 2 infections. *Front Immunol*. 2022;13:832394.

doi: 10.3389/fimmu.2022.832394

45. Stegeman SK, Kourko O, Amsden H, *et al*. RNA viruses, toll-like receptors, and cytokines: The perfect storm? *J Innate Immun*. 2025;17:126-153.

doi: 10.1159/000543608

46. Lu T, Yan H, Luo J, Wang S, Xia Y, Xu X. Elevated thrombosis-related biomarkers as predictors of disease severity and mortality in patients with severe fever with thrombocytopenia syndrome. *BMC Infect Dis*. 2025;25:235.

doi: 10.1186/s12879-025-10574-6

47. Krishnamachary B, Cook C, Kumar A, Spikes L, Chalise P,

Dhillon NK. Extracellular vesicletors of disease severity and mortality in patients with severe fever with thrombocytopenia syndrome. *J Extracell Vesicles*. 2021;10(9):e12117.

doi: 10.1002/jev2.12117

48. Ramaswamy A, Brodsky NN, Sumida TS, *et al*. Immune dysregulation and autoreactivity correlate with disease severity in SARS-CoV-2-associated multisystem inflammatory syndrome in children. *Immunity*. 2021;54(5):1083-1095.e7.

doi: 10.1016/j.immuni.2021.04.003

49. Mohite P, Yadav V, Pandhare R, *et al*. Revolutionizing cancer treatment: Unleashing the power of viral vaccines, monoclonal antibodies, and proteolysis-targeting chimeras in the new era of immunotherapy. *ACS Omega*. 2024;9(7):7277-7295.

doi: 10.1021/acsomega.3c06501

50. Paudyal B, McNee A, Rijal P, *et al*. Low dose pig anti-influenza virus monoclonal antibodies reduce lung pathology but do not prevent virus shedding. *Front Immunol*. 2021;12:790918.

doi: 10.3389/fimmu.2021.790918

51. Li N, Parkes JE, Spathis R, *et al*. The effect of immunomodulatory treatments on anti-dystrophin immune response after AAV gene therapy in dystrophin deficient mdx mice. *J Neuromuscul Dis*. 2021;8(s2):S325-S340.

doi: 10.3233/JND-210706

52. Xu C, Hao M, Zai X, *et al*. A new perspective on gut-lung axis affected through resident microbiome and their implications on immune response in respiratory diseases. *Arch Microbiol*. 2024;206(3):107.

doi: 10.1007/s00203-024-03843-6

53. Song Z, Meng Y, Fricker M, Tian H, Tan Y, Qin L. The role of gut-lung axis in COPD: Pathogenesis, immune response, and prospective treatment. *Heliyon*. 2024;10(9):e30612.

doi: 10.1016/j.heliyon.2024.e3061

54. De Oliveira GLV, Oliveira CNS, Pinzan CF, De Salis LVV, Cardoso CRB. Microbiota modulation of the gut-lung axis in COVID-19. *Front Immunol*. 2021;12:635471.

doi: 10.3389/fimmu.2021.635471

55. Loera-Muro A, Guerrero-Barrera A, Tremblay DNY, Hathroubi S, Angulo C. Bacterial biofilm-derived antigens: A new strategy for vaccine development against infectious diseases. *Expert Rev Vaccines*. 2021;20(4):385-396.

doi: 10.1080/14760584.2021.1892492

56. Worley MJ. Immune evasion and persistence in enteric bacterial pathogens. *Gut Microbes*. 2023;15(1):2163839.

doi: 10.1080/19490976.2022.2163839

57. Johnston SL, Goldblatt DL, Evans SE, Tuvim MJ, Dickey BF. Airway epithelial innate immunity. *Front Physiol*. 2021;12:749077.

doi: 10.3389/fphys.2021.749077

58. Paradis T, Bègue H, Basmaciyan L, Dalle F, Bon F. Tight junctions as a key for pathogens invasion in intestinal epithelial cells. *Int J Mol Sci*. 2021;22(5):2506.

doi: 10.3390/ijms22052506

59. Ishihara N, Tanaka M, Namba K, *et al*. Long-term exposure to urban particulate matter exacerbates mortality after ischemic stroke in mice. *J Toxicol Sci*. 2025;50(3):147-159.

doi: 10.2131/jts.50.147

60. Hu D, Jia X, Cui L, *et al*. Exposure to fine particulate matter promotes platelet activation and thrombosis via obesity-related inflammation. *J Hazard Mater*. 2021;413:125341.

doi: 10.1016/j.jhazmat.2021.125341

61. Koul A, Bawa RK, Kumar Y. Artificial intelligence techniques to predict the airway disorders illness: A systematic review. *Arch Computat Methods Eng*. 2023;30(2):831-864.

doi: 10.1007/s11831-022-09818-4

62. Yan C, Wang L, Lin J, *et al*. A fully automatic artificial intelligence-based CT image analysis system for accurate detection, diagnosis, and quantitative severity evaluation of pulmonary tuberculosis. *Eur Radiol*. 2022;32:2188-2199.

doi: 10.1007/s00330-021-08365-z

63. Mettelman RC, Allen EK, Thomas PG. Mucosal immune responses to infection and vaccination in the respiratory tract. *Immunity*. 2022;55(5):749-780.

doi: 10.1016/j.immuni.2022.04.013

64. Fraser R, Orta-Resendiz A, Mazein A, Dockrell DH. Upper respiratory tract mucosal immunity for SARS-CoV-2 vaccines. *Trends Mol Med*. 2023;29(4):255-267.

doi: 10.1016/j.molmed.2023.01.003

65. Jung M, Dourado M, Maksymetz J, *et al*. Cross-species transcriptomic atlas of dorsal root ganglia reveals species-specific programs for sensory function. *Nat Commun*. 2023;14(1):366.

doi: 10.1038/s41467-023-36014-0

66. Mogilenko DA, Shpynov O, Andhey PS, *et al*. Comprehensive profiling of an aging immune system reveals clonal GZMK+ CD8+ T cells as conserved hallmark of inflammaging. *Immunity*. 2021;54(1):99-115.e12.

doi: 10.1016/j.immuni.2020.11.005

ACCSCIENCE PUBLISHING

Microbes & Immunity

REVIEW ARTICLE

Management of obesity-related diseases through the gut microbiome

Amar P. Garg[1]*, Rashmi Goley[2], and Anchal Bamal[2]

[1]Research and Development Cell, Swami Vivekanand Subharti University, Meerut, Uttar Pradesh, India

[2]Department of Biotechnology, School of Biotechnology and Life Sciences, Shobhit Institute of Engineering and Technology, Meerut, Uttar Pradesh, India

(This article belongs to the *Special Issue: Obesity and Human Microbiome*)

Abstract

Obesity is a multifactorial disease that results in the excessive accumulation of adipose tissue in humans. It poses a major global public health crisis, as it increases the risk of several pathologies. The gut microbiome is considered a potential modulator in the development of obesity, alongside environmental factors, lifestyle, and genetic makeup. The qualitative and quantitative composition of the gut microbiome is greatly influenced by the type, quality, and quantity of diet. We have found that a vegetarian diet facilitates the growth and development of beneficial bacteria in the gut. This review discusses the relationship between the human gut microbiome, energy balance, and various obesity-related diseases. The metabolic products of the gut microbiome (such as short-chain fatty acids and secondary bile acids) and their effects on the gut microbiome, intestinal barrier function, and immune homeostasis are explored in the context of obesity. However, the specific roles of individual gut microbiota species and their interactions with the gut environment, host genetics, and medications (including antibiotics) require further investigation. We also discuss the potential of the gut microbiome in managing obesity-related diseases through dietary modifications, with reference to dietary fiber, resistant starch, gluten, high-fat diets, and proteins and carbohydrates from both vegetarian and animal sources.

Keywords: Obesity; Gut microbiome; Metabolism; Homeostasis; Diet and microbiota; Fecal microbiota; Probiotics

***Corresponding author:**
Amar P. Garg
(director_research@subharti.org)

Citation: Garg AP, Goley R, Bamal A. Management of obesity-related diseases through the gut microbiome. *Microbes & Immunity*. 2025;2(4):40-60.
doi: 10.36922/MI025160036

Received: April 18, 2025

1st revised: May 13, 2025

2nd revised: May 29, 2025

Accepted: June 12, 2025

Published online: July 1, 2025

1. Introduction

Obesity has emerged as a major global public health challenge, with prevalence rates rising rapidly across both developed and developing nations.[1] At present, over 600 million adults and 107 million children worldwide are affected by obesity, and if trends continue, it is estimated that 18% of men and 21% of women will be obese by 2025, with 20% of the global adult population projected to be obese by 2030.[2,3] Obesity is strongly associated with numerous comorbidities, including type 2 diabetes, cardiovascular disease, and various cancers, contributing significantly to both economic and social burdens.[4] Conventionally, obesity has been recognized as an interconnected condition influenced by genetic, behavioral, socioeconomic, and environmental factors. In recent

years, however, the significance of the gut microbiota in obesity has garnered increasing attention, revealing its profound impact on host energy storage and metabolic processes.[5,6] Pioneering research has demonstrated that altered gut bacterial composition, specifically, a decrease in the abundance of *Bacteroidetes* and an increase in *Firmicutes*, correlates with obesity.[7] Moreover, studies involving the transplantation of microbiota from obese and lean individuals into germ-free mice have shown that microbiota from obese individuals promote greater fat accumulation, highlighting the potential role of gut microbiota in the development of obesity.[3,7] This observation, combined with emerging theories, such as the hypothesis of metaflammation, suggests that genetic adaptations that evolved to combat infectious diseases may inadvertently contribute to the modern obesity epidemic.[8] Understanding the evolutionary origins and the complex interplay between genetics, the microbiome, and environmental factors is essential for addressing this global health crisis.[9]

Obesity is also strongly linked to an elevated risk of a range of diseases, including cardiovascular complications, diabetes, respiratory issues, and certain cancers. While the causes of obesity are multifactorial and not yet fully understood, contributing factors include unhealthy eating habits, sedentary lifestyles, environmental influences, and genetic predisposition. One of the most intriguing environmental factors linked to obesity is the gut microbiota, which has been shown to play a pivotal purpose in the development and progression of obesity and other metabolic disorders, such as diabetes and non-alcoholic fatty liver disease (NAFLD). The gut microbiota, a complex ecosystem of microorganisms inhabiting the human gastrointestinal tract, includes bacteria, fungi, viruses, archaea, and protists.[3] With a total weight of about 1 – 2 kg and containing more than 100 times the number of genes in the human genome, the gut microbiota contributes to various essential physiological functions. These include digesting and absorbing nutrients, defending against harmful microbes, and maintaining immune system balance. However, when the microbiota becomes dysbiotic, meaning it falls out of balance, it can contribute to a range of diseases, including obesity. Gut dysbiosis is thought to influence obesity through multiple mechanisms, including disruption of energy homeostasis, altered lipid synthesis and storage, modulation of central appetite and feeding behaviors, and promotion of chronic low-grade inflammation.[10] While several effective interventions for obesity exist, such as healthy lifestyle changes, weight-reducing drugs, and bariatric surgery, maintaining long-term weight loss remains a challenge. In addition, side effects associated with drugs and surgeries can further complicate treatment. Given the prominent role of the gut microbiota in obesity progression, it presents a promising target for novel therapeutic strategies. Future research should focus on better understanding the relationship between obesity and gut microbiota, uncovering the mechanisms by which the microbiota influences obesity, and evaluating the safety and efficacy of microbiota-targeted therapies as potential treatments for obesity.[11]

2. Human gut microbiome and its relation to obesity

The gut microbiota plays a central role in obesity progression, affecting microbial diversity, metabolic pathways, inflammation, immunity, and hormone regulation. Dysbiosis in obesity results in imbalanced bacterial populations, increased inflammatory markers, reduced gut barrier integrity, and alterations in metabolic functions. The gut microbiome influences energy homeostasis, shaping fat accumulation, insulin resistance, and immune responses. While beneficial microbes offer anti-inflammatory and metabolically protective effects, harmful bacteria and microbial-derived metabolites contribute to chronic inflammation and metabolic disorders. Understanding these intricate mechanisms may pave the way for microbiota-targeted interventions, offering potential therapeutic strategies to improve metabolic health and combat obesity.[12] In obese individuals, the gut microbiome is often characterized by intestinal dysbiosis, involving reduced microbial diversity, imbalanced bacterial composition, and altered metabolic functions. This dysbiosis leads to a loss of beneficial commensal bacteria, an overgrowth of pathogenic or conditionally pathogenic microbes, and an overall decline in microbial gene richness. Several studies have reported reduced gut microbiome diversity in obese populations, suggesting that a less diverse microbiota may contribute to metabolic disturbances and obesity development.

A widely observed trend in obesity is an increased *Firmicutes*/*Bacteroidetes* ratio, with *Firmicutes* being more abundant and *Bacteroidetes* being significantly reduced. Some studies have confirmed this pattern across various populations, indicating a correlation between gut microbiota composition and obesity.[13] However, newer research suggests that relying solely on phylum-level classification may be oversimplified, as differences within bacterial genera and species reveal more nuanced microbiome changes in obesity. For instance, while certain *Firmicutes* species, such as *Clostridium, Lactobacillus,* and *Ruminococcus* are found in greater abundance in obese individuals, the levels of *Faecalibacterium prausnitzii* (also within the *Firmicutes* phylum) decrease. This species is

associated with anti-inflammatory effects and metabolic health. Similarly, studies across different populations have noted variability in microbiota composition, suggesting that bacterial groups beyond the *Firmicutes/Bacteroidetes* dichotomy influence obesity risk. Beyond compositional changes, gut microbiota-derived metabolites play a major role in obesity. Short-chain fatty acids (SCFAs), including propionate, acetate, and butyrate, are produced through microbial fermentation of dietary fiber. These compounds have dual effects on metabolism – they can increase satiety, enhance energy expenditure, and reduce fat accumulation; however, excessive SCFA production may also promote lipid synthesis, potentially contributing to obesity. In addition, secondary bile acids, another group of microbial metabolites, help regulate lipid metabolism and gut hormone secretion, reinforcing their influence on energy balance. A key feature of obesity is chronic low-grade inflammation, which is largely influenced by the gut microbiota. Lipopolysaccharides (LPS), derived from Gram-negative bacteria, such as *Bacteroidetes*, are major triggers for inflammation. These endotoxins compromise intestinal barrier integrity, allowing microbial byproducts to enter systemic circulation, which activates immune responses and disrupts metabolic disruption. Elevated plasma LPS levels have been correlated with increased fat deposition, insulin resistance, and heightened inflammation**,** emphasizing the gut microbiota's role in obesity-related inflammatory responses.[14] Conversely, certain Gram-positive bacteria, such as *Lactobacillus* and *Bifidobacterium*, help strengthen gut barrier function and reduce inflammation, highlighting the potential protective role of beneficial microbiota.

The gut microbiota also interacts with intestinal immunity, influencing both innate and adaptive immune responses. Immune cells, including goblet cells, Paneth cells, and intestinal epithelial cells, maintain gut homeostasis, with antimicrobial peptides (AMPs) playing a crucial role in pathogen defense. *Akkermansia muciniphila*, a beneficial gut bacterium, has been found to restore AMPs diminished by obesogenic diets, thereby reinforcing gut protection. In addition, Toll-like receptors (TLRs) and nucleotide-binding oligomerization domain-like receptors recognize bacterial components, such as LPS, flagellin, and peptidoglycan**,** triggering immune activation. In adaptive immunity, the intestinal microbiota influences T helper 17 cells, which release interleukin (IL) 17 and IL-22, cytokines that enhance AMP production and gut barrier integrity. Reduced immunoglobulin A (IgA) production observed in obesity has been linked to impaired immune defenses, increasing susceptibility to metabolic disturbances. The gut microbiota also modulates host immunity through microbial metabolites, including imidazole propionate and tryptophan derivatives, which influence insulin resistance and metabolic syndrome. Disrupted aryl hydrocarbon receptor (AhR) signaling, caused by altered tryptophan metabolism, contributes to obesity-related inflammation. Reduced AhR ligand production diminishes IL-22 synthesis, exacerbating gut permeability and metabolic dysfunction. Meanwhile, microbial-derived components, such as flagellin and muramyl dipeptide show potential benefits in alleviating diet-induced inflammation and insulin resistance.

3. Metabolite production by gut microbiota

The gut microbiota secretes a variety of metabolites that influence host metabolism, immune responses, and overall health. In obesity and metabolic disorders, dysbiosis disrupts the balance of microbial metabolites, leading to increased adiposity, inflammation, oxidative stress, and metabolic dysfunction. These metabolites originate from both dietary sources and endogenous compounds and include indole derivatives, SCFAs, polyamines (putrescine, spermidine, and spermine), secondary bile acids, and adenosine triphosphate (ATP). SCFAs**,** produced by bacterial fermentation of dietary fiber, play crucial roles in immune signaling by activating receptors on neutrophils, macrophages, and dendritic cells (DCs). This activation promotes the production of IL-18, IL-22, IgA, and the satiety hormone glucagon-like peptide-1 (GLP-1). SCFAs also influence intestinal gluconeogenesis through gut–brain signaling pathways and inhibit histone deacetylase activity through G protein-coupled receptor (GPCR) activation, thereby impacting metabolic regulation. Tryptophan metabolism occurs through multiple pathways, including the kynurenine and serotonin pathways.[15] Its metabolism products affect intestinal motility and insulin regulation, with indole derivatives modulating gut hormone release (e.g., GLP-1), appetite suppression, and gastric emptying. Indole compounds also regulate immune responses by activating the AhR, thereby promoting IL-22 production to maintain mucosal immunity and gut barrier integrity.

4. Bacterial metabolite production from dietary components

4.1. SCFAs

The gut microbiota plays a crucial role in energy production and metabolism by fermenting non-digestible carbohydrates in the cecum, generating SCFAs, amino acids, and vitamins. Among SCFAs, propionate, acetate, and butyrate are the most abundant, with *Bacteroides thetaiotaomicron* primarily producing acetate and *F. prausnitzii* generating butyrate. SCFAs influence metabolic pathways by activating transcription factors,

such as carbohydrate-responsive element-binding protein (CHREBP) and sterol regulatory binding protein 1 (SREBP1), promoting lipogenesis and triglyceride storage. They also inhibit fasting-induced adipocyte factor, leading to triglyceride accumulation in adipocytes. In addition, SCFAs bind to GPCRs, playing roles in lipid, glucose, and cholesterol metabolism, regulation of gut inflammation, and neurogenesis. Early studies show that SCFAs modulate adiposity and glucose tolerance by stimulating GLP-1 secretion through G protein-coupled receptor (GPR) 41 and GPR43 receptors, with GPR43 capable of dual signaling through different pathways.

Butyric acid contributes to immune homeostasis by stimulating IL-18 secretion and suppressing inflammation through GPR109A activation and histone deacetylase inhibition. Moreover, gut microbiota-derived propionate and butyrate activate intestinal gluconeogenesis through free fatty acid receptor 3 or a gut–brain neural circuit, influencing glucose metabolism. While microbiota-derived acetate serves as a pre-cursor for fatty acids and *de novo* lipogenesis in the liver, excessive acetate generation has been linked to obesity and NAFLD. Microbiota–immune system interactions further regulate metabolic homeostasis. Studies indicate that fiber-derived SCFA binding to free fatty acid receptors suppresses high-fat diet (HFD)-induced metabolic syndrome by restoring IL-22-mediated enterocyte function. In addition, *Lactobacillus johnsonii Q1–7* deficiency contributes to reduced food intake and body mass through mammalian target of rapamycin complex 1 signaling, affecting IgA production. In clinical cases, *Bacteroidetes* abundance increases while SCFA-producing *Firmicutes* decline in NAFLD patients, further emphasizing the microbiota's role in metabolic disorders. Understanding these microbial interactions highlights their significance in metabolism, immune regulation, and obesity, paving the way for microbiota-targeted therapies to enhance metabolic health.[14]

4.2. Indole derivatives

Indole and its derivatives produced by commensal bacteria, such as *Lactobacillus*, *Escherichia coli*, and *Bacteroides*, play a significant role in bacterial communication and host interactions. These metabolites are generated from dietary tryptophan through the action of tryptophanase and can reach high concentrations in the digestive tract and systemic circulation.[15,16] Indole is metabolized in the liver by cytochrome P450 2E1 into 3-indoxyl sulfate (3-IS), with low urinary levels of 3-IS indicating gut dysbiosis. Indole derivatives – including indole-3-lactic acid, indole-3-aldehyde, indole-3-acetic acid, and indole-3-propionic acid – act as ligands for AhRs, which regulate immune responses and inflammation by modulating IL-22 production and lymphoid function in the intestine. Studies suggest that reduced tryptophan metabolism into AhR agonists is a hallmark of metabolic syndrome, contributing to insulin resistance, liver steatosis, and increased intestinal permeability due to elevated LPS translocation.[17] Therapeutic approaches include administration of AhR agonists or probiotic supplementation with *Lactobacillus reuteri* to improve intestinal barrier function and increase GLP-1 secretion, thereby reversing metabolic disorders, such as low-grade inflammation and intestinal barrier dysfunction. Indole administration has been found to prevent LPS-induced abnormalities in cholesterol metabolism and liver inflammation. Research also shows that inhibiting indoleamine 2,3-dioxygenase (IDO) – a key enzyme in the kynurenine pathway – can help mitigate HFD-induced obesity and associated metabolic alterations. IDO overactivation leads to increased concentrations of inflammatory metabolites, such as xanthurenic acid, kynurenic acid, and quinolinic acid, while reducing plasma tryptophan levels, thereby contributing to metabolic dysfunction. Serotonin, another tryptophan-derived metabolite, plays a role in obesity regulation by modulating appetite and satiety. However, excessive serotonin levels suppress brown adipose tissue thermogenesis, resulting in fat accumulation. Elevated levels of 5-hydroxyindole-3-acetic acid, the end-product of serotonin metabolism, have been observed in individuals with metabolic disorders compared to healthy controls.[18] This highlights the importance of gut microbiota-derived indole metabolites in regulating inflammation, metabolic health, and obesity, suggesting potential therapeutic applications through microbiota-based interventions.

5. Metabolite production by the host and biochemical alteration by gut bacteria

5.1. Secondary bile acids

Secondary bile acids, metabolized by gut microbiota, play a pivotal role in fat digestion, lipid metabolism, glucose regulation, and inflammation. They shape the bile acid pool and influence bile acid-activated receptors, including farnesoid X receptors (FXRs), pregnane X receptors, and GPCRs, which regulate various metabolic processes.[19] Dysregulation of these pathways can contribute to metabolic disorders. Among the major secondary bile acids, deoxycholic acid and lithocholic acid support energy homeostasis by activating Takeda G protein-coupled receptor 5, thereby influencing metabolic functions. Clinical studies suggest that bile acid composition is modulated by diet and medication. For instance, the anti-diabetic drug acarbose alters bile acid profiles, while HFDs elevate overall bile acid levels and shift the balance

between primary and secondary bile acids.[20,21] Research indicates that gut microbiome deficiency can modulate cytochrome P450 family 7 subfamily A member 1 expression, alleviating HFD-induced metabolic syndrome, and thus represents a potential therapeutic target for obesity.[16] Experimental treatments further demonstrate the significance of bile acid modulation in metabolic health. In obese mice, colesevelam (a bile acid sequestrant) enhanced GLP-1 secretion and improved glucose levels through FXR-dependent mechanisms, suggesting potential for type 2 diabetes treatment. In addition, antibiotic interventions have been shown to suppress FXR signaling, improving glucose tolerance and reducing hepatic steatosis. Dietary interventions also influence bile acid metabolism. A high-protein diet increased the abundance of *Eubacterium* species, which metabolize bile acids through 7α-dehydroxylation, resulting in elevated deoxycholic acid and lithocholic acid levels. Specific dietary modifications appear beneficial for metabolic regulation and obesity prevention. Methionine restriction stabilizes lipid profiles in HFD-induced metabolic disorders, while extruded legumes and cereals enhance bile acid excretion, promoting lipid homeostasis. Notably, common buckwheat supplementation has shown promise in preventing NAFLD and dyslipidemia by regulating primary bile acid biosynthesis and modulating gut microbiome composition. Overall, secondary bile acids play an integral role in metabolic regulation, with potential therapeutic applications through dietary and pharmacological interventions.[22]

5.2. Taurine, ATP, and polysaccharide A (PSA)

Several key metabolites, including taurine, ATP, and PSA, play pivotal roles in immune regulation within the gut. ATP, secreted by certain intestinal bacteria, interacts with P2X and P2Y receptors, amplifying T cell receptor signaling, promoting inflammatory responses in macrophages and DCs, and influencing immune activation. It binds to seven P2X receptors (P2X1R–P2X7R) and eight GPCRs (P2Y1R–P2Y14R), leading to ion exchange and cellular immune modulation. Taurine, an essential amino acid found abundantly in immune cells, supports intestinal microbial metabolism, enhances T cell proliferation, stimulates SCFA production, and reduces LPS levels, thereby contributing to gut homeostasis. PSA, produced by gut bacteria, plays a protective role by activating TLR2 on DCs, stimulating IL-10 secretion by T cells, and directly binding to TLR2 on forkhead box P3-positive regulatory T cells, further increasing IL-10 production to regulate inflammation.[23] PSA has also been shown to counteract gut inflammation by suppressing mucosal effector T cell (T helper 17 cell) activity, thereby mitigating conditions, such as colitis. Together, these metabolites help maintain immune balance, gut health, and metabolic stability, making them essential for overall wellbeing.[24]

6. Mechanisms of impact of gut microbiota on obesity

The human gut microbiome, composed of trillions of bacteria, plays a crucial role in digestion, immune function, and brain activity. Recent studies challenge the traditional belief that obesity results solely from excessive calorie intake, highlighting the significant role of the gut microbiota in metabolic disorders that lead to weight gain. Certain bacterial species, such as *Firmicutes*, enhance energy extraction from food by fermenting complex carbohydrates into SCFAs, which regulate metabolism, satiety, and energy expenditure through interactions with gut hormones. Microbial metabolites, including bile acids and SCFAs, influence lipid absorption, glucose balance, and thermogenesis. Disruptions in the gut microbiota can impair intestinal barrier integrity, allowing harmful LPS to enter circulation and triggering inflammation and metabolic dysfunction.[9] Furthermore, the gut–brain axis plays a vital role in appetite regulation, with gut bacteria producing neurotransmitters, such as gamma-aminobutyric acid (GABA) and serotonin, which influence feeding behavior and mood. Dietary choices significantly impact the gut microbiota; diets rich in saturated fats and low in fiber promote pro-inflammatory bacteria, contributing to insulin resistance, fat storage, and adipose tissue inflammation – key features of obesity. Understanding these mechanisms has opened new possibilities for microbiota-based interventions to improve metabolic health and address obesity.[25]

7. Energy homeostasis disruption

The fate of energy extracted by the gut microbiota from dietary components that escape digestion and absorption in the small intestine represents a fundamental bioenergetic principle linking diet, microbial activity, and the energy ultimately available to the human host. This energy, derived from microbial fermentation, is predominantly generated from carbohydrates in the host's diet and, to a lesser extent, from proteins. Approximately 90% of the caloric intake from a meal is absorbed in the small intestine, with absorption rates ranging between 83% and 97%.[26,27] Upon reaching the colon, undigested dietary components undergo microbial fermentation, producing energy that is either absorbed by the host, utilized for microbial biomass growth, or excreted in feces. The energy absorbed by the host is typically estimated as a percentage of consumed energy, after deducting energy lost in a feces that is not fully utilized by either the host or the microbiota; this is referred to as metabolizable energy.[28]

In the context of precision nutrition, fecal energy loss varies among individuals (ranging from 2% to 16%) due to methodological and biological differences.[26,27]

7.1. Digestible energy uptake

Research suggests that the gut microbiota in obese individuals enhances energy extraction from food compared to non-obese controls. This occurs through increased secretion of nutrient transporters and fermentation of enzymes. Specifically, an elevation in *Clostridium ramosum* (from the *Firmicutes* phylum) has been associated with upregulated expression of GLUT2 (a glucose transporter) and CD36 (a fatty acid translocase), thereby improving energy absorption. In addition, a higher *Firmicutes*/*Bacteroidetes* ratio in obese individuals correlates with increased digestion of polysaccharides, leading to greater production of monosaccharides and SCFAs, such as acetate and butyrate. SCFAs contribute significantly to the body's energy supply – providing around 5 – 15% of total caloric intake and fulfilling 60 – 70% of the energy requirements of colonic epithelial cells. Furthermore, interspecies hydrogen (H_2) transfer between bacteria and archaea enhances energy uptake in obesity.[29] The coexistence of H_2-utilizing methanogenic archaea alongside H_2-producing bacteria facilitates the breakdown of polysaccharides into SCFAs by relieving thermodynamic constraints during fermentation processes.

7.2. Energy expenditure

The absorption of food energy in the small intestine determines the fraction that can reach the colon. The energy that arrives in the colon then becomes available to the gut microbiota for fermentation. The ultimate fate of the energy extracted by gut microorganisms remains unclear, yet it is a crucial component of overall energy balance.[26,27] A compelling set of hypotheses has emerged regarding the quantitative exchange of energy between humans and gut microbes. It has been established that the negative energy balance achieved through the alteration of the gut microbiota through a high-fiber, whole-food diet is partially due to the diversion of energy from microbial activity in the colon toward microbial biomass proliferation rather than host energy reserves.[26] This is likely a significant quantitative factor in energy balance, as mathematical modeling and previous studies[30,31] indicate that 25 – 50% of fecal energy originates from microbial biomass. The correlation observed between microbial biomass and changes in energy absorption on a high-fiber, whole-food diet suggests that microbial growth serves as a mechanism to modify energy balance through precision nutrition.[26] Further research is needed to quantify the bidirectional energy transfer between microorganisms and the host and to identify the biological, physiological, and sociodemographic factors that contribute to interindividual variability.[32]

7.2.1. Energy regulation

Multiple bacterial taxa have been associated with energy absorption or obesity.[33] However, the mechanisms underlying these associations in humans remain unclear, due to the reliance on relative abundance metrics of microbial composition and the lack of investigation into community-wide functional interactions. *A. muciniphila* is a widely studied species inversely correlated with obesity in various model systems.[34] A distinctive feature of *A. muciniphilla*'s action is that a surface protein (a postbiotic) mediates several of its metabolic effects. Its protective mechanisms against obesity involve enhanced energy expenditure and increased fecal energy loss.[35] *B. thetaiotaomicron* has shown decreased relative abundance in individuals with obesity. Treatment of mice with live *B. thetaiotaomicron*, but not heat-killed variants, has been shown to reduce fat accumulation and increase lean mass.[36] *Methanobrevibacter smithii*, the predominant methanogen in the gastrointestinal tract, is thought to contribute to energy extraction by interacting with SCFA-producing bacteria.[37] Activation of the Takeda G protein-coupled receptor 5 in brown adipose tissue enhances mitochondrial biogenesis and thermogenesis by increasing thyroid hormone activation. Similarly, activation of *FXR* in the intestine stimulates fibroblast growth factor 15/19 secretion, which alters bile acid composition and promotes fat burning. However, gut dysbiosis associated with obesity reduces beneficial bile acid levels, impairing these energy-expending processes.[7]

7.3. SCFAs and metabolic impact

Fecal and circulatory metabolites can indicate host–diet–microbiome interactions that influence energy balance.[38] It is improbable that metabolites derived from microbes significantly influence energy absorption directly, as the energy content lost in feces is anticipated to be minimal.[39] Nonetheless, there may be indirect involvement in energy balance associated with signaling processes or due to these metabolites serving as indicators of fermentation. The signaling roles of SCFAs are well-documented in pre-clinical models and are thought to influence adipose tissue through enhanced expression and signaling from G-protein-coupled receptors 41 and 43.[40] SCFAs may also induce a transition from lipogenesis to fat oxidation through peroxisome proliferator-activated receptor gamma-mediated signaling.[40] Nonetheless, there is debate as to whether individuals with obesity generate a greater or lesser quantity of SCFAs, rendering

the mechanisms in humans ambiguous.[41] The most compelling evidence regarding the significance of SCFAs in human energy balance comes from a study conducted by Canfora *et al.*[42] They administered colonic infusions of SCFA combinations in men with obesity (n = 12) at concentrations and ratios similar to those achieved with a high-fiber diet. The study revealed enhancements in fat oxidation, energy expenditure, and peptide YY, accompanied by elevated lipolysis due to SCFA colonic infusion.[42] While fermentation products, such as SCFAs serve as readily absorbable energy sources for both bacteria and the host, the quantitative effect on energy balance remains uncertain and likely varies among individuals.[42] SCFAs (propionate, acetate, butyrate) are produced through bacterial fermentation of dietary fiber. Increased SCFA levels in obese individuals are linked to a higher abundance of *Firmicutes* and H_2-utilizing methanogenic archaea. SCFAs can influence energy expenditure in conflicting ways – some studies suggest they suppress fasting-induced adipose factor, reducing fat oxidation. Conversely, butyrate can enhance mitochondrial activity, stimulate thermogenesis, and increase fatty acid oxidation in brown adipose tissue.[43]

7.4. Overall contribution to obesity

The gut microbiota contributes to obesity progression through both elevated digestible energy intake (via enhanced nutrient absorption and fermentation) and reduced energy expenditure (due to bile acid depletion and uncertain SCFA effects). While SCFAs show potential for promoting fat burning, their role remains controversial and requires further research.[44]

7.5. Lipid synthesis and storage

Altered gut microbiota in obese individuals influences lipid synthesis and storage through several mechanisms.

7.6. Bile acid reduction and lipogenesis

A decrease in *Bacteroides* and *Lactobacillus* leads to lower bile acid levels, weakening FXR activation in the liver. This results in increased SREBP1c expression, promoting hepatic *de novo* lipogenesis. Similarly, reduced fibroblast growth factor 19 signaling further enhances lipogenesis.[45]

7.7. Digestible energy absorption and lipid synthesis

A key physiological element that may influence variations in energy absorption is intestinal transit time. Colonic transit time exhibits significant variability across individuals and influences gut microbial metabolism, as it determines the duration during which colonic bacteria can ferment food substrates.[46] The interplay between gut bacteria and colonic transit may be significant for human energy absorption. A mathematical model indicated that, although intestinal transit time was not directly correlated with metabolizable energy, it was essential for explaining interindividual variability in metabolizable energy.[26,39] Research indicates that colonic transit time correlates with fecal energy losses, with individuals exhibiting faster transit times experiencing reduced fecal energy losses.[47] A study comparing diets rich versus poor in microbiota-accessible carbohydrates found no difference in colonic transit time by diet; however, transit time accounted for 5% of the diversity in the gut microbiome.[48] Additional gastrointestinal physiological traits may influence energy absorption. Gastric emptying regulates the rate at which nutrients are delivered to the small and large intestines, thereby influencing satiety and body weight.[49] Consequently, it may affect the absorption of microbially derived energetic substrates. Nonetheless, the role of gastric emptying in energy absorption has not been established in either rats or humans.[26,49] An augmented intestinal mucus layer may result in diminished energy absorption by the host.[50] This corresponds with findings that Western diets are linked to increased energy absorption and a microbial community more inclined to utilize the mucus layer as an energy source. A diminished mucus layer correlates with increased intestinal permeability, which may be the mechanism enhancing the absorption of energetic substrates.[26,32] Higher GLUT2 expression elevates serum glucose levels, stimulating key transcription factors (SREBP1, ChREBP) that drive lipid accumulation. Increased SCFAs, especially acetate, provide pre-cursors for fatty acid and cholesterol synthesis, contributing to lipid buildup.

7.8. Inflammation and lipid storage

Elevated levels of LPS in obese individuals induce metabolic endotoxemia, leading to chronic inflammation. This inflammatory state increases the expression of pro-inflammatory cytokines, such as IL-6 and tumor necrosis factor-alpha (TNF-α), thereby disrupting insulin signaling and contributing to insulin resistance and excess fat storage. In addition, LPS promotes adipocyte pre-cursor proliferation, further amplifying fat accumulation.[51]

7.9. Gut microbiota and fat regulation

The gut flora may also influence bodily energy reserves through alterations in energy expenditure. To date, human studies have not demonstrated a correlation between the gut microbiome and energy expenditure.[26,32] The extent of anaerobic microbial thermogenic activity in humans remains unknown. Microbial thermogenesis cannot be quantified using the indirect calorimetry techniques currently employed to assess human energy

expenditure. Innovative approaches must be developed to determine whether gut bacteria influence thermogenesis in humans.[52] Dysbiosis suppresses neuropeptide-related genes involved in energy homeostasis, including *GCG* (encoding preproglucagon) and *BDNF* (encoding brain-derived neurotrophic factor), and induces leptin resistance through suppressor of cytokine signaling-3, thereby exacerbating obesity. The reduction of *L. paracasei* removes its inhibition of lipoprotein lipase, allowing more triglycerides to be absorbed by adipocytes, thereby facilitating lipid storage (Figure 1).

8. Feeding behavior and central appetite

8.1. The gut–brain axis

The gut–brain axis is a complex, bidirectional communication system that transmits nutritional and metabolic information between the gut and the central neurological system through various pathways, including the vagus nerve, the neural system, and the gut endocrine system. Recent research has highlighted the significant role of the gut microbiota in this interaction, leading to the concept of the microbiota–gut–brain axis. Studies suggest that this correlation plays an important in both gastrointestinal and neurological conditions, such as Parkinson's disease and irritable bowel syndrome. Given that the gut–brain axis plays a major role in regulating appetite and feeding behavior, disruptions in the gut microbiota (gut dysbiosis) in obese individuals may impact food intake and contribute to obesity progression. This underscores the importance of gut microbiota in both metabolic and neurological health.[53]

8.2. The functions of gut microbiota: Feeding behavior and regulation of central appetite

The gut microbiota plays a critical part in regulating central appetite and feeding behavior through multiple mechanisms, as outlined in the following subsections.

8.3. Bacterial metabolites and satiety

Certain bacteria (*Bifidobacterium*, *Lactobacillus*) produce lactate, which supports neuronal activity and prolongs satiety. SCFAs, such as acetate and butyrate, derived from bacterial fermentation, influence appetite regulation by affecting neuropeptides in the hypothalamus and activating the vagus nerve.

8.4. Gut hormones and appetite control

Intestinal hormones, such as GLP-1 and peptide YY are produced by enteroendocrine cells and are modulated by bile acids, SCFAs, and indoles. These hormones act as anorexigenic signals, binding to receptors in neurons, the hypothalamus, and the brainstem to suppress appetite.[54]

8.5. Neurotransmitters and feeding behavior

Gut bacteria contribute to the production of neurotransmitters, including serotonin and GABA, which regulate appetite. GABA stimulates feeding behavior, while serotonin suppresses appetite by modulating melanocortin neurons, which help maintain energy balance.

8.6. Mood and reward pathways

The gut microbiota influences mood through immune responses, microbial metabolites, and vagus nerve

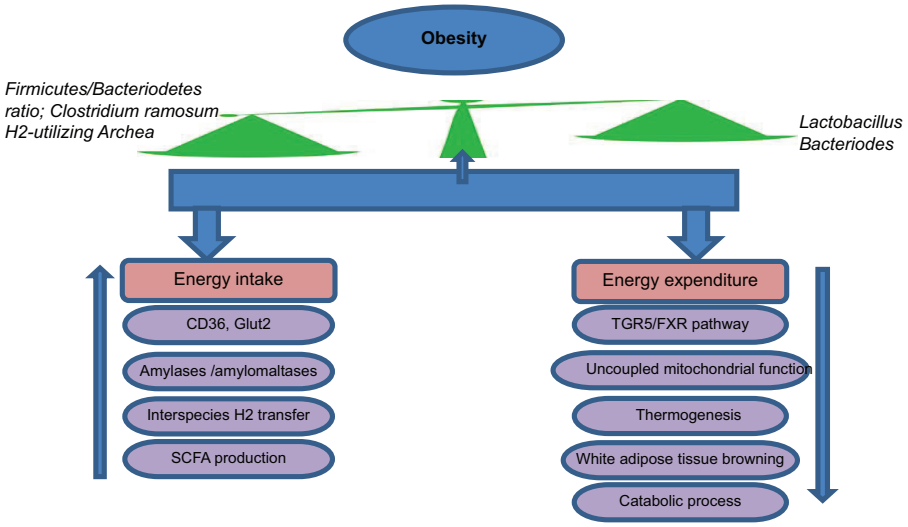

Figure 1. Energy homeostasis disruption
Abbreviations: CD36: Cluster of differentiation 36; FXR: Farnesoid X receptor; Glut2: Glucose transporter 2; H2: Hydrogen; TGR5: Takeda G-protein-coupled receptor 5.

activation. Psychological stress can trigger hedonic signaling pathways, leading to increased consumption of high-calorie foods. In addition, bacterial fermentation products, such as propionate have been linked to reduced reward responses to unhealthy food, thereby influencing feeding behavior.[55]

8.7. Chronic inflammation

Chronic low-grade inflammation is a key trait of obesity, primarily driven by increased levels of LPS – endotoxins released by Gram-negative bacteria, such as *Veillonella*. In obese individuals, excessive LPS disrupts the gut barrier by activating the TLR4/myeloid differentiation primary response 88 (MyD88)/IL-1 receptor-associated kinase 4 (IRAK4) signaling pathway, allowing bacterial byproducts to enter the bloodstream. Reduced levels of *A. muciniphila*, which helps maintain gut barrier integrity, further contribute to this process. In addition, high-fat diets (HFD) facilitate LPS absorption and transport into circulation through chylomicrons. Once in the bloodstream, LPS triggers immune responses in adipose tissue and the liver. It forms complexes with LPS-binding protein and cluster of differentiation 14**,** leading to the stimulation of nuclear factor kappa B (NF-κB) and activator protein 1, which drive the release of pro-inflammatory cytokines, such as TNF-*α*, IL-6, and monocyte chemoattractant protein (MCP) 1. These cytokines, in turn, stimulate adipocytes to secrete additional inflammatory signals, exacerbating metabolic dysfunction. Despite the inflammatory effects of LPS, SCFAs – especially butyrate – exert anti-inflammatory properties. Butyrate promotes IL-18 secretion, supports regulatory T cell differentiation, and suppresses NF-κB activation, thereby reducing inflammation.[56] However, it remains unclear whether these beneficial effects are sufficient to counteract LPS-induced chronic inflammation, indicating the need for further research.

9. Factors affecting homeostasis

9.1. Composition of infants' microbiota

The composition and development of the infant gut microbiota differ significantly from that of adults, undergoing a dynamic process of establishment. Colonization begins at birth, with some evidence suggesting maternal bacterial transmission may occur during gestation. In neonates, the gut microbiota consists primarily of *Enterococcus, Escherichia/Shigella, Streptococcus,* and *Rothia* species, while infants aged 1 – 6 months show increased colonization of *Bifidobacterium* and *Collinsella*. By 4 months of age, additional bacteria, such as *Lactobacillus, Granulicatella,* and *Veillonella* become prevalent, although full microbiome maturation continues until at least two years of age, reaching adult-like complexity by age three. Several factors influence early microbiota development, including mode of delivery, maternal microbiota, feeding practices, antibiotic exposure, and dietary changes. The maternal gut microbiota directly affects infant colonization, with *Bifidobacteria* being a dominant species transmitted through breast milk and fecal matter.[57] Mode of delivery also plays a significant role in microbiota composition, with vaginally born infants showing higher levels of *Bacteroides*, while Cesarean-section-delivered infants exhibit increased levels of *Hungatella*. Feeding practices shape microbial diversity – formula feeding leads to greater microbiome development compared to breastfeeding. In addition, antibiotic use rapidly alters the gut microbiota, reducing beneficial bacterial populations, while dietary changes, such as the introduction of complementary foods, further influence microbiome diversity.[58]

9.2. Composition of the adult microbiota

In healthy adults, the gut microbiota is comparatively stable, unlike in infants, whose microbiome is still developing, and the elderly, who tend to have a less diverse and more unstable gut microbiome (Figure 2). The dominant bacterial phyla in the adult gut microbiota are *Firmicutes* and *Bacteroidetes*, alongside other phyla, such as *Actinobacteria*, *Verrucomicrobia,* and *Proteobacteria*. While microbial diversity varies among individuals, gut bacteria consistently perform essential physiological functions, including metabolism, fermentation, methanogenesis, and immune regulation.[59]

However, several factors can disrupt microbiota homeostasis, including host genetics, diet, medications, infections, and circadian rhythm disturbances**.** Diet-induced obesity is associated with shifts in microbiota composition that differ from those of normal-weight individuals. Antibiotics and other xenobiotics can rapidly alter microbiome diversity and function, and prolonged exposure may lead to antibiotic resistance and microbiome imbalance. Maintaining a stable microbiota is critical for immune system homeostasis, as it helps resist pathogenic infections; however, infections can significantly disrupt microbiota composition. In addition, circadian rhythm plays a role in microbiota balance – disruptions in feeding patterns can lead to gut flora imbalances and metabolic disorders, including obesity. Overall, maintaining gut microbiota stability is essential for supporting metabolic health and immune function, with various internal and external factors influencing its composition and resilience.[60]

10. Alteration of gut microbiota by antibiotics leading obesity

Diet and antibiotics play a fundamental role in shaping gut microbiota composition, with diet exerting a more

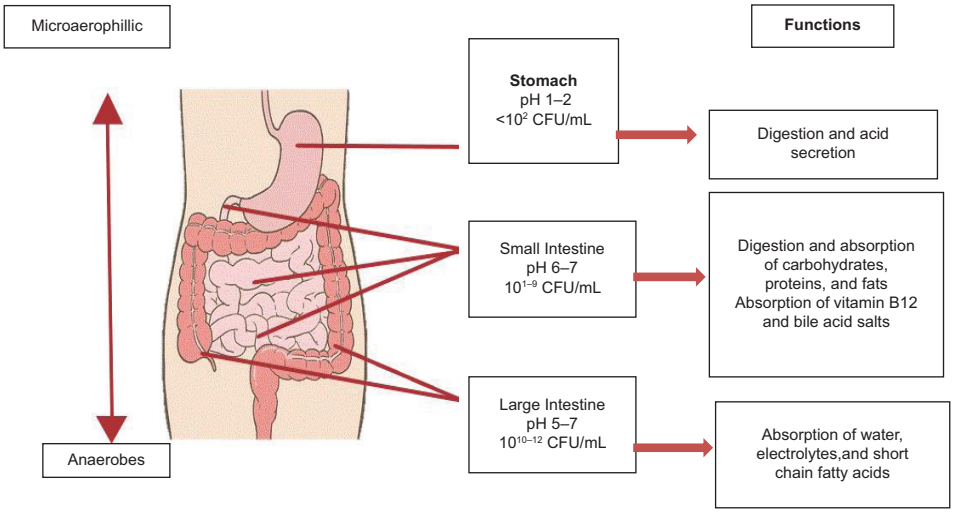

Figure 2. Key physiologic and microbiological features of the gut

substantial influence than obesity itself. Studies comparing resistin-like molecule b-deficient mice – which are resistant to high-fat diet-stimulated obesity – with wild-type mice showed that both groups experienced similar gut microbiota shifts, reinforcing the idea that dietary intake is the primary determinant of microbiota changes, rather than obesity alone. Beyond dietary impact, long-term antibiotic use can cause lasting alterations in gut microbiota. Research has demonstrated that a 7-day clindamycin regimen in humans irreversibly modified *Bacteroides* populations for up to two years, without signs of recovery. Similarly, exposure to ciprofloxacin significantly reduced gut microbial diversity, and while most species restored their populations within a month, certain bacterial taxa failed to recover even 6 months after treatment.[61]

Alterations caused by antibiotics extend beyond gut microbiota and can significantly influence metabolic health and obesity progression. For instance, administering norfloxacin and ampicillin improved glycemic control in diet-induced obese mice, suggesting a potential role for antibiotics in obesity management. However, early-life exposure to antibiotics has been linked to increased adiposity, particularly in newborn mice, highlighting a critical time window during which antibiotic intervention can lead to lasting metabolic consequences. Studies found that newborn mice were more vulnerable to low-dose penicillin than mice treated later, with early exposure leading to increased fat storage and metabolic shifts. Moreover, transplanting microbiota from penicillin-exposed mice into germ-free mice induced obesity-like phenotypes, further establishing a causal connection between gut microbiota alterations and obesity development. Human studies reinforce this connection, showing that antibiotic therapy has been associated with increased obesity risk**,** particularly when administered in early childhood. Research in Finnish pre-school children using metagenomics identified significant correlations between infant antibiotic exposure and obesity prevalence, suggesting long-term effects on microbial diversity and metabolic health. Given the widespread use of antibiotics, their unintended influence on gut microbiota could contribute to metabolic dysfunctions, insulin resistance, and weight gain over time (Figure 3). Overall, dietary patterns and antibiotic interventions strongly shape gut microbiota balance, impacting metabolic regulation, immune function, and obesity risk.[62] While targeted antibiotic use may offer therapeutic potential, caution is necessary regarding early-life exposure, as disruptions in microbiota composition can have lasting metabolic consequences.

11. Microbiota and diseases associated with obesity

Obesity induces persistent low-grade inflammation in multiple organs, which is linked to metabolic disorders, including glucose intolerance, insulin resistance, and cardiovascular illnesses (Table 1).[63] Inflammation is a significant risk factor for metabolic disorders associated with diabetes, metabolic syndrome, and cardiovascular disease.[64] Hotamisligil *et al.*[65] were the first to elucidate inflammation in metabolic disease, demonstrating that adipocytes can express the cytokine TNF-α, with its expression being heightened in the adipocytes of obese mice. The gut microbiota intensifies inflammation by the action of LPS, a crucial element of the cell walls of Gram-

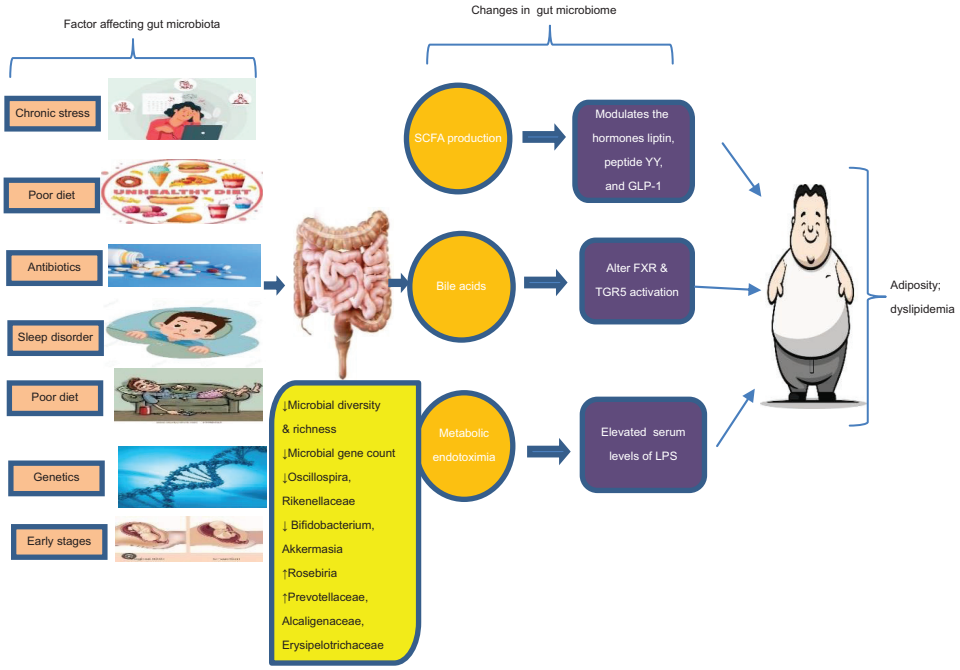

Figure 3. Factors altering gut microbiome leading to obesity
Abbreviations: FXR: Farnesoid X receptors; LPS: Lipopolysaccharide; SCFA: Short-chain fatty acid; TGR5: Takeda G-protein-coupled receptor 5c.

Table 1. Microbial taxa in obese individuals with metabolic disorders

Metabolic disorders	Risk-enhancing Bacteria	Protective or risk-lowering bacteria
Metabolic syndrome	*Coriobacteriaceae*	*Faecalibacterium prausnitzii, Parabacteroides, Bacteroides caccae, Parabacteroides distasonis,* and *Oscillospira*
Impaired glucose tolerance or insulin resistance	*Bacteroides ovatus* and *Enterobacteriaceae Prevotellaceae* and *Veillonella*	*Coprococcus, Haemophilus parainfluenzae, Parabacteroides, Bacteroides caccae* *Oscillibacter sp., Agathobaculum butyriciproducens, Haemophilus parainfluenzae, Veillonella parvula, Dialister invisus*
High diastolic blood pressure	*Clostridium* and *Clostridiaceae*	-
Low HDL cholesterol	*Lachnospiraceae*, *Gemellaceae*, and *Turicibacter*	-
Cardiovascular disorders	*Prevotellaceae* and *Veillonella*	*Coriobacteriaceae*

negative bacteria.[66-68] The proliferation of Gram-negative bacteria in obese individuals, such as *Veillonella*, can result in an increased concentration of LPS in the colon.[69] The increase of LPS can compromise the gut barrier by stimulating the TLR4/MyD88/IRAK4 signaling pathway in intestinal epithelial cells, subsequently leading to the transfer of LPS from the intestine into the systemic circulation.[70] Furthermore, the reduction of *A. muciniphila* facilitates the transfer of microbial by-products due to its role in preserving gut barrier integrity.[71] Moreover, a high-fat diet facilitates the integration of LPS into chylomicrons, thereby enhancing the absorption of LPS in the intestine and its subsequent transfer to the systemic circulation through lymphatic fluid.[72] These pathways lead to increased LPS levels in circulation. LPS can trigger immunological reactions in adipose tissue and the liver during systemic circulation. LPS initially associates with the LPS-binding protein and then forms a complex with cluster of differentiation 14.[73] This complex subsequently stimulates the NF-κB and activator protein 1 by activating TLR4 present on macrophages and adipose tissue, thereby facilitating the production of pro-inflammatory chemokines and cytokines, including MCP-1, TNF-α, and IL-6.[43,73] These cytokines can influence adipocytes, prompting them to release more cytokines and chemokines through paracrine and autocrine mechanisms.[74] Furthermore, overexpression

of MCP-1 in adipose tissue has been established as associated with heightened macrophage infiltration in rodents.[75] Significantly, SCFAs serve as a crucial link between inflammatory reactions and the gut microbiota, demonstrating strong anti-inflammatory characteristics, particularly butyrate.[76] Butyrate safeguards the gut against inflammation by inducing IL-18 production and facilitating the development of regulatory IL-10-producing T cells and T cells through GPR109a.[32,77] Moreover, butyrate can upregulate peroxisome proliferator-activated receptor gamma, enhance the production of anti-inflammatory cytokines, and inhibit NF-κB activation triggered by LPS, thereby demonstrating its anti-inflammatory effects.[78,79] The genera *Fusobacterium*, *Pseudomonas*, *Escherichia-Shigella*, and *Campylobacter* are commonly associated with obesity.[80,81] LPS from members of the *Desulfovibrionaceae* and *Enterobacteriaceae* families exhibit endotoxin activity that is 1,000-fold greater than that of LPS from *Bacteroideaceae*.[82]

12. Effects of diet on obesity

The composition of the gut microbiota is significantly influenced by dietary habits. A diet rich in fats and sugars, characteristic of Western cuisine, increases the relative prevalence of *Firmicutes* while diminishing *Bacteroidetes* in animal models.[83] Furthermore, transitioning from a low-fat, plant polysaccharide-rich diet to a high-fat/high-sugar "Western" diet can alter microbiota formation within a single day in gnotobiotic mice colonized with human fecal bacteria.[84] The nature of diet, combined with elevated caloric intake along with reduced physical activity, is among the principal factors contributing to the rising incidence of obesity.[85] The origins and progression of obesity can be explained by the carbohydrate-insulin model and/or the energy balance model (EBM).[86] The EBM model posits that the brain, particularly the hypothalamus, regulates body weight by controlling food intake through complex internal endocrine, metabolic, and neural signals from peripheral organs, as well as external cues from the food environment.[87] The increased availability of ultra-processed foods (UPFs), characterized by high energy density and elevated levels of fat and sugar, but low in protein, fiber, vitamins, and minerals, may result in a positive energy balance and fat accumulation (adiposity), regardless of the diet's macronutrient composition. Typical examples of UPFs include refined cereals, sweet and savory snacks, margarine, reconstituted and ready-to-eat frozen meals, and carbonated and alcoholic beverages.[88] The carbohydrate-insulin model emphasizes diet quality, namely, chemical composition, over quantity.[89] UPFs and other refined products are high in sugars, which elevate both glycemic index and glycemic load. Elevated glycemia triggers excessive insulin production, leading to increased adiposity and the inhibition of energy release from adipose tissue. Post-prandial energy substrate deficiency in the bloodstream is detected by the hypothalamus, stimulating appetite and reducing energy expenditure, potentially resulting in a positive energy balance due to hyperphagia.[90] Excessive consumption of UPFs can affect gut flora and has been associated with a higher incidence of obesity, metabolic syndrome, hypercholesterolemia, and hypertension.[91] Diets high in protein and fat are typically linked to *Bacteroides*-dominant (enterotype I) microbiota, while high-carbohydrate diets are associated with *Prevotella*-driven (enterotype II) microbiota profiles. This aligns with the findings of Wu *et al.*,[92] who reported that *Bacteroidetes* and *Actinobacteria* positively correlate with dietary fat and negatively with dietary fiber, while *Firmicutes* and *Proteobacteria* show the opposite trend. Conversely, Brinkworth *et al.*[93] found that high-fat/low-fiber diets reduced the abundance of *Bifidobacteria* compared to low-fat/high-fiber diets. Lower carbohydrate and fiber intake resulted in a decline in bacteria, such as *Eubacterium rectale*, *Roseburia* spp., and *Bifidobacterium* spp. in obese adults.[94] Dietary fiber increased the abundance of *Prevotella*, whereas bile-resistant taxa, such as *Bilophila* and *Bacteroides* were associated with high-fat, animal-based diets.[95]

Vegetarians generally exhibit greater bacterial diversity, higher *Prevotella* to *Bacteroides* ratios, and reduced levels of *Enterobacteriaceae*, including *E. coli*, compared to omnivores.[96] Moreover, vegetarians and vegans show a greater abundance of *Lachnospiraceae* (e.g., *Roseburia*, *Anaerostipes*, *Blautia* genera) and *Ruminococcaceae* (e.g., *Ruminococcus* and *F. prauznitzii* genera), along with a reduced presence of *Bacteroides*, *Parabacteroides*, and *Alistipes*.[97]

The Western-style diet, marked by a high intake of protein and fats (particularly saturated fats), is associated with an increased prevalence of metabolic disorders, such as type 2 diabetes, cardiovascular diseases, and obesity.[98] It also correlates with increased abundances of *Bacteroides*, *Alistipes*, and *Bilophila*, and decreased levels of *Lactobacillus*, *Roseburia*, *Eubacterium*, and *Enterococcus* genera.[99] In contrast, the Mediterranean diet – rich in dietary fiber from cereals, vegetables, legumes, nuts, and fruits; unsaturated fatty acids from fish and vegetable oils; and antioxidants, such as flavonoids and polyphenols – enhances overall microbial diversity.[100] This includes increases in families, such as *Clostridiaceae* and *Lactobacillaceae*, and genera, such as *Bacteroides*, *Prevotella*, *Bifidobacterium*, *Roseburia*, *Lactobacillus*, *Clostridium*, and *Faecalibacterium* (Table 2), while reducing the abundance of *Proteobacteria*.[101]

Table 2. Comparison of gut microbiota in obese and non-obese individuals

Group	↑ Gut microbes	↓ Gut microbes	*Firmicutes: Bacteroidetes*	References
Non-obese individuals	*Actinobacteria* (phylum), *Bacteroidetes* (phylum), *Bifidobacterium*, *Bacteroides*, *Prevotella*	*Firmicutes* (phylum), *Lactobacillales* (order), *Clostridium*	0.9	127
Obese individuals	*Firmicutes* (phylum), *Lactobacillales* (order), *Clostridium*	*Actinobacteria* (phylum), *Bacteroidetes* (phylum), *Bifidobacterium*, *Bacteroides*, *Prevotella*	1.7	127

13. Obesity and cardiovascular disorders

The gut microbiota, when subjected to unhealthy dietary patterns, metabolizes dietary nutrients into metabolically harmful substances. Examples include imidazole propionate, branched-chain amino acids (BCAAs), and trimethylamine N-oxide (TMAO).[102] The microorganisms *Bacteroides vulgatus* and *Prevotella copri* promote the synthesis of BCAAs, whereas *Eggerthella lenta* and *Streptococcus mutans* are known to produce imidazole propionate. Elevated circulating levels of BCAAs are significant risk factors for insulin resistance, and BCAA-related microbial metabolites, such as imidazole propionate, adversely affect insulin signaling cascades. TMAO has garnered significant interest because of its potential role in cardiovascular disease.[103] Trimethylamine is produced by the gut microbiota from compounds, such as choline, phosphatidylcholine, betaine, and L-carnitine, which are abundant in seafood, egg yolks, dairy products, and red meat. Trimethylamine is absorbed into the portal circulation and oxidized to TMAO in the liver by flavin-containing monooxygenase 3.[104] TMAO and its dietary pre-cursors promote arteriosclerosis through pathways involving inflammation, platelet aggregation, oxidative stress, and thrombosis.[96] Consequently, gut dysbiosis results in elevated plasma TMAO levels, which are associated with cardiovascular disease and increased overall mortality.[103]

LPSs are glycolipid molecules that constitute crucial components of the outer membrane components of Gram-negative bacteria and act as bacterial endotoxins, contributing to cardiometabolic abnormalities. Elevated LPS levels can induce the expression of pro-inflammatory cytokines, leading to endothelial damage, enhanced oxidation of low-density cholesterol particles, and foam cell formation, processes that collectively accelerate atherosclerosis.[105]

14. Prevention of obesity by modulation of gut microbiota

14.1. Probiotics

The World Health Organization defines probiotics as "living microorganisms that provide the host with beneficial effects when administered in sufficient quantities."[106] Probiotics are currently widely applied in the prevention and treatment of various diseases, including periodontal conditions and gastrointestinal infections, with particular emphasis on *Lactobacillus* and *Bifidobacterium* species.[107] As commensal microorganisms in the human gut, probiotics are believed to exert beneficial effects through mechanisms, such as competing with pathogenic bacteria, enhancing gut barrier function, and regulating immune responses.[108] Recent studies involving both animals and humans have demonstrated that probiotics can effectively improve metabolic disorders, reduce inflammation, and mitigate weight gain in individuals with obesity. The probiotic VSL#3, which includes *Bifidobacteria* and *Lactobacillus* strains, has been utilized in mouse models to address obesity by enhancing insulin sensitivity, decreasing food intake, and inhibiting weight gain.[109] In a randomized controlled trial, VSL#3 usage in human subjects demonstrated improvements in insulin sensitivity and lipid profiles.[110] The probiotic powder *Lactobacillus plantarum* Dad-13 demonstrated the ability to alter gut microbiota composition in a double-blind, placebo-controlled trial, resulting in a decrease in *Firmicutes* and an increase in *Bacteroidetes*, alongside significant reductions in body weight and body mass index.[111] Another double-blind, randomized trial found that the supplementation with a probiotic mix (*Bifidobacterium*, *Lactococcus*, and *Lactobacillus*) in overweight and obese individuals increased antioxidant enzyme activity and reduced abdominal adiposity. Nonetheless, a recent meta-analysis of randomized controlled human studies indicated that the association between weight loss and probiotics treatment was not statistically significant.[112] Furthermore, the specific bacterial species, optimal dosages, and treatment durations necessary to effectively enhance obesity management require additional research.

14.2. Prebiotics

Prebiotics are indigestible components specifically used by host microbiota, offering beneficial effects primarily by alleviating gut dysbiosis.[113] Several studies have indicated that prebiotics may improve dysbiosis, metabolic disorders, and chronic inflammation associated with obesity.[114] Common prebiotics include inulin, various forms of lactulose, oligosaccharides, and resistant starch. It is

generally accepted that all fermentable dietary fibers possess prebiotic properties.[115] A functional food strategy has been implemented to incorporate inulin into widely consumed items, such as cereals, biscuits, infant foods, yogurts, breads, and beverages at levels capable of eliciting a prebiotic effect.[116] Various dietary supplements containing fructo-oligosaccharides, mainly inulin, are also commercially available. Gut hormones, such as GLP-1 are essential for transmitting signals regarding nutritional and energy status from the gut to the central nervous system, thereby regulating appetite. Research indicates that prebiotics upregulate *Glp1* expression in obese mice, indicating that changes in gut microbiota may influence gastrointestinal hormone secretion.[117] In genetically obese mice, prebiotic treatment was associated with weight loss, improved glucose tolerance, and reduced inflammation, alongside an increase in *Bacteroidetes* and a decrease in the *Firmicutes* phylum. In a double-blind, placebo-controlled trial, supplementation with oligofructose-enriched inulin in overweight or obese children led to a significant reduction in serum IL-6 levels and body weight.[118] In addition, a randomized, placebo-controlled trial examining fecal samples from obese individuals consuming inulin-type fructans revealed an increase in *Bifidobacterium* abundance and a reduction in fecal calprotectin, a marker of gut inflammation, compared to controls.[119] Consequently, incorporating prebiotics into the diet holds significant potential to beneficially modulate gut microbiota composition.

14.3. Synbiotics

A synbiotic refers to a combination of a probiotic and a prebiotic. Synbiotics may have a more significant impact on gut microbiota and host health compared to the isolated consumption of either prebiotics or probiotics. This is because they provide probiotic bacteria along with a prebiotic component that enhances the survival and growth of these beneficial microbes within the digestive tract. Evidence suggests that synbiotics can be effective in modifying the composition of the gut microbiota. For instance, the synbiotic combination of particular oligofructose-enriched inulin (SYN1) with *Lactobacillus rhamnosus* GG and *Bifidobacterium lactis* Bb12 over a 12-week period resulted in a 16% and 18% increase in *Bifidobacterium* and *Lactobacillus* populations, while also leading to a 31% reduction in *Clostridium perfringens* counts.[120] *In vitro* investigations have shown that synbiotics outperform prebiotics and probiotics in their ability to modulate gut microflora. However, it is essential to document these findings through rigorously controlled human intervention studies. At present, there is a limited number of human studies examining the potential benefits of synbiotics in relation to obesity.[121]

14.4. Fecal microbiota transplantation

Fecal microbiota transplantation (FMT) is defined as the introduction of fecal suspension from healthy donors into

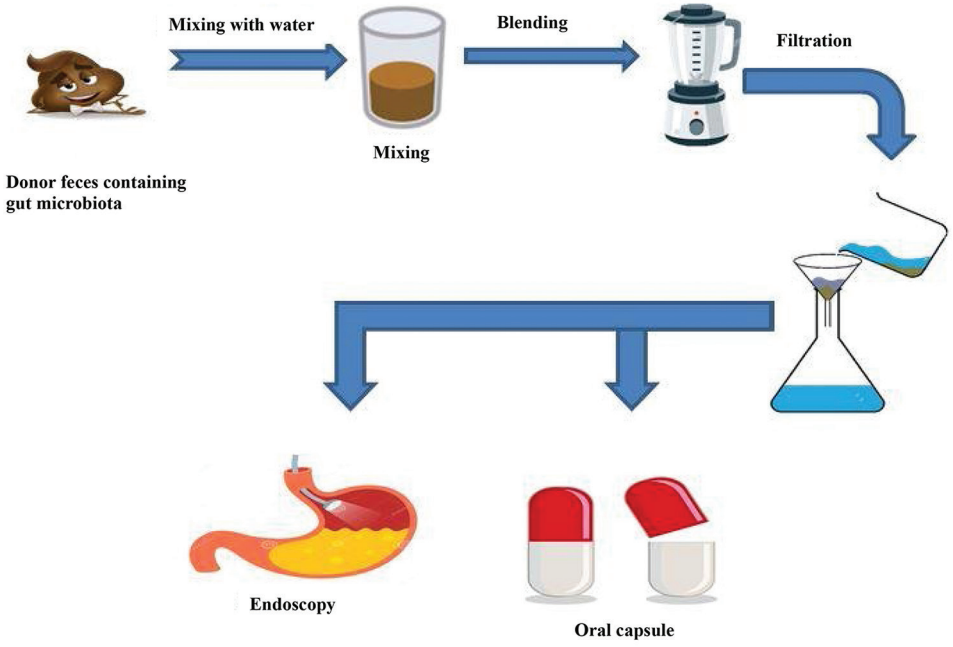

Figure 4. Schematic diagram of the fecal microbiota transplantation process

a patient's gastrointestinal tract, with the aim of restoring gut microbiota and treating related disorders.[122] Unlike probiotics, FMT provides recipients with a complete community of gut microbiota and its metabolites from healthy donors, rendering it a potentially more effective therapeutic intervention.[123] The remarkable efficacy of FMT in treating *Clostridium difficile* infections suggests that it is becoming a promising therapeutic option for other conditions linked to gut dysbiosis, including persistent irritable bowel syndrome, constipation, and ulcerative colitis.[124] A pilot human study demonstrated a substantial improvement in peripheral insulin sensitivity among nine obese individuals with metabolic syndrome following the transplantation of fecal microbiota from lean donors. Nevertheless, in several recent randomized clinical trials, FMT did not demonstrate significant effects on metabolic profiles and weight reduction.[125] There are also risks associated with FMTs, as viral pathogens cannot be eliminated through filtration. Therefore, FMT should be utilized only as a last resort for conditions, such as recurrent *C. difficile* infection (Figure 4). Furthermore, FMTs may have detrimental impacts in the context of obesity. A recent case report described a patient who underwent a successful FMT for *C. difficile* infection but subsequently developed new-onset obesity after receiving stool from an overweight donor.[126]

15. Conclusion

In conclusion, the gut microbiome plays a pivotal role in obesity development and associated metabolic disorders by influencing energy metabolism, immune responses, inflammation, and nutrient absorption. The intricate relationship between diet, antibiotic exposure, and microbiota composition demonstrates how external factors shape gut health, potentially leading to obesity when dysbiosis occurs. Understanding the mechanisms by which gut microbiota impacts obesity, including microbial metabolites and immune modulation, offers valuable insights into prevention and treatment strategies. Dietary interventions, particularly plant-based diets, contribute to greater microbial diversity, fostering a healthier gut environment. Moreover, strategies, such as probiotic, prebiotic, and synbiotic supplementation, as well as fecal microbiota transplantation, have emerged as promising therapeutic approaches for restoring microbial balance, improving metabolic function, and preventing obesity-related complications. However, the effects of microbiota treatments may vary from person to person, over time, and depending on factors, such as diet, concurrent medical treatments, and coexisting diseases. The complex interactions between the native gut microbiota, the quality and quantity of transplanted microbiota, the gut environment, host genetics, and interactions with various medications, including antibiotics, still require further investigation. The role of different species of gut microbial species also warrants greater focus in future microbiological research. Various studies have revealed that metabolic activities of gut microbiota facilitate the extraction of energy (calories) from ingested dietary food and aid in storing this energy for later usage by the host. By leveraging gut microbiota modulation, novel treatments can pave the way for sustainable obesity management, providing effective alternatives to conventional weight-loss strategies. Advancing research on microbiome-targeted therapies will be essential for optimizing clinical applications and ensuring that interventions are tailored to individual microbiota profiles for improved health outcomes.

Acknowledgments

The authors are thankful to the Vice Chancellor, Maj. Gen. Dr. G.K. Thapaliyal, Swami Vivekanand Subharti University, Meerut, for his valuable suggestions during the finalization of this paper.

Funding

None.

Conflict of interest

The authors declare that they have no competing interest.

Author contributions

Conceptualization: Amar P. Garg
Visualization: Rashmi Goley, Anchal Bamal
Writing – original draft: All authors
Writing – review & editing: Amar P. Garg

Ethics approval and consent to participate

Not applicable.

Consent for publication

Not applicable.

Availability of data

Not applicable.

Further disclosure

Part of this paper was presented as a keynote address at the International Conference on Pediatrics and Child Health in Dubai, UAE, on May 15–16, 2025.

References

1. NCD Risk Factor Collaboration (NCD-RisC). Trends in adult body-mass index in 200 countries from 1975

to 2014: A pooled analysis of 1698 population-based measurement studies with 19.2 million participants. *Lancet*. 2016;387:1377e96.

doi: 10.1016/S0140-6736(16)30472-X

2. Kelly T, Yang W, Chen CS, Reynolds K, He J. Global burden of obesity in 2005 and projections to 2030. *Int J Obes (Lond)*. 2008;32:1431-1437.

doi: 10.1038/ijo.2008.102

3. Haslam DW, James WP. Obesity. *Lancet*. 2005;366:1197-1209.

doi: 10.1016/S0140-6736(05)67483-1

4. Ghosh S, Bouchard C. Convergence between biological, behavioural and genetic determinants of obesity. *Nat Rev Genet*. 2017;18:731-748.

doi: 10.1038/nrg.2017.72

5. Hruby A, Hu FB. The epidemiology of obesity: A big picture. *Pharmacoeconomics*. 2015;33:673-689.

doi: 10.1038/nrmicro3089

6. Zhao L. The gut microbiota and obesity: From correlation to causality. *Nat Rev Microbiol*. 2013;11:639-647.

doi: 10.1038/nrmicro3089

7. Bäckhed F, Ding H, Wang T, *et al*. The gut microbiota as an environmental factor that regulates fat storage. *Proc Natl Acad Sci U S A*. 2004;101(44):15718-15723.

doi: 10.1073/pnas.0407076101

8. Ley RE, Backhed F, Turnbaugh P, Lozupone CA, Knight RD, Gordon JI. Obesity alters gut microbial ecology. *Proc Natl Acad Sci U S A*. 2005;102:11070-11075.

doi: 10.1073/pnas.0504978102

9. Turnbaugh PJ, Ley RE, Mahowald MA, Magrini V, Mardis ER, Gordon JI. An obesity-associated gut microbiome with increased capacity for energy harvest. *Nature*. 2006;444(7122):1027-1031.

doi: 10.1038/nature05414.

10. Martins Dos Santos V, Müller M, De Vos W. Systems biology of the gut: The interplay of food, microbiota and host at the mucosal interface. *Curr Opin Biotechnol*. 2010;21(4):539-550.

doi: 10.1016/j.copbio.2010.08.003

11. Rajani C, Jia W. Disruptions in gut microbial-host co-metabolism and the development of metabolic disorders. *Clin Sci (Lond)*. 2018;132(7):791-811.

doi: 10.1042/CS20171328

12. Agus A, Clemen TK, Soko LH. Gut microbiota-derived metabolites as central regulators in metabolic disorders. *Gut*. 2021;70(6):1174-1182.

doi: 10.1136/gutjnl-2020-323071

13. Khan MJ, Gerasimidis K, Edwards CA, Shaikh MG. Role of gut microbiota in the aetiology of obesity: Proposed mechanisms and review of the literature. *J Obes*. 2016;2016:7353642.

doi: 10.1155/2016/7353642

14. Tolhurst G, Heffron H, Lam YS, *et al*. Short-chain fatty acids stimulate glucagon-like peptide-1 secretion via the G-protein-coupled receptor FFAR2. *Diabetes*. 2012;61(2):364-371.

doi: 10.2337/db11-1019

15. Softic S, Cohen DE, Kahn CR. Role of dietary fructose and hepatic *de novo* lipogenesis in fatty liver disease. *Dig Dis Sci*. 2016;61(5):1282-1293.

doi: 10.1007/s10620-016-4054-0

16. Da Silva HE, Teterina A, Comelli EM, *et al*. Nonalcoholic fatty liver disease is associated with dysbiosis independent of body mass index and insulin resistance. *Sci Rep*. 2018;8:1466.

doi: 10.1038/s41598-018-19753-9

17. Beaumont M, Neyrinck AM, Olivares M, *et al*. The gut microbiota metabolite indole alleviates liver inflammation in mice. *FASEB J*. 2018;32(10):5445-5455.

doi: 10.1096/fj.201800544

18. Matsubara T, Li F, Gonzalez FJ. FXR signaling in the enterohepatic system. *Mol Cell Endocrinol*. 2013; 368(1-2):17-29.

doi: 10.1016/j.mce.2012.05.004

19. Harrison SA, Rinella ME, Abdelmalek MF, *et al*. NGM282 for treatment of non-alcoholic steatohepatitis: A multicentre, randomised, double-blind, placebo-controlled, phase 2 trial. *Lancet*. 2018;391(10126):1174-1185.

doi: 10.1016/S0140-6736(18)30474-4

20. Trabelsi MS, Daoudi M, Prawitt J, *et al*. Farnesoid X receptor inhibits glucagon-like peptide-1 production by enteroendocrine L cells. *Nat Commun*. 2015;6:7629.

doi: 10.1038/ncomms8629

21. Wang L, Ren B, Zhang Q, *et al*. Methionine restriction alleviates high-fat diet-induced obesity: Involvement of diurnal metabolism of lipids and bile acids. *Biochim Biophys Acta Mol Basis Dis*. 2020;1866(11):165908.

doi: 10.1016/j.bbadis.2020.165908

22. Huang ZR, Deng JC, Li QY, *et al*. Protective mechanism of common buckwheat (*Fagopyrum esculentum Moench*.) against nonalcoholic fatty liver disease associated with dyslipidemia in mice fed a high-fat and high-cholesterol diet. *J Agric Food Chem*. 2020;68(24):6530-6543.

doi: 10.1021/acs.jafc.9b08211

23. Yaron JR, Gangaraju S, Rao MY, *et al*. K(+) regulates Ca(2+) to drive inflammasome signaling: Dynamic visualization of

ion flux in live cells. *Cell Death Dis*. 2015;6:e1954.

doi: 10.1038/cddis.2015.277

24. Round JL, Lee SM, Li J, *et al*. The toll-like receptor 2 pathway establishes colonization by a commensal of the human microbiota. *Science*. 2011;332(6032):974-977.

doi: 10.1126/science.1206095

25. Ridlon JM, Kang DJ, Hylemon PB. Bile salt biotransformations by human intestinal bacteria. *J Lipid Res*. 2006;47(2):241-259.

doi: 10.1194/jlr.R500013-JLR200

26. Corbin KD, Carnero EA, Dirks B, *et al*. Host-diet-gut microbiome interactions influence human energy balance: A randomized clinical trial. *Nat Commun*. 2023;14:3161.

doi: 10.1038/s41467-023-38778-x

27. Lund J, Gerhart-Hines Z, Clemmensen C. Role of energy excretion in human body weight regulation. *Trends Endocrinol Metab*. 2020;31:705-708.

doi: 10.1016/j.tem.2020.06.002

28. Elia M, Cummings JH. Physiological aspects of energy metabolism and gastrointestinal effects of carbohydrates. *Eur J Clin Nutr*. 2007;61(Suppl 1):S40-S74.

doi: 10.1038/sj.ejcn.1602938

29. Watanabe M, Houten SM, Mataki C, *et al*. Bile acids induce energy expenditure by promoting intracellular thyroid hormone activation. *Nature*. 2006;439(7075):484-489.

doi: 10.1038/nature04330

30. Stephen AM, Cummings JH. The microbial contribution to human faecal mass. *J Med Microbiol*. 1980;13:45-56.

doi: 10.1099/00222615-13-1-45

31. Achour L, Nancey S, Moussata D, Graber I, Messing B, Flourié B. Faecal bacterial mass and energetic losses in healthy humans and patients with a short bowel syndrome. *Eur J Clin Nutr*. 2007;61:233-238.

doi: 10.1038/sj.ejcn.1602496

32. Corbin KD, Igudesman D, Smith SR, Zengler K, Krajmalnik-Brown R. Targeting the gut microbiota's role in host energy absorption with precision nutrition interventions for the prevention and treatment of obesity. *Nutr Rev*. 2025:nuaf046.

doi: 10.1093/nutrit/nuaf046

33. Abuqwider JN, Mauriello G, Altamimi M. *Akkermansia muciniphila*, a new generation of beneficial microbiota in modulating obesity: A systematic review. *Microorganisms*. 2021;9:1098.

doi: 10.1093/nutrit/nuaf046

34. Saad MJA, Santos A. The microbiota and evolution of obesity. *Endocr Rev*. 2025;46:300-316.

doi: 10.1210/endrev/bnae033

35. Depommier C, Van Hul M, Everard A, Delzenne NM, De Vos WM, Cani PD. Pasteurized *Akkermansia muciniphila* increases whole-body energy expenditure and fecal energy excretion in diet-induced obese mice. *Gut Microbes*. 2020;11:1231-1245.

doi: 10.1080/19490976.2020.1737307

36. Liu R, Hong J, Xu X, *et al*. Gut microbiome and serum metabolome alterations in obesity and after weight-loss intervention. *Nat Med*. 2017;23:859-868.

doi: 10.1038/nm.4358

37. Dirks B, Davis TL, Carnero EA, *et al*. *Methanogens are Associated with Altered Microbial Production of Short-Chain Fatty Acids and Human-Host Metabolizable Energy*. bioRxiv. [Preprint]; 2025.

doi: 10.1093/ismejo/wraf103

38. Koh A, Backhed F. From association to causality: The role of the gut microbiota and its functional products on host metabolism. *Mol Cell*. 2020;78:584-596.

doi: 10.1016/j.molcel.2020.03.005

39. Marcus A, Davis TL, Rittmann BE, *et al*. Developing a model for estimating the activity of colonic microbes after intestinal surgeries. *PLoS One*. 2021;16:e0253542.

doi: 10.1371/journal.pone.0253542

40. Den Besten G, Bleeker A, Gerding A, *et al*. Short-chain fatty acids protect against high-fat diet-induced obesity via a PPARγ-dependent switch from lipogenesis to fat oxidation. *Diabetes*. 2015;64:2398-2408.

doi: 10.2337/db14-1213

41. Ecklu-Mensah G, Choo-Kang C, Maseng MG, *et al*. Gut microbiota and fecal short chain fatty acids differ with adiposity and country of origin: The METS-Microbiome study. *Nat Commun*. 2023;14:5160.

doi: 10.1038/s41467-023-40874-x

42. Canfora EE, Van Der Beek CM, Jocken JW, *et al*. Colonic infusions of short-chain fatty acid mixtures promote energy metabolism in overweight/obese men: A randomized crossover trial. *Sci Rep*. 2017;7:2360.

doi: 10.1038/s41598-017-02546-x

43. Vijay-Kumar RM, Aitken JD, Carvalho FA, *et al*. Metabolic syndrome and altered gut microbiota in mice lacking toll-like receptor 5. *Science*. 2010;328(5975):228-231.

doi: 10.1126/science.1179721

44. Van Son J, Koekkoek LL, La Fleur SE, Serlie MJ, Nieuwdorp M. The role of the gut microbiota in the gut-brain axis in obesity: Mechanisms and future implications. *Int J Mol Sci*. 2021;22(6):2993.

doi: 10.3390/ijms22062993

45. Dinan TG, Cryan JF. Mood by microbe: Towards clinical

translation. *Genome Med.* 2016;8(1):36.

doi: 10.1186/s13073-016-0292-1

46. Procházková N, Falony G, Dragsted LO, Licht TR, Raes J, Roager HM. Advancing human gut microbiota research by considering gut transit time. *Gut*. 2023;72:180-191.

doi: 10.1136/gutjnl-2022-328166

47. Boekhorst J, Venlet N, Prochazkova N, *et al*. Stool energy density is positively correlated to intestinal transit time and related to microbial enterotypes. *Microbiome*. 2022;10:223.

doi: 10.1186/s40168-022-01418-5

48. Prochazkova N, Venlet N, Hansen ML, *et al*. Effects of a wholegrain-rich diet on markers of colonic fermentation and bowel function and their associations with the gut microbiome: A randomised controlled cross-over trial. *Front Nutr*. 2023;10:1187165.

doi: 10.3389/fnut.2023.1187165

49. Mushref MA, Srinivasan S. Effect of high fat-diet and obesity on gastrointestinal motility. *Ann Transl Med*. 2012;1:14.

doi: 10.3978/j.issn.2305-5839.2012.11.01

50. Herath M, Hosie S, Bornstein JC, Franks AE, Hill-Yardin EL. The role of the gastrointestinal mucus system in intestinal homeostasis: Implications for neurological disorders. *Front Cell Infect Microbiol*. 2020;10:248.

doi: 10.3389/fcimb.2020.00248

51. Schellekens H, Finger BC, Dinan TG, Cryan JF. Ghrelin signalling and obesity: At the interface of stress, mood and food reward. *Pharmacol Ther.* 2012;135(3):316-326.

doi: 10.1016/j.pharmthera.2012.06.004

52. Riedl RA, Burnett CML, Pearson NA, *et al*. Gut microbiota represent a major thermogenic biomass. *Function (Oxf)*. 2021;2: zqab019.

doi: 10.1093/function/zqab019

53. Gribble FM, Reimann F. Enteroendocrine cells: Chemosensors in the intestinal epithelium. *Annu Rev Physiol*. 2016;78:277-299.

doi: 10.1146/annurev-physiol-021115-105439

54. De Silva A, Bloom SR. Gut hormones and appetite control: A focus on pyy and glp-1 as therapeutic targets in obesity. *Gut Liver.* 2012;6(1):10-20.

doi: 10.5009/gnl.2012.6.1.10

55. Xu Y, Jones JE, Kohno D, *et al*. 5-Ht2crs expressed by pro-opiomelanocortin neurons regulate energy homeostasis. *Neuron*. 2008;60(4):582-589.

doi: 10.1016/j.neuron.2008.09.033

56. Singh N, Gurav A, Sivaprakasam S, *et al*. Activation of Gpr109a, receptor for niacin and the commensal metabolite butyrate, suppresses colonic inflammation and carcinogenesis. *Immunity.* 2014;40(1):128-139.

doi: 10.1016/j.immuni.2013.12.007

57. Bisht N, Garg AP. Isolation, characterization and probiotic value of lactic acid bacteria from milk and milk products. *Biotech Today*. 2019;9(2):54-63.

doi: 10.21786/bbrc/14.1/28

58. Medina DA, Pinto F, Ortuzar V, Garrido D. Simulation and modeling of dietary changes in the infant gut microbiome. *FEMS Microbiol Ecol.* 2018;94(9):1-11.

doi: 10.1093/femsec/fiy140

59. Arya RK, Tahilramani H, Garg AP. Impact of human colostrum associated population on neonatal health. *Int J Med Sci Innova Res.* 2018;3(5):86-90.

60. Thaiss CA, Zeevi D, Levy M, *et al*. Transkingdom control of microbiota diurnal oscillations promotes metabolic homeostasis. *Cell*. 2014;159(3):514-529.

doi: 10.1016/j.cell.2014.09.048

61. Jernberg C, Lofmark S, Edlund C, Jansson JK. Long-term ecological impacts of antibiotic administration on the human intestinal microbiota. *ISME J.* 2007;1:56-66.

doi: 10.1038/ismej.2007.3

62. Scott FI, Horton DB, Mamtani R, *et al*. Administration of antibiotics to children before age 2 years increases risk for childhood obesity. *Gastroenterology.* 2016;151:120-129.e5.

doi: 10.1053/j.gastro.2016.03.006

63. Sarmiento-Andrade Y, Suárez R, Quintero B, Garrochamba K, Chapela SP. Gut microbiota and obesity: New insights. *Front Nutr*. 2022;9:1018212.

doi: 10.3389/fnut.2022.1018212

64. Li Z, Gurung M, Rodrigues RR, *et al*. Microbiota and adipocyte mitochondrial damage in type 2 diabetes are linked by Mmp12+ macrophages. *J Exp Med*. 2022;219:e20220017.

doi: 10.1084/jem.20220017

65. Hotamisligil GS, Shargill NS, Spiegelman BM. Adipose expression of tumor necrosis factor-alpha: Direct role in obesity-linked insulin resistance. *Science*. 1993; 259(5091):87-91.

doi: 10.1126/science.7678183

66. Ley RE. Obesity and the human microbiome. *Curr Opin Gastroenterol*. 2010;26(1):5-11.

doi: 10.1097/MOG.0b013e328333d751

67. Cani PD, Bibiloni R, Knau FC, *et al*. Changes in gut microbiota control metabolic endotoxemia-induced inflammation in high-fat diet-induced obesity and diabetes in mice. *Diabetes*. 2008;57(6):1470-1481.

doi: 10.2337/db07-1403

68. Cani PD, Neyrinck AM, Fava F, *et al*. Selective increases

of bifidobacteria in gut microflora improve high-fat-diet-induced diabetes in mice through a mechanism associated with endotoxaemia. *Diabetologia*. 2007;50(11):2374-2383.

doi: 10.1007/s00125-007-0791-0

69. Yun Y, Kim HN, Kim SE, *et al*. Comparative analysis of gut microbiota associated with body mass index in a Large Korean cohort. *BMC Microbiol*. 2017;17(1):151.

doi: 10.1186/s12866-017-1052-0

70. Guo S, Nighot M, Al-Sadi R, Alhmoud T, Nighot P, Ma TY. Lipopolysaccharide regulation of intestinal tight junction permeability is mediated by Tlr4 signal transduction pathway activation of fak and Myd88. *J Immunol*. 2015; 195(10):4999-5010.

doi: 10.4049/jimmunol.1402598

71. Derrien M, Vaughan EE, Plugge CM, De Vos WM. *Akkermansia muciniphila* gen. Nov., sp. Nov., a human intestinal mucin-degrading bacterium. *Int J Syst Evol Microbiol*. 2004;54(Pt 5):1469-1476.

doi: 10.1099/ijs.0.02873-0

72. Torres-Fuentes C, Schellekens H, Dinan TG, Cryan JF. The microbiota-gut-brain axis in obesity. *Lancet Gastroenterol Hepatol*. 2017;2(10):747-756.

doi: 10.1016/S2468-1253(17)30147-4

73. Neal MD, Leaphart C, Levy R, *et al*. Enterocyte Tlr4 mediates phagocytosis and translocation of bacteria across the intestinal barrier. *J Immunol*. 2006;176(5):3070-3079.

doi: 10.4049/jimmunol.176.5.3070

74. Amabebe E, Robert FO, Agbalalah T, Orubu ESF. Microbial dysbiosis-induced obesity: Role of gut microbiota in homoeostasis of energy metabolism. *Br J Nutr*. 2020;123(10):1127-1137.

doi: 10.1017/S0007114520000380

75. Kanda H, Tateya S, Tamori Y, *et al*. Mcp-1 contributes to macrophage infiltration into adipose tissue, insulin resistance, and hepatic steatosis in obesity. *J Clin Invest*. 2006;116(6):1494-1505.

doi: 10.1172/JCI26498

76. Lin HV, Frassetto A, Kowalik EJ Jr., *et al*. Butyrate and propionate protect against diet-induced obesity and regulate gut hormones via free fatty acid receptor 3-independent mechanisms. *PLoS One*. 2012;7(4):e35240.

doi: 10.1371/journal.pone.0035240

77. Macia L, Tan J, Vieira AT, *et al*. Metabolite-sensing receptors Gpr43 and Gpr109a facilitate dietary fibre-induced gut homeostasis through regulation of the inflammasome. *Nat Commun*. 2015;6:6734.

doi: 10.1038/ncomms7734

78. Mattace Raso G, Simeoli R, Russo R, *et al*. Effects of sodium butyrate and its synthetic amide derivative on liver inflammation and glucose tolerance in an animal model of steatosis induced by high fat diet. *PLoS One*. 2013;8(7):e68626.

doi: 10.1371/journal.pone.0068626

79. Chen G, Ran X, Li B, *et al*. Sodium butyrate inhibits inflammation and maintains epithelium barrier integrity in a tnbs-induced inflammatory bowel disease mice model. *EBioMedicine*. 2018;30:317-325.

doi: 10.1016/j.ebiom.2018.03.030

80. Gao R, Zhu C, Li H, *et al*. Dysbiosis signatures of gut microbiota along the sequence from healthy, young patients to those with overweight and obesity. *Obesity (Silver Spring)*. 2018;26(2):351-361.

doi: 10.1038/nature12506

81. Le Chatelier E, Nielsen T, Qin J, *et al*. Richness of human gut microbiome correlates with metabolic markers. *Nature*. 2013;500(7464):541-546.

doi: 10.1038/nature12506

82. Lindberg AA, Weintraub A, Zähringer U, Rietschel ET. Structure-activity relationships in lipopolysaccharides of *Bacteroides fragilis*. *Rev Infect Dis*. 1990;12(Suppl 2):S133-S141.

doi: 10.1093/clinids/12.supplement_2.s133

83. Turnbaugh PJ, Backhed F, Fulton L, Gordon JI. Diet-induced obesity is linked to marked but reversible alterations in the mouse distal gut microbiome. *Cell Host Microbe*. 2008;3:213-223.

doi: 10.1016/j.chom.2008.02.015

84. Turnbaugh PJ, Ridaura VK, Faith JJ, Rey FE, Knight R, Gordon JI. The effect of diet on the human gut microbiome: A metagenomic analysis in humanized gnotobiotic mice. *Sci Transl Med*. 2009;1:6ra14.

doi: 10.1126/scitranslmed.3000322

85. Teodoro JS, Varela AT, Rolo AP, Palmeira CM. High-fat and obesogenic diets: Current and future strategies to fight obesity and diabetes. *Genes Nutr*. 2014;9:406.

doi: 10.1007/s12263-014-0406-6

86. Ludwig DS, Apovian CM, Aronne LJ, *et al*. Competing paradigms of obesity pathogenesis: Energy balance versus carbohydrate-insulin models. *Eur J Clin Nutr*. 2022;76:1209-1221.

doi: 10.1038/s41430-022-01179-2

87. Hall KD, Farooqi IS, Friedman JM, *et al*. The energy balance model of obesity: Beyond calories in, calories out. *Am J Clin Nutr*. 2022;115:1243-1254.

doi: 10.1093/ajcn/nqac031

88. Monda A, De Stefano MI, Villano I, *et al*. Ultra-processed

food intake and increased risk of obesity: A narrative review. *Foods*. 2024;13:2627.

doi: 10.3390/foods13162627

89. Heindel JJ, Lustig RH, Howard S, Corkey BE. Obesogens: A unifying theory for the global rise in obesity. *Int J Obes (Lond)*. 2024;48:449-460.

doi: 10.1038/s41366-024-01460-3

90. Flier JS. Moderating "the great debate": The carbohydrate-insulin vs. The energy balance models of obesity. *Cell Metab.* 2023;35:737-741.

doi: 10.1016/j.cmet.2023.03.020

91. Poti JM, Braga B, Qin B. Ultra-processed food intake and obesity: What really matters for health-processing or nutrient content? *Curr Obes Rep.* 2017;6:420-431.

doi: 10.1007/s13679-017-0285-4

92. Wu GD, Chen J, Hoffmann C, *et al*. Linking long-term dietary patterns with gut microbial enterotypes. *Science.* 2011;334:105-108.

doi: 10.1126/science.1208344

93. Brinkworth GD, Noakes M, Clifton PM, Bird AR. Comparative effects of very low-carbohydrate, high-fat and highcarbohydrate, low-fat weight-loss diets on bowel habit and faecal short-chain fatty acids and bacterial populations. *Br J Nutr.* 2009;101:1493-1502.

doi: 10.1017/S0007114508094658

94. Duncan SH, Belenguer A, Holtrop G, Johnstone AM, Flint HJ, Lobley GE. Reduced dietary intake of carbohydrates by obese subjects results in decreased concentrations of butyrate and butyrate-producing bacteria in feces. *Appl Environ Microbiol.* 2007;73:1073-1078.

doi: 10.1128/AEM.02340-06

95. David LA, Maurice CF, Carmody RN, *et al*. Diet rapidly and reproducibly alters the human gut microbiome. *Nature*. 2014;505:559-563.

doi: 10.1038/nature12820

96. Zimmer J, Lange B, Frick JS, *et al*. A vegan or vegetarian diet substantially alters the human colonic faecal microbiota. *Eur J Clin Nutr*. 2012;66:53-60.

doi: 10.1038/ejcn.2011.141

97. Sidhu SRK, Kok CW, Kunasegaran T, Ramadas A. Effect of plant-based diets on gut microbiota: A systematic review of interventional studies. *Nutrients*. 2023;15:1510.

doi: 10.3390/nu15061510

98. Clemente-Suárez VJ, Beltrán-Velasco AI, Redondo-Flórez L, Martín-Rodríguez A, Tornero-Aguilera JF. Global impacts of western diet and its effects on metabolism and health: A narrative review. *Nutrients.* 2023;15:2749.

doi: 10.3390/nu15122749

99. Beam A, Clinger E, Hao L. Effect of diet and dietary components on the composition of the gut microbiota. *Nutrients*. 2021;13:2795.

doi: 10.3390/nu13082795

100. Borrego-Ruiz A, Borrego JJ. Human gut microbiome, diet, and mental disorders. *Int Microbiol*. 2025;28(1):1-15.

doi: 10.1007/s10123-024-00518-6

101. Nagpal R, Neth BJ, Wang S, Craft S, Yadav H. Modified mediterranean-ketogenic diet modulates gut microbiome and short-chain fatty acids in association with alzheimer's disease markers in subjects with mild cognitive impairment. *EBioMedicine*. 2019;47:529-542.

doi: 10.1016/j.ebiom.2019.08.032

102. Bamal A, Goley R, Garg AP. Health managements through gut microbiota. *Am J Biomed Sci Res.* 2025;25(5):700-727.

doi: 10.34297/AJBSR.2025.25.003368

103. Koh A, Molinaro A, Ståhlman M, *et al*. Microbially produced imidazole propionate impairs insulin signaling through mTORC1. *Cell.* 2018;175:947-961.e17.

doi: 10.1016/j.cell.2018.09.055

104. Liu Y, Dai M. Trimethylamine N-Oxide generated by the gut microbiota is associated with vascular inflammation: New insights into atherosclerosis. *Mediators Inflamm*. 2020;2020:4634172.

doi: 10.1155/2020/4634172

105. Schicho R, Marsche G, Storr M. Cardiovascular complications in inflammatory bowel disease. *Curr Drug Targets*. 2015;16:181-188.

doi: 10.2174/1389450116666150202161500

106. Beyaz Coşkun A, Sağdiçoğlu Celep AG. Therapeutic modulation methods of gut microbiota and gut-liver axis. *Crit Rev Food Sci Nutr.* 2021;62(23):6505-6515.

doi: 10.1080/10408398.2021.1902263

107. Hu H, Lin A, Kong M, *et al*. Intestinal microbiome and nafld: Molecular insights and therapeutic perspectives. *J Gastroenterol*. 2020;55(2):142-158.

doi: 10.1007/s00535-019-01649-8

108. Bisht N, Garg AP. Role of gut microbiota in human health. *Res J Biotech*. 2021;16(1):202-212.

109. Yadav H, Lee JH, Lloyd J, Walter P, Rane SG. Beneficial metabolic effects of a probiotic Via butyrate-induced glp-1 hormone secretion. *J Biol Chem*. 2013;288(35):25088-25097.

doi: 10.1074/jbc.M113.452516

110. Rajkumar H, Mahmood N, Kumar M, Varikut SR, Challa HR, Myakala SP. Effect of probiotic (Vsl#3) and omega-3 on lipid profile, insulin sensitivity, inflammatory markers, and gut colonization in overweight adults: A randomized, controlled trial. *Mediators Inflamm*. 2014;2014:348959.

doi: 10.1155/2014/348959

111. Rahayu ES, Mariyatun M, Putri Manurung NE, *et al*. Effect of probiotic *Lactobacillus plantarum* dad-13 powder consumption on the gut microbiota and intestinal health of overweight adults. *World J Gastroenterol*. 2021;27(1): 107-128.

doi: 10.3748/wjg.v27.i1.107

112. Dror T, Dickstein Y, Dubourg G, Paul M. Microbiota manipulation for weight change. *Microb Pathog*. 2017; 106:146-161.

doi: 10.1016/j.micpath.2016.01.002

113. Gibson GR, Hutkins R, Sanders ME, *et al*. Expert consensus document: The international scientific association for probiotics and prebiotics (Isapp) consensus statement on the definition and scope of prebiotics. *Nat Rev Gastroenterol Hepatol*. 2017;14(8):491-502.

doi: 10.1038/nrgastro.2017.75

114. Parnell JA, Reimer RA. Prebiotic fibres dose-dependently increase satiety hormones and alter *Bacteroidetes* and *Firmicutes* in lean and obese Jcr: La-cp rats. *Br J Nutr*. 2012;107(4):601-613.

doi: 10.1017/S0007114511003163

115. Lim CC, Ferguson LR, Tannock GW. Dietary fibres as "prebiotics": Implications for colorectal cancer. *Mol Nutr Food Res*. 2005;49:609-619.

doi: 10.1002/mnfr.200500015

116. Kolinda S, Gibson GR. Prebiotic capacity of inulin-type fructans. *J Nutr*. 2007;137:2503S-2506S.

doi: 10.1093/jn/137.11.2503S

117. Delzenne NM, Cani PD, Daubioul C, Neyrinck AM. Impact of inulin and oligofructose on gastrointestinal peptides. *Br J Nutr*. 2005;93:S157-S161.

doi: 10.1079/bjn20041342

118. Nicolucci AC, Hume MP, Martınez I, Mayengbam S, Walter J, Reimer RA. Prebiotics reduce body fat and alter intestinal microbiota in children who are overweight or with obesity. *Gastroenterology*. 2017;153(3):711-722.

doi: 10.1053/j.gastro.2017.05.055

119. Neyrinck AM, Rodriguez J, Zhang Z, *et al*. Prebiotic dietary fibre intervention improves fecal markers related to inflammation in obese patients: Results from the Food4gut randomized placebo-controlled trial. *Eur J Nutr*. 2021;60(6):3159-3170.

doi: 10.1007/s00394-021-02484-5

120. Rafter J, Bennett M, Caderni G, *et al*. Dietary synbiotics reduce cancer risk factors in polypectomized and colon cancer patients. *Am J Clin Nutr*. 2007;85:488-496.

doi: 10.1093/ajcn/85.2.488

121. Beserra BTS, Fernandes R, Do Rosario VA, Mocellin MC, Kuntz MG, Trindade EB. A systematic review and meta-analysis of the prebiotics and synbiotics effects on glycaemia, insulin concentrations and lipid parameters in adult patients with overweight and obesity. *Clin Nutr*. 2015;34:845-858.

doi: 10.1016/j.clnu.2014.10.004

122. Milosevic I, Vujovic A, Barac A, *et al*. Gut-liver axis, gut microbiota, and its modulation in the management of liver diseases: A review of the literature. *Int J Mol Sci*. 2019;20(2):395.

doi: 10.3390/ijms20020395

123. Lee P, Yacyshyn BR, Yacyshyn MB. Gut microbiota and obesity: An opportunity to alter obesity through faecal microbiota transplant (Fmt). *Diabetes Obes Metab*. 2019;21(3):479-490.

doi: 10.1111/dom.13561

124. Bron PA, Kleerebezem M, Brummer RJ, *et al*. Can probiotics modulate human disease by impacting intestinal barrier function? *Br J Nutr*. 2017;117(1):93-107.

doi: 10.1017/S0007114516004037

125. Leong KSW, Jayasinghe TN, Wilson BC, *et al*. Effects of fecal microbiome transfer in adolescents with obesity: The gut bugs randomized controlled trial. *JAMA Netw Open*. 2020;3(12):e2030415.

doi: 10.1001/jamanetworkopen.2020.30415

126. Alang N, Kelly CR. Weight gain after fecal microbiota transplantation. *Open Forum Infect Dis*. 2015;2:ofv004.

doi: 10.1093/ofid/ofv004

127. Kasai C, Sugimoto K, Moritani I, *et al*. Comparison of the gut microbiota composition between obese and non-obese individuals in a Japanese population, as analyzed by terminal restriction fragment length polymorphism and next-generation sequencing. *BMC Gastroenterol*. 2015;15:100.

doi: 10.1186/s12876-015-0330-2

ACCSCIENCE PUBLISHING

Microbes & Immunity

PERSPECTIVE ARTICLE

Mx. BIOME: A bioinformatics and big data analysis platform in a data explosion era

Patrick C. Y. Woo[1,2*], Yu-Hsi Lin[3], Shao-Yu Huang[3], Mei-Hui Chen[1], Ming-Hon Hou[4,5,6], and Chieh-Chen Huang[3,7,8*]

[1]Doctoral Program in Translational Medicine and Department of Life Sciences, National Chung Hsing University, Taichung 402, Taiwan

[2]The iEGG and Animal Biotechnology Research Center, National Chung Hsing University, Taichung 402, Taiwan

[3]Department of Life Sciences, National Chung Hsing University, Taichung 402, Taiwan

[4]Institute of Genomics and Bioinformatics and Department of Life Sciences, National Chung Hsing University, Taichung 402, Taiwan

[5]Doctoral Program in Medical Biotechnology, National Chung Hsing University, Taichung 402, Taiwan

[6]Biotechnology Center, National Chung Hsing University, Taichung 402, Taiwan

[7]Innovation and Development Center of Sustainable Agriculture, National Chung Hsing University, Taichung 402, Taiwan

[8]Advanced Plant and Food Crop Biotechnology Center, National Chung Hsing University, Taichung 402, Taiwan

***Corresponding authors:**
Chieh-Chen Huang
(cchuang@dragon.nchu.edu.tw)
Patrick C. Y. Woo
(pcywoo@hku.hk)

Citation: Woo PCY, Lin Y, Huang S, Chen M, Hou M, Huang C. Mx. BIOME: A bioinformatics and big data analysis platform in a data explosion era. *Microbes & Immunity*. 2025;2(4):61-66. doi: 10.36922/mi.5077

Received: October 8, 2024

Revised: December 4, 2024

Accepted: January 2, 2025

Published online: February 3, 2025

Abstract

With the development of next-generation sequencing and other technologies, there has been an exponential increase in DNA, RNA, and protein sequences and protein structures in the last two decades, paralleled with the advancement of user-friendly bioinformatics tools. Furthermore, the enormous improvement in computational power and accumulation of massive amounts of data has given rise to the development of big data analysis, which can unveil novel patterns, associations, and trends. In view of the unprecedented biological data explosion, we have recently developed a platform known as Mx. BIOME, which provides a collection of some of the most popular and cutting-edge tools in the fields of bioinformatics and big data analysis. Such a collection would facilitate end-users to identify suitable tools for analyzing their specific datasets. Further studies and reviews on various *in silico* tools are necessary to compare the advantages and limitations.

Keywords: Bioinformatics; DNA; Sequencing; Big data; Analysis; SARS-CoV-2

The unprecedented explosive growth of DNA sequences and other biological data in the past 50 years comes with an ever-growing need for rapid and accurate analysis of vast amounts of data. First developed by Fred Sanger in the 1970s, DNA sequencing entails a highly labor-intensive process. Also known as Sanger sequencing, this technique works on the principle of the chain termination method, which requires labeling bases with radioactive phosphorus, running long polyacrylamide sequencing gel, developing and fixing X-ray films, and manually analyzing and interpreting the sequencing results.[1] Automation of the traditional Sanger sequencing methods became possible with the development of the automated sequencer toward the end of the last millennium. In

the subsequent years, efficiency was further improved following the capacity expansion of the sequencing machine from handling one sample to multiple samples at a time. Such remarkable improvements in Sanger sequencing technologies led to the tremendous growth in DNA sequencing data across various fields.

In the past two decades, DNA sequencing technology has undergone a further breakthrough, transitioning from the traditional Sanger sequencing to several high-throughput, short-read, second-generation sequencing technologies. This significant development started with the launch of the 454 pyrosequencing platform 20 years ago.[2] However, the Illumina platform emerged as the market leader, and the HiSeq™ Sequencing System has become the most popular one. An approach different from Sanger sequencing, the sequencing by synthesis technology from the Illumina HiSeq™ platform requires DNA template amplification before sequencing. Fluorescent-labeled reversible terminator nucleotides are incorporated into the elongating DNA strands and then imaged through fluorophore excitation at the genomic composition bias.

Another significant development happened in 2011 when Pacific Biosciences launched the first PacBio® RS sequencing platform to the market. This sequencing platform did not require genomic DNA amplification, hence addressing one of the major challenges of second-generation sequencing technologies. This platform employed a real-time single molecule detection technology, enabling real-time sequencing of individual polymerase molecules with lesser bias and longer reads.[3,4] However, this technology was noted to be associated with a tendency to sequence errors. With enhancements in its chemistry and software, iterations of the subsequent sequencer have demonstrated substantial improvements in accuracy, throughput, and read length compared to earlier models. Recently, the MinION sequencer (Oxford Nanopore Technologies) has made next-generation sequencing even more user-friendly.[5] Featured with short turnaround time, portable size, and low equipment cost, this device enables small laboratories to perform their own in-house next-generation sequencing experiments. The advent of these robust next-generation sequencing technology platforms has resulted in the generation of DNA sequencing data on a massive, industrial scale, an obvious example of which is the exponential growth of the GenBank database.

Alongside the rapid generation of DNA and RNA sequences, there has been a huge expansion of other biological data, such as protein sequences and protein structures. Across biomedical science fields, analysis of vast amounts of these biological data for deciphering their meaning, testing hypotheses, and generating novel ideas essentially requires the most advanced bioinformatics tools that have effectively harnessed the exponential expansion in computation power, as observed by Moore's Law. Thirty years ago, having some knowledge of computer programming and the expertise in inputting commands were often prerequisites for using the *state-of-the-art* bioinformatics tools. However, bioinformatics tools have gradually become more user-friendly in the last 20 years, a metamorphosis similar to the evolution of the *IBM* word processor in the 1980s to *Microsoft Word*. In the present day, bioinformatics analysis can be easily executed even by scientists with minimal knowledge of computer programming. On the other hand, the proliferation of bioinformatics tools could have bewildered students, post-doctoral fellows, and even some experienced scientists.

For many centuries, scientific discoveries have typically been made following the conventional approach of *The Scientific Method*, which involves the step-by-step process from formulating a hypothesis to gathering relevant, high-quality data for hypothesis testing, analyzing the data collected, and finally drawing conclusions. In recent times, the immense advancements in computational power, coupled with the accumulation of massive amounts of data generated over the years, have given rise to the development of big data analysis as a fast-growing discipline with wide applications across various industries and sectors.[6,7] The huge amounts of structured and unstructured data used in big data analysis often consist of retrospective data that are pooled from multiple sources, involving hundreds or even thousands of individuals or parties with varying levels of expertise and training in data collection. Such datasets are typically stored in databases which are made accessible to the public, or in cases where the datasets are owned by an organization, they can be readily retrieved by its members. Using advanced statistical tools to examine large, complex datasets, big data analysis is capable of unveiling novel patterns, associations, and trends. As a result, it offers fresh conclusions and new insights, which conventional analysis of smaller datasets generated by individual research groups would not have the capacity to achieve. However, it is necessary to be mindful of "garbage in, garbage out" data quality: To derive reliable conclusions, it is crucial that the data used for analysis are of high quality.[8]

In view of the unparalleled explosion of data on all fronts of biology, we have recently developed a platform named Mx. BIOME, which provides a collection of some of the most popular and cutting-edge tools suitable for use in multiple disciplines of bioinformatics analysis and big data analysis (http://mxbiome.nchu.edu.tw). The designation "Mx. BIOME" symbolizes the entirety of living cells, each comprising informational components regardless of

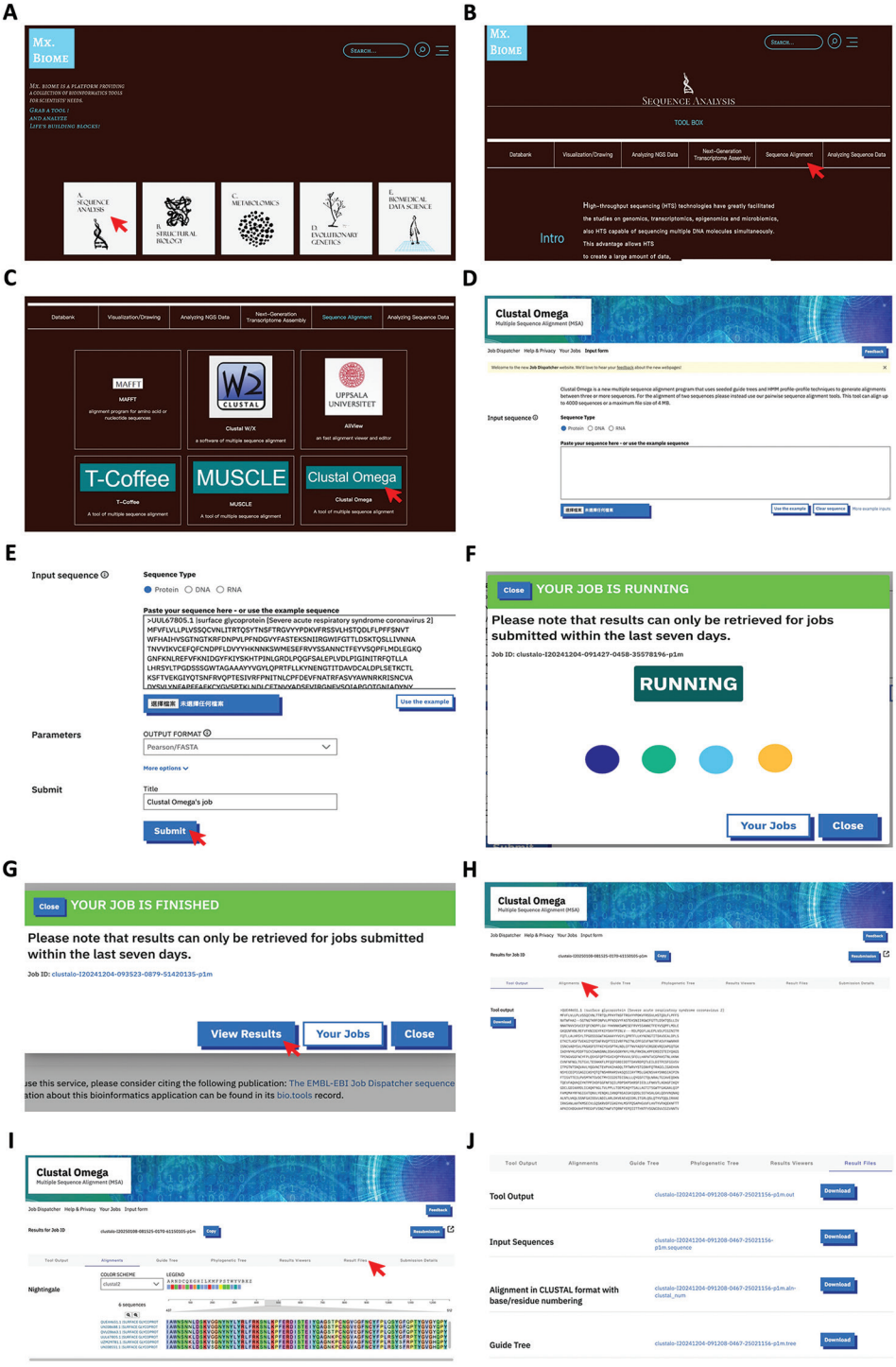

Figure 1. Use of Mx. BIOME for multiple sequence alignment of spike protein sequences from SARS-CoV-2 isolated from different phases of the COVID-19 pandemic in Taiwan. (A) Front page of Mx. BIOME. (B) Introduction page of "Sequence Analysis." (C) "Sequence Alignment" section of "Sequence Analysis." (D) Main page of Clustal Omega from the EBI website. (E) Six spike protein sequences of SARS-CoV-2 were pasted to the input box of Clustal Omega. (F) Running page of Clustal Omega. (G): Completing the running status page of Clustal Omega. (H) Output page of the sequences is displayed in FASTA format. (I) Snapshot of multiple sequence alignment results (AA 437 to AA 512), showing the difference among the ACE2 binding regions of the spike proteins. (J) Download page of the alignment results.

Abbreviations: AA: Amino acid; COVID-19: Coronavirus disease 2019; SARS-CoV-2: Severe acute respiratory syndrome coronavirus 2.

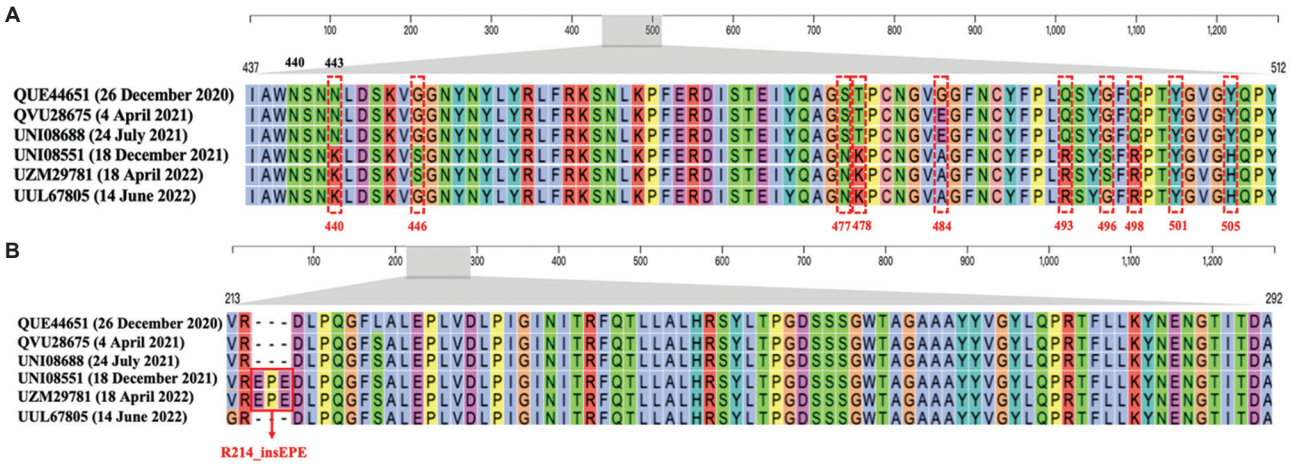

Figure 2. Multiple sequence alignment of S protein sequences from SARS-CoV-2 found in Taiwan. (A) Manual annotation of AA 437 to AA 512 of the multiple sequence alignment results shown in Figure 1I (after rearranging the strains in chronological order), indicating the difference in amino acid sequences of the six spike proteins at 10 amino acid positions. The numbers in red and the dashed boxes represent the amino acid positions described by Zhou *et al.*[20] for the different SARS-CoV-2 variants.[20] The discrepancy between the amino acid position numbers in the present alignment and those by Zhou *et al.*[20] is due to an insertion of three amino acids EPE at AA 215 to AA 217 for the two omicron variant sublineage BA.1 strains. (B) Multiple sequence alignment of AA 213 to AA 292 shows the unique insertion of the three amino acids EPE for the two omicron variant sublineage BA.1 strain (red box).

Abbreviations: AA: Amino acid; SARS-CoV-2: Severe acute respiratory syndrome coronavirus 2.

their individual attributes, and the perpetual flux of life finds manifestation through bioinformation. The tools in this platform were broadly grouped into five categories: sequence analysis, structural biology, metabolomics, evolutionary genetics, and biomedical data science, with some of them developed by scientists from our university.[9-19] Such a collection of tools would facilitate end-users to identity suitable tools for analyzing their specific datasets. Further studies and reviews on the various *in silico* tools are necessary to compare their advantages and limitations.

To illustrate the use of Mx. BIOME for microorganism study, we performed multiple sequence alignment for six spike protein sequences from six severe acute respiratory syndrome coronavirus 2 (SARS-CoV-2) strains isolated from different phases of the COVID-19 pandemic in Taiwan. Multiple sequence alignment is one of the first steps in analyzing microbial DNA/RNA or protein sequences, which involves the alignment of nucleotide or amino acid sequences to identify regions of identity and similarity. Such regions are important because they represent functional and evolutionary relationships between the sequences. In multiple sequence alignment tools, the nucleotide or amino acid residues are represented as rows in a matrix, with gaps inserted between the residues so as to generate the most optimal alignments with maximum identity and similarity as determined by the algorithm used in the tool. The commonly used multiple sequence alignment tools include T-Coffee, MUSCLE, Clustal Omega, and MAFFT. These tools differ by the algorithms used, maximum number of sequences they can handle, the level of user-friendliness of the interface, etc.

In the current exercise, Clustal Omega was chosen as the multiple sequence alignment tool. To begin the multiple sequence alignment exercise, we downloaded six spike protein sequences from six SARS-CoV-2 genomes from the NCBI virus database (https://www.ncbi.nlm.nih.gov/labs/virus/vssi/#/), representing SARS-CoV-2 isolated from different phases of the COVID-19 pandemic in Taiwan.

From the front page of Mx BIOME, "Sequence Analysis" was clicked (Figure 1A), then "Sequence Alignment" (Figure 1B), then "Clustal Omega" (Figure 1C), which brought us to the main page of Clustal Omega from the EBI website (Figure 1D). The six spike protein sequences were pasted into the input box, and FASTA was chosen as the output format (Figure 1E). The alignment process started when "Submit" was clicked (Figure 1F). A few seconds later, when the screen indicated that the alignment was finished, "View Results" was clicked (Figure 1G), and the input sequences were shown again (Figure 1H). When "Alignments" was clicked, the multiple sequence alignment of the six spike protein sequences was displayed (Figure 1I). When "Results Files" was clicked, the page on which the results could be downloaded appeared (Figure 1J).

Further manual analysis confirmed that the three spike proteins from SARS-CoV-2 strains isolated on December 26, 2020, April 4, 2021, and July 24, 2021, with specific mutation A570D, belonged to the alpha variant sublineage

B.1.1.7; the two spike proteins from SARS-CoV-2 strains isolated on December 18, 2021 and April 18, 2022, with specific insertion R214_insEPE, belonged to the omicron variant sublineage BA.1; and that from the SARS-CoV-2 strain isolated on June 14, 2022, with specific mutation V213G, belonged to the omicron variant sublineage BA.2 (Figure 2). Similar to multiple sequence alignment, phylogenetic analysis, three-dimensional structural modeling, the interaction of spike protein with its ACE2 receptor, etc., could be analyzed rapidly using various bioinformatics tools cataloged in Mx. BIOME.

Acknowledgments

None.

Funding

This work was partly supported by the National Science and Technology Council (NSTC 112-2311-B-005-006-MY3) and the Feature Areas Research Center Program within the framework of the Higher Education Sprout Project by the Ministry of Education (MOE-113-S-0023-A) in Taiwan.

Conflict of interest

Patrick C. Y. Woo is an Editorial Board Member of this journal but was not in any way involved in the editorial and peer-review process conducted for this paper, directly or indirectly. Separately, other authors declared that they have no known competing financial interests or personal relationships that could have influenced the work reported in this paper.

Author contributions

Conceptualization: Patrick C. Y. Woo, Ming-Hon Hou, Chieh-Chen Huang
Writing – original draft: All authors
Writing – review & editing: All authors

Ethics approval and consent to participate

Not applicable.

Consent for publication

Not applicable.

Availability of data

Not applicable.

References

1. Sanger F, Nicklen S, Coulson AR. DNA sequencing with chain-terminating inhibitors. *Proc Natl Acad Sci U S A*. 1977;74(12):5463-5467.
doi: 10.1073/pnas.74.12.5463

2. Margulies M, Egholm M, Altman WE, *et al*. Genome sequencing in microfabricated high-density picolitre reactors. *Nature*. 2005;437(7057):376-380.
doi: 10.1038/nature03959

3. Eid J, Fehr A, Gray J, *et al*. Real-time DNA sequencing from single polymerase molecules. *Science*. 2009;323(5910):133-138.
doi: 10.1126/science.1162986

4. Teng JLL, Yeung ML, Chan E, *et al*. Pacbio but not illumina technology can achieve fast, accurate and complete closure of the high GC, complex *Burkholderia pseudomallei* two-chromosome genome. *Front Microbiol*. 2017;8:1448.
doi: 10.3389/fmicb.2017.01448

5. Lu H, Giordano F, Ning Z. Oxford nanopore MinION sequencing and genome assembly. *Genomics Proteomics Bioinformatics*. 2016;14(5):265-279.
doi: 10.1016/j.gpb.2016.05.004

6. Castillo M. The scientific method: A need for something better? *AJNR Am J Neuroradiol*. 2013;34(9):1669-1671.
doi: 10.3174/ajnr.A3401

7. Khamisy-Farah R, Gilbey P, Furstenau LB, *et al*. Big data for biomedical education with a focus on the Covid-19 era: An integrative review of the literature. *Int J Environ Res Public Health*. 2021;18(17):8989.
doi: 10.3390/ijerph18178989

8. Lau SKP, Woo PCY. Pitfalls in big data analysis: Next-generation technologies, last-generation data. *Diagn Microbiol Infect Dis*. 2019;94(2):209-210.
doi: 10.1016/j.diagmicrobio.2018.12.006

9. Chu YW, Chang KP, Chen CW, Liang YT, Soh ZT, Hsieh LC. miRgo: Integrating various off-the-shelf tools for identification of microRNA-target interactions by heterogeneous features and a novel evaluation indicator. *Sci Rep*. 2020;10(1):1466.
doi: 10.1038/s41598-020-58336-5

10. Huang CC, Chang CC, Chen CW, Ho SY, Chang HP, Chu YW. PClass: Protein quaternary structure classification by using bootstrapping strategy as model selection. *Genes* (*Basel*). 2018;9(2):91.
doi: 10.3390/genes9020091

11. Pan WJ, Chen CW, Chu YW. siPRED: Predicting siRNA efficacy using various characteristic methods. *PLoS One*. 2011;6(11):e27602.
doi: 10.1371/journal.pone.0027602

12. Tung CH, Chen CW, Guo RC, Ng HF, Chu YW. QuaBingo: A prediction system for protein quaternary structure attributes using block composition. *Biomed Res Int*. 2016;2016:9480276.

doi: 10.1155/2016/9480276

13. Tung CH, Chen CW, Sun HH, Chu YW. Predicting human protein subcellular localization by heterogeneous and comprehensive approaches. *PLoS One*. 2017;12(6):e0178832.

    doi: 10.1371/journal.pone.0178832

14. Chen CW, Lin MH, Liao CC, Chang HP, Chu YW. IStable 2.0: Predicting protein thermal stability changes by integrating various characteristic modules. *Comput Struct Biotechnol J*. 2020;18:622-630.

    doi: 10.1016/j.csbj.2020.02.021

15. Tung CH, Chien CH, Chen CW, Huang LY, Liu YN, Chu YW. QUATgo: Protein quaternary structural attributes predicted by two-stage machine learning approaches with heterogeneous feature encoding. *PLoS One*. 2020;15(4):e0232087.

    doi: 10.1371/journal.pone.0232087

16. Chen CW, Chang KP, Ho CW, Chang HP, Chu YW. KStable: A computational method for predicting protein thermal stability changes by K-Star with Regular-mRMR feature selection. *Entropy* (*Basel*). 2018;20(12):988.

    doi: 10.3390/e20120988

17. Chang CC, Tung CH, Chen CW, Tu CH, Chu YW. SUMOgo: Prediction of sumoylation sites on lysines by motif screening models and the effects of various post-translational modifications. *Sci Rep.* 2018;8(1):15512.

    doi: 10.1038/s41598-018-33951-5

18. Chien CH, Chang CC, Lin SH, Chen CW, Chang ZH, Chu YW. N-GlycoGO: Predicting protein N-glycosylation sites on imbalanced data sets by using heterogeneous and comprehensive strategy. *IEEE Access*. 8 2020;8:165944-165950.

    doi: 10.1109/ACCESS.2020.3022629

19. Chen CW, Huang LY, Liao CF, Chang KP, Chu YW. GasPhos: Protein phosphorylation site prediction using a new feature selection approach with a GA-aided ant colony system. *Int J Mol Sci*. 2020;21(21):7891.

    doi: 10.3390/ijms21217891

20. Zhou Z, Zhu Y, Chu M. Role of Covid-19 vaccines in sars-Cov-2 variants. *Front Immunol*. 2022;13:898192.

    doi: 10.3389/fimmu.2022.898192

ACCSCIENCE PUBLISHING

Microbes & Immunity

ORIGINAL RESEARCH ARTICLE

Impact of dietary emulsifiers on the presence of adherent-invasive *Escherichia coli* in Crohn's disease

Yu Lin[1,2†], Xiangqian Dong[3,4†], Hein Min Tun[2,5], Wenli Huang[1,2], Yinglei Miao[3,4], Juan Luo[3,4], Fengrui Zhang[3,4], Caroline Chevarin[6], Anthony Buisson[6,7], Nicolas Barnich[6], Jean-Frédéric Colombel[8], Francis Ka Leung Chan[2,9], Yang Sun[3,4*], Zhilu Xu[1,2*], and Siew Chien Ng[1,2*]

[1]Department of Medicine and Therapeutics, Faculty of Medicine, The Chinese University of Hong Kong, Hong Kong SAR, China

[2]Microbiota I-Center (MagIC), Hong Kong SAR, China

[3]Department of Gastroenterology, The First Affiliated Hospital of Kunming Medical University, Kunming, Yunnan, China

[4]Yunnan Province Clinical Research Center for Digestive Diseases, Kunming, Yunnan, China

[5]The Jockey Club School of Public Health and Primary Care, Faculty of Medicine, The Chinese University of Hong Kong, Hong Kong SAR, China

[6]Université Clermont Auvergne, Inserm U1071, INRAE USC 1382, Microbes, Intestin, Inflammation et Susceptibilité de l'Hôte (M2iSH), Clermont-Ferrand, France

[7]Université Clermont Auvergne, Inserm, 3iHP, CHU Clermont-Ferrand, Service d'Hépato-Gastro Entérologie, Clermont-Ferrand, France

[8]Department of Medicine, Division of Gastroenterology, Icahn School of Medicine at Mount Sinai, New York, United States of America

[9]Center for Gut Microbiota Research, Faculty of Medicine, The Chinese University of Hong Kong, Hong Kong SAR, China

[†]*These authors contributed equally to this work.*

***Corresponding authors:**
Siew Chien Ng
(siewchienng@cuhk.edu.hk)
Zhilu Xu
(lulux719@gmail.com)
Yang Sun
(sunyang_doctor@vip.sina.com)

Citation: Lin Y, Dong X, Tun HM, *et al*. Impact of dietary emulsifiers on the presence of adherent-invasive *Escherichia coli* in Crohn's disease. *Microbes & Immunity.* 2025;2(4):67-78.
doi: 10.36922/MI025230051

Received: June 6, 2025

Revised: July 18, 2025

Accepted: August 1, 2025

Published online: August 21, 2025

Abstract

Adherent-invasive *Escherichia coli* (AIEC) has been implicated in Crohn's disease (CD) pathogenesis. We aimed to evaluate the impact of dietary factors on the presence of AIEC in patients with CD and to identify AIEC-associated mucosa microbial signatures in regions with different urbanization levels. A total of 112 CD patients and healthy controls were recruited from a rural area in China (Yunnan). Clinical demographics, food additive questionnaires, and ileal biopsies were collected from subjects in rural China. AIEC was isolated from biopsy samples by an antibiotic protection assay. Correlation between AIEC presence and food additives was evaluated using multivariate logistic regression. In addition, a secondary dataset of an urban CD cohort (Hong Kong) was included for microbiome analysis. AIEC was detected in the ileal mucosa in 20.83% of patients with CD in rural China. Multivariate analysis showed that living in an urban area was associated with the presence of AIEC in CD patients. Carrageenan consumption was positively correlated with AIEC presence in CD. AIEC-positive CD patients with primary education consumed more carrageenan than AIEC-negative CD patients (p=0.008). AIEC presence in CD patients was associated with 23 microbial genera in both urban and rural areas. AIEC-positive CD patients showed a decrease in anti-inflammatory pathways. AIEC colonizes the gut mucosa of CD patients in a rural area of China, with its presence significantly

associated with higher carrageenan consumption. These findings suggest a potential link between dietary emulsifiers, microbial dysbiosis, and AIEC-related CD pathogenesis.

Keywords: Adherent-invasive *Escherichia coli*; Crohn's disease; Dietary emulsifiers

1. Introduction

Crohn's disease (CD) is an intestinal inflammatory disorder that predominantly affects the distal small intestine. The pathogenesis of CD involves a complex interplay between environmental factors, genetic variants, and abnormal gut microbiota, associated with a dysregulated immunological response.[1] Studies have shown that patients with CD had a reduced abundance of beneficial microbes such as *Faecalibacterium, Roseburia,* and *Clostridium* and an increased abundance of pathogenic commensals, including *Fusobacterium*, *Shigella*, and *Escherichia,* compared to healthy controls.[2,3] In particular, an increased abundance of adherent-invasive *Escherichia coli* (AIEC) is commonly detected in the terminal ileum of patients with CD.[4] AIEC has the ability to bind to the adhesion molecule receptor CEACAM6 on the membrane of enterocytes through type 1 pili,[5] and can invade and replicate in the intestinal epithelial cells. Moreover, the CEACAM6 receptor has been shown to be overexpressed in patients with CD, further facilitating AIEC adhesion in the intestinal epithelial cells.[6] Mechanistic studies have revealed that AIEC can infect macrophages and lead to the release of proinflammatory cytokines, including tumor necrosis factor-alpha and interleukin (IL)-1β.[7] AIEC could also prevent the restoration of normal gut microbiota in dextran sodium sulfate-induced colitis mice models after fecal microbiota transplantation.[8] Furthermore, AIEC is involved in the synthesis of propanediol dehydratase, which can increase the fermentation of propanediol and trigger T cells-induced intestinal inflammation in mice model.[9] Altogether, these findings suggest that AIEC can potentially aggravate abnormal immune responses in CD and contribute to chronic mucosal inflammation.

CD incidence has substantially increased in newly industrialized countries over the past few decades in parallel with rapid urbanization in these regions.[10] Some of the major culprits include early life exposure, consumption of highly processed foods, and changes in hygiene and socioeconomic status.[11-13] The interaction between the host and environment during urbanization may play a role in initiating CD.[14] A migrant study from Canada reported that immigration from developing countries at a younger age was associated with an increased risk of inflammatory bowel disease (IBD), suggesting that early exposure to an urbanized environment may contribute to the development of IBD.[15] Food additives in processed foods, such as emulsifiers, have recently been shown to induce chronic intestinal inflammation in rodents and may potentially play a role in the development and exacerbation of IBD in humans.[16] Common food emulsifiers, such as polysorbate-80 and carboxymethylcellulose, promoted gut inflammation in gnotobiotic mice colonized by AIEC.[17] Another emulsifier, carrageenan, was associated with altered gut microbiome composition and increased expression of pro-inflammatory molecules in an *in vitro* cultivation system.[18]

Importantly, despite experimental evidence linking emulsifiers to AIEC pathogenicity, no human population studies have examined this interaction. Our work addresses this gap by providing the first human evidence linking dietary carrageenan to AIEC prevalence in CD patients and uncovering diet-microbe-pathogen interactions in CD pathogenesis. We further identify AIEC-associated mucosal microbiota signatures, providing novel insights into how urban environmental exposures and diet may interact with microbial factors in the pathogenesis of CD. These findings offer translational insights into how urbanization and diet may synergistically promote AIEC-driven CD.

2. Materials and methods

2.1. Study population

The study population consisted of patients with CD residing in urban and rural areas of China and their corresponding controls. The rural cohort was recruited from the First Affiliated Hospital of Kunming Medical University in Yunnan (population density <1000/km^2)[19] between August 2018 and January 2019. Patients with CD were diagnosed based on endoscopic, radiological, and histological examinations. Healthy controls were subjects who underwent colonoscopies without gastrointestinal diseases in the same hospital. All subjects filled out questionnaires that measured the social demographics and clinical characteristics, and questionnaires that recorded the consumption of food additives. The estimation of food additive intake in each subject was described in the Supplementary Methods section

(Supplementary File). The food additives questionnaire was validated in a CD survey across Australia, Hong Kong, and mainland China to identify the exposure to food additives in CD patients and healthy controls.[11,20] Our study also incorporated a secondary dataset of CD patients and healthy controls from Hong Kong as an urban cohort.[8] The subjects in the urban cohort were recruited from the Prince of Wales Hospital in Hong Kong (population density = 6582.6/km^2).[21] All participants had not been exposed to antibiotics, probiotics, or prebiotics in the past three months before enrollment. All participants gave informed consent, and the study was conducted in accordance with the Declaration of Helsinki. The identification of AIEC presence, sample DNA extraction, and 16S amplicon sequencing were detailed in the Supplementary Methods section. The study was approved by the Research Ethics Committee of the First Affiliated Hospital of Kunming Medical School (reference no. 2017.L.15-1).

2.2. Statistical analysis

Characteristics of CD patients with and without AIEC presence were reported. Data were presented as counts for categorical variables with percentages, and the mean or median for continuous variables with standard deviation or interquartile range. In univariate analysis, the Wilcoxon rank sum test was applied to determine the statistical significance for continuous variables, and Pearson's Chi-squared test was used to identify the statistical difference for categorical variables. The food additives difference between CD patients with and without AIEC presence was calculated using the smd package to obtain the Standardized Mean Difference. Multivariate logistic regression was used to assess the relationship between the risk factors and outcome, with confounders adjusted. We evaluated the association between CD and AIEC presence and the association between AIEC presence and consumption of food additives in the rural cohort. Finally, the impact of urbanization on AIEC prevalence was analyzed in CD patients from rural and urban regions.

2.3. The 16S amplicon sequencing analysis

The taxonomy annotation and functional prediction for the mucosal microbiome sequencing data are detailed in the Supplementary Methods section. For alpha diversity analysis, Shannon diversity and Observed Features were calculated using the operational taxonomic units table that was rarefied to 10,000 sequences per sample. In addition, Bray–Curtis distance was calculated for all samples, and the analysis of similarities (ANOSIM) test was used to identify the statistical difference in beta diversity. The explanation of host factors on the microbiome composition variation was identified by the permutational multivariate analysis of variance (PERMANOVA) test. Differentially abundant taxa and functional modules were identified using a linear mixed model with the geographic region as a random effect. The batch effect of microbiome data was adjusted by the MMUPHin method.[22] A sensitivity analysis was performed to verify the robustness of differentially abundant taxa using the adjusted microbiome data. After selecting the significantly different genera, we validated the discrimination ability of selected microbial genera using the random forest model. Five-fold cross-validation was applied during the model training. The model was trained in 80% of CD patients from two cohorts and validated on the remaining 20% of CD patients and those patients from different regions. We also compared the functional differences in CD patients with and without AIEC presence using a linear mixed model.

3. Results

3.1. The presence of AIEC was significantly associated with CD risk and carrageenan intake

The study design is illustrated in the Graphical Abstract. A total of 112 subjects, including 72 CD patients and 40 healthy controls from a rural area (Yunnan, China), were recruited (Figure S1). AIEC was detected in 20.83% of CD patients and 12.50% of healthy controls (p=0.270, Table 1). Among CD patients, AIEC presence was significantly associated with lower educational attainment (p=0.023), with 33.0% of AIEC-positive patients having no formal education compared to 7.0% of AIEC-negative patients (Table 2). Multivariate logistic regression showed a significant association between AIEC presence and increased CD risk (adjusted Odds Ratio [aOR] = 7.50, 95% confidence interval [CI]: 1.04–54.23, p=0.046, Figure 1A and Table S1). Low education level (middle school) was positively associated with CD risk (aOR = 8.20, 95% CI: 1.35–49.71, p=0.022), whereas body mass index (BMI) was negatively associated with CD risk (aOR = 0.77, 95% CI: 0.65–0.9, p=0.001). CD patients consumed more aluminum silicate (8382 mg/year vs. 2092 mg/year, p=0.038) and titanium dioxide (127151 mg/year vs. 29664 mg/year,

Table 1. AIEC prevalence in the urban and rural cohorts

Area	AIEC-positive rate (%)	AIEC-positive	AIEC-negative	p-value†
Rural CD	20.83	15	57	0.270
Rural HC	12.50	5	35	
Urban CD	30.00	18	42	0.003
Urban HC	7.14	4	52	

Notes: †p-value was calculated according to Pearson's Chi-squared test. Abbreviations: AIEC: Adherent-invasive *Escherichia coli*; CD: Crohn's disease; HC: Healthy controls.

Table 2. The characteristics of CD patients in AIEC-positive and AIEC-negative groups in the rural cohort

Characteristic	AIEC-positive (*n*=15)	AIEC-negative (*n*=57)	*p*-value
Age[†]	45 (20)	39 (23)	0.220
BMI[†]	20.8 (4.6)	20.8 (5.3)	0.792
Surgery history[‡] (%)	9 (60.0)	29 (50.9)	0.735
Education level[§] (%)			
College/University	6 (40.0)	18 (31.6)	0.023
Middle school	2 (13.3)	24 (42.1)	
No formal schooling	5 (33.3)	4 (7.0)	
Primary school	2 (13.3)	11 (19.3)	
Smoker status[§] (%)			
Ex-smoker	3 (20.0)	5 (8.8)	0.400
Non-smoker	11 (73.3)	42 (73.7)	
Smoker	1 (6.7)	10 (17.5)	
Alcohol consumption[§] (%)			
Current drinker	2 (12.3)	2 (3.5)	0.481
Former drinker	1 (6.7)	7 (12.3)	
Lifetime abstainer	12 (80)	47 (82.4)	
Other	0 (0)	1 (1.8)	
CD Location[§]			
L1	2 (13.3)	6 (10.5)	0.476
L2	4 (26.7)	8 (14.0)	
L3	9 (60.0)	38 (66.7)	
Other	0 (0)	5 (8.8)	

Notes: The number in each cell denotes the median (interquartile range) for the continuous variables or *n* (%) for the categorical variables. CD Location indicates areas in the gastrointestinal tract affected by CD: ileal (L1), colonic (L2), ileocolonic (L3), and others. [†]Wilcoxon rank sum test; [‡]Pearson's Chi-squared test; [§]Fisher's exact test.
Abbreviations: AIEC: Adherent-invasive *Escherichia coli*; BMI: Body mass index; CD: Crohn's disease.

p=0.035) than healthy controls (Table S2). Among CD patients, AIEC presence was associated with higher carrageenan consumption (aOR = 4.49, CI: 1.28–15.75, *p*=0.019, Figure 1B and Table S3), with the largest observed difference among patients with primary education (Standardized Mean Difference, SMD = 3.810, *p*=0.008; Table S4 and Figure S2).

3.2. The presence of AIEC was associated with urbanization and mucosal microbiota dysbiosis

To assess the impact of urbanization on mucosal microbiota and AIEC prevalence, we compared data from the current rural cohort with our previous cohort of 116 patients with CD and healthy controls recruited from an urban area (Hong Kong).[8] We found that the prevalence of AIEC was significantly higher in patients with CD only in the urban area (*p*=0.003) but not in the rural area (*p*=0.31) (Table 1). Multivariate analysis showed a positive association between AIEC risk and living in an urban area in CD patients (aOR = 2.56, 95% CI: 1.03–6.38, *p*=0.04, Table S5). Principal coordinates analysis showed that there were two distinct clusters of individuals living in urban and rural areas (ANOSIM test R = 0.22, *p*=0.001, Figure 2A). PERMANOVA test indicated that geographic regions accounted for larger differences in the gut microbiome composition and functional pathways than CD diagnosis and the presence of AIEC (Figure 2B). For the alpha diversity, Shannon and Observed Features were significantly decreased in AIEC-positive CD patients in the urban area (*p*=0.011) but not in the rural area (Figure S3A and B). A linear mixed model identified 23 microbial genera associated with AIEC presence (Figure 2C). Among these genera, *Bacillus*, *Delftia*, and *Roseburia* were also decreased in AIEC-positive CD patients in our previous study.[8] *Finegoldia* and *Rhodococcus* have been reported as pathogens in the periprosthetic joint infection[23] and pneumonia.[24]

We further performed sensitivity analysis using MMUPHin to eliminate potential batch effect and found 16 microbial genera were significantly different in AIEC-positive CD patients (Figure 3A). Fifteen of them were also identified as differentially abundant taxa before batch effect correction, indicating that the selected taxa were relatively robust. A random forest model showed stronger classification performance for AIEC status in urban patients than in rural patients (median AUC from rural: 0.700 vs. median AUC from urban: 0.850, Figure 3B), suggesting that AIEC-associated microbiome signatures were more distinct in urban settings.

3.3. AIEC presence was associated with reduced acetate production capacity

We identified nine functional pathways associated with AIEC presence in rural and urban CD patients using the linear mix model, with most of these pathways being depleted in AIEC-positive groups. Among these pathways, anti-inflammatory pathways such as L-glutamate and L-glutamine biosynthesis (*p*=0.009), chondroitin sulfate degradation I (*p*=0.031), and acetylene degradation (*p*=0.017) were reduced in AIEC-positive groups (Figure 4A and Table S6). Acetylene degradation is a crucial pathway for acetate (one of the short-chain fatty acids [SCFAs]) production.[25] Among 23 microbial genera that were associated with AIEC presence, 21 AIEC were positively associated with these nine functional pathways (Figure 4B), suggesting that the genera depleted in AIEC-positive CD patients may contribute to the reduced functional pathways.

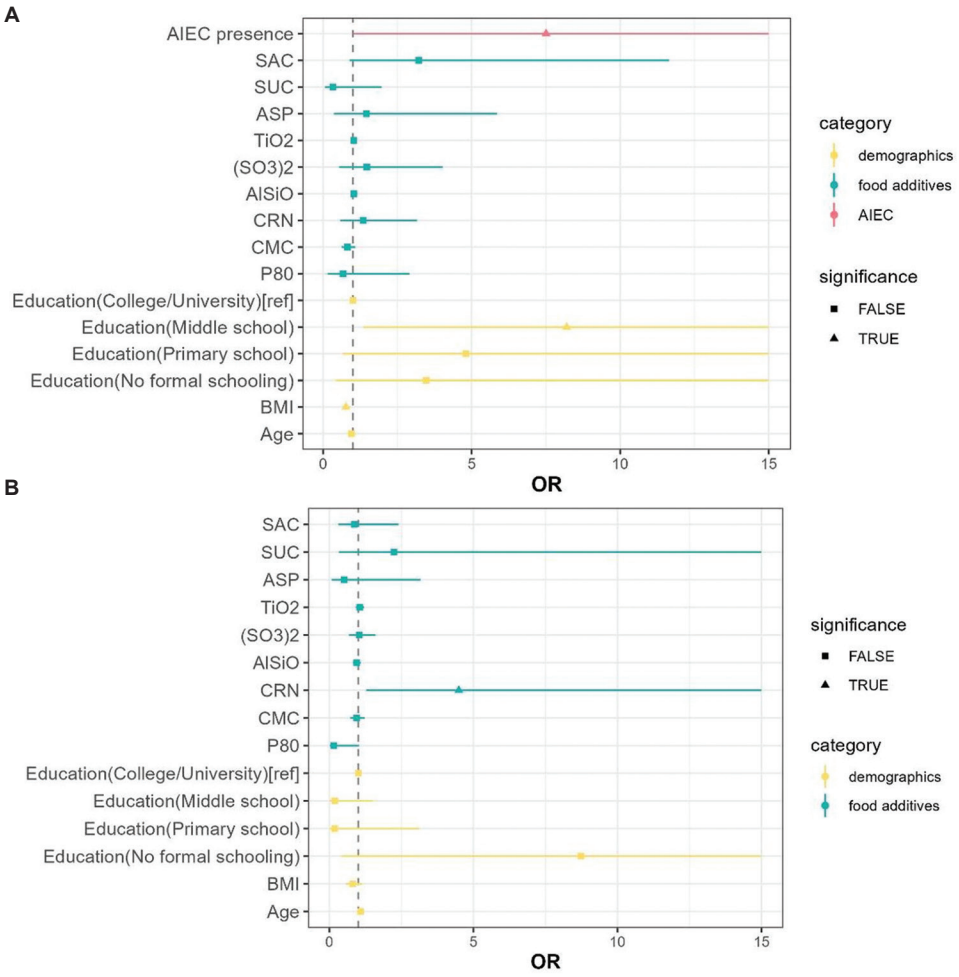

Figure 1. The association between AIEC presence, CD risk, and food additives exposure in the rural cohort. (A) Logistic regression analysis showing factors associated with CD risk. Predictors are grouped into three categories: AIEC presence (pink), demographic variables (yellow), and food additives (blue). Odds ratios with 95% confidence intervals are shown. Triangles indicate statistically significant associations ($p<0.05$), and squares indicate non-significant results. (B) Factors associated with AIEC presence in CD patients from the same rural cohort. Food additives and demographic variables are assessed for their contribution to AIEC presence.

Abbreviations: AIEC: Adherent-invasive *Escherichia coli*; AlSiO: Aluminum silicate; ASP: Aspartame; CD: Crohn's disease; CMC: Carboxymethylcellulose; CRN: Carrageenan; P80: Polysorbate-80; SAC: Saccharine; $(SO_3)_2$: Sulfite; SUC: Sucralose; TiO_2: Titanium dioxide.

4. Discussion

Our study provides the first human population-based evidence linking dietary factors to AIEC prevalence in CD patients. We demonstrate that AIEC is present in CD patients residing in a rural area, with the prevalence lower than that in urban areas. We found that urbanization was associated with increased AIEC prevalence, and that AIEC presence was significantly associated with CD risk and carrageenan intake. These results suggest that dietary emulsifiers may promote AIEC colonization and contribute to CD pathogenesis.

Our study revealed a significant association between AIEC and CD risk after adjusting for education level and food additives. This is consistent with a positive correlation between AIEC and CD reported in a meta-analysis.[26] We found that nearly half of AIEC-positive CD patients had lower education levels compared to AIEC-negative patients. AIEC-positive CD patients with low education levels consumed higher amounts of food additives, specifically carrageenan, than AIEC-negative CD patients. It is highly possible that subjects with low education levels tend to choose foods containing additives than those with high education levels.[27]

Our findings indicate a positive association between urbanization and AIEC prevalence, which may be influenced by accompanying changes in diet and lifestyle. Prior studies from our team reported that the dietary habits differed significantly between people living in Yunnan and

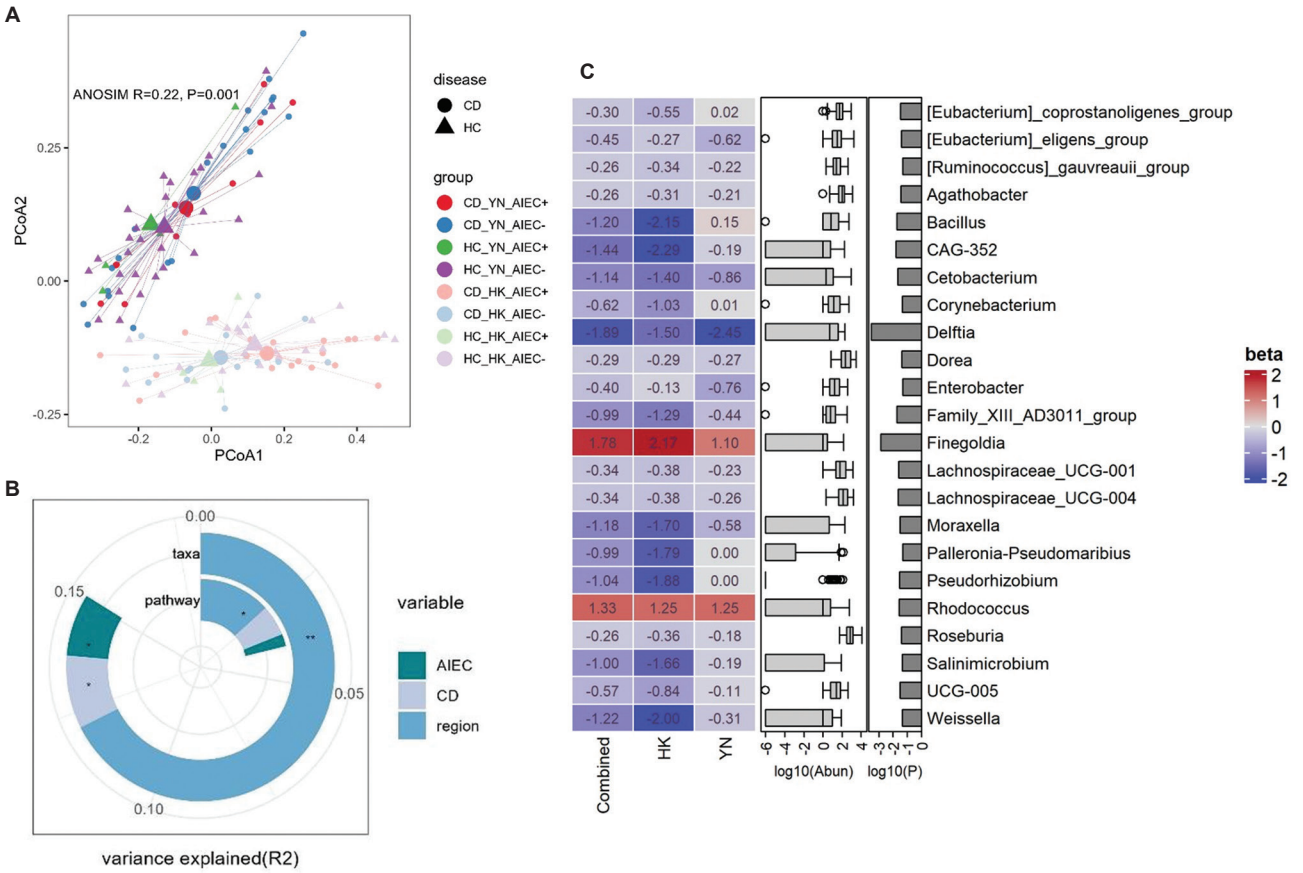

Figure 2. The effect of AIEC on mucosal microbiome composition across rural and urban cohorts. (A) Principal coordinates analysis based on Bray–Curtis distance, comparing microbiome profiles between AIEC-positive and AIEC-negative individuals across CD patients and HCs. The microbiome composition difference between groups was identified by the analysis of similarities test. (B) Permutational analysis of variance (PERMANOVA) showing the proportion of variation in microbiome composition explained by AIEC presence, disease status (CD vs. HC), and geographic region (Hong Kong vs. Yunnan). *p<0.05, **p<0.001. (C) Differentially abundant microbial genera associated with AIEC presence. Heatmap displays the beta coefficients of genera in combined CD patients were calculated using the linear mixed model with the formula ($\log_{10}$(taxa abundance) ~ AIEC presence + (1|region)). The beta coefficients of genera in each cohort were calculated using the linear regression model with the formula ($\log_{10}$(taxa abundance) ~ AIEC presence). Boxplots show the $\log_{10}$-transformed abundance of each genus. Boxplots show p-values with the $\log_{10}$ transformation identified from the linear mixed model.

Abbreviations: AIEC: Adherent-invasive *Escherichia coli*; CD: Crohn's disease; HC: Healthy control; HK: Hong Kong; YN: Yunnan.

Hong Kong, with work stress and dietary habits as the most important factors in explaining the gut mycobiome and virome variation.[28,29] Although Yunnan's vegetable- and mushroom-rich diet likely reduces additive exposure, the persistent association between AIEC and CD, similar to Western populations, suggests that diet and urbanization may not be the only factors affecting the association between AIEC and CD. Absence of dietary fiber was shown to promote AIEC colonization in mice.[30] However, no significant differences in AIEC prevalence and AIEC-associated virulence genes were found between omnivores and vegans consuming high-fiber diets in a human study.[31] Another possible factor was antibiotic usage, as our previous studies reported a higher prevalence of antibiotic-resistant genes in Hong Kong AIEC strains versus France AIEC strains.[8,32] Nevertheless, we did observe lower AIEC prevalence in Yunnan, compared to Hong Kong and France. These findings reinforce that while multiple environmental factors may influence AIEC epidemiology, dietary emulsifiers associated with urbanized lifestyles appear to play a prominent role.

Carrageenan can impact gut health in many ways. The degradation product of carrageenan, poligeenan, can be produced during gastric digestion of carrageenan, triggering the release of inflammatory cytokines.[33] Carrageenan can activate toll-like receptor-4 and stimulate the production of IL-6 in the immune response in mice, further exacerbating gut inflammation.[34] Furthermore, piglets receiving both carrageenan and AIEC infusion exhibited higher fecal

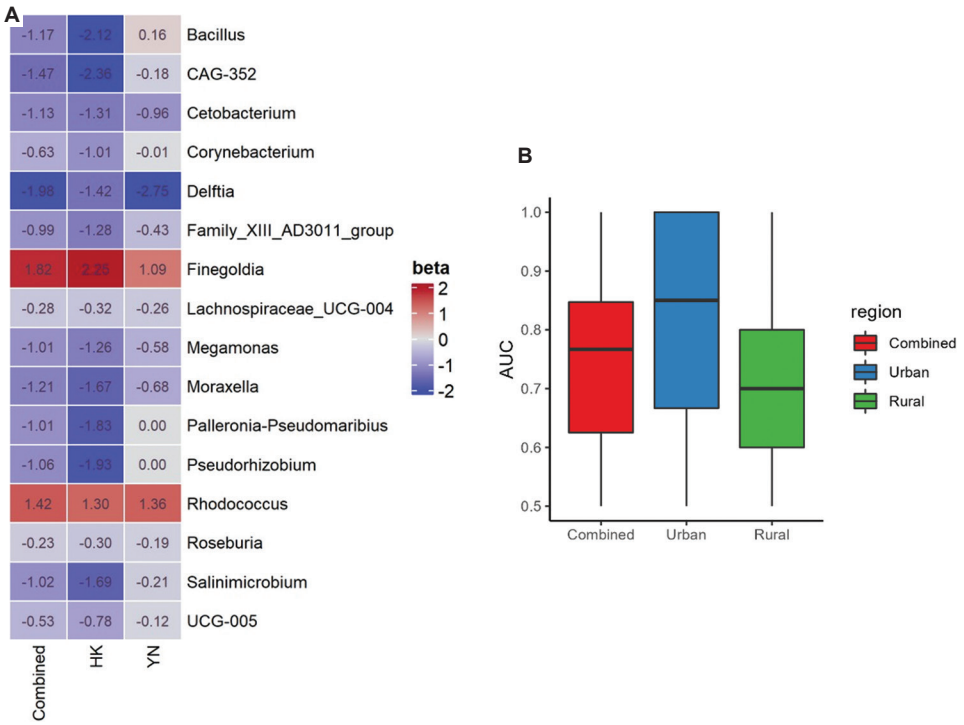

Figure 3. Sensitivity analysis and classification modeling of AIEC presence in CD patients. (A) Heatmap of differentially abundant mucosal microbial genera associated with AIEC presence, after adjusting for batch effect using the MMUPHin approach. For the combined cohort, the beta coefficients of genera based on adjusted data were calculated using a linear mixed model with the formula ($\log_{10}$(taxa abundance) ~ AIEC presence + (1|region)). The beta coefficients of genera in each cohort were calculated using the linear regression model with the formula ($\log_{10}$(taxa abundance) ~ AIEC presence). (B) Performance of a random forest model trained to predict AIEC presence in CD using the selected 23 microbial taxa. Five-fold cross-validation was performed to distinguish AIEC presence in CD patients. The model was validated on the combined CD patients (red), and CD patients from the urban (blue), and rural cohorts (green) in each fold of cross-validation.
Abbreviations: AIEC: Adherent-invasive *Escherichia coli*; CD: Crohn's disease; HK: Hong Kong; YN: Yunnan.

score and IL-6 levels in the ileum compared to the group receiving carrageenan alone.[35] Our findings align with preclinical evidence that: (i) Emulsifiers in mice disrupts the balance between cell proliferation and apoptosis, thereby altering the intestinal microenvironment;[36] (ii) emulsifiers have no significant effect on germ-free mice, indicating that their impact is dependent on the gut microbiome;[16] (iii) emulsifiers can enhance the expression of virulent genes in AIEC, promote its penetration of the mucus layer, and subsequently induce intestinal inflammation and increase disease susceptibility.[17] Taken together, these findings support the hypothesis that emulsifiers influence AIEC pathogenicity through microbiota-mediated mechanisms that compromise intestinal homeostasis. Our study provided the first human evidence that there is an association between dietary emulsifiers and AIEC presence in CD patients. However, given the observational nature of our study, we cannot infer a causal relationship between carrageenan intake and AIEC colonization or inflammation.

We identified several co-differentially abundant microbial genera that were associated with the presence of AIEC. Among them, *Finegoldia* has been associated with CD relapses, inducing gut inflammation through the interaction with human neutrophils,[37,] and *Rhodococcus* was reported to be increased in patients with ulcerative colitis.[38] Several anti-inflammatory SCFAs producers, including *Roseburia*, *Dorea*, *and* Agathobacter, were significantly reduced in AIEC-positive CD patients. One of the SCFAs, butyrate, was known to protect against AIEC-induced mitochondrial dysfunction to reduce gut inflammation.[39] In addition, we found a depletion of *Ruminococcus gauvreauii* group in AIEC-positive CD patients, and the deficiency of *Ruminococcus* was also reported in the recurrent CD patients with AIEC colonization.[40] In the functional analysis, several anti-inflammatory functional pathways were reduced in AIEC-positive CD patients, such as the L-glutamate and L-glutamine biosynthesis, acetylene degradation, and chondroitin sulfate degradation I. Glutamine was shown to alleviate inflammation in CD patients by maintaining the integrity of the intestinal mucosa through increasing the level of heat shock proteins and reducing the expression

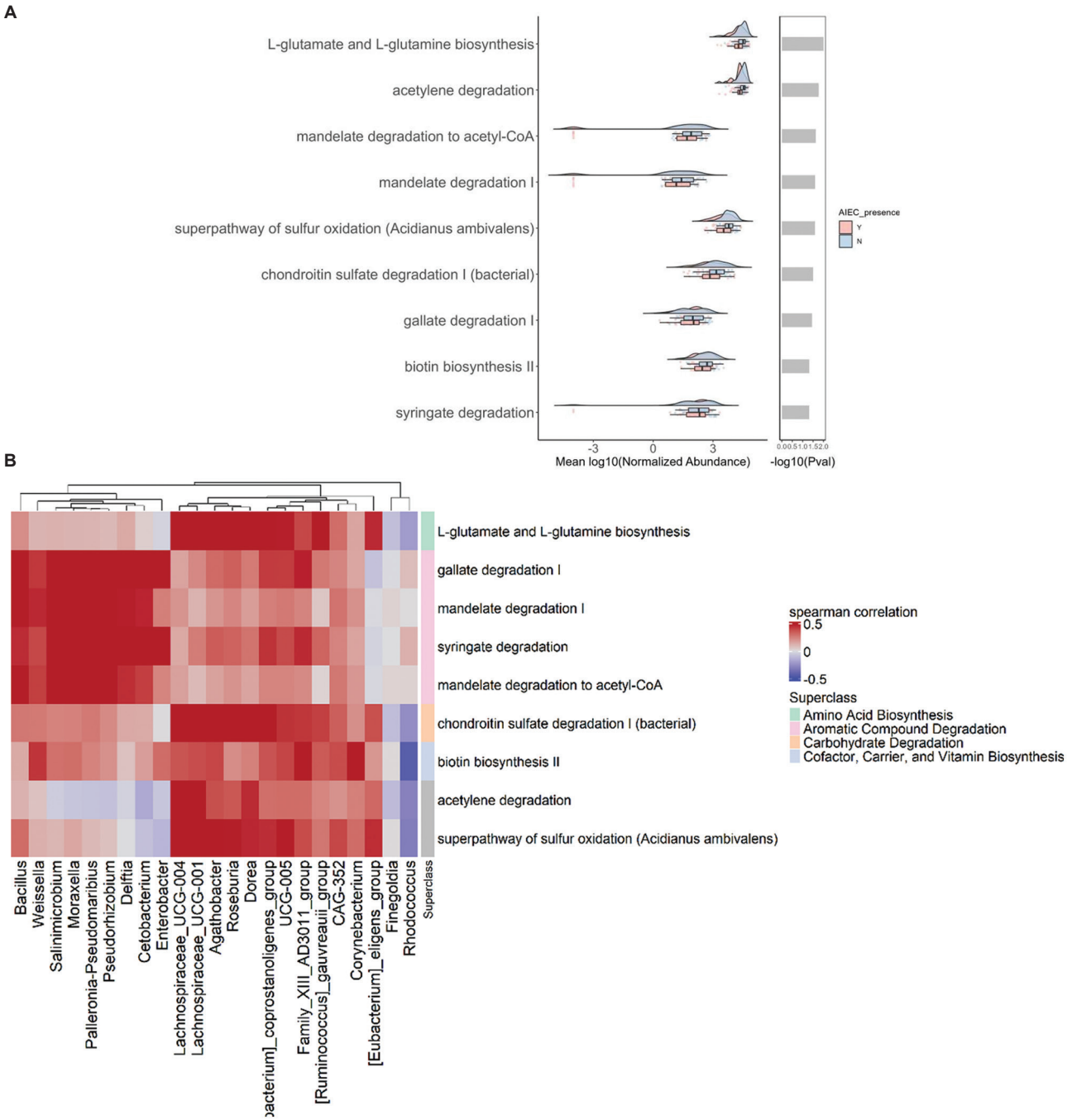

Figure 4. Function analysis of AIEC-related pathways in CD patients. (A) Differential functional pathways associated with AIEC presence in CD patients, as identified by a linear mixed model. The left panel displays boxplots showing $\log_{10}$-transformed normalized abundance of each pathway, stratified by AIEC-positive (pink) and AIEC-negative (blue) CD patients. Overlaid density plots denote the abundance distribution of functional pathways in each group. The right panel shows the corresponding -$\log_{10}$ transformed p-value from the linear mixed model, indicating the statistical significance of group differences. (B) Spearman correlation heatmap showing associations between significantly altered microbial genera and functional pathways for AIEC presence in CD patients. The color-coded bar on the right denotes the Superclass level of each functional pathway, including amino acid biosynthesis, aromatic compound degradation, cofactor/carrier/vitamin biosynthesis, and others.
Abbreviations: AIEC: Adherent-invasive *Escherichia coli*; CD: Crohn's disease.

of inflammation-related transcription factors such as Nuclear factor kappa B.[41] Acetylene degradation is an important pathway for producing acetate—which latter was known to reduce intestinal inflammation.[42] It has

been reported that chondroitin sulfate could reduce IBD relapse in a prospective follow-up study.[43] Altogether, these microbiome alterations may reflect a more dysbiotic gut environment in AIEC-positive individuals.

Given the observed associations among carrageenan intake, AIEC presence, and increased CD risk, our findings suggest that a potential dietary modification strategy, particularly those aimed at reducing the intake of emulsifiers such as carrageenan, may help lower the risk of AIEC colonization and mitigate gut dysbiosis. Promoting nutritional education and reducing the consumption of processed foods, especially among individuals with lower education levels, could be valuable in reducing the risk of CD. Although our study cannot establish causal relationships, these strategies may serve as practical interventions to support the management of high-risk populations. Future interventional studies are warranted to evaluate the effectiveness of these approaches in reducing AIEC colonization and improving clinical outcomes.

This study had several limitations. First of all, dietary and environmental data were only available for the rural subjects. Second, since this is an observational study, the association between carrageenan intake with AIEC presence and the gut microbiome is descriptive, and the causal relationship could not be proven. Further studies using prospective, well-characterized cohorts and mechanistic animal studies or *in vitro* experiments are needed to confirm the findings and make causal inferences.

5. Conclusion

Our findings suggest that reducing dietary emulsifiers, particularly carrageenan, might mitigate AIEC colonization risk—especially among high-risk groups such as less-educated populations who may consume more processed foods in rural areas. This hypothesis is supported by a clinical trial demonstrating that carrageenan exposure increased relapse risk and IL-6 levels in ulcerative colitis patients.[44] Together with our observation of urban-rural differences in AIEC prevalence, these results highlight how both dietary factors and urbanization may shape gut microbiome composition and CD risk. Most importantly, we provide population-based evidence that AIEC should be considered a global risk factor for CD pathogenesis. Future intervention studies should evaluate whether emulsifier-restricted diets can reduce AIEC colonization and improve clinical outcomes in CD patients.

Acknowledgments

We thank Winnie Lin for her assistance in processing the food questionnaire data to estimate food additive content. We would also like to extend our thanks to Alan Chu and Natalie Chen for their guidance during the experimental phase of this project.

Funding

The study was funded by The French National Research Agency (ANR)/Research Grants Council (RGC) Joint Research Scheme (A-CUHK402/17); National Natural Science Foundation of China (82060107, 82160113); "Xingdian Talents" Support Project of Yunnan Province, China; and Applied Basic Research Projects of Yunnan Province, China (202201AW070019, 2019FE001(-039)). Authors affiliated with MagIC are partially supported by InnoHK, the Government of Hong Kong, Special Administrative Region of the People's Republic of China.

Conflict of interest

Francis Ka Leung Chan is a Board Member of CUHK Medical Centre. He is a co-founder, non-executive Board Chairman, non-executive scientific advisor, and shareholder of GenieBiome Ltd. He receives patent royalties through his affiliated institutions. He has received fees as an advisor and honoraria as a speaker for Eisai Co. Ltd., AstraZeneca, Pfizer Inc., Takeda Pharmaceutical Co., and Takeda (China) Holdings Co. Ltd. Siew Chien Ng has served as an advisory board member for Pfizer, Ferring, Janssen, and Abbvie and received honoraria as a speaker for Ferring, Tillotts, Menarini, Janssen, Abbvie, and Takeda. Siew Chien Ng has received research grants through her affiliated institutions from Olympus, Ferring, and AbbVie. Siew Chien Ng is a founder member, non-executive director, non-executive scientific advisor, and shareholder of GenieBiome Ltd. Siew Chien Ng receives patent royalties through her affiliated institutions. RIL is a Medical Affairs Manager of GenieBiome Ltd. Francis Ka Leung Chan, Siew Chien Ng, Zhilu Xu, and RIL are named inventors of patent applications held by the CUHK and MagIC that cover the therapeutic and diagnostic use of microbiome and receive patent royalties through their affiliated institutions.

Author contributions

Conceptualization: Siew Chien Ng, Zhilu Xu, Nicolas Barnich, Caroline Chevarin, Anthony Buisson
Data curation: Xiangqian Dong, Yang Sun, Yinglei Miao, Juan Luo, Fengrui Zhang
Formal analysis: Yu Lin
Investigation: Yu Lin, Zhilu Xu, Wenli Huang
Methodology: Yu Lin, Zhilu Xu
Supervision: Siew Chien Ng, Yang Sun, Zhilu Xu, Francis Ka Leung Chan
Writing–original draft: Yu Lin
Writing–review & editing: Siew Chien Ng, Zhilu Xu, Hein

Min Tun, Nicolas Barnich, Jean-Frédéric Colombel

Ethical approval and consent to participate

The study was approved by the Research Ethics Committee of the First Affiliated Hospital of Kunming Medical School (reference no. 2017.L.15-1). The study was conducted in accordance with the Declaration of Helsinki. Informed consent was obtained from all participants.

Consent for publication

Participants consented to the publication of their data.

Availability of data

The 16S rRNA sequencing data of the rural and urban cohorts have been deposited in the SRA database under the accession numbers: PRJNA986689 and PRJNA641238.

References

1. Torres J, Mehandru S, Colombel JF, Peyrin-Biroulet L. Crohn's disease. *Lancet*. 2017;389(10080):1741-1755.

   doi: 10.1016/S0140-6736(16)31711-1

2. Pascal V, Pozuelo M, Borruel N, *et al*. A microbial signature for Crohn's disease. *Gut*. 2017;66(5):813-822.

   doi: 10.1136/gutjnl-2016-313235

3. Wright EK, Kamm MA, Teo SM, Inouye M, Wagner J, Kirkwood CD. Recent advances in characterizing the gastrointestinal microbiome in Crohn's disease: A systematic review. *Inflamm Bowel Dis*. 2015;21(6):1219-1228.

   doi: 10.1097/MIB.0000000000000382

4. Palmela C, Chevarin C, Xu Z, *et al*. Adherent-invasive *Escherichia coli* in inflammatory bowel disease. *Gut*. 2018;67(3):574-587.

   doi: 10.1136/gutjnl-2017-314903

5. Barnich N, Darfeuille-Michaud A. Abnormal CEACAM6 expression in Crohn disease patients favors gut colonization and inflammation by adherent-invasive *E. coli*. *Virulence*. 2010;1(4):281-282.

   doi: 10.4161/viru.1.4.11510

6. Barnich N, Carvalho FA, Glasser AL, *et al*. CEACAM6 acts as a receptor for adherent-invasive *E. coli*, supporting ileal mucosa colonization in Crohn disease. *J Clin Invest*. 2007;117(6):1566-1574.

   doi: 10.1172/jci30504

7. Glasser AL, Boudeau J, Barnich N, Perruchot MH, Colombel JF, Darfeuille-Michaud A. Adherent invasive *Escherichia coli* strains from patients with Crohn's disease survive and replicate within macrophages without inducing host cell death. *Infect Immun*. 2001;69(9):5529-5537.

   doi: 10.1128/iai.69.9.5529-5537.2001

8. Zhilu X, Xiangqian D, Keli Y, *et al*. Association of adherent-invasive *Escherichia coli* with severe gut mucosal dysbiosis in Hong Kong Chinese population with Crohn's disease. *Gut Microbes*. 2021;13(1):1994833.

   doi: 10.1080/19490976.2021.1994833

9. Viladomiu M, Metz ML, Lima SF, *et al*. Adherent-invasive *E. coli* metabolism of propanediol in Crohn's disease regulates phagocytes to drive intestinal inflammation. *Cell Host Microbe*. 2021;29(4):607-619.e8.

   doi: 10.1016/j.chom.2021.01.002

10. Kaplan GG, Ng SC. Understanding and preventing the global increase of inflammatory bowel disease. *Gastroenterology*. 2017;152(2):313-321.e2.

    doi: 10.1053/j.gastro.2016.10.020

11. Trakman GL, Lin WYY, Hamilton AL, *et al*. Processed food as a risk factor for the development and perpetuation of crohn's disease-the ENIGMA study. *Nutrients*. 2022;14(17):3627.

    doi: 10.3390/nu14173627

12. Mark-Christensen A, Lange A, Erichsen R, *et al*. Early-life exposure to antibiotics and risk for crohn's disease: A nationwide danish birth cohort study. *Inflamm Bowel Dis*. 2022;28(3):415-422.

    doi: 10.1093/ibd/izab085

13. Anyane-Yeboa A, Quezada S, Rubin DT, Balzora S. The Impact of the social determinants of health on disparities in inflammatory bowel disease. *Clin Gastroenterol Hepatol*. 2022;20(11):2427-2434.

    doi: 10.1016/j.cgh.2022.03.011

14. Zuo T, Kamm MA, Colombel JF, Ng SC. Urbanization and the gut microbiota in health and inflammatory bowel disease. *Nat Rev Gastroenterol Hepatol*. 2018;15(7):440-452.

    doi: 10.1038/s41575-018-0003-z

15. Benchimol EI, Mack DR, Guttmann A, *et al*. Inflammatory bowel disease in immigrants to Canada and their children: A population-based cohort study. *Am J Gastroenterol*. 2015;110(4):553-563.

    doi: 10.1038/ajg.2015.52

16. Chassaing B, Koren O, Goodrich JK, *et al*. Dietary emulsifiers impact the mouse gut microbiota promoting colitis and metabolic syndrome. *Nature*. 2015;519(7541):92-96.

    doi: 10.1038/nature14232

17. Viennois E, Bretin A, Dube PE, *et al*. Dietary Emulsifiers directly impact adherent-invasive *E. coli* Gene expression to drive chronic intestinal inflammation. *Cell Rep*. 2020;33(1):108229.

    doi: 10.1016/j.celrep.2020.108229

18. Naimi S, Viennois E, Gewirtz AT, Chassaing B. Direct

impact of commonly used dietary emulsifiers on human gut microbiota. *Microbiome*. 2021;9(1):66.

doi: 10.1186/s40168-020-00996-6

19. CEIC. *China Population: Census: Yunnan: Kunming*. CEIC. Available from: https://www.ceicdata.com [Lastb accessed on 2023 May 01].

20. Trakman GL, Lin W, Wilson-O'Brien AL, *et al*. Development and Validation of surveys to estimate food additive intake. *Nutrients*. 2020;12(3):812.

doi: 10.3390/nu12030812

21. CEIC. *Hong Kong SAR, China Population*. CEIC. Available from: https://www.ceicdata.com [Last accessed on 2023 May 01].

22. Ma S, Shungin D, Mallick H, *et al*. Population structure discovery in meta-analyzed microbial communities and inflammatory bowel disease using MMUPHin. *Genome Biol*. 2022;23(1):208.

doi: 10.1186/s13059-022-02753-4

23. Levy PY, Fenollar F, Stein A, Borrione F, Raoult D. Finegoldia magna: A forgotten pathogen in prosthetic joint infection rediscovered by molecular biology. *Clin Infect Dis*. 2009;49(8):1244-1247.

doi: 10.1086/605672

24. Stewart A, Sowden D, Caffery M, Bint M, Broom J. *Rhodococcus equi* infection: A diverse spectrum of disease. *IDCases*. 2019;15:e00487.

doi: 10.1016/j.idcr.2019.e00487

25. Akob DM, Sutton JM, Fierst JL, *et al.* Acetylenotrophy: A hidden but ubiquitous microbial metabolism? *FEMS Microbiol Ecol*. 2018;94(8):fiy103.

doi: 10.1093/femsec/fiy103

26. Nadalian B, Yadegar A, Houri H, *et al.* Prevalence of the pathobiont adherent-invasive *Escherichia coli* and inflammatory bowel disease: A systematic review and meta-analysis. *J Gastroenterol Hepatol*. 2021;36(4):852-863.

doi: 10.1111/jgh.15260

27. Kayışoğlu S, Çoşkun F. Determinatıon of the level of knowledge of consumers about food additives. *IOSR J Environ Sci Toxicol Food Technol*. 2016;10:53-56.

28. Sun Y, Zuo T, Cheung CP, *et al.* Population-Level configurations of gut mycobiome across 6 ethnicities in urban and rural China. *Gastroenterology*. 2021;160(1):272-286.e11.

doi: 10.1053/j.gastro.2020.09.014

29. Zuo T, Sun Y, Wan Y, *et al*. Human-Gut-DNA virome variations across geography, ethnicity, and urbanization. *Cell Host Microbe*. 2020;28(5):741-751.e4.

doi: 10.1016/j.chom.2020.08.005

30. Lau TC, Fiebig-Comyn AA, Shaler CR, McPhee JB, Coombes BK, Schertzer JD. Low dietary fiber promotes enteric expansion of a Crohn's disease-associated pathobiont independent of obesity. *Am J Physiol Endocrinol Metab*. 2021;321(3):E338-E350.

doi: 10.1152/ajpendo.00134.2021

31. Veca R, O'Dea C, Burke J, Hatje E, Kuballa A, Katouli M. A Comparative study of the adherent-invasive *Escherichia coli* Population and gut microbiota of healthy vegans versus omnivores. *Microorganisms*. 2020;8(8):1165.

doi: 10.3390/microorganisms8081165

32. Chevarin C, Xu Z, Martin L, *et al*. Comparison of Crohn's disease-associated adherent-invasive *Escherichia coli* (AIEC) from France and Hong Kong: Results from the Pacific study. *Gut Microbes*. 2024;16(1):2431645.

doi: 10.1080/19490976.2024.2431645

33. Borsani B, De Santis R, Perico V, *et al*. The role of carrageenan in inflammatory bowel diseases and allergic reactions: Where do we stand? *Nutrients*. 2021;13(10):3402.

doi: 10.3390/nu13103402

34. Tsuji RF, Hoshino K, Noro Y, *et al*. Suppression of allergic reaction by lambda-carrageenan: Toll-like receptor 4/MyD88-dependent and -independent modulation of immunity. *Clin Exp Allergy*. 2003;33(2):249-258.

doi: 10.1046/j.1365-2222.2003.01575.x

35. Munyaka PM, Sepehri S, Ghia JE, Khafipour E. Carrageenan gum and adherent invasive *Escherichia coli* in a piglet model of inflammatory bowel disease: Impact on Intestinal mucosa-associated microbiota. *Front Microbiol*. 2016;7:462.

doi: 10.3389/fmicb.2016.00462

36. Viennois E, Merlin D, Gewirtz AT, Chassaing B. Dietary emulsifier-induced low-grade inflammation promotes colon carcinogenesis. *Cancer Res*. 2017;77(1):27-40.

doi: 10.1158/0008-5472.CAN-16-1359

37. Buffet-Bataillon S, Bouguen G, Fleury F, Cattoir V, Le Cunff Y. Gut microbiota analysis for prediction of clinical relapse in Crohn's disease. *Sci Rep.* 2022;12(1):19929.

doi: 10.1038/s41598-022-23757-x

38. Sasaki M, Klapproth JM. The role of bacteria in the pathogenesis of ulcerative colitis. *J Signal Transduct*. 2012;2012:704953.

doi: 10.1155/2012/704953

39. Hamed S. *Butyrate Alleviates Crohn's Diseases' Adherent Invasive E coli-Induced Mitochondrial Dysfunction in Intestinal Epithelium.* (Master's thesis, Calgary, Canada: University of Calgary). 2022.

40. Buisson A, Sokol H, Hammoudi N, *et al*. Role of adherent and invasive *Escherichia coli* in Crohn's disease: Lessons from

the postoperative recurrence model. *Gut*. 2023;72(1):39-48.

doi: 10.1136/gutjnl-2021-325971

41. Deters BJ, Saleem M. The role of glutamine in supporting gut health and neuropsychiatric factors. *Food Sci Hum Wellness*. 2021;10(2):149-154.

doi: 10.1016/j.fshw.2021.02.003

42. Parada Venegas D, De la Fuente MK, Landskron G, *et al*. Short chain fatty acids (SCFAs)-mediated gut epithelial and immune regulation and its relevance for inflammatory bowel diseases. *Front Immunol*. 2019;10:277.

doi: 10.3389/fimmu.2019.00277

43. Linares PM, Chaparro M, Algaba A, *et al*. Effect of chondroitin sulphate on pro-inflammatory mediators and disease activity in patients with inflammatory bowel disease. *Digestion*. 2015;92(4):203-210.

doi: 10.1159/000439522

44. Bhattacharyya S, Shumard T, Xie H, *et al.* A randomized trial of the effects of the no-carrageenan diet on ulcerative colitis disease activity. *Nutr Healthy Aging*. 2017;4(2):181-192.

doi: 10.3233/NHA-170023

ACCSCIENCE PUBLISHING

Microbes & Immunity

ORIGINAL RESEARCH ARTICLE

Identification and characterization of novel outer membrane proteins of *Brachyspira pilosicoli*

Amisha Panda[1], Jahnvi Kapoor[1], Batchu Hareramadas[2], Ilmas Naqvi[2], Ravindresh Chhabra[3], Sanjiv Kumar[4]*, and Anannya Bandyopadhyay[1]*

[1]Department of Zoology, Faculty of Science, University of Delhi, New Delhi, Delhi, India

[2]Department of Zoology, Zakir Husain Delhi College, University of Delhi, New Delhi, Delhi, India

[3]Department of Biochemistry, School of Basic Sciences, Central University of Punjab, Bathinda, Punjab, India

[4]Independent Researcher, Stockholm, Sweden

Abstract

Brachyspira pilosicoli is a globally prevalent, anaerobic, Gram-negative spirochete that causes intestinal spirochetosis in birds, pigs, and humans. It colonizes the large intestine, causing colitis, diarrhea, and impaired growth. Despite its pathogenic relevance, the outer membrane proteins of *B. pilosicoli* remain largely uncharacterized. In this study, we computationally identified a total of 42 outer membrane β-barrel (OMBB) proteins within the *B. pilosicoli* proteome using a consensus-based computational framework. Structural models generated using AlphaFold 3 confirmed the β-barrel architectures of the predicted proteins. Structure- and sequence-based functional annotations revealed homologs of *β*-barrel assembly machinery BamA protein, lipopolysaccharide-assembly protein LPS-assembly protein D, TolC, transporter proteins, enzymes, diffusion channels, and porins. Notably, seven of the predicted OMBB proteins were previously unannotated in UniProt and the National Center for Biotechnology Information; we report their putative functions here for the 1st time. Sequence variation analysis among the homologs of OMBB proteins across nine *B. pilosicoli* strains revealed that many of the variations were present within surface-exposed loop regions, suggesting roles in host interaction and immune modulation. Our *in silico* study expands the functional repertoire of *B. pilosicoli* outer membrane proteins, highlighting potential targets for diagnostics, vaccine development, and therapeutic interventions.

Keywords: *Brachyspira pilosicoli;* Intestinal spirochetosis; Outer membrane proteins; β-barrel structures; Structural models; Sequence variations; Functional annotations; *In silico*

***Corresponding authors:**
Anannya Bandyopadhyay (anannya@zoology.du.ac.in)
Sanjiv Kumar (drsanjivk@gmail.com)

Citation: Panda A, Kapoor J, Hareramadas B, *et al*. Identification and characterization of novel outer membrane proteins of *Brachyspira pilosicoli*. *Microbes & Immunity*. 2025;2(4):79-109. doi: 10.36922/MI025230050

Received: June 6, 2025

Revised: July 9, 2025

Accepted: August 1, 2025

Published online: August 25, 2025

1. Introduction

Brachyspira pilosicoli, previously known as *Serpulina pilosicoli*, is a zoonotic bacterium belonging to the family Brachyspiraceae, within the order *Spirochaetales* and phylum Spirochaetota.[1] It is a Gram-negative, anaerobic, slow-growing, double-membraned, flagellated bacterium. *B. pilosicoli* causes intestinal spirochetosis (IS) in higher animals, including avian intestinal spirochetosis (AIS) in birds, porcine intestinal spirochetosis

(PIS) in pigs, and human intestinal spirochetosis (HIS) in humans. Spirochetal infections have been reported in the United Kingdom, continental Europe, Scandinavia, North America, Oceania, Iran, Malaysia, and South America.[2-7] *B. pilosicoli* has a broad host range,[8,9] including dogs, monkeys, water birds, game birds, and humans.[8]

In IS, numerous brachyspiral cells penetrate the mucosal layer overlying enterocytes in the small intestine, attaching one end to the luminal surface of the enterocytes, aided by surface lipoproteins. This attachment forms a distinctive layer resembling a "false brush border."[8] *B. pilosicoli* is the sole etiological agent of PIS, which is marked by diarrhea and impaired growth in pigs.[9,10] AIS in chickens is associated with the delayed onset of egg laying, wet and bloody feces, reduced growth rate, and diarrhea.[3,8,11] HIS is associated with a range of non-specific clinical symptoms, including abdominal pain, altered bowel patterns, chronic diarrhea, and rectal bleeding.[3,12-15]

Common risk factors for zoonotic transmission of *B. pilosicoli* to humans include exposure to fecally contaminated water,[9,16-18] rural or animal exposure, overcrowding, socioeconomic depression, travel to less developed countries, immunosuppression due to HIV infection, or being a homosexual male.[8] AIS and PIS are underreported diseases, bearing significant economic consequences for global food production. Although no comprehensive cost analysis for PIS exists, AIS alone is estimated to cost the poultry industry approximately GBP 18 million annually in the United Kingdom.[3] Extrapolating from these figures, combined global economic losses to both industries could reach approximately USD 1–2 billion annually.[19]

Antibiotics are used to treat AIS, PIS, and HIS; however, resistance has been reported.[18] Antibiotics such as co-amoxicillin and metronidazole are used to treat HIS, whereas pleuromutilins, macrolides, and lincosamides are used for AIS and PIS.[18] Although antibiotics are commonly used, no vaccines are currently available to prevent HIS, AIS, or PIS, highlighting the urgent need for vaccine development.

The reference strain (i.e., *B. pilosicoli* strain 95/1000) possesses a single circular chromosome of approximately 2.59 Mb and lacks any extrachromosomal elements. The *B. pilosicoli* genome comprises 2338 genes, with coding regions accounting for approximately 85% of the total genome.[20] Like other Gram-negative bacteria, *B. pilosicoli* consists of a central protoplasmic cylinder enclosed by a membrane sheath known as the outer membrane (OM).[21] The exact composition of *B. pilosicoli*'s OM is not fully understood; however, it is known to be extremely labile due to its high sterol content, which results in low resistance to osmotic stress and destabilisation when exposed to low-ionic-strength buffers.[22]

The *B. pilosicoli* outer envelope contains lipooligosaccharides (LOS) rather than lipopolysaccharides (LPS), exhibiting serological diversity across multiple strains.[23] Bacteria with diderm envelopes possess a diverse family of OM proteins (OMPs), characterized by *β-barrel* structures (OMBBs) and LOS.[24,25] β-barrels are protein structures composed of amphipathic, anti-parallel β-strands that close in on themselves, forming a cylindrical structure. The β-barrels of OMPs are typically composed of an even number of β-strands, typically ranging from 8 to 36.[26] These β-strands are alternately connected on each side of the OM by long loops on the extracellular surface and by shorter turns on the periplasmic side.[27] OMBB proteins are involved in a range of functions, including nutrient acquisition, membrane biogenesis, assembly of OMPs, adhesion, biofilm formation, efflux, proteolysis, and pilus formation.[28] Thus, OMBB proteins represent a crucial area of research and a promising target for developing antibacterial therapies to combat pathogenic microbes.

Notably, few OMPs of *B. pilosicoli* have been studied, including BmpC (a 23 kDa lipoprotein),[22] a 45 kDa surface-exposed lipoprotein,[29] and Bmp72.[30] Christodoulides *et al.*[19] employed an *in silico* reverse vaccinology approach to identify potential vaccine candidates from predicted OMBB proteins. Although a few OMPs and lipoproteins of *B. pilosicoli* have been identified,[22,29-31] the identification and characterization of the complete OM proteome are needed to define their potential roles in disease pathogenesis, particularly in processes such as attachment, virulence, and eliciting host immune responses.

In this study, a comprehensive *in silico* approach was employed to identify novel OMBB proteins in *B. pilosicoli.* A consensus of the outputs from OM localization prediction tools and *β*-barrel conformation prediction tools was considered for OMBB protein prediction. Through stringent screening criteria and manual curation, 42 putative OMBB proteins were selected. In addition, deep-learning-based structural models of the proteins were generated. Structural homologs were identified using the digital addressable lighting interface (DALI) server and Foldseek tool, revealing the functional roles of the proteins. Furthermore, sequence-based annotations were performed using PANNZER and eggNOG-mapper. Amino acid sequence variations in the predicted proteins were obtained from nine strains of *B. pilosicoli* and mapped onto the structural models. This study identified a total of 42 OMBB proteins of *B. pilosicoli*, computationally characterized their structure and function, and identified peptide regions potentially crucial for bacterial pathogenesis.

2. Materials and methods

2.1. OM β-barrel (OMBB) protein prediction

Given that reference genomes provide a streamlined, standardized, and taxonomically diverse representation of the RefSeq collection,[32] we selected the reference strain *B. pilosicoli* 95/1000, a porcine isolate, for our study. Using genome assembly ASM14372v1, the sequences of all proteins from the *B. pilosicoli* 95/1000 genome were downloaded from the National Center for Biotechnology Information (NCBI) (https://www.ncbi.nlm.nih.gov/).[32]

Peptide length, molecular weight, charge, and isoelectric point for all protein sequences were determined using the Pepstats tool from the EMBOSS package (https://www.ebi.ac.uk/jdispatcher/seqstats/emboss_pepstats).[33] The presence of signal peptide was determined using SignalP 5.0 (https://services.healthtech.dtu.dk/services/SignalP-6.0/; accessed on April 20, 2024) and LipoP 1.0 (https://services.healthtech.dtu.dk/services/LipoP-1.0/; accessed on April 17, 2024). SignalP was employed to predict the presence and cleavage position of signal peptides in the protein sequences.

The SignalP server generates output for each protein sequence in the following categories: Secretory signal peptide ("Sec/SPI"), lipoprotein signal peptide ("Sec/SPII"), Tat signal peptide ("Tat/SPI"), Tat lipoprotein signal peptide ("Tat/SPII"), pilin signal peptide ("Sec/SPIII"), or the absence of any signal peptide ("Other").[34]

The LipoP server predicts lipoproteins in Gram-negative bacteria and distinguishes between lipoprotein signal peptides, other signal peptides, and N-terminal transmembrane helices (TMHs). The output is classified into four classes: Secretory signal peptide ("SpI"), lipoprotein signal peptide ("SpII"), N-terminal TMH ("TMH"), and cytoplasmic protein ("Cyt").[35] The N-terminal TMH serves as an anchor, stabilizing the protein within the membrane. Therefore, LipoP was used as a secondary tool to predict signal peptides.

CELLO v.2.5 (http://cello.life.nctu.edu.tw/; accessed on April 19, 2024)[36] and PSORTb 3.0 (https://www.psort.org/psortb/; accessed on April 30, 2024)[37] were utilized to predict the subcellular localization of proteins. Essential proteins from *B. pilosicoli* were predicted by performing BLASTP searches against the Database of Essential Genes (DEG) v15.2 (https://ngdc.cncb.ac.cn/databasecommons/database/id/229; accessed on April 2, 2024).[38] The DEG database is a repository of essential proteins from archaea, bacteria, and eukaryotes, and assumes that proteins essential in one organism are likely to be essential in others. Specifically, proteins with an $E < 1\times10^{-3}$ and a bit score >100 were considered essential.

The computational framework designed to select OMPs is detailed and schematically represented in Figure 1. We employed a consensus-based computational approach to identify OMBB proteins, where the outputs from four OMP prediction tools were considered: One from OMPdb (http://aias.biol.uoa.gr/OMPdb/; accessed on April 21, 2024),[39] MCMBB (http://athina.biol.uoa.gr/bioinformatics/mcmbb/; accessed on May 1, 2024),[40] TMBETADISC-radial basis function (RBF) (http://rbf.bioinfo.tw/~sachen/OMP.html; accessed on April 23, 2024),[41] and TMbed (https://github.com/BernhoferM/TMbed; accessed on April 20, 2024).[42] Protein sequences were searched against those in the OMPdb database to identify homologous proteins (with $E < 1\times10^{-3}$; bit score > 100). OMPdb is a database of integral β-barrel OMPs from Gram-negative bacteria.

MCMBB distinguishes β-barrel OMPs from globular proteins and α-helical membrane proteins. In MCMBB, a score > 0 indicates a higher likelihood of β-barrel conformation, whereas a score lower than zero suggests the protein is not a β-barrel. The TMBETADISC-RBF server predicts OMPs using an RBF network and position-specific scoring matrix profiles. TMbed, based on embeddings from protein language models, predicts the propensity of each residue to form TMHs, transmembrane β-strands, signal peptides, or other structural elements.

Using a consensus-based approach, predictions from the aforementioned tools were used to identify potential OMBB proteins. A final list of 42 OMBB proteins was compiled based on the number of tools predicting β-barrel architecture for each protein. These proteins were categorized based on the number of tools providing positive predictions. Higher confidence was assigned to proteins predicted as OMBBs by a greater number of tools.

2.2. Structural modeling

Structural models of the predicted OMBB proteins were generated using the AlphaFold server, powered by AlphaFold 3 (https://alphafoldserver.com/; accessed on July 21, 2024).[43] The modeling process incorporates physical and chemical constraints to accurately predict protein folding, resulting in atomic coordinates for each OMBB protein. Outputs of AlphaFold 3 include confidence metrics, namely: Predicted local distance difference test, predicted aligned error, predicted template modeling (pTM), and interface predicted template modeling (ipTM) scores. The pTM and ipTM scores assess the accuracy of the overall structure.[44,45] A pTM score above 0.5 and an ipTM score above 0.8 indicate highly reliable predictions. The top-ranked predictions, based on predicted local distance difference test scores, were selected for figure generation

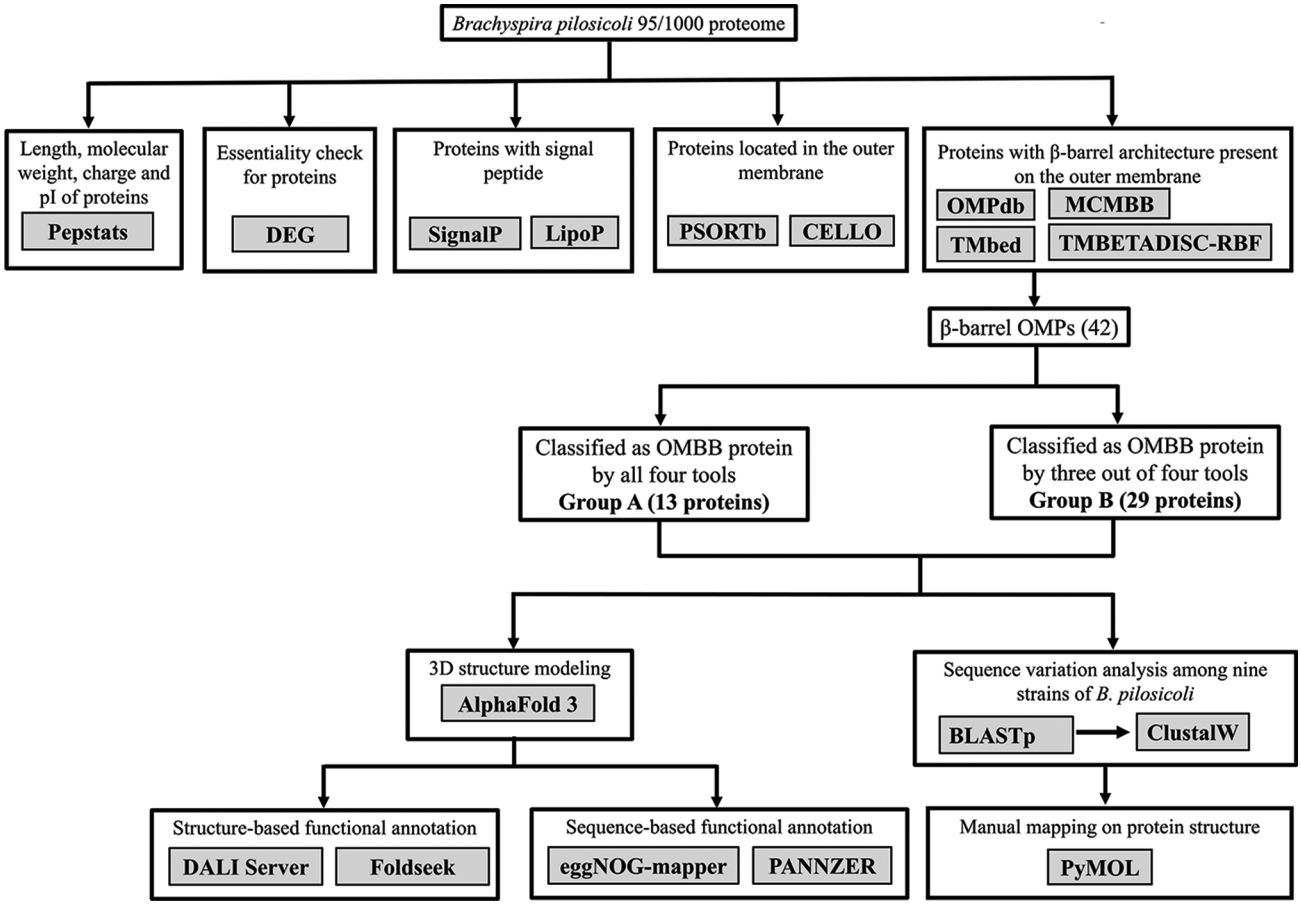

Figure 1. Computational framework for predicting outer membrane-localized β-barrel proteins from *Brachyspira pilosicoli* 95/1000. The *B. pilosicoli* proteome was mined *in silico* using various tools, including SignalP, LipoP, PSORTb, CELLO, OMPdb, MCMBB, TMbed, and TMBETADISC-RBF. Protein essentiality was assessed using the Database of Essential Genes (DEG). Protein size, net charge, and isoelectric point of proteins were predicted using Pepstats. Structural models were generated using the AlphaFold 3 server and used as queries in the DALI server and Foldseek to annotate putative functions. Additionally, sequence-based annotation tools (eggNOG-mapper and PANNZER) were used to predict functional roles. Amino acid sequence variation across nine strains of *B. pilosicoli* was analyzed using ClustalW and mapped onto the structural models using PyMOL.
Abbreviations: OMBB: Outer membrane β-barrel; OMP: Outer membrane protein; pI: Isoelectric point.

and further analysis. The resulting atomic coordinate files were visualized using PyMOL (Warren Lyford DeLano, Schrödinger Inc., USA).[46]

To validate the structures generated by AlphaFold 3, comparative models were also generated using other structure prediction tools: ESMFold (https://colab.research.google.com/github/sokrypton/ColabFold/blob/main/ESMFold.ipynb; accessed on January 23, 2025),[47] SWISS-MODEL (https://swissmodel.expasy.org/; accessed on January 23, 2025),[48] RoseTTA (https://robetta.bakerlab.org/; accessed on January 23, 2025),[49] and TrRosetta (https://yanglab.qd.sdu.edu.cn/trRosetta/; accessed on January 23, 2025).[50]

2.3. Functional annotation of the predicted proteins

Given that many of the OMBB proteins were unannotated hypothetical proteins, a structure-based approach was employed to unravel their functional roles. Atomic coordinates of the structural models were used as queries in the DALI server (http://ekhidna.biocenter.helsinki.fi/dali/; accessed on May 23, 2024)[51] with the full Protein Data Bank (PDB) search option, ensuring that the query was compared against all protein structures available in the PDB. The top-hit protein with the highest Z-score was selected for functional annotation. The Z-score is an optimized similarity score based on the sum of equivalent Cα–Cα distances between two proteins. A score >20 indicates definite homology, 8–20 suggests potential homology, whereas scores <8 indicate insignificant similarity.[52] Functions of the top-hit proteins were retrieved from the available literature to annotate the predicted OMBB proteins.

In addition, the Foldseek tool (https://search.foldseek.com/search; accessed on February 2, 2025) was employed to

identify structural homologs across five protein databases: PDB100, CATH50, AFDB50, AFDB-SWISSPROT, and AFDB-Proteome.[53] The top hit, based on the template modeling score, was selected for functional annotation. Sequence-based functional annotation was performed using PANNZER (http://ekhidna.biocenter.helsinki.fi/pannzer; accessed on February 13, 2025) and eggNOG-mapper v2 (https://eggnog-mapper.embl.de/; accessed on February 2, 2025).[54,55]

2.4. Amino acid sequence variation among different strains of *B. pilosicoli*

Predicted OMBB proteins from the reference genome 95/1000 were searched for similar proteins using BLASTP (E-value < 1×10^{-3}; bit score > 100) across nine completed genomes of *B. pilosicoli* to analyze the amino acid sequence variation in the predicted β-barrel proteins (Table S1). Multiple sequence alignment (MSA) was performed for orthologous sequences of each protein using ClustalW (Thompson JD, Gibson TJ, Higgins DG; EMBL, Heidelberg, Germany).[56] Analysis of the MSA revealed amino acid substitutions among the orthologs. Mapping of these variations onto the structural models was conducted using PyMOL.[46]

In addition, the 16S rRNA gene sequence of *B. pilosicoli* strain P43/6/78 was retrieved from the NCBI database and used as a query for BLASTn against available *B. pilosicoli* genome sequences. From the BLASTn results, strains previously included in the sequence variation analysis were identified, and their corresponding 16S rRNA gene sequences were extracted. A multi-FASTA file was created, followed by MSA using Multiple Sequence Comparison by Log Expectation (Robert C. Edgar, USA). Subsequently, a phylogenetic tree was constructed using the Neighbor-Joining method in MEGA12 software (Kumar S, Tamura K; Temple University, Philadelphia, USA, and Tokyo Metropolitan University, Japan) to determine the evolutionary relationships among the selected strains (Figure S1).[57]

2.5. Structure alignment using the US-align server

Structural models were aligned using the US-align server (https://zhanggroup.org/US-align/; accessed on July 23, 2024)[58] an online web server to assess structural similarities and variations. Structural alignments were visualized, and figures were generated using PyMOL.

3. Results and discussion

3.1. Prediction of OMBB proteins using a consensus-based computational approach

A consensus-based computational framework was applied to the *B. pilosicoli* 95/1000 proteome, consisting of 2,275 proteins, to identify OMBB proteins (Figure 1). Ten computational tools were used for predictions: Pepstats, DEG database, SignalP, LipoP, CELLO, PSORTb, OMPdb, MCMBB, TMBETADISC-RBF, and TMbed (Table S2). Prediction outputs from all tools were combined for each protein. Tools that specifically predict OMBB proteins (e.g., OMPdb, MCMBB, TMBETADISC-RBF, and TMbed) were prioritized for OMBB protein prediction (Table S2).

Through stringent screening criteria and manual curation, a total of 42 OMBB proteins were selected and classified into two groups: Group A (13 proteins, predicted as OMBB by all four tools) and Group B (29 proteins, predicted as OMBB by any three out of four tools) (Table 1).

To gain structural insights into the predicted proteins, we searched for their structures in the PDB but found no experimentally determined models available. Using AlphaFold 3,[43] structural models of the predicted proteins were generated, revealing typical features of OMPs, such as β-barrel architectures with central pores, periplasmic loops, and surface-exposed loops.

Given that most proteins were unannotated, both structure- and sequence-based approaches were employed to assign putative functions. Top-ranking hits were considered for functional annotation. This analysis revealed structural and sequence homologs of well-characterized proteins, including OMP assembly factor BamA, LPS-assembly protein D (LptD), Neisserial surface protein NspA, OM porin F (OmpF), OM phospholipase A (OMPLA), and vitamin B_{12} transporter protein BtuB, thereby providing valuable insights into their possible roles (Tables 2 and S3).

OMPs are located on the bacterial surface, serving as the primary interface between host and pathogen. Due to exposure to the host environment, these proteins are subjected to strong selection pressures, making the analysis of their sequence variability essential for understanding pathogen evolution (Table 3).[59] Building on this, we analyzed the amino acid sequences of the predicted OMBB proteins for residues exhibiting sequence variation across nine *B. pilosicoli* strains (Table S4). Mapping these variations onto the structural models revealed that many variations were located on extracellular loops (ECLs), which are more likely to interact with the host environment (Table 3).

3.2. Identification of OMPs

3.2.1. Group A

Group A comprised of 13 proteins, consisting of three proteins with 16 stranded β-barrel domain (BP951000_RS05730, BP951000_RS10215, and BP951000_RS04760); seven proteins with eight-stranded β-barrel domain

Table 1. Predicted outer membrane β-barrel proteins from *Brachyspira pilosicoli* 95/1000

Locus identifier	Protein name[a]	SignalP	PSORTb	CELLO	TMBETADISC. RBF_AADP	OMPdb Match	MCMBB	Tmbed	No. of β-strands[b]
Group A									
BP951000_RS05730	OMP assembly factor/ BamA	+	+	+	+	+	+	+	16
BP951000_RS10215	Variable surface protein (VspE)	+	U	+	+	+	+	+	16
BP951000_RS04760	Variable surface protein (VspD)	+	U	+	+	+	+	+	16
BP951000_RS01125	CsgG/HfaB family protein	+	U	+	+	+	+	+	8
BP951000_RS03440	OMBB protein	+	U	+	+	+	+	+	8
BP951000_RS05600	TolC family protein	+	–	+	+	+	+	+	18 (trimer of six-stranded protomer)
BP951000_RS09000	TolC family protein	+	U	+	+	+	+	+	18 (trimer of six-stranded protomer)
BP951000_RS06235	TolC family protein	+	+	+	+	+	+	+	12 (trimer of four-stranded protomer)
BP951000_RS04880	Serpentine receptor domain-containing protein	+	+	+	+	+	+	+	8
BP951000_RS02055	Serpentine receptor domain-containing protein	+	+	+	+	+	+	+	8
BP951000_RS02050	Serpentine receptor domain-containing protein	+	+	+	+	+	+	+	8
BP951000_RS07540	Serpentine receptor domain-containing protein	+	+	+	+	+	+	+	8
BP951000_RS00180	Serpentine receptor domain-containing protein	+	U	+	+	+	+	+	8
Group B									
BP951000_RS09575	Lipopolysaccharide-assembly protein (LptD)	+	+	+	+	–	+	+	26
BP951000_RS03215	TonB-dependent siderophore receptor	+	+	+	–	+	+	+	22
BP951000_RS04405	Toxin A	+	+	+	+	–	+	+	18
BP951000_RS09655	DUF5723 domain-containing protein	+	U	+	+	–	+	+	16
BP951000_RS04440	Hypothetical protein	+	U	+	+	–	+	+	16
BP951000_RS08285	Trep protein	–	U	+	+	–	+	+	16
BP951000_RS04505	Variable surface protein (VspH)	–	U	+	–	+	+	+	16
BP951000_RS08455	PorV/PorQ family protein	+	U	+	+	–	+	+	14

(Cont'd...)

Table 1. ***(Continued)***

Locus identifier	Protein name[a]	SignalP	PSORTb	CELLO	TMBETADISC. RBF_AADP	OMPdb Match	MCMBB	Tmbed	No. of β-strands[b]
BP951000_RS01090	Variable surface protein (VspH)	+	+	+	+	−	+	+	14
BP951000_RS06935	Hypothetical protein	+	−	+	+	−	+	+	12
BP951000_RS11380	Toxin A	+	U	+	+	−	+	+	12
BP951000_RS03405	Hypothetical protein	+	U	+	+	−	+	+	12
BP951000_RS00185	Hypothetical protein	+	+	+	+	−	+	+	12
BP951000_RS10320	Hypothetical protein	+	U	+	+	−	+	+	10
BP951000_RS05445	DUF3575 domain-containing protein	+	U	+	+	−	+	+	8
BP951000_RS08300	Tia invasion determinant	+	U	+	−	+	+	+	8
BP951000_RS05490	Tia invasion determinant	+	U	+	+	−	+	+	8
BP951000_RS07500	Hypothetical protein	+	−	+	+	−	+	+	8
BP951000_RS01590	Hypothetical protein	−	−	+	+	−	+	+	8
BP951000_RS08295	Tia invasion determinant	+	U	−	−	+	+	+	8
BP951000_RS08975	TonB-dependent receptor domain-containing protein	+	U	+	+	−	+	+	13
BP951000_RS06930	Serpentine receptor domain-containing protein	−	−	−	+	−	+	+	8
BP951000_RS03290	Serpentine receptor domain-containing protein	+	−	+	+	−	+	+	8
BP951000_RS00765	Serpentine receptor domain-containing protein	+	+	+	+	−	+	+	8
BP951000_RS01280	Serpentine receptor domain-containing protein	+	+	+	+	−	+	+	8
BP951000_RS10445	Serpentine receptor domain-containing protein	+	+	+	+	−	+	+	8
BP951000_RS00365	Serpentine receptor domain-containing protein	+	U	+	+	−	+	+	8
BP951000_RS04620	Serpentine receptor domain-containing protein	+	+	+	+	−	+	+	8
BP951000_RS04220	Serpentine receptor domain-containing protein	+	−	+	+	−	+	+	8

Notes: [a]Protein names follow annotations in the National Center for Biotechnology Information and UniProt databases, retrieved using protein accession numbers (accessed on March 28, 2024). [b]The number of β-strands was predicted using AlphaFold 3. "U" indicates an unknown output from PSORTb, where the tool could not determine the exact cellular localization of the protein. "+" denotes a positive result, and "−" represents a negative result as reported by the respective computational tool.

Abbreviations: DUF: Domain of unknown function; OMBB: Outer membrane β-barrel; OMP: Outer membrane protein; Trep: transcriptional regulating protein.

Table 2. Classification of outer membrane β-barrel proteins based on functional annotation

Functional categories[a]	Subtypes	Protein accession number	Locus identifier	Protein name[a]
Transport and nutrient uptake	Porins	WP_013243854.1	BP951000_RS04405	Toxin A
		WP_013243193.1	BP951000_RS01125	CsgG/HfaB family protein
	Diffusion channels	WP_013244641.1	BP951000_RS08455	PorV/PorQ family protein
		WP_013243185.1	BP951000_RS01090	Variable surface protein (VspH)
		WP_013244339.1	BP951000_RS06935	Hypothetical protein
	TonB-dependent receptors	WP_013244745.1	BP951000_RS08975	TonB-dependent receptor domain-containing protein
		WP_013244607.1	BP951000_RS08285	Trep protein
		WP_041747581.1	BP951000_RS03215	TonB-dependent siderophore receptor
Secretion and export	Secretins	WP_013244995.1	BP951000_RS10215	VspE
		WP_013243917.1	BP951000_RS04760	VspD
		WP_015274839.1	BP951000_RS04505	VspH
	Autotransporters	WP_013244339.1	BP951000_RS06935[d]	Hypothetical protein
	Efflux pumps	WP_013244081.1	BP951000_RS05600	TolC family protein
		WP_013244750.1	BP951000_RS09000	TolC family protein
		WP_041747714.1	BP951000_RS06235	TolC family protein
Structural integrity	OM scaffolding proteins	WP_013243377.1	BP951000_RS02055	Serpentine receptor domain-containing protein[c]
		WP_013243376.1	BP951000_RS02050	Serpentine receptor domain-containing protein[c]
		WP_013244459.1	BP951000_RS07540	Serpentine receptor domain-containing protein[c]
		WP_013242998.1	BP951000_RS00180	Serpentine receptor domain-containing protein[c]
		WP_187287137.1	BP951000_RS07500	Hypothetical protein
		WP_014936494.1	BP951000_RS03290	Serpentine receptor domain-containing protein[c]
		WP_014933009.1	BP951000_RS00765	Serpentine receptor domain-containing protein[c]
		WP_013245039.1	BP951000_RS10445	Serpentine receptor domain-containing protein[c]
		WP_013243896.1	BP951000_RS04620	Serpentine receptor domain-containing protein[c]
		WP_013243815.1	BP951000_RS04220	Serpentine receptor domain-containing protein[c]
	OM biogenesis machinery	WP_013244106.1	BP951000_RS05730	BamA
		WP_041747843.1	BP951000_RS09575	Lipopolysaccharide-assembly protein (LptD)
Adhesion and virulence	Adhesins	WP_013243917.1	BP951000_RS04760[d]	VspD
		WP_013243655.1	BP951000_RS03440	OMBB
		WP_013243940.1	BP951000_RS04880	Serpentine receptor domain-containing protein[c]
		WP_041747873.1	BP951000_RS10320	Hypothetical protein
		WP_013244050.1	BP951000_RS05445	DUF3575 domain-containing protein

(Cont'd...)

Table 2. ***(Continued)***

Functional categories[a]	Subtypes	Protein accession number	Locus identifier	Protein name[a]
		WP_013244610.1	BP951000_RS08300	Tia invasion determinant
		WP_013244059.1	BP951000_RS05490	Tia invasion determinant
		WP_228369485.1	BP951000_RS08295	Tia invasion determinant
		WP_013243225.1	BP951000_RS01280	Serpentine receptor domain-containing protein
		WP_013244338.1	BP951000_RS06930	Serpentine receptor domain-containing protein
		WP_013243037.1	BP951000_RS00365	Serpentine receptor domain-containing protein
	Immune evasion proteins	WP_013244610.1	BP951000_RS08300[d]	Tia invasion determinant
		WP_013242999.1	BP951000_RS00185	Hypothetical protein
		WP_228369485.1	BP951000_RS08295[d]	Tia invasion determinant
Signal transduction	Receptor-like OMPs	WP_181893515.1	BP951000_RS01590	Hypothetical protein
		WP_013243193.1	BP951000_RS01125[d]	CsgG/HfaB family protein
Enzymatic functions	Lipases	WP_013243647.1	BP951000_RS03405	Hypothetical protein

Notes: [a]Protein names follow annotations in the National Center for Biotechnology Information and UniProt databases, retrieved using protein accession numbers (accessed on March 28, 2024). [b]Functional categories were assigned based on consensus predictions from structure- and sequence-based annotation tools (Table S3). [c]As serpentine receptors, or G-protein coupled receptors, are absent in prokaryotes and all tools predicted transmembrane β-barrel structures rather than α-helices, these proteins are likely misannotated as serpentine receptor proteins in UniProt. [d]These proteins were predicted to possess dual roles.
Abbreviations: DUF: Domain of unknown function; OM: Outer membrane; OMBB: Outer membrane β-barrel; OMP: Outer membrane protein; Trep: transcriptional regulating protein.

(BP951000_RS02055, BP951000_RS02055, BP951000_RS07540, BP951000_RS01125, BP951000_RS00180, BP951000_RS03440, and BP951000_RS04880), and three TolC family proteins (BP951000_RS05600, BP951000_RS09000, and BP951000_RS06235) (Table 1). Out of the seven eight-stranded β-barrel proteins, five are annotated as serpentine receptor (SR) domain-containing proteins (BP951000_RS02055, BP951000_RS02055, BP951000_RS07540, BP951000_RS00180, and BP951000_RS04880).

3.2.1.1. BP951000_RS05730

BP951000_RS05730 is annotated as BamA in *B. pilosicoli* strain 95/1000. BamA, along with BamB, BamC, BamD, and BamE, forms the β-barrel assembly machinery complex, which is involved in the assembly and insertion of β-barrel proteins into the OM.[60] BP951000_RS05730 is identified as an essential protein in the DEG database. Its structural model exhibits a characteristic BamA bipartite structure, consisting of a periplasmic N-terminal region and a C-terminal *β*-barrel domain (Figure 2A). The N-terminal segment contains five polypeptide transport-associated (POTRA) domains (P1–P5), each comprising a characteristic β1-α1-α2-β2-β3 motif. In other well-characterized BamA proteins, these domains form a scaffold for the binding of BamB, BamC, BamD, and BamE proteins, and facilitate the folding of OMPs.[61]

Brachyspira pilosicoli BamA consists of 16 antiparallel β-strands, with a characteristic lateral gate between strands 1 and 16. A structural homology search using the DALI server revealed the closest match with BamA of *Escherichia coli* O157:H7 (PDB ID: 7NRE) (Tables 2 and S3). The consensus predictions from other annotation tools (Foldseek, PANNZER, and eggNOG-mapper) validated the functional annotation of BamA in *B. pilosicoli* (Table S3).

Sequence comparison of BP951000_RS05730 across nine strains of *B. pilosicoli* revealed five variations (D60, A184, V465, A467, and F512) (Tables 3 and S4). When mapped onto the structural model, V465, A467, and F512 were present in the β-barrel transmembrane (TM) domain, whereas D60 and V184 were located in the periplasmic region of the protein (Tables 3 and S4).

3.2.1.2. BP951000_RS10215

BP951000_RS10215 is annotated as a hypothetical protein in NCBI. However, it is annotated as a variable surface protein (Vsp), specifically VspE, in the UniProt database. Vsps are OMPs identified in *Brachyspira hyodysenteriae* and *Mycoplasma bovis*, and are used by these pathogenic bacteria to adapt to host conditions and enhance colonization.[62,63] These proteins can undergo reversible on/off expression

Table 3. Sequence variations among nine strains: Total variations and variations in the extracellular loops of predicted outer membrane β-barrel proteins

Locus identifier	Protein names[a]	Total variations	Variations present on the predicted extracellular loop region
Group A			
BP951000_RS05730	OMP assembly factor BamA	Six variations: D60, A184, V465, A467, and F512	None
BP951000_RS10215[b]	Variable surface protein (VspE)	208 variations	Not determined[c]
BP951000_RS04760[b]	Variable surface protein (VspD)	260 variations	Not determined[c]
BP951000_RS01125	CsgG/HfaB family protein	Five variations: S63, D79, T190, I210, and L380	None
BP951000_RS03440	OMBB protein	Six variations: F24, V47, V64, N110, D169, and A197	V47
BP951000_RS05600	TolC family protein	Two variations: T246 and N499	None
BP951000_RS09000	TolC family protein	Two variations: S90 and S131	S90
BP951000_RS06235	TolC family protein	18 variations: K2, N3, F5, V6, F7, I8, I10, L12, S16, S25, N33, I42, E43, L93, S105, E136, I137, and T210	L93
BP951000_RS04880	Serpentine receptor domain-containing protein	One variation: N69	None
BP951000_RS02055	Serpentine receptor domain-containing protein	Three variations: H101, N163 and M235	N163 and M235
BP951000_RS02050	Serpentine receptor domain-containing protein	Five variations: A27, L28, T108, A228, and I247	T108 and A228
BP951000_RS07540	Serpentine receptor domain-containing protein	Six variations: M1, K2, K3, I4, I5, and L6	None
BP951000_RS00180	Serpentine receptor domain-containing protein	Two variations: I64 and M115	None
Group B			
BP951000_RS09575	Lipopolysaccharide-assembly protein (LptD)	Seven variations: N14, G137, I257, I382, E454, D600, and G944	D600
BP951000_RS03215[b]	TonB-dependent siderophore receptor	59 variations	Not determined[c]
BP951000_RS04405	Toxin A	23 variations: M1, H2, R3, I4, I6, L8, T9, M18, V19, T24, N32, S34, N41, F84, K90, N98, I101, S102, N104, S175, Q183, I264, and T303	N41, F84, K90, N98, S175, and Q183
BP951000_RS09655[b]	DUF5723 domain-containing protein	315 variations	Not determined[c]
BP951000_RS04440	Hypothetical protein	13 variations: K104, K113, S117, Y124, I132, T134, N151, G153, L243, V252, L254, S308, N321	K104 and L243
BP951000_RS08285[b]	Trep protein	43 variations	Not determined[c]
BP951000_RS04505[b]	Variable surface protein (VspH)	247 variations	Not determined[c]
BP951000_RS08455	PorV/PorQ family protein	Six variations: L12, S20, N22, A117, R187, and S253	N22 and A117
BP951000_RS01090	Variable surface protein (VspH)	One variation: E258	E258
BP951000_RS06935	Hypothetical protein	Four variations: S9, I10, V13, and R298	None
BP951000_RS11380	Toxin A	Three variations: M126, M154, and I278	M126

(Cont'd...)

Table 3. ***(Continued)***

Locus identifier	Protein names[a]	Total variations	Variations present on the predicted extracellular loop region
BP951000_RS03405	Hypothetical protein	24 variations: M1, R2, L3, K4, F5, F6, F7, L8, I9, F10, L11, F12, L13, S14, L15, S16, L17, Y18, T19, Q20, D21, N22, E23, and A24	None
BP951000_RS00185[b]	Hypothetical protein	58 variations	Not determined[c]
BP951000_RS10320	Hypothetical protein	25 variations: L18, D48, E55, F251, G285, E400, Y401, G402, I403, F404, T405, K406, Q407, L408, A409, I410, S411, F412, I413, P414, I415, N416, I417, R418, and F419	None
BP951000_RS05445	DUF3575 domain-containing protein	Six variations: K2, I7, A79, N87, H89, and K158	N87 and H89
BP951000_RS08300	Tia invasion determinant	Three variations: L143, N156, and S200	None
BP951000_RS05490[b]	Tia invasion determinant	61 variations	Not determined[c]
BP951000_RS07500[b]	Hypothetical protein	183 variations	Not determined[c]
BP951000_RS01590	Hypothetical protein	Three variations: V205, I215, and V221	None
BP951000_RS08295	Tia invasion determinant	Six variations: N34, I49, V123, S141, I144, and V167	N34
BP951000_RS08975	TonB-dependent receptor domain-containing protein	Two variations: D32 and T371	D32
BP951000_RS06930[b]	Serpentine receptor domain-containing protein	135 variations	Not determined[c]
BP951000_RS03290	Serpentine receptor domain-containing protein	None	None
BP951000_RS00765[b]	Serpentine receptor domain-containing protein	70 variations	Not determined[c]
BP951000_RS01280	Serpentine receptor domain-containing protein	Five variations: V32, A83, V124, E210, and T237	E210
BP951000_RS10445	Serpentine receptor domain-containing protein	G228	None
BP951000_RS00365	Serpentine receptor domain-containing protein	11 variations: V72, Q77, I84, D156, D159, V168, N177, A200, T216, I222, and Y226	D156, D159, and A200
BP951000_RS04620	Serpentine receptor domain-containing protein	Four variations: K2, E95, A140, and V194	None
BP951000_RS04220[b]	Serpentine receptor domain-containing protein	218 variations	Not determined[c]

Notes: [a]Protein names follow annotations in the National Center for Biotechnology Information and UniProt databases, retrieved using protein accession numbers (accessed on March 28, 2024). [b]Sequence comparison of these proteins across nine strains of *Brachyspira pilosicoli* revealed variations at more than 40 positions. Therefore, they have been listed in Table S5. [c]Given that sequence variations were present at more than 40 positions, we have not determined whether these variations are present on the transmembrane region or loop region of the predicted proteins.
Abbreviations: DUF: Domain of unknown function; OMBB: Outer membrane β-barrel; OMP: Outer membrane protein; Trep: transcriptional regulating protein.

switching or antigenic variation by expressing alternative protein phenotypes.[62] They may function as mediators for bacterial attachment to host cells.[64] Vsp-like proteins have been identified in *B. hyodysenteriae*, *B. pilosicoli*, and *Mycoplasma*;[29,62,65] however, homologs in other bacterial genera remain undiscovered, highlighting their unique role in these pathogens.

Brachyspira pilosicoli VspE, BP951000_RS10215, contains a secretory signal peptide. The structural model generated by AlphaFold 3 revealed a β-barrel architecture consisting of 16 β-strands, with the ninth and 10th strands longer than the others, giving an elliptical shape to the extracellular surface of the barrel (Figure 2B). BP951000_RS10215 exhibited the best structural alignment with the

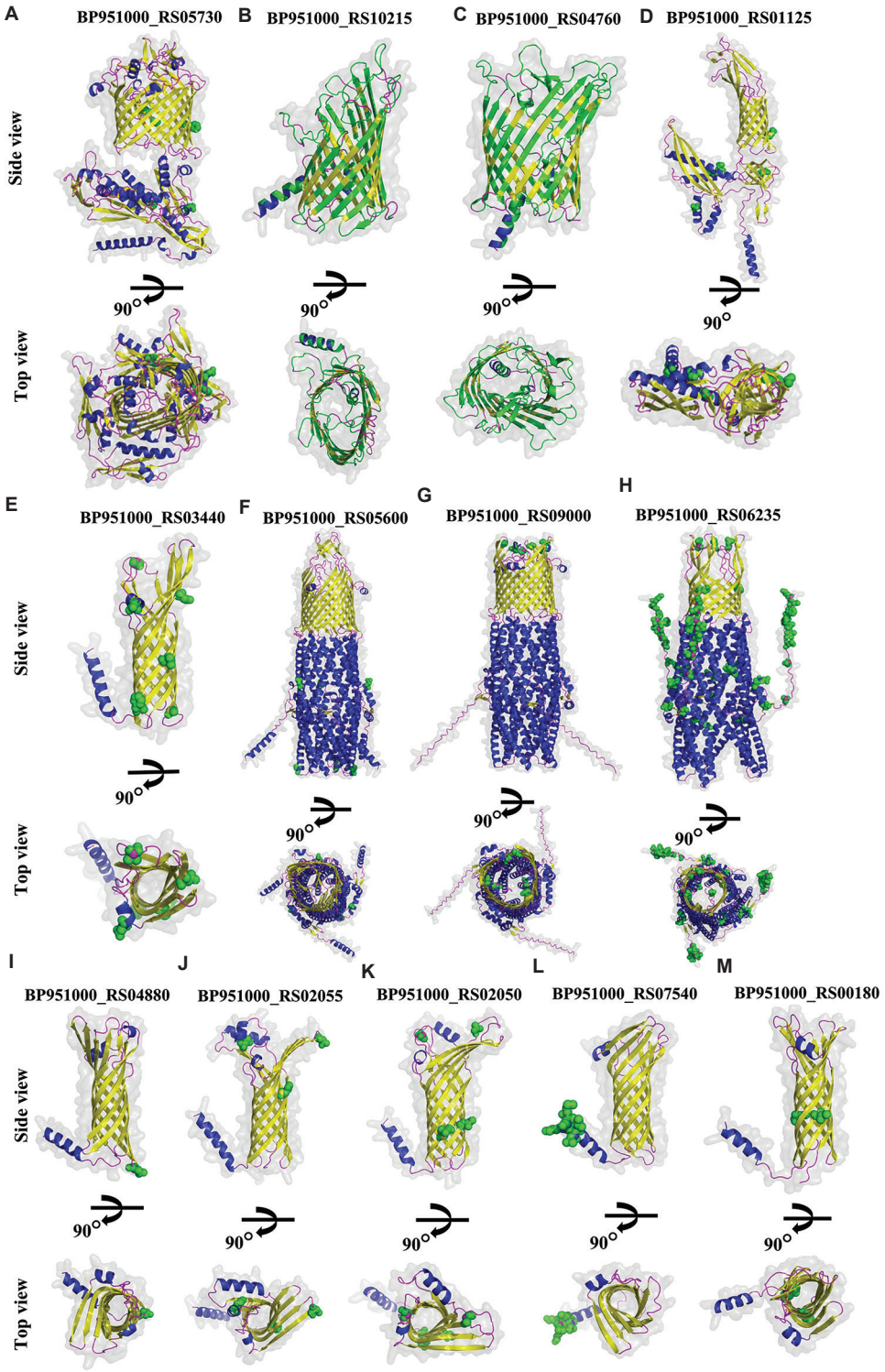

Figure 2. Structural models of β-barrel outer membrane proteins in Group A. Group A consists of 13 proteins. (A-C) Proteins with 16 *β*-strands; (F-H) predicted trimeric structures of TolC family proteins. The remaining proteins exhibit eight-stranded β-barrel structures (D-E, I-M). β-strands, α-helices, and loops are colored yellow, blue, and magenta, respectively. Green spheres indicate amino acid variations identified across nine strains of *Brachyspira pilosicoli*. Proteins with more than 40 variations are shown in green ribbon representation.

C-terminal β-barrel domain of poly-β-1,6-N-acetyl-D-glucosamine (PNAG) export protein PgaA of *E. coli* K-12 (PDB ID: 4Y25) (Tables 2 and S3). *E. coli* PgaA comprises a 16-stranded β-barrel domain at the C-terminal and eight periplasmic tetratricopeptide repeats (TPRs) at the N-terminal. In contrast, BP951000_RS10215 lacks periplasmic TPR domains. PgaA facilitates the translocation of PNAG polymer from the periplasm to the cell surface, a key step in biofilm formation.[66-68] The structural similarity of β-barrels between *E. coli* PgaA and BP951000_RS10215 implies a possible role of the Brachyspiral protein in translocation. Consistently, the Foldseek tool identified its closest match with the bacterial polysaccharide OM secretion of *E. coli* K-12, supporting a potential role in polysaccharide secretion.

In parallel, PANNZER annotated BP951000_RS10215 as VspB, suggesting a possible involvement in surface antigenic variation. Together, these findings suggest a possible dual function in secretion with surface variability (Tables 2 and S2). Given its high sequence and structural homology with *B. hyodysenteriae,* there is a strong likelihood that BP951000_RS10215 plays a role in adherence and host colonization.[62-64] Sequence variation analysis across nine strains of *B. pilosicoli* revealed 208 amino acid substitutions and several deletions (Table S5). These variations are distributed throughout the protein (Figure 2B), suggesting the ability of *B. pilosicoli* to rapidly adapt to changing environments or host immune responses.[62]

3.2.1.3. BP951000_RS04760

BP951000_RS04760 is annotated as VspD in the UniProt database and as a variable surface family protein in NCBI. As discussed in Section 3.2.2, Vsps are involved in bacterial attachment to host cells.[64] *B. hyodysenteriae* VspD is a virulence factor and a potential vaccine development target.[69] Our predictions revealed that BP951000_RS04760 carries a signal peptide and comprises a 16-stranded β-barrel architecture, with varying strand lengths creating an elliptical barrel surface on the extracellular side (Figure 2C). The protein showed the closest structural match with the β-barrel domain of the cellulose synthase operon protein C (BcsC porin; PDB ID: 6TZK) from *E. coli* K-12 (Tables 2 and S3), as determined using the DALI server. BcsC is a 16-stranded β-barrel protein with a periplasmic domain consisting of 19 TPRs, which facilitate the secretion of phosphoethanolamine-cellulose across the OM.[70-74] In contrast, BP951000_RS04760 lacks TPRs. The structural homology between the β-barrel domains of *E. coli* BcsC and BP951000_RS04760 implies a possible role for BP951000_RS04760 in translocation. This structural insight is reinforced by the Foldseek tool, which identified its closest match with the bacterial polysaccharide OM secretin of *E. coli* K-12, further supporting involvement of this protein in secretion. Complementing this, PANNZER annotated BP951000_RS10215 as VspD, which, in *B. hyodysenteriae*, is associated with adhesion and virulence. Together, these findings suggest a dual role for the protein in secretion and adhesion. (Tables 2 and S3). Among nine strains of *B. pilosicoli*, BP951000_RS04760 exhibited 260 amino acid substitutions and multiple deletions, indicating high variability (Table S5). These variations were distributed throughout the protein (Figure 2C).

3.2.1.4. BP951000_RS01125

BP951000_RS01125 is annotated as the curli production assembly/transport component CsgG in both the NCBI and UniProt databases. SignalP predicted a lipoprotein signal peptide, whereas LipoP predicted it as a cytoplasmic protein. The structural model of the protein showed a β-barrel architecture comprising eight β-strands extending into the periplasm via the periplasmic domain (Figure 2D). DALI server results showed that BP951000_RS01125 exhibited the best structural match with OmpF (PDB ID: 4RLC) of *Pseudomonas aeruginosa* (Tables 2 and S3). *P. aeruginosa* OmpF is involved in biofilm formation, OM vesicle production, adhesion, and host immune system modulation.[75-81] The Foldseek tool identified its closest structural match with an uncharacterized protein from the marine metagenome. Sequence-based annotation using PANNZER and eggNOG-mapper confirmed BP951000_RS01125 to be a CsgG homolog (Tables 2 and S3).

The CsgG curli production assembly/transport component OMP is essential for the secretion of curli—functional amyloid fibers that constitute the primary protein component of biofilm extracellular matrices in *Bacteroidetes* and Proteobacteria—and play key roles in pathogenesis.[82] Curli fimbriae are involved in the initial colonization of the host, as well as in bacterial persistence and invasion.[83-85] Considering that both OmpF and CsgG are functionally linked to surface-associated processes and virulence, the combined structural and sequence-level analyses strongly suggest that BP951000_RS01125 may play a similar role in *B. pilosicoli*. Across *B. pilosicoli* strains, BP951000_RS01125 exhibited sequence variations at five positions (S63, D79, T190, I210, and L380) (Tables 3 and S4). Structural mapping revealed that L380 is located within the β-barrel domain, whereas the remaining variations are positioned in the periplasmic region of the protein (Table S4).

3.2.1.5. BP951000_RS03440

BP951000_RS03440 is annotated as a hypothetical protein in the UniProt database, whereas NCBI identifies it as an

"OMBB protein." Our study supports the latter annotation, revealing the presence of a secretory signal peptide. Structural modeling using AlphaFold 3 showed a β-barrel architecture comprising eight β-strands (Figure 2E). Structural similarity assessment using the DALI server identified the closest match with *Neisseria meningitidis* NspA (PDB ID: 1P4T) (Tables 2 and S3). NspA, an eight-stranded β-barrel protein, is involved in bacterial attachment and interaction with the host immune system and has been proposed as a potential vaccine candidate.[86-89] Foldseek analysis identified an uncharacterized protein of *Brachyspira murdochii* as its closest structural homolog, suggesting potential species-specific divergence.

Sequence-based annotation using PANNZER predicted the presence of an OMBB domain (Tables 2 and S3). Together, the structure- and sequence-based data strongly support the classification of BP951000_RS03440 as an OMBB protein, likely involved in host-pathogen interaction. MSA across *B. pilosicoli* strains identified six variations (F24, V47, V64, N110, D169, and A197) (Tables 3 and S4). Structural mapping localized one variation (V47) to the ECL region, four variations (F24, V64, N110, A197) to the TM region, and one variation (D169) to the intracellular region of the protein (Table S4).

3.2.1.6. BP951000_RS05600

BP951000_RS05600 is annotated as a putative OM component of a multidrug efflux system in UniProt and as a TolC family protein in NCBI. Both SignalP and LipoP predicted a secretory signal peptide. The AlphaFold 3 model revealed a trimer 18-stranded β-barrel, with each subunit (protomer) contributing six β-strands (i.e., one-third of the barrel) (Figure 2F). As no known 18-stranded TolC structures have been discovered to date, we validated this model using TrRosetta, RoseTTAFold, ESMFold, and SWISS-MODEL. All models showed high similarity and aligned closely with the AlphaFold 3 model. Alignment of the five monomeric models yielded a root mean square deviation (RMSD) of 3.96 Å, supporting model reliability (Figure S2). Like canonical TolC, the TM barrel extends into the periplasm as an α-helical tunnel, connected to the OM (Figure 2F),[90] with its periplasmic entry blocked, likely to prevent leakage through the OM, as the β-barrel domain remains constantly open.[91]

BP951000_RS05600 showed the best structural match with *E. coli* K-12 TolC (PDB ID: 6WXI) (Tables 2 and S3). TolC functions in hemolysin secretion,[92,93] colicin import,[94,95] antibiotic efflux,[96] and serves as a bacteriophage receptor.[97] PANNZER and eggNOG-mapper respectively annotated the protein as "integral OMP TolC" and "efflux TM transporter" (Tables 2 and S3), suggesting similar roles in *B. pilosicoli*. Sequence comparison across nine strains of *B. pilosicoli* revealed two variations (T246 and N499) (Tables 3 and S4), both mapped to the periplasmic α-helical regions of the protein (Table S4).

3.2.1.7. BP951000_RS09000

BP951000_RS09000 is annotated as an OM efflux protein in UniProt and as a TolC family protein in NCBI. It carries a secretory signal peptide. The AlphaFold 3 model revealed a trimeric 18-stranded β-barrel, with each protomer contributing six β-strands (Figure 2G). Similar to BP951000_RS05600 (Section 3.2.6), we validated this structure using TrRosetta, RoseTTAFold, ESMFold, and SWISS-MODEL. Structural alignment of monomeric models from all five tools yielded an RMSD value of 3.85 Å (Figure S3), confirming strong agreement with the AlphaFold 3 prediction. Consistent with canonical TolC proteins, the barrel extends into the periplasm as an α-helical tunnel (Figure 2G).[90] Structural alignment identified *E. coli* K-12 TolC (PDB ID: 6WXI) as the closest match (Tables 2 and S3). As described in Section 3.2.6, *E. coli* TolC mediates hemolysin secretion,[92,93] colicin import,[94,95] antibiotic efflux,[96] and bacteriophage recognition.[97] The Foldseek tool identified its closest structural match with an uncharacterized protein from a *Spirochaete* bacterium. PANNZER and eggNOG-mapper similarly annotated BP951000_RS09000 as an integral OMP and efflux transporter (Tables 2 and S3). Amino acid sequence comparison across nine *B. pilosicoli* strains revealed two variations: S90 (in the ECL region) (Figure 2G) and S131 (within the β-barrel domain) (Tables 3 and S4).

3.2.1.8. BP951000_RS06235

BP951000_RS06235 is annotated as a TolC family protein in UniProt. The AlphaFold 3 model predicted a trimeric 12-stranded β-barrel, with each subunit contributing four β-strands (Figure 2H). As in Section 3.2.6, we validated this structure using ESMFold, SWISS-MODEL, RoseTTAFold, and TrRosetta. Structural alignment of monomeric models from all tools yielded an RMSD of 3.26 Å (Figure S4), confirming model consistency. The barrel extends into the periplasm as an α-helical tunnel connecting to the OM (Figure 2H).[90] DALI analysis showed the highest similarity to *E. coli* K-12 TolC (PDB ID: 6WXI) (Tables 2 and S3). Foldseek identified the closest homolog as TolC from a *Spirochaete* bacterium. PANNZER and eggNOG-mapper consistently annotated the protein as an OM efflux protein (Tables 2 and S3), suggesting a TolC-like function. Sequence alignment across nine *B. pilosicoli* strains revealed variations at 18 positions: K2, N3, F5, V6, F7, I8, I10, L12, S16, S25, N33, I42, E43, L93, S105, E136, I137, and T210 (Tables 3 and S4). Mapping showed L93

in the ECL region (Figure 2H), S105 in the β-barrel, and the remaining residues within the periplasmic domain (Table S4).

3.2.1.9. Eight-stranded β-barrel proteins annotated as SR domain-containing proteins

Thirteen *B. pilosicoli* proteins annotated in UniProt as "SR domain-containing proteins" were predicted in this study as OMBB proteins. Five proteins—BP951000_RS04880, BP951000_RS02055, BP951000_RS02050, BP951000_RS07540, and BP951000_RS00180—were classified as group A (predicted as OMBB proteins by all tools). Except for BP951000_RS02055 (annotated as an OMBB in NCBI), the rest are listed as hypothetical in NCBI. SRs, or G-protein-coupled receptors (GPCRs), are eukaryote-specific heptahelical membrane proteins.[98,99] However, AlphaFold 3 models of these *B. pilosicoli* proteins displayed eight-stranded β-barrel architectures with four extracellular and three periplasmic loops (Figure 2I–M). These conformations were consistently supported by ESMFold, SWISS-MODEL, RoseTTAFold, and TrRosetta tools. As GPCRs are absent in prokaryotes, and given that all tools predicted TM β-barrel structures rather than α-helices, we conclude that these proteins are misannotated as SR proteins in UniProt. The reason for this misannotation is that UniProtKB/TrEMBL annotates proteins automatically using computational pipelines. These annotations are not manually curated and rely on sequence similarity and automated rule-based systems.[100]

DALI analysis showed that BP951000_RS02055, BP951000_RS07540, and BP951000_RS00180 best matched the N-terminal β-barrel domain of *E. coli* K-12 OM protein A (OmpA) (PDB ID: 9FZC), whereas BP951000_RS02050 exhibited the best structural match with another *E. coli* K-12 OmpA structure (PDB ID: 9FZD) (Tables 2 and S3). Unlike *E. coli* OmpA, which includes both β-barrel and periplasmic domains, these *B. pilosicoli* proteins lack the periplasmic domain. *E. coli* OmpA functions in phage recognition, colicin transport, conjugation, membrane integrity maintenance, solute diffusion, and virulence. It also contributes to the virulence and pathogenicity of *E. coli*, making it a key target in the immune response.[101-109] BP951000_RS04880 aligned best with NspA of *N. meningitidis* (PDB ID: 1P4T) (Tables 2 and S3), a potential vaccine candidate involved in host adhesion and immune interaction.[86-89] This suggests that BP951000_RS04880 might have a role in adhesion and may be explored experimentally as a potential vaccine candidate.

PANNZER annotated all five proteins as OMBB domain-containing proteins. Foldseek identified BP951000_RS02055 and BP951000_RS02050 to be structurally closest to an OMBB protein of *B. hyodysenteriae*, whereas the remaining three proteins matched to an uncharacterized protein of *Brachyspira* spp. (Tables 2 and S3). Functional roles of these five proteins remain uncertain, highlighting the need for experimental validation. Amino acid sequence comparison across nine *B. pilosicoli* strains revealed several variations (Tables 3 and S4). BP951000_RS02055 and BP951000_RS02050 had variations in ECL regions (Figure 2J and 2K); variations in the remaining proteins were located in TM or periplasmic regions (Figure 2I, L, and M, Tables 3 and S4).

3.2.2. Group B

Group B included 29 proteins with diverse β-barrel architectures: a 26-stranded barrel (BP951000_RS09575); a 22-stranded barrel (BP951000_RS03215); an 18-stranded barrel (BP951000_RS04405); four 16-stranded barrels (BP951000_RS09655, BP951000_RS04440, BP951000_RS08285, and BP951000_RS04505); two 14-stranded barrels (BP951000_RS08455 and BP951000_RS01090); one 13-stranded barrel (BP951000_RS08975); four 12-stranded barrels (BP951000_RS06935, BP951000_RS11380, BP951000_RS03405, and BP951000_RS00185); one 10-stranded barrel (BP951000_RS10320); and six 8-stranded barrels (BP951000_RS05445, BP951000_RS08300, BP951000_RS05490, BP951000_RS07500, BP951000_RS01590, and BP951000_RS08295). In addition, eight 8-stranded β-barrel SR domain-containing proteins (BP951000_RS06930, BP951000_RS03290, BP951000_RS00765, BP951000_RS01280, BP951000_RS10445, BP951000_RS00365, BP951000_RS04620, and BP951000_RS04220) were identified (Table 1).

3.2.2.1. BP951000_RS09575

BP951000_RS09575 is annotated as LptD in *B.pilosicoli,*[20] a component of the LPS transport (LPT) system responsible for transporting LPS from the inner OM leaflet to the Gram-negative bacterial surface.[110] It carries a predicted secretory signal peptide. The AlphaFold 3 structural model revealed a 26-stranded β-barrel spanning the OM, with a lateral opening between strands 1 and 26, and a distinctive periplasmic β-jelly roll domain (Figure 3A). DALI analysis showed the best structural alignment with *Yersinia pestis* LptD (PDB ID: 5IXM) (Tables 2 and S3). Functional annotation by PANNZER and eggNOG-mapper confirmed roles in cell envelope biogenesis and LPT function, respectively, further validating its identity as LptD in *B. pilosicoli* (Tables 2 and S3). Sequence variation analysis across nine *B. pilosicoli* strains revealed seven variations: N14, G137, I257, I382, E454, D600, and G944 (Figure 3A, Tables 3 and S1). Structural mapping showed G944 in the ICL region, D600 in the ECL, I382 and E454 in the TM region, and the remaining variations in the β-jelly roll domain (Table S4).

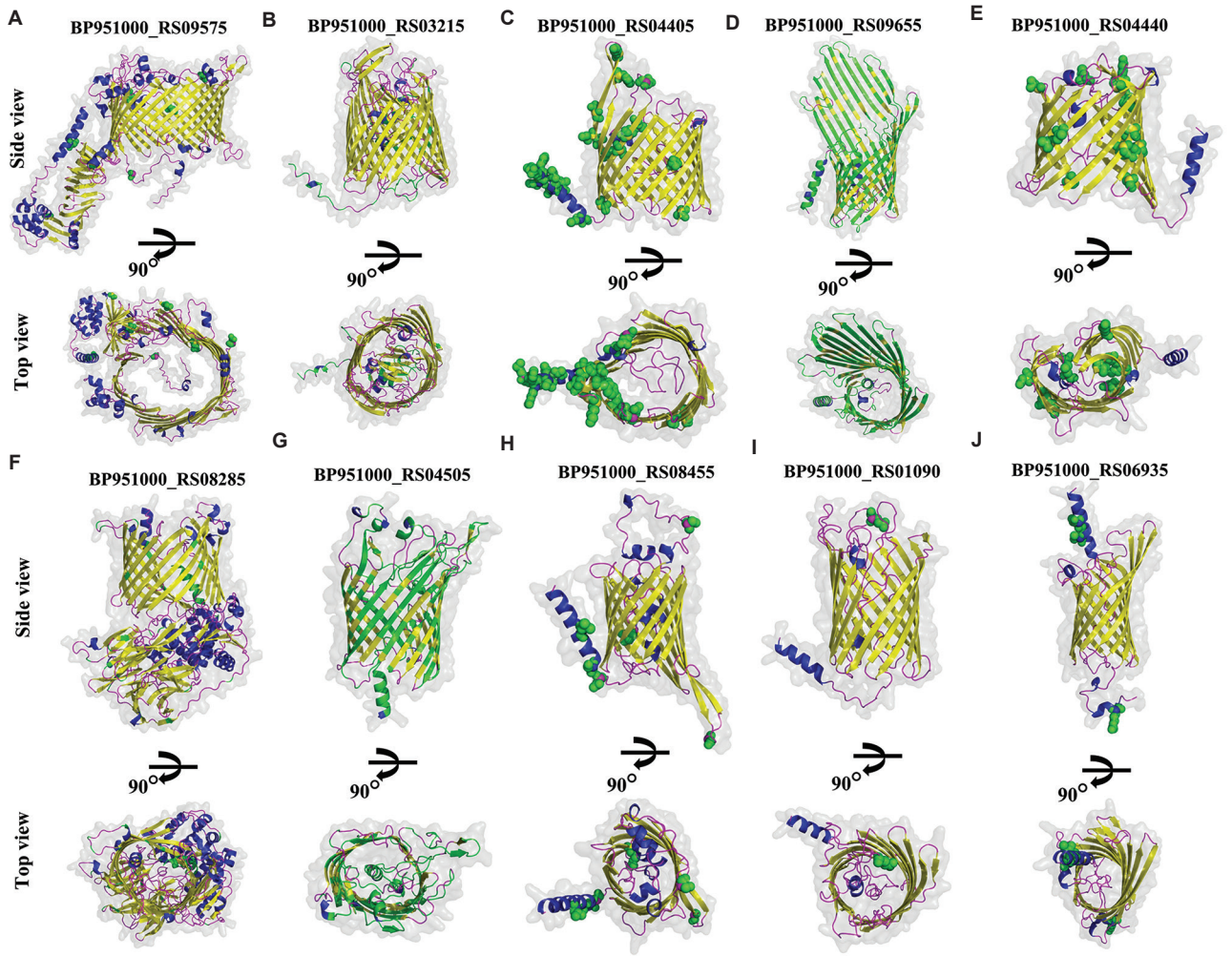

Figure 3. Structural models of β-barrel outer membrane proteins in group B. Group B includes 29 proteins, of which 10 are illustrated here (A-J). β-strands, α-helices, and loops are colored yellow, blue, and magenta, respectively. Green spheres indicate amino acid variations identified across nine strains of *Brachyspira pilosicoli*. Proteins with more than 40 variations are shown in green ribbon representation.

3.2.2.2. BP951000_RS03215

BP951000_RS03215 is annotated as a TonB-dependent siderophore receptor in *B. pilosicoli*. SignalP predicted a secretory signal peptide, while LipoP predicted a cytoplasmic localization. The AlphaFold 3 model revealed a 22-stranded C-terminal β-barrel and an N-terminal plug domain (Figure 3B). DALI analysis showed the best structural alignment with *E. coli* K-12 BtuB (PDB ID: 3RGM) (Tables 2 and S3), a TonB-dependent transporter (TBDT) with a 22-stranded β-barrel and an N-terminal plug domain that occludes the lumen.[111] *E. coli* BtuB mediates vitamin B_{12} (cobalamin) uptake via ECLs.[111-113] TBDTs also transport heme, ferric-siderophores, sucrose, and maltodextrin.[114,115] BP951000_RS03215 shares the same overall architecture as *E. coli* BtuB, and its high Z-score (32.1) confirms strong homology. Foldseek further identified a TonB-dependent receptor (TBDR) from a member of the phylum *Bacteroidetes* as the closest match, supporting a role in nutrient uptake. Sequence-based annotation using PANNZER and eggNOG-mapper, respectively, classified the protein as an OM receptor and linked it to cobalamin transport activity (Tables 2 and S3). Together, these results strongly suggest that BP951000_RS03215 functions as a TonB-dependent OM receptor involved in vitamin B_{12} transport. Sequence variation analysis across nine *B. pilosicoli* strains identified 59 variations (Table S5), which were mapped onto the structural model (Figure 3B).

3.2.2.3. BP951000_RS04405

BP951000_RS04405 is annotated as Toxin A in UniProt[20] but as a hypothetical protein in NCBI. It contains a predicted secretory signal peptide. The AlphaFold 3

structural model revealed a β-barrel comprising 18 β-strands, nine ECLs, and eight periplasmic loops (Figure 3C). DALI analysis showed the highest structural similarity to *P. aeruginosa* PAO1 porin OM channel protein K (OccK)-7 (PDB ID: 4FRT) (Tables 2 and S3). The OccK protein family contains a ladder of basic residues (arginine + lysine = 11%) that form a positively charged channel for the uptake of small, carboxyl-containing substrates.[116-119] BP951000_RS04405 exhibited a lower arginine + lysine content (7.6%), suggesting that while structurally similar to OccK, it may facilitate the transport of alternative substrates. Foldseek identified its closest structural match with an uncharacterized protein from *Treponema vincentii*. PANNZER annotated it as Toxin A, a known virulence factor (Tables 2 and S3).[120]

These findings suggest that BP951000_RS04405 is a porin-like protein with potential functional divergence, warranting further experimental annotation. A total of 23 amino acid sequence variations were identified across nine *B. pilosicoli* strains (Tables 3 and S4). Structural mapping showed six variations (N41, F84, K90, N98, S175, and Q183) in the ECL region, eight (T24, N32, S34, I101, S102, N104, I264, and T303) in the TM β-barrel region, and the remainder in the periplasmic region (Figure 3C and Table S4).

3.2.2.4. BP951000_RS09655

BP951000_RS09655 is annotated as a hypothetical protein in NCBI and as a domain of unknown function (DUF) 5723 domain-containing protein in UniProt. It carries a secretory signal peptide. The AlphaFold model predicted a 16-stranded β-barrel, with strands 3–12 longer than the rest, giving the barrel an asymmetric extracellular profile (Figure 3D).

DALI analysis identified the closest structural match with the tetraheme c-type cytochrome CymA from *Klebsiella oxytoca* (PDB ID: 4V3G) (Tables 2 and S3). CymA, a 14-stranded OMP, facilitates passive diffusion of large molecules such as cyclodextrins and linear maltooligosaccharides.[121,122] It aligned with 14 of the 16 β-strands in BP951000_RS09655. The comparable pore diameter suggests a similar function in passive diffusion channels in *B. pilosicoli*. Structural alignment using the US-Align server yielded an RMSD of 4.28 Å, supporting high structural homology. PANNZER annotated the protein as a cell surface protein (Tables 2 and S3). Sequence comparison across nine strains of *B. pilosicoli* revealed 315 variations and multiple deletions, indicating high variability across the full length of the protein (Figure 3D and Table S5).

3.2.2.5. BP951000_RS04440

BP951000_RS04440, annotated as a hypothetical protein, contains a secretory signal peptide. The AlphaFold 3 model predicted a 16-stranded β-barrel structure with a lateral gate between strands 1 and 16 (Figure 3E). DALI analysis revealed its closest structural match with the translocation and assembly module protein A (TamA) from *E. coli* (PDB ID: 4C00) (Tables 2 and S3), an Omp85 superfamily protein featuring three N-terminal POTRA domains and a C-terminal 16-stranded β-barrel.[123] TamA facilitates autotransporter β-barrel membrane insertion and passenger domain translocation into the extracellular space.[123-125] Foldseek also identified a structural match with an Omp85 domain-containing protein from *Dracunculus medinensis*. While BP951000_RS04440 closely resembles the TamA β-barrel domain, it lacks the POTRA domains, suggesting functional divergence. BP951000_RS04440 is thus predicted to be a structural homolog of TamA, but its specific role in *B. pilosicoli* remains to be clarified. Notably, PANNZER annotated the protein as Toxin A (Tables 2 and S3). Sequence comparison across nine *B. pilosicoli* strains revealed 10 variations (K104, K113, S117, Y124, I132, T134, N151, G153, L243, and V252) (Tables 3 and S4). Structural mapping showed K104 and L243 in the ECL region, with the remaining variations located within the TM β-barrel domain (Figure 3E and Table S4).

3.2.2.6. BP951000_RS08285

BP951000_RS08285 is annotated as a transcriptional regulating protein (Trep) in *B. pilosicoli*. In *Pseudomonas fluorescens*, Trep catalyzes trehalose phosphorylation and its translocation across the OM.[126] LipoP predicted BP951000_RS08285 as cytoplasmic, whereas SignalP predicted no signal peptide. The AlphaFold 3 predicted a 16-stranded C-terminal β-barrel with a large N-terminal periplasmic domain and a lateral opening between strands 1 and 16 (Figure 3F). Structure-based annotation showed the closest match with TolB proteins from *E. coli* K-12 (PDB ID: 3IAX) and *Citrobacter freundii* (PDB ID: 2IVZ) (Tables 2 and S3). *E. coli* TolB is a periplasmic protein with a two-domain structure: an α/β N-terminal domain and a six-bladed β-propeller C-terminal domain (Figure S5).[127] The periplasmic domain of BP951000_RS08285 closely resembles the TolB C-terminal domain, suggesting a similar role in porin assembly and cell envelope integrity.[128-130] However, unlike TolB, BP951000_RS08285 includes an additional TM β-barrel domain, indicating potential functions unique to *B. pilosicoli*.

When the β-barrel domain alone was queried, the top DALI hit was filamentous hemagglutinin (FHA) transporter FhaC (PDB ID: 4QL0) from *Bordetella pertussis*, a 16-stranded β-barrel protein that transports FHA (Figure S5).[131] While FhaC includes POTRA domains for substrate recognition,[132] BP951000_RS08285 lacks them, suggesting it may function as a translocation pore

with distinct specificity. Foldseek identified the closest structural match with an uncharacterized protein from a *Spirochaete* bacterium (Tables 2 and S3). PANNZER annotated BP951000_RS08285 as Trep, while eggNOG-mapper linked it to TonB-independent uptake pathways. BLASTp analysis showed no sequence homologs in other spirochetes (e.g., *Treponema*, *Borrelia*, and *Leptospira*), indicating species-specific uniqueness. MSA across nine *B. pilosicoli* strains revealed 43 variations (Table S5).

3.2.2.7. BP951000_RS04505

BP951000_RS04505 is annotated as VspH in *B. pilosicoli*.[20] As described in Section 3.2.3, Vsps mediate bacterial adherence to host cells.[64] SignalP predicted no signal peptide, whereas LipoP predicted the presence of N-terminal TMHs. The AlphaFold 3 model revealed a 16-stranded β-barrel (Figure 3G).

Structural alignment identified the closest match with *E. coli* K-12 PgaA (PDB ID: 4Y25) (Tables 2 and S3). As discussed in Section 3.2.2, PgaA facilitates polysaccharide translocation across the OM. Additionally, Foldseek identified its best alignment with a bacterial polysaccharide OM secretin from *E. coli* K-12, supporting this hypothesis. PANNZER annotated the protein as a cell surface protein. Based on both structural and sequence analyses, BP951000_RS04505 is likely involved in polysaccharide secretion across the OM. Notably, its homolog in *B. hyodysenteriae* (VspH) has been evaluated as a potential vaccine candidate.[69] Sequence comparison across nine *B. pilosicoli* strains revealed 247 amino acid variations and multiple deletions, indicating high variability throughout the protein (Figure 3G and Table S5).

3.2.2.8. BP951000_RS08455

BP951000_RS08455 is annotated as a PorV/PorQ family protein in UniProt and as a hypothetical protein in NCBI. PorV and PorQ are integral components of the type IX secretion system, involved in protein export in Gram-negative members of the Fibrobacteres–Chlorobi–Bacteroidetes superphylum.[133] The AlphaFold 3 model revealed a 14-stranded β-barrel structure with seven ECLs and an interior blocked by an N-terminal hatch domain (Figure 3H). Foldseek identified structural similarity to a PorV/PorQ family protein, and the best DALI match was *E. coli* long-chain fatty acid transporter FadL (PDB ID: 2R88) (Tables 2 and S3). Like FadL, BP951000_RS08455 adopts a monomeric 14-stranded β-barrel,[134] though it lacks the lateral opening formed by the inward bend in a β-strand that is essential for fatty acid transport in FadL.[135] Despite this structural difference, the remaining structural resemblance suggests a potential role in transporting hydrophobic molecules.[136] Although PANZZER annotated the protein as uncharacterized, structure-based evidence strongly supports its function as a transporter of hydrophobic substrates. Sequence comparison across nine *B. pilosicoli* strains revealed an insertion at position 255 and six variations (L12, S20, N22, A117, R187, and S253) (Figure 3H, Tables 3 and S4). Mapping these onto the model placed N22 and A117 in the ECL region, S253 in the ICL region, R187 in the β-barrel TM region, and the remaining variations in the N-terminal domain (Table S4).

3.2.2.9. BP951000_RS01090

BP951000_RS01090 is annotated as a hypothetical protein in NCBI but as a VspH in UniProt. SignalP predicted a secretory signal peptide. The AlphaFold 3 model revealed a 14-stranded β-barrel architecture (Figure 3I). Sequence-based annotation using PANNZER supported the VspH designation. DALI analysis identified *K. oxytoca* CymA (PDB ID: 4V3G) as the closest structural homolog (Tables 2 and S3). As discussed in Section 3.2.13, CymA functions as a diffusion channel for bulky substrates. Foldseek further indicated similarity to an uncharacterized protein from a *Chitinophagaceae* bacterium. Sequence comparison across nine *B. pilosicoli* strains revealed a single variation, E258, located in the ECL region (Figure 3I; Tables 3 and S4). Structural alignment of BP951000_RS04760, BP951000_RS02055, BP951000_RS04505, and BP951000_RS01090 using the US-align server resulted in an RMSD of 4.00 Å (Figure S6).

3.2.2.10. BP951000_RS06935

BP951000_RS06935 is annotated as a hypothetical protein in UniProt and NCBI. It is predicted to contain a secretory signal peptide. The AlphaFold 3 model revealed a 12-stranded β-barrel structure with six ECLs (Figure 3J). Structural homology search identified the closest match as the β-barrel domain of the *E. coli* hemoglobin-binding protease (Hbp) autotransporter (PDB ID: 3AEH) (Tables 2 and S3). Hbp, a member of the serine protease autotransporters of Enterobacteriaceae family, consists of an N-terminal serine protease passenger domain and a C-terminal β-barrel that facilitates its extracellular secretion.[137-139] While BP951000_RS06935 lacks a periplasmic or passenger domain, its β-barrel homology suggests a role in substrate translocation across the OM.

Foldseek identified the best match with a 12-stranded β-barrel OMP from Cluster of Orthologous Groups (COG) 4313 of *Pseudomonas putida* F1, which has a dynamic lateral opening that permits the passage of hydrophobic molecules.[140] Sequence-based annotation by PANNZER linked BP951000_RS06935 to Toxin A. Collectively, structure- and sequence-based analyses suggest that BP951000_RS06935 may act as an autotransporter or facilitate hydrophobic molecule transport. Sequence

variation analysis across nine *B. pilosicoli* strains revealed four variations (S9, I10, V13, and R298) (Figure 3J, Tables 3 and S4). When mapped onto the structural model, these variations were present in the N-terminal and C-terminal regions of the β-barrel structure (Table S4).

3.2.2.11. BP951000_RS11380

BP951000_RS11380, annotated as a hypothetical protein in NCBI, was predicted to contain a secretory signal peptide. UniProt classified the protein as Toxin A. It has an N-terminal TMH, predicted by LipoP. The AlphaFold 3 model revealed a 12-stranded β-barrel (Figure 4A). Structural alignment using DALI showed the closest match to *E. coli* O157:H7 serine protease EspP (PDB ID: 2QOM) (Tables 2 and S3), a member of the serine protease autotransporters of *Enterobacteriaceae* family of autotransporters.[141] These specialized porins contain a C-terminal β-barrel that facilitates the secretion of an N-terminal virulence-associated passenger domain. Some autotransporters consist solely of the β-barrel autotransporter domain, with the passenger or toxin-encoding gene located upstream in the genome.[142] The EspP passenger domain exhibits serine protease activity, cleaving host proteins such as pepsin A and human coagulation factor V.[143-145] Given the structural similarity, BP951000_RS11380 might function as an autotransporter for a serine protease or virulence factor encoded elsewhere in the genome. Foldseek identified the closest structural homolog with an uncharacterized protein from *Candidatus margulis*. Sequence-based analysis by PANNZER also aligned it with Toxin A. Sequence comparison across nine *B. pilosicoli* strains revealed three variations (M126, M154, and I278), with M126 located in the ECL region and the other two (M154 and I278) in the TM β-barrel region (Figure 4A, Tables 3 and S4).

3.2.2.12. BP951000_RS03405

BP951000_RS03405, annotated as a hypothetical protein, contains a secretory signal peptide. The AlphaFold 3 model revealed a 12-stranded β-barrel (Figure 4B). DALI analysis showed *E. coli* OMPLA as the closest structural homolog (PDB ID: 1ILD) (Tables 2 and S3). OMPLA is an acyl hydrolase that cleaves ester bonds in phospholipids and lysophospholipids, and contributes to colicin secretion.[146-148] BP951000_RS03405, as a structural homolog of *E. coli* OMPLA, may serve similar functions in *B. pilosicoli*. Although OMPLA contains a catalytic histidine (His)–serine (Ser)–asparagine (Asn) triad, BP951000_RS03405 lacks this exact motif; however, Ser and Asn residues are present at adjacent positions 224 and 225. Foldseek indicated homology to a DUF1207 domain-containing protein from *Ignavibacteria*, suggesting possible functional diversity, while PANNZER annotated BP951000_RS03405 simply as an OMP. Sequence alignment across nine strains of *B. pilosicoli* revealed 24 variations, all located within the periplasmic region of the β-barrel structure (Figure 4, Tables 3 and S4).

3.2.2.13. BP951000_RS00185

BP951000_RS00185, annotated as a hypothetical protein, contains a secretory signal peptide with a cleavage site between residues 20 and 21. The AlphaFold 3 model predicted a 12-stranded β-barrel (Figure 4C). DALI analysis identified *E. coli* K-12 OMPLA as the closest structural match (PDB ID: 1QD6; Z-score = 18.3, RMSD = 3.1 Å) (Tables 2 and S3). As discussed in Section 3.2.21, OMPLA hydrolyzes acyl ester bonds in phospholipids and lysophospholipids and is involved in colicin secretion.[146-148] Although OMPLA contains a catalytic His–Ser–Asn triad, BP951000_RS00185 lacks this motif. However, adjacent Ser–Asn residues were identified at positions 25–26 and 73–74. Foldseek identified structural homology to a DUF1207 domain-containing protein from *Ignavibacteria*. Sequence-based annotation indicated similarity to Toxin A, a known virulence factor.[120] Sequence variation across nine strains of *B. pilosicoli* revealed 58 variations predominantly present in the signal peptide region (Figure 4C and Table S5).

3.2.2.14. BP951000_RS10320

BP951000_RS10320, annotated as a hypothetical protein, is predicted to contain a secretory signal peptide. The AlphaFold 3 model revealed a 10-stranded β-barrel with several TM β-strands extending toward the periplasmic side, forming an elliptical pore (Figure 4D). Periplasmic loops from the TM barrel are also folded into α-helices and β-strands. Structural homology using Foldseek identified the best match with an uncharacterized protein from *B. murdochii*. DALI analysis returned synthetic TM β-barrels as the top four hits; the fifth hit, *N. meningitidis* opacity-associated protein A (OpcA) (PDB ID: 2VDF), was considered the best structural homolog (Tables 2 and S3). OpcA is a 10-stranded β-barrel OMP that mediates adhesion by binding host cell proteoglycans.[149,150] Sequence analysis using PANNZER also indicated homology with a cell surface protein, supporting a potential role in host cell interaction and adhesion. Sequence analysis across nine *B. pilosicoli* strains revealed 25 variations, none of which were located in the ECL region (Figure 4D, Tables 3 and S4).

3.2.2.15. BP951000_RS05445

BP951000_RS05445, annotated as a DUF3575 domain-containing protein in UniProt and as a hypothetical protein in NCBI, carries a predicted secretory signal peptide (SignalP), although LipoP classified it as a cytoplasmic

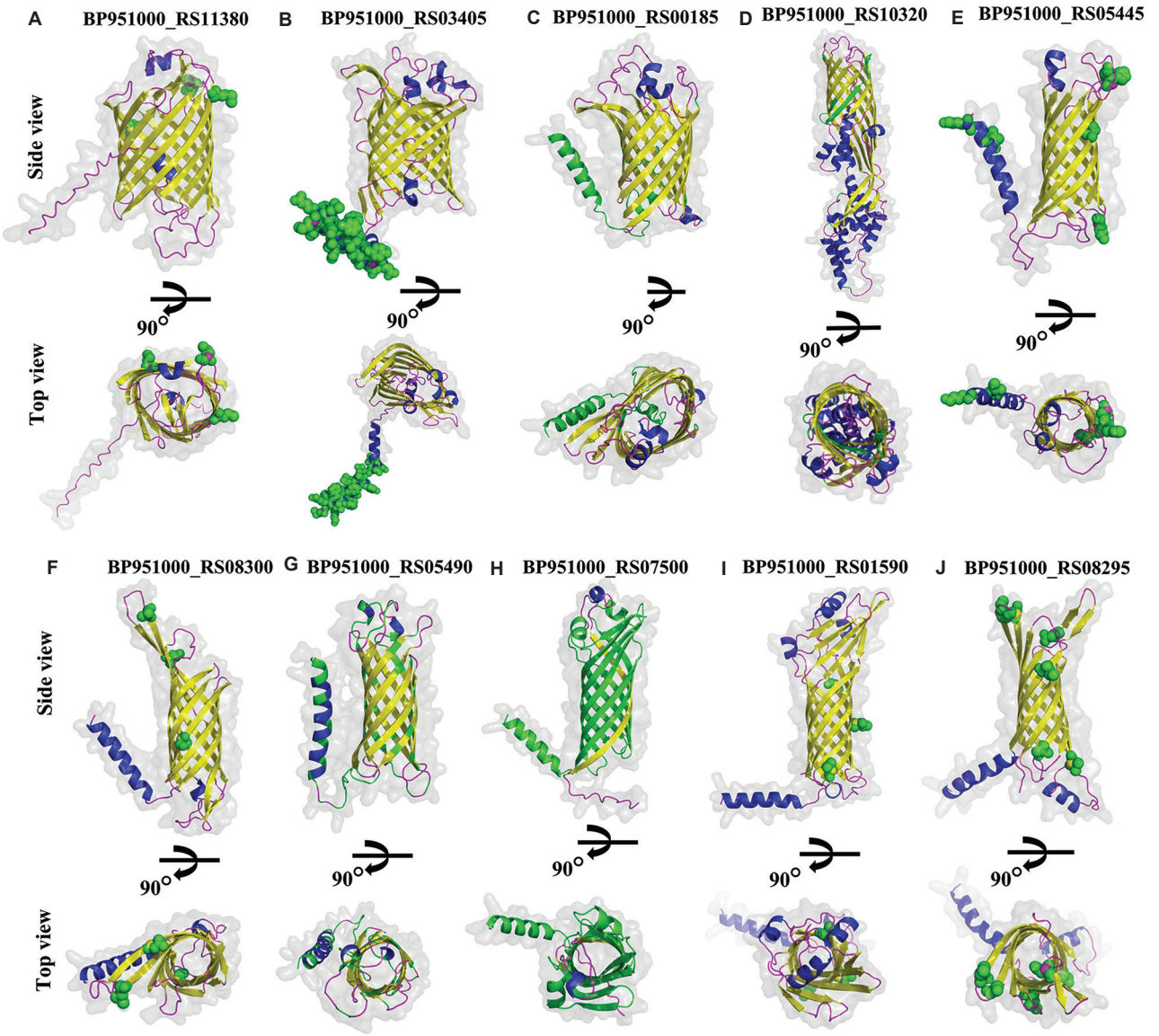

Figure 4. Structural models of β-barrel outer membrane proteins in Group B (continued). Structural models of 10 Group B proteins are shown (A-J), arranged in descending order based on the number of β-strands in their β-barrel architectures. β-strands, α-helices, and loops are colored yellow, blue, and magenta, respectively. Green spheres indicate amino acid variations identified across nine strains of *Brachyspira pilosicoli*. Proteins with more than 40 variations are shown in green ribbon representation.

protein. The AlphaFold 3 model revealed an eight-stranded β-barrel architecture (Figure 4E). DALI analysis for structural homology showed the best matches with two proteins: OmpF (PDB ID: 4RLC) of *P. aeruginosa* PAO1 and NspA (PDB ID: 1P4T) of *N. meningitidis* (Tables 2 and S3). Given the established roles of OmpF and NspA in adhesion, immune modulation, and biofilm formation (as discussed in Sections 3.2.4 and 3.2.5), BP951000_RS05445 may serve similar functions in *B. pilosicoli*.

Sequence-based annotation identified it as Tia invasion protein, supporting its potential role as an adhesin involved in host cell interaction. Comparative sequence analysis across nine *B. pilosicoli* strains revealed six variations (K2, I7, A79, N87, H89, and K158) (Figure 4E, Tables 3 and S4). Mapping onto the structural model showed N87 and H89 in the ECL region, K158 in the ICL region, A79 in the β-barrel domain, and the remaining two in the N-terminal region of the protein (Table S4).

3.2.2.16. BP951000_RS08300

BP951000_RS08300 is annotated as a Tia invasion determinant. Tia proteins, known in enterotoxigenic *E.*

coli, function as both adhesins and invasins.[151] Tia proteins consist of eight TM β-sheets with four surface-exposed loops and bind specific receptors on HCT8 human ileocecal epithelial cells.[152]

BP951000_RS08300 is predicted to contain a secretory signal peptide, and its AlphaFold 3 model revealed an elliptical eight-stranded β-barrel, with two extended β-strands projecting extracellularly (Figure 4F). Structural alignment showed the highest similarity to *N. meningitidis* NspA (PDB ID: 1P4T) (Tables 2 and S3). Foldseek analysis identified structural homology with an OmpA family protein of *Brachyspira hampsonii* 30446, suggesting potential involvement in adhesion, invasion, intracellular survival, or immune modulation. EggNOG mapper further predicted lipid A 3-O-deacylase activity, which modifies lipid A structure to facilitate immune evasion. Collectively, structure- and sequence-based evidence suggests that BP951000_RS08300 is a multifunctional OMP, potentially involved in host interaction and immune modulation. Sequence comparison across nine *B. pilosicoli* strains revealed three variations (L143, N156, and S200) (Figure 4F; Tables 3 and S4), all located in the β-barrel domain (Table S4).

3.2.2.17. BP951000_RS05490

BP951000_RS05490 is annotated as a hypothetical protein in NCBI and as a Tia invasion determinant in UniProt. SignalP predicted a secretory signal peptide, whereas LipoP classified it as cytoplasmic. The AlphaFold 3 model revealed an eight-stranded β-barrel architecture (Figure 4G). DALI analysis identified *N. meningitidis* NspA (PDB ID: 1P4T) as the closest structural match (Tables 2 and S3). As a structural homolog of NspA, BP951000_RS05490 may play similar roles in host interaction and immune modulation, as discussed in Section 3.2.5. PANNZER annotation also identified the protein as a Tia invasion determinant, aligning with its UniProt classification. Comparative sequence analysis across nine *B. pilosicoli* strains revealed 61 variations distributed throughout the sequence and two deletions (Figure 4G and Table S5).

3.2.2.18. BP951000_RS07500

BP951000_RS07500, annotated as a hypothetical protein, is predicted to contain a secretory signal peptide. The AlphaFold 3 model predicted an eight-stranded β-barrel structure (Figure 4H). Structural alignment identified the closest match with the β-barrel domain of *E. coli* K-12 OmpA (PDB ID: 9FZC) (Tables 2 and S3). Unlike *E. coli* OmpA, BP951000_RS07500 lacks the periplasmic domain. Given that OmpA is involved in phage binding, vesicle transport, conjugation, and membrane integrity, BP951000_RS07500 may perform similar functions.[101-109] Sequence-based annotation using PANNZER identified it as an OMBB protein. Sequence comparison across nine *B. pilosicoli* strains revealed 183 variations within the first seven strands of the β-barrel (Figure 4H and Table S5), indicating high variability across its 232-residue sequence.

3.2.2.19. BP951000_RS01590

BP951000_RS01590, annotated as a hypothetical protein, is predicted to contain a secretory signal peptide. LipoP predicted a TMH at the N-terminal. The structural model revealed an eight-stranded β-barrel architecture (Figure 4I) and additional short β-strands and α-helices extending extracellularly. As identified by DALI, structural homology was highest with *P. aeruginosa* OprG (PDB ID: 2X27) (Tables 2 and S3), an OmpW family protein involved in catabolism and uptake of hydrophobic molecules, including hydrocarbons.[153] Foldseek identified the closest structural match with an uncharacterized protein of *B. pilosicoli* P43/6/78. PANNZER analysis predicted the protein to be a cell surface protein, suggesting a possible role in host–pathogen interaction. Sequence variation analysis across nine *B. pilosicoli* strains revealed three variations (V205, I215, and V221), all located in the TM β-barrel domain (Figure 4I, Tables 3 and S4).

3.2.2.20. BP951000_RS08295

BP951000_RS08295, annotated as a Tia invasion determinant, is predicted to carry a secretory signal peptide. The AlphaFold 3 model revealed an eight-stranded β-barrel with two elongated strands, forming an elliptical pore on the extracellular side (Figure 4J). DALI analysis identified the best structural alignment with *N. meningitidis* NspA (PDB ID: 1P4T) (Tables 2 and S3), suggesting potential roles in adhesion and immune evasion, similar to NspA (Section 3.2.5). Sequence-based annotation indicated adhesive function and potential lipid A 3-O-deacylase activity, potentially contributing to immune evasion. Among nine *B. pilosicoli* strains, six variations were detected (N34, I49, V123, S141, I144, and V167), with N34 located in the ECL region and the others in the β-barrel domain (Figure 4J, Tables 3 and S4).

3.2.2.21. BP951000_RS08975

BP951000_RS08975 is annotated as a TonB-dependent receptor (TBDR) domain-containing protein in NCBI,[20] and as a Ser/Threonine protein kinase in UniProt. TBDR domain-containing proteins transport substrates across the OM using the proton motive force, transmitted via the TonB–ExbB–ExbD complex.[114,154] SignalP predicted a secretory signal peptide. AlphaFold 3 revealed a 13-stranded incomplete β-barrel, likely forming a dimer or a higher-order oligomer (Figure 5A). Attempts to model a

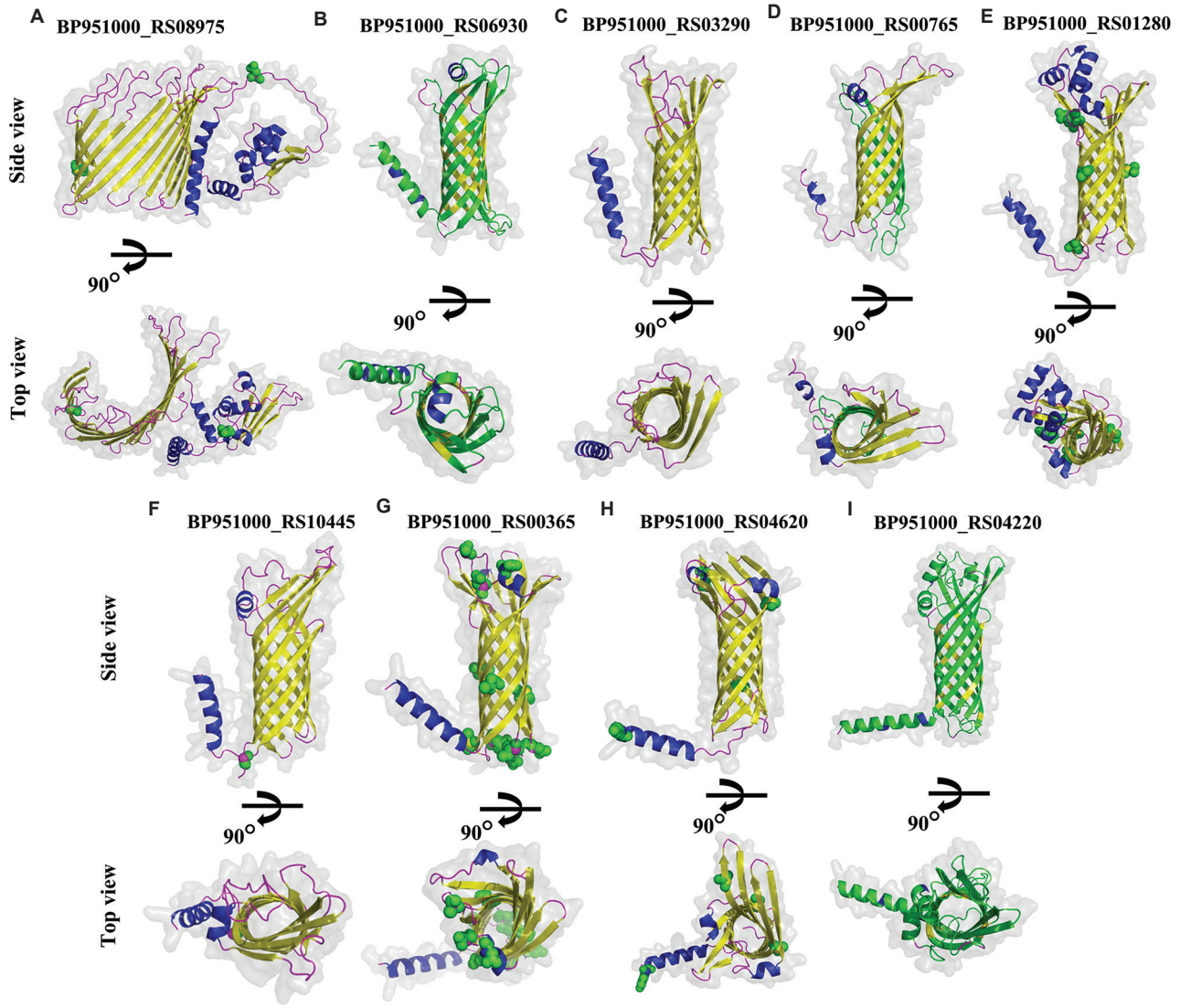

Figure 5. Structural models of β-barrel outer membrane proteins in Group B (continued). Structural models of the remaining nine proteins of Group B are shown (A-I). Proteins are arranged based on the decreasing number of β-strands. Structural model of BP951000_RS08975 revealed an incomplete β-barrel structure consisting of 13 β-strands. β-strands, α-helices, and loops are colored yellow, blue, and magenta, respectively. Green spheres indicate amino acid variations identified across nine strains of *Brachyspira pilosicoli*. Proteins with more than 40 variations are shown in green ribbon representation.

dimer using AlphaFold 3 were inconclusive (pTM = 0.35; ipTM = 0.19).

Structural models generated using ESMFold, SWISS-MODEL, RoseTTAFold, and TrRosetta aligned well with the AlphaFold 3 prediction (RMSD = 4.61 Å). Foldseek identified structural homology with an uncharacterized protein from *B. hampsonii*, whereas the DALI server matched it to *E. coli* BtuB (PDB ID: 2GSK), a vitamin B_{12} transporter (Tables 2 and S3). However, the high RMSD suggests significant structural differences, and functional BtuB homology is unlikely. Unlike canonical BtuB, BP951000_RS08975 does not possess a full β-barrel. Furthermore, BP951000_RS08975 showed no homologs in the spirochete genera—*Treponema*, *Borrelia*, or *Leptospira*—by BLASTp. PANNZER annotation also identified the protein as a Ser/Threonine protein kinase, aligning with its UniProt classification. Sequence comparison across nine *B. pilosicoli* strains revealed two variations: D32 in the ECL and T371 in the TM region (Figure 5A, Tables 3 and S4).

3.2.2.22. Eight-stranded β-barrel proteins annotated as Serpentine receptor domain-containing proteins

Eight *B. pilosicoli* proteins of Group B—BP951000_RS06930, BP951000_RS03290, BP951000_RS00765,

BP951000_RS01280, BP951000_RS10445, BP951000_RS00365, BP951000_RS04620, and BP951000_RS04220—are annotated in UniProt as SR domain-containing proteins, but listed as hypothetical in NCBI. All are predicted to contain a signal peptide. Five similarly annotated proteins (Group A) were previously discussed in Section 3.2.9.

The AlphaFold 3 models revealed a conserved eight-stranded β-barrel architecture (Figure 5B-I). Structural alignment analysis using DALI showed that BP951000_RS01280, BP951000_RS00365, and BP951000_RS06930 closely matched with *N. meningitidis* NspA (PDB ID: 1P4T), whereas BP951000_RS04620, BP951000_RS00765, BP951000_RS03290, BP951000_RS04220, and BP951000_RS10445 aligned best with the N-terminal β-barrel domain of *E. coli* K-12 OmpA (PDB ID: 9FZC) (Tables 2 and S3).

As described in Sections 3.2.5 and 3.2.9, NspA contributes to host colonization and immune evasion and is a potential vaccine candidate,[86-89] whereas OmpA plays roles in phage recognition, conjugation, membrane integrity, diffusion, and virulence.[101-109] Foldseek analysis further revealed that seven of the eight proteins showed the closest structural match with uncharacterized proteins from the *Brachyspira* genus. Notably, BP951000_RS01280 aligned with an OMBB protein from *B. hyodysenteriae*, supporting its role as a conserved OMP component.

Consistent with structural data, PANNZER annotated BP951000_RS06930, BP951000_RS00765, BP951000_RS01280, BP951000_RS10445, and BP951000_RS04620 as OMBB proteins, whereas BP951000_RS03290, BP951000_RS00365, and BP951000_RS04220 remained uncharacterized. The convergence of structure- and sequence-based annotations supports their classification as OMBB proteins, although experimental validation is needed to confirm their functional roles. Sequence comparison across nine *B. pilosicoli* strains revealed variations at several positions (Tables 3, S4, and S5).

This study did not include experimental validation of OMBBs, which is a limitation. Future research should focus on validating these predictions through experimental characterization and functional analysis.

4. Conclusion

Brachyspira pilosicoli is a globally prevalent enteric spirochete associated with IS in both animals and humans. Despite its clinical significance, the molecular mechanisms underlying its pathogenesis remain poorly understood, particularly the role of OMPs, which are critical for nutrient uptake, adhesion, immune evasion, and virulence. In this study, we addressed this knowledge gap by systematically identifying and characterizing the OMBB proteome of *B. pilosicoli* using a consensus-based computational approach.

We predicted 42 OMBB proteins and validated their β-barrel architectures using AlphaFold 3. These proteins exhibited diverse topologies, ranging from 8 to 26 strands. Structural homology-based functional annotation revealed putative homologs of BamA, LptD, TolC, TBDRs, NspA, OmpA, FadL, and others, suggesting roles in membrane biogenesis, LPT, efflux activity, substrate uptake, host colonization, and immune modulation.

Among the 42 OMBB proteins, seven lacked annotation in both UniProt and NCBI. Combined structure- and sequence-based analyses enabled putative functional assignment for these hypothetical proteins. Comparative sequence analysis across nine *B. pilosicoli* strains revealed extensive polymorphisms in 12 proteins, each containing 40 or more variations, suggesting potential roles in immune evasion and host adaptation.

This study expands current knowledge of the *B. pilosicoli* OMP repertoire and provides a framework for identifying potential targets for diagnostic, prophylactic, and therapeutic development. The functional predictions and structural insights reported here lay the foundation for future experimental work aimed at elucidating the precise roles of these OMPs in IS pathogenesis.

Acknowledgements

None.

Funding

Amisha Panda is a recipient of a junior research fellowship from the Department of Biotechnology, Government of India (grant number: DBT/2023-24/UOD/2326). Jahnvi Kapoor is a recipient of a junior research fellowship from the University Grants Commission, Government of India (grant number: 231620067077).

Conflict of interest

The authors declare that they have no competing interests.

Author contributions

Conceptualization: Sanjiv Kumar
Data curation: Amisha Panda
Formal analysis: Amisha Panda, Jahnvi Kapoor, Ravindresh Chhabra, Anannya Bandyopadhyay
Investigation: Amisha Panda
Methodology: Amisha Panda, Sanjiv Kumar, Anannya Bandyopadhyay
Software: Amisha Panda, Sanjiv Kumar
Supervision: Sanjiv Kumar

Visualization: Jahnvi Kapoor, Batchu Hareramadas, Ilmas Naqvi

Writing–original draft: Amisha Panda, Ravindresh Chhabra, Anannya Bandyopadhyay

Writing–review & editing: Jahnvi Kapoor, Batchu Hareramadas, Ilmas Naqvi, Ravindresh Chhabra, Sanjiv Kumar, Anannya Bandyopadhyay

Ethics approval and consent to participate

Not applicable.

Consent for publication

Not applicable.

Availability of data

The data supporting the findings of this study are available from the corresponding author upon reasonable request.

References

1. Ludwig W, Euzéby J, Whitman WB. Taxonomic outlines of the phyla bacteroidetes, spirochaetes, tenericutes (mollicutes), acidobacteria, fibrobacteres, fusobacteria, dictyoglomi, gemmatimonadetes, lentisphaerae, verrucomicrobia, chlamydiae, and planctomycetes. In: Krieg NR, Staley JT, Brown DR, *et al*, editors. *Bergey's Manual® of Systematic Bacteriology: Volume Four The Bacteroidetes, Spirochaetes, Tenericutes (Mollicutes), Acidobacteria, Fibrobacteres, Fusobacteria, Dictyoglomi, Gemmatimonadetes, Lentisphaerae, Verrucomicrobia, Chlamydiae, and Planctomycetes*. New York: Springer; 2010. p. 21-24.
2. Hampson DJ, Oxberry SL, La T. Potential for zoonotic transmission of *Brachyspira pilosicoli*. *Emerg Infect Dis*. 2006;12(5):869-870.

   doi: 10.3201/eid1205.051180
3. Le Roy CI, Mappley LJ, La Ragione RM, Woodward MJ, Claus SP. *Brachyspira pilosicoli*-induced avian intestinal spirochaetosis. *Microb Ecol Health Dis*. 2015;26(1):28853.

   doi: 10.3402/mehd.v26.28853
4. Bano L, Merialdi G, Bonilauri P, *et al*. Prevalence, disease associations and risk factors for colonization with intestinal spirochaetes (*Brachyspira* spp.) in flocks of laying hens in North-Eastern Italy. *Avian Pathol*. 2008;37(3):281-286.

   doi: 10.1080/03079450802043726
5. Myers SE, Dunn PA, Phillips ND, La T, Hampson DJ. *Brachyspira* intermedia and *Brachyspira pilosicoli* are commonly found in older laying flocks in Pennsylvania. *Avian diseases*. 2009;53(4):533-537.

   doi: 10.1637/8900-042709-Reg.1
6. Amin MM, Phillips ND, La T, Robertson ID, Hampson DJ. Intestinal spirochaetes (*Brachyspira* spp.) colonizing flocks of layer and breeder chickens in Malaysia. *Avian Pathol*. 2014;43(6):501-505.

   doi: 10.1080/03079457.2014.966056
7. Zarabi M, Jamshidi A, Khanzadi S, Razmyar J. Intestinal colonization of different *Brachyspira* spp. In laying hens. *Iran J Vet Med*. 2014;8:213-218.
8. Hampson DJ. The spirochete *Brachyspira pilosicoli*, enteric pathogen of animals and humans. *Clin Microbiol Rev*. 2018;31(1):e00087-17.

   doi: 10.1128/cmr.00087-17
9. Smith JL. Colonic spirochetosis in animals and humans. *J Food Prot*. 2005;68(7):1525-1534.

   doi: 10.4315/0362-028X-68.7.1525
10. Trott DJ, Stanton TB, Jensen NS, Duhamel GE, Johnson JL, Hampson DJ. *Serpulina pilosicoli* sp. Nov., the agent of porcine intestinal spirochetosis. *Int J Syst Bacteriol*. 1996;46(1):206-215.

    doi: 10.1099/00207713-46-1-206
11. Stephens CP, Hampson DJ. Intestinal spirochete infections of chickens: A review of disease associations, epidemiology and control. *Anim Health Res Rev*. 2001;2(1):83-91.
12. Gad A, Willén R, Furugård K, Fors B, Hradsky M. Intestinal spirochaetosis as a cause of longstanding diarrhoea. *Ups J Med Sci*. 1977;82(1):49-54.

    doi: 10.3109/03009737709179059
13. Gan J, Bryant C, Arul D, Parmar C. Intestinal spirochaetosis mimicking acute appendicitis with review of the literature. *BMJ Case Rep*. 2017;2017:bcr2017221574.

    doi: 10.1136/bcr-2017-221574
14. Nishii S, Higashiyama M, Ogata S, *et al*. Human intestinal spirochetosis mimicking ulcerative colitis. *Clin J Gastroenterol*. 2018;11:145-149.

    doi: 10.1007/s12328-017-0807-3
15. Marthinsen L, Willén R, Carlén B, Lindberg E, Värendh G. Intestinal spirochetosis in eight pediatric patients from Southern Sweden. *APMIS*. 2002;110(7-8):571-579.

    doi: 10.1034/j.1600-0463.2002.11007809.x
16. Oxberry SL, Trott DJ, Hampson DJ. *Serpulina pilosicoli*, waterbirds and water: Potential sources of infection for humans and other animals. *Epidemiol Infect*. 1998;121(1):219-225.

    doi: 10.1017/S0950268898008863
17. Trott DJ, Mikosza AS, Combs BG, Oxberry SL, Hampson DJ. Population genetic analysis of *Serpulina pilosicoli* and its molecular epidemiology in villages in the Eastern Highlands of Papua New Guinea. *Int J Syst Bacteriol*. 1998;48(3):659-668.

    doi: 10.1099/00207713-48-3-659

18. Hampson DJ, Lugsomya K, La T, Phillips ND, Trott DJ, Abraham S. Antimicrobial resistance in *Brachyspira* - an increasing problem for disease control. *Vet Microbiol*. 2019;229:59-71.

doi: 10.1016/j.vetmic.2018.12.019

19. Christodoulides M, De Oliveira D, Cleary DW, Humbert MV, Machado-De-Ávila RA, La Ragione RM. An *in silico* reverse vaccinology study of *Brachyspira pilosicoli*, the causative organism of intestinal spirochaetosis, to identify putative vaccine candidates. *Process Biochem*. 2022;122:128-148.

doi: 10.1016/j.procbio.2022.08.014

20. Wanchanthuek P, Bellgard MI, La T, *et al*. The complete genome sequence of the pathogenic intestinal spirochete *Brachyspira pilosicoli* and comparison with other *Brachyspira* genomes. *PLoS One*. 2010;5(7):e11455.

doi: 10.1371/journal.pone.0011455

21. Erlandson KM, Klingler ET. Intestinal spirochetosis: Epidemiology, microbiology, and clinical significance. *Clin Microbiol Newsl*. 2005;27(12):91-96.

doi: 10.1016/j.clinmicnews.2005.05.002

22. Trott DJ, Alt DP, Zuerner RL, *et al*. Identification and cloning of the gene encoding BmpC: an outer-membrane lipoprotein associated with *Brachyspira pilosicoli* membrane vesicles. *Microbiology (Reading)*. 2004;150(4):1041-1053.

doi: 10.1099/mic.0.26755-0

23. Lee BJ, Hampson DJ. Lipo-oligosaccharide profiles of *Serpulina pilosicoli* strains and their serological cross-reactivities. *J Med Microbiol*. 1999;48(4):411-415.

doi: 10.1099/00222615-48-4-411

24. Koebnik R, Locher KP, Van Gelder P. Structure and function of bacterial outer membrane proteins: Barrels in a nutshell. *Mol Microbiol*. 2000;37(2):239-253.

doi: 10.1046/j.1365-2958.2000.01983.x

25. Fairman JW, Noinaj N, Buchanan SK. The structural biology of β-barrel membrane proteins: A summary of recent reports. *Curr Opin Struct Biol*. 2011;21(4):523-531.

doi: 10.1016/j.sbi.2011.05.005

26. Horne JE, Brockwell DJ, Radford SE. Role of the lipid bilayer in outer membrane protein folding in gram-negative bacteria. *J Biol Chem*. 2020;295(30):10340-10367.

doi: 10.1074/jbc.REV120.011473

27. Kleinschmidt JH. Folding of β-barrel membrane proteins in lipid bilayers - unassisted and assisted folding and insertion. *Biochim Biophys Acta*. 2015;1848(9):1927-1943.

doi: 10.1016/j.bbamem.2015.05.004

28. Solan R, Pereira J, Lupas AN, Kolodny R, Ben-Tal N. Gram-negative outer-membrane proteins with multiple β-barrel domains. *Proc Natl Acad Sci U S A*. 2021;118(31):e2104059118.

doi: 10.1073/pnas.2104059118

29. Trott DJ, Alt DP, Zuerner RL, Wannemuehler MJ, Stanton TB. The search for *Brachyspira* outer membrane proteins that interact with the host. *Anim Health Res Rev*. 2001;2(1):19-30.

doi: 10.1079/AHRR200112

30. Tenaya IW, Penhale WJ, Hampson DJ. Preparation of diagnostic polyclonal and monoclonal antibodies against outer envelope proteins of *Serpulina pilosicoli*. *J Med Microbiol*. 1998;47(4):317-324.

doi: 10.1099/00222615-47-4-317

31. La T, Phillips ND, Hampson DJ. Vaccination of chickens with the 34 kDa carboxy-terminus of Bpmp72 reduces colonization with *Brachyspira pilosicoli* following experimental infection. *Avian Pathol*. 2019;48(1):80-85.

doi: 10.1080/03079457.2018.1546377

32. Medicine NLo. *National Center for Biotechnology Information (NCBI)*. Bethesda (MD): Medicine NLo; 1988.

doi: 10.1093/nar/gkaa892

33. Rice P, Longden I, Bleasby A. EMBOSS: The European molecular biology open software suite. *Trends Genet*. 2000;16(6):276-277.

doi: 10.1016/S0168-9525(00)02024-2

34. Teufel F, Almagro Armenteros JJ, Johansen AR, *et al*. SignalP 6.0 predicts all five types of signal peptides using protein language models. *Nat Biotechnol*. 2022;40(7):1023-1025.

doi: 10.1038/s41587-021-01156-3

35. Juncker AS, Willenbrock H, Von Heijne G, Brunak S, Nielsen H, Krogh A. Prediction of lipoprotein signal peptides in gram-negative bacteria. *Protein Sci*. 2003;12(8):1652-1662.

doi: 10.1110/ps.0303703

36. Yu CS, Lin CJ, Hwang JK. Predicting subcellular localization of proteins for gram-negative bacteria by support vector machines based on n-peptide compositions. *Protein Sci*. 2004;13(5):1402-1406.

doi: 10.1110/ps.03479604

37. Yu NY, Wagner JR, Laird MR, *et al*. PSORTb 3.0: Improved protein subcellular localization prediction with refined localization subcategories and predictive capabilities for all prokaryotes. *Bioinformatics*. 2010;26(13):1608-1615.

doi: 10.1093/bioinformatics/btq249

38. Luo H, Lin Y, Liu T, *et al*. DEG 15, an update of the database of essential genes that includes built-in analysis tools. *Nucleic Acids Res*. 2021;49(D1):D677-D686.

doi: 10.1093/nar/gkaa917

39. Roumia AF, Tsirigos KD, Theodoropoulou MC, Tamposis IA, Hamodrakas SJ, Bagos PG. OMPdb: A global hub of

beta-barrel outer membrane proteins. *Front Bioinform*. 2021;1:646581.

doi: 10.3389/fbinf.2021.646581

40. Bagos PG, LiakopoulipopTD, Hamodrakas SJ. Finding beta-barrel outer membrane proteins with a markov chain model. *WSEAS Trans Biol Biomed*. 2004;2(1):186-189.

41. Ou YY, Gromiha MM, Chen SA, Suwa M. TMBETADISC-RBF: Discrimination of beta-barrel membrane proteins using RBF networks and PSSM profiles. *Comput Biol Chem*. 2008;32(3):227-231.

doi: 10.1016/j.compbiolchem.2008.03.002

42. Bernhofer M, Rost B. TMbed: Transmembrane proteins predicted through language model embeddings. *BMC Bioinformatics*. 2022;23(1):326.

doi: 10.1186/s12859-022-04873-x

43. Abramson J, Adler J, Dunger J, *et al*. Accurate structure prediction of biomolecular interactions with AlphaFold 3. *Nature*. 2024;630:493-500.

doi: 10.1038/s41586-024-07487-w

44. Xu J, Zhang Y. How significant is a protein structure similarity with TM-score= 0.5? *Bioinformatics*. 2010;26(7):889-895.

doi: 10.1093/bioinformatics/btq066

45. Zhang Y, Skolnick J. Scoring function for automated assessment of protein structure template quality. *Proteins*. 2004;57(4):702-710.

doi: 10.1002/prot.20264

46. DeLano WL. *The PyMOL Molecular Graphics System*; 2002. https://www/pymol/org [Last accessed on 2025 Jan 25].

47. Lin Z, Akin H, Rao R, *et al*. Evolutionary-scale prediction of atomic-level protein structure with a language model. *Science*. 2023;379(6637):1123-1130.

doi: 10.1126/science.ade2574

48. Waterhouse A, Bertoni M, Bienert S, *et al*. SWISS-MODEL: Homology modelling of protein structures and complexes. *Nucleic Acids Res*. 2018;46(W1):W296-W303.

doi: 10.1093/nar/gky427

49. Baek M, DiMaio F, Anishchenko I, *et al*. Accurate prediction of protein structures and interactions using a three-track neural network. *Science*. 2021;373(6557):871-876.

doi: 10.1126/science.abj8754

50. Du Z, Su H, Wang W, *et al*. The trRosetta server for fast and accurate protein structure prediction. *Nat Protoc*. 2021;16(12):5634-5651.

doi: 10.1038/s41596-021-00628-9

51. Holm L. Dali server: Structural unification of protein families. *Nucleic Acids Res*. 2022;50(W1):W210-W215.

doi: 10.1093/nar/gkac387

52. Holm L. Using dali for protein structure comparison. *Methods Mol Biol*. 2020;2112:29-42.

doi: 10.1007/978-1-0716-0270-6_3

53. Van Kempen M, Kim SS, Tumescheit C, *et al*. Fast and accurate protein structure search with foldseek. *Nat Biotechnol*. 2024;42(2):243-246.

doi: 10.1038/s41587-023-01773-0

54. Törönen P, Holm L. PANNZER-a practical tool for protein function prediction. *Protein Sci*. 2022;31(1):118-128.

doi: 10.1002/pro.4193

55. Cantalapiedra CP, Hernández-Plaza A, Letunic I, Bork P, Huerta-Cepas J. EggNOG-mapper v2: Functional annotation, orthology assignments, and domain prediction at the metagenomic scale. *Mol Biol Evol*. 2021;38(12):5825-5829.

doi: 10.1093/molbev/msab293

56. Larkin MA, Blackshields G, Brown NP, *et al*. Clustal W and clustal X version 2.0. *Bioinformatics*. 2007;23(21):2947-2948.

doi: 10.1093/bioinformatics/btm404

57. Kumar S, Stecher G, Suleski M, Sanderford M, Sharma S, Tamura K. MEGA12: Molecular evolutionary genetic analysis version 12 for adaptive and green computing. *Mol Biol Evol*. 2024;41(12):msae263.

doi: 10.1093/molbev/msae263

58. Zhang C, Shine M, Pyle AM, Zhang Y. US-align: Universal structure alignments of proteins, nucleic acids, and macromolecular complexes. *Nat Methods*. 2022;19(9):1109-1115.

doi: 10.1038/s41592-022-01585-1

59. Derbyshire MC. Bioinformatic detection of positive selection pressure in plant pathogens: The neutral theory of molecular sequence evolution in action. *Front Microbiol*. 2020;11:644.

doi: 10.3389/fmicb.2020.00644

60. Bakelar J, Buchanan SK, Noinaj N. The structure of the β-barrel assembly machinery complex. *Science*. 2016;351(6269):180-186.

doi: 10.1126/science.aad3460

61. Konovalova A, Kahne DE, Silhavy TJ. Outer membrane biogenesis. *Annu Rev Microbiol*. 2017;71(1):539-556.

doi: 10.1146/annurev-micro-090816-093754

62. Lysnyansky I, Ron Y, Sachse K, Yogev D. Intrachromosomal recombination within the vsp locus of *Mycoplasma bovis* generates a chimeric variable surface lipoprotein antigen. *Infect Immun*. 2001;69(6):3703-3712.

doi: 10.1128/iai.69.6.3703-3712.2001

63. Gabe JD, Dragon E, Chang RJ, McCaman MT. Identification of a linked set of genes in Serpulina hyodysenteriae (B204) predicted to encode closely related 39-kilodalton

extracytoplasmic proteins. *J Bacteriol*. 1998;180(2):444-448.

doi: 10.1128/jb.180.2.444-448.1998

64. Gömmel M, Barth S, Heydel C, Baljer G, Herbst W. Adherence of *Brachyspira* hyodysenteriae to porcine intestinal epithelial cells is inhibited by antibodies against outer membrane proteins. *Curr Microbiol*. 2013;66:286-292.

doi: 10.1007/s00284-012-0267-4

65. Bellgard MI, Wanchanthuek P, La T, *et al*. Genome sequence of the pathogenic intestinal spirochete *Brachyspira* hyodysenteriae reveals adaptations to its lifestyle in the porcine large intestine. *PLoS One*. 2009;4(3):e4641.

doi: 10.1371/journal.pone.0004641

66. Wang Y, Pannuri AA, Ni D, *et al*. Structural basis for translocation of a biofilm-supporting exopolysaccharide across the bacterial outer membrane. *J Biol Chem*. 2016;291(19):10046-10057.

doi: 10.1074/jbc.M115.711762

67. Itoh Y, Rice JD, Goller C, *et al*. Roles of pgaABCD genes in synthesis, modification, and export of the *Escherichia coli* biofilm adhesin poly-beta-1,6-N-acetyl-D-glucosamine. *J Bacteriol*. 2008;190(10):3670-3680.

doi: 10.1128/jb.01920-07

68. Wang X, Preston JF 3rd, Romeo T. The pgaABCD locus of *Escherichia coli* promotes the synthesis of a polysaccharide adhesin required for biofilm formation. *J Bacteriol*. 2004;186(9):2724-2734.

doi: 10.1128/jb.186.9.2724-2734.2004

69. Bellgard M, Hampson DJ, La T. *Genes and Proteins of Brachyspira Hyodysenteriae and uses Thereof*. Google Patents; 2015.

70. Zimmer J. A molecular description of cellulose biosynthesis. *Biophys J*. 2015;108(2):499a.

doi: 10.1016/j.bpj.2014.11.2734

71. Römling U, Galperin MY. Bacterial cellulose biosynthesis: Diversity of operons, subunits, products, and functions. *Trends Microbiol*. 2015;23(9):545-557.

doi: 10.1016/j.tim.2015.05.005

72. Acheson JF, Derewenda ZS, Zimmer J. Architecture of the cellulose synthase outer membrane channel and its association with the periplasmic TPR domain. *Structure*. 2019;27(12):1855-1861.e3.

doi: 10.1016/j.str.2019.09.008

73. Mathes A, Engelhardt H. Nonlinear and asymmetric open channel characteristics of an ion-selective porin in planar membranes. *Biophys J*. 1998;75(3):1255-1262.

doi: 10.1016/S0006-3495(98)74045-7

74. Zeth K, Diederichs K, Welte W, Engelhardt H. Crystal structure of Omp32, the anion-selective porin from comamonas acidovorans, in complex with a periplasmic peptide at 2.1 Å resolution. *Structure*. 2000;8(9):981-992.

doi: 10.1016/S0969-2126(00)00189-1

75. Azghani AO, Idell S, Bains M, Hancock RE. *Pseudomonas aeruginosa* outer membrane protein F is an adhesin in bacterial binding to lung epithelial cells in culture. *Microb Pathog*. 2002;33(3):109-114.

doi: 10.1006/mpat.2002.0514

76. Wu L, Estrada O, Zaborina O, *et al*. Recognition of host immune activation by *Pseudomonas aeruginosa*. *Science*. 2005;309(5735):774-777.

doi: 10.1126/science.1112422

77. Fito-Boncompte L, Chapalain A, Bouffartigues E, *et al*. Full virulence of *Pseudomonas aeruginosa* requires OprF. *Infect Immunity*. 2011;79(3):1176-1186.

doi: 10.1128/iai.00850-10

78. Wessel AK, Liew J, Kwon T, Marcotte EM, Whiteley M. Role of *Pseudomonas aeruginosa* peptidoglycan-associated outer membrane proteins in vesicle formation. *J Bacteriol*. 2013;195(2):213-219.

doi: 10.1128/jb.01253-12

79. Abellón-Ruiz J, Zahn M, Baslé A, Van Den Berg B. Crystal structure of the *Acinetobacter baumannii* outer membrane protein Omp33. *Acta Crystallogr D Struct Biol*. 2018;74(9):852-860.

doi: 10.1107/S205979831800904X

80. Alhede M, Bjarnsholt T, Givskov M, Alhede M. *Pseudomonas aeruginosa* biofilms: Mechanisms of immune evasion. *Adv Appl Microbiol*. 2014;86:1-40.

doi: 10.1016/B978-0-12-800262-9.00001-9

81. Mayeux G, Gayet L, Liguori L, *et al*. Cell-free expression of the outer membrane protein OprF of *Pseudomonas aeruginosa* for vaccine purposes. *Life Sci Alliance*. 2021;4(6):e202000958.

doi: 10.26508/lsa.202000958

82. Goyal P, Krasteva PV, Van Gerven N, *et al*. Structural and mechanistic insights into the bacterial amyloid secretion channel CsgG. *Nature*. 2014;516(7530):250-253.

doi: 10.1038/nature13768

83. La Ragione RM, Sayers AR, Woodward MJ. The role of fimbriae and flagella in the colonization, invasion and persistence of *Escherichia coli* O78:K80 in the day-old-chick model. *Epidemiol Infect*. 2000;124(3):351-363.

doi: 10.1017/S0950268899004045

84. La Ragione RM, Cooley WA, Woodward MJ. The role of fimbriae and flagella in the adherence of avian strains of *Escherichia coli* O78:K80 to tissue culture cells and tracheal and gut explants. *J Med Microbiol*. 2000;49(4):327-338.

doi: 10.1099/0022-1317-49-4-327

85. La Ragione RM, Woodward MJ. Virulence factors of *Escherichia coli* serotypes associated with avian colisepticaemia. *Res Vet Sci*. 2002;73(1):27-35.

doi: 10.1016/S0034-5288(02)00075-9

86. Vandeputte-Rutten L, Bos MP, Tommassen J, Gros P. Crystal structure of neisserial surface protein A (NspA), a conserved outer membrane protein with vaccine potential. *J Biol Chem*. 2003;278(27):24825-24830.

doi: 10.1074/jbc.M302803200

87. Martin D, Cadieux N, Hamel J, Brodeur BR. Highly conserved *Neisseria meningitidis* surface protein confers protection against experimental infection. *J Exp Med*. 1997;185(7):1173-1184.

doi: 10.1084/jem.185.7.1173

88. Moe GR, Tan S, Granoff DM. Differences in surface expression of NspA among *Neisseria meningitidis* group B strains. *Infect Immun*. 1999;67(11):5664-5675.

doi: 10.1128/iai.67.11.5664-5675.1999

89. Moe GR, Zuno-Mitchell P, Lee SS, Lucas AH, Granoff DM. Functional activity of anti-neisserial surface protein A monoclonal antibodies against strains of *Neisseria meningitidis* serogroup B. *Infect Immun*. 2001;69(6):3762-3771.

doi: 10.1128/iai.69.6.3762-3771.2001

90. Koronakis V, Eswaran J, Hughes C. Structure and function of TolC: The bacterial exit duct for proteins and drugs. *Annu Rev Biochem*. 2004;73(1):467-489.

doi: 10.1146/annurev.biochem.73.011303.074104

91. Koronakis V, Sharff A, Koronakis E, Luisi B, Hughes C. Crystal structure of the bacterial membrane protein TolC central to multidrug efflux and protein export. *Nature*. 2000;405(6789):914-919.

doi: 10.1038/35016007

92. Vakharia H, German GJ, Misra R. Isolation and characterization of *Escherichia coli* tolC mutants defective in secreting enzymatically active alpha-hemolysin. *J Bacteriol*. 2001;183(23):6908-6916.

doi: 10.1128/jb.183.23.6908-6916.2001

93. Wandersman C, Delepelaire P. TolC, an *Escherichia coli* outer membrane protein required for hemolysin secretion. *Proc Natl Acad Sci*. 1990;87(12):4776-4780.

doi: 10.1073/pnas.87.12.4776

94. Clowes R. Transmission and elimination of colicin factors and some aspects of immunity to colicin E1 in *Escherichia coli*. *Zentrabl Bakteriol Parasiten Abt I Orig*. 1965;196:152-157.

95. Davies JK, Reeves P. Genetics of resistance to colicins in *Escherichia coli* K-12: Cross-resistance among colicins of group A. *J Bacteriol*. 1975;123(1):102-117.

doi: 10.1128/jb.123.1.102-117.1975

96. Fralick JA. Evidence that TolC is required for functioning of the Mar/AcrAB efflux pump of *Escherichia coli*. *J Bacteriol*. 1996;178(19):5803-5805.

doi: 10.1128/jb.178.19.5803-5805.1996

97. German GJ, Misra R. The TolC protein of *Escherichia coli* serves as a cell-surface receptor for the newly characterized TLS bacteriophage. *J Mol Biol*. 2001;308(4):579-585.

doi: 10.1006/jmbi.2001.4578

98. Fredriksson R, Lagerström MC, Lundin LG, Schiöth HB. The G-protein-coupled receptors in the human genome form five main families. Phylogenetic analysis, paralogon groups, and fingerprints. *Mol Pharmacol*. 2003;63(6):1256-1272.

doi: 10.1124/mol.63.6.1256

99. Pierce KL, Premont RT, Lefkowitz RJ. Seven-transmembrane receptors. *Nat Rev Mol Cell Biol*. 2002;3(9):639-650.

doi: 10.1038/nrm908

100. Consortium TU. UniProt: The universal protein knowledgebase in 2025. *Nucleic Acids Res*. 2024;53(D1):D609-D617.

doi: 10.1093/nar/gkae1010

101. Van Alphen L, Havekes L, Lugtenberg B. Major outer membrane protein d of *Escherichia coli* K12. Purification and *in vitro* activity of bacteriophage k3 and f-pilus mediated conjugation. *FEBS Lett*. 1977;75:285-290.

doi: 10.1016/0014-5793(77)80104-x

102. Datta DB, Arden B, Henning U. Major proteins of the *Escherichia coli* outer cell envelope membrane as bacteriophage receptors. *J Bacteriol*. 1977;131(3):821-829.

doi: 10.1128/jb.131.3.821-829.1977

103. Chai T, Foulds J. Demonstration of a missing outer membrane protein in tolG mutants of *Escherichia* cell. *J Mol Biol*. 1974;85(3):465-474.

doi: 10.1016/0022-2836(74)90445-8

104. Skurray RA, Hancock RE, Reeves P. Con--mutants: Class of mutants in *Escherichia coli* K-12 lacking a major cell wall protein and defective in conjugation and adsorption of a bacteriophage. *J Bacteriol*. 1974;119(3):726-735.

doi: 10.1128/jb.119.3.726-735.1974

105. Schweizer M, Henning U. Action of a major outer cell envelope membrane protein in conjugation of *Escherichia coli* K-12. *J Bacteriol*. 1977;129(3):1651-1652.

doi: 10.1128/jb.129.3.1651-1652.1977

106. Braun V. Covalent lipoprotein from the outer membrane of *Escherichia coli*. *Biochim Biophys Acta*. 1975;415(3):335-377.

doi: 10.1016/0304-4157(75)90013-1

107. Sonntag I, Schwarz H, Hirota Y, Henning U. Cell envelope and shape of *Escherichia coli*: Multiple mutants missing

the outer membrane lipoprotein and other major outer membrane proteins. *J Bacteriol*. 1978;136(1):280-285.

doi: 10.1128/jb.136.1.280-285.1978

108. Sugawara E, Nikaido H. Pore-forming activity of OmpA protein of *Escherichia coli*. *J Biol Chem*. 1992;267(4):2507-2511.

doi: 10.1016/S0021-9258(18)45908-X

109. Krishnan S, Prasadarao NV. Outer membrane protein A and OprF: Versatile roles in gram-negative bacterial infections. *FEBS J*. 2012;279(6):919-931.

doi: 10.1111/j.1742-4658.2012.08482.x

110. Laguri C, Sperandeo P, Pounot K, *et al*. Interaction of lipopolysaccharides at intermolecular sites of the periplasmic Lpt transport assembly. *Sci Rep.* 2017;7(1):9715.

doi: 10.1038/s41598-017-10136-0

111. Pieńko T, Trylska J. Extracellular loops of BtuB facilitate transport of vitamin B12 through the outer membrane of *E. Coli*. *PLoS Comput Biol*. 2020;16(7):e1008024.

doi: 10.1371/journal.pcbi.1008024

112. Di Girolamo PM, Kadner RJ, Bradbeer C. Isolation of vitamin B 12 transport mutants of *Escherichia coli*. *J Bacteriol*. 1971;106(3):751-757.

doi: 10.1128/jb.106.3.751-757.1971

113. White JC, Di Girolamo PM, Fu ML, Preston YA, Bradbeer C. Transport of vitamin B 12 in *Escherichia coli*. Location and properties of the initial B 12 -binding site. *J Biol Chem*. 1973;248(11):3978-3986.

doi: 10.1016/S0021-9258(19)43828-3

114. Noinaj N, Guillier M, Barnard TJ, Buchanan SK. TonB-dependent transporters: Regulation, structure, and function. *Annu Rev Microbiol*. 2010;64(1):43-60.

doi: 10.1146/annurev.micro.112408.134247

115. Schauer K, Rodionov DA, De Reuse H. New substrates for TonB-dependent transport: Do we only see the 'tip of the iceberg'? *Trends Biochem Sci*. 2008;33(7):330-338.

doi: 10.1016/j.tibs.2008.04.012

116. Biswas S, Mohammad MM, Patel DR, Movileanu L, Van Den Berg B. Structural insight into OprD substrate specificity. *Nat Struct Mol Biol*. 2007;14(11):1108-1109.

doi: 10.1038/nsmb1304

117. Moraes TF, Bains M, Hancock RE, Strynadka NC. An arginine ladder in OprP mediates phosphate-specific transfer across the outer membrane. *Nat Struct Mol Biol*. 2007;14(1):85-87.

doi: 10.1038/nsmb1189

118. Eren E, Vijayaraghavan J, Liu J, *et al*. Substrate specificity within a family of outer membrane carboxylate channels. *PLoS Biol*. 2012;10(1):e1001242.

doi: 10.1371/journal.pbio.1001242

119. Biswas S, Mohammad MM, Movileanu L, Van Den Berg B. Crystal structure of the outer membrane protein OpdK from *Pseudomonas aeruginosa*. *Structure*. 2008;16(7):1027-1035.

doi: 10.1016/j.str.2008.04.009

120. Kuehne SA, Cartman ST, Heap JT, Kelly ML, Cockayne A, Minton NP. The role of toxin A and toxin B in *Clostridium* difficile infection. *Nature*. 2010;467(7316):711-713.

doi: 10.1038/nature09397

121. Van Den Berg B, Prathyusha Bhamidimarri S, Dahyabhai Prajapati J, Kleinekathöfer U, Winterhalter M. Outer-membrane translocation of bulky small molecules by passive diffusion. *Proc Natl Acad Sci*. 2015;112(23):E2991-E2999.

doi: 10.1073/pnas.1424835112

122. Pajatsch M, Andersen C, Mathes A, Böck A, Benz R, Engelhardt H. Properties of a cyclodextrin-specific, unusual porin from *Klebsiella oxytoca*. *J Biol Chem*. 1999;274(35):25159-25166.

doi: 10.1074/jbc.274.35.25159

123. Gruss F, Zähringer F, Jakob RP, Burmann BM, Hiller S, Maier T. The structural basis of autotransporter translocation by TamA. *Nat Struct Mol Biol*. 2013;20(11):1318-1320.

doi: 10.1038/nsmb.2689

124. Selkrig J, Mosbahi K, Webb CT, *et al*. Discovery of an archetypal protein transport system in bacterial outer membranes. *Nat Struct Mol Biol*. 2012;19(5):506-510.

doi: 10.1038/nsmb.2261

125. Pavlova O, Peterson JH, Ieva R, Bernstein HD. Mechanistic link between β barrel assembly and the initiation of autotransporter secretion. *Proc Natl Acad Sci*. 2013;110(10):E938-E947.

doi: 10.1073/pnas.1219076110

126. Matthijs S, Koedam N, Cornelis P, De Greve H. The trehalose operon of *Pseudomonas* fluorescens ATCC 17400. *Res Microbiol*. 2000;151(10):845-851.

doi: 10.1016/S0923-2508(00)01151-7

127. Abergel C, Bouveret E, Claverie JM, *et al*. Structure of the *Escherichia coli* TolB protein determined by MAD methods at 1.95 Å resolution. *Structure*. 1999;7(10):1291-1300.

doi: 10.1016/S0969-2126(00)80062-3

128. Rigal A, Bouveret E, Lloubes R, Lazdunski C, Benedetti H. The TolB protein interacts with the porins of *Escherichia coli*. *J Bacteriol*. 1997;179(23):7274-7279.

doi: 10.1128/jb.179.23.7274-7279.1997

129. Fognini-Lefebvre N, Lazzaroni JC, Portalier R. tolA, tolB and excC, three cistrons involved in the control of pleiotropic release of periplasmic proteins by *Escherichia coli* K12. *Mol Gen Genet*. 1987;209:391-395.

doi: 10.1007/BF00329670

130. Lazzaroni JC, Fognini-Lefebvre N, Portalier R. Cloning of the excC and excD genes involved in the release of periplasmic proteins by *Escherichia coli* K12. *Mol Gen Genet*. 1989;218:460-464.

doi: 10.1007/BF00332410

131. Maier T, Clantin B, Gruss F, *et al*. Conserved Omp85 lid-lock structure and substrate recognition in FhaC. *Nat Commun*. 2015;6(1):7452.

doi: 10.1038/ncomms8452

132. Delattre AS, Saint N, Clantin B, *et al*. Substrate recognition by the POTRA domains of TpsB transporter FhaC. *Mol Microbiol*. 2011;81(1):99-112.

doi: 10.1111/j.1365-2958.2011.07680.x

133. Lauber F, Deme JC, Lea SM, Berks BC. Type 9 secretion system structures reveal a new protein transport mechanism. *Nature*. 2018;564(7734):77-82.

doi: 10.1038/s41586-018-0693-y

134. Van Den Berg B, Black PN, Clemons WM Jr., Rapoport TA. Crystal structure of the long-chain fatty acid transporter FadL. *Science*. 2004;304(5676):1506-1509.

doi: 10.1126/science.1097524

135. Black PN, Said B, Ghosn CR, Beach JV, Nunn WD. Purification and characterization of an outer membrane-bound protein involved in long-chain fatty acid transport in *Escherichia coli*. *J Biol Chem*. 1987;262(3):1412-1419.

doi: 10.1016/S0021-9258(19)75801-3

136. Lauber F, Deme JC, Liu X, *et al*. Structural insights into the mechanism of protein transport by the type 9 secretion system translocon. *Nat Microbiol*. 2024;9(4):1089-1102.

doi: 10.1038/s41564-024-01644-7

137. Otto BR, Sijbrandi R, Luirink J, *et al*. Crystal structure of hemoglobin protease, a heme binding autotransporter protein from pathogenic *Escherichia coli*. *J Biol Chem*. 2005;280(17):17339-17345.

doi: 10.1074/jbc.M412885200

138. Otto BR, Van Dooren SJ, Dozois CM, Luirink J, Oudega B. *Escherichia coli* hemoglobin protease autotransporter contributes to synergistic abscess formation and heme-dependent growth of *Bacteroides fragilis*. *Infect Immun*. 2002;70(1):5-10.

doi: 10.1128/iai.70.1.5-10.2002

139. Otto BR, Van Dooren SJ, Nuijens JH, Luirink J, Oudega B. Characterization of a hemoglobin protease secreted by the pathogenic *Escherichia coli* strain EB1. *J Exp Med*. 1998;188(6):1091-1103.

doi: 10.1084/jem.188.6.1091

140. Berg BVD, Bhamidimarri SP, Winterhalter M. Crystal structure of a COG4313 outer membrane channel. *Sci Rep*. 2015;5(1):11927.

doi: 10.1038/srep11927

141. Henderson IR, Nataro JP. Virulence functions of autotransporter proteins. *Infect Immun*. 2001;69(3):1231-1243.

doi: 10.1128/iai.69.3.1231-1243.2001

142. Yen MR, Peabody CR, Partovi SM, Zhai Y, Tseng YH, Saier MH Jr. Protein-translocating outer membrane porins of gram-negative bacteria. *Biochim Biophys Acta*. 2002;1562(1-2):6-31.

doi: 10.1016/S0005-2736(02)00359-0

143. Henderson IR, Navarro-Garcia F, Nataro JP. The great escape: Structure and function of the autotransporter proteins. *Trends Microbiol*. 1998;6(9):370-378.

doi: 10.1016/S0966-842X(98)01318-3

144. Dutta PR, Cappello R, Navarro-García F, Nataro JP. Functional comparison of serine protease autotransporters of Enterobacteriaceae. *Infect Immun*. 2002;70(12):7105-7113.

doi: 10.1128/iai.70.12.7105-7113.2002

145. Brunder W, Schmidt H, Karch H. EspP, a novel extracellular serine protease of enterohaemorrhagic *Escherichia coli* O157:H7 cleaves human coagulation factor V. *Mol Microbiol*. 1997;24(4):767-778.

doi: 10.1046/j.1365-2958.1997.3871751.x

146. Scandella CJ, Kornberg A. Membrane-bound phospholipase A1 purified from *Escherichia coli*. *Biochemistry*. 1971;10(24):4447-4456.

doi: 10.1021/bi00800a015

147. Pugsley AP, Schwartz M. Colicin E2 release: Lysis, leakage or secretion? Possible role of a phospholipase. *EMBO J*. 1984;3(10):2393-2397.

doi: 10.1002/j.1460-2075.1984.tb02145.x

148. Van Der Wal FJ, Luirink J, Oudega B. Bacteriocin release proteins: Mode of action, structure, and biotechnological application. *FEMS Microbiol Rev*. 1995;17(4):381-399.

doi: 10.1111/j.1574-6976.1995.tb00221.x

149. De Vries FP, Cole R, Dankert J, Frosch M, Van Putten JP. *Neisseria meningitidis* producing the Opc adhesin binds epithelial cell proteoglycan receptors. *Mol Microbiol*. 1998;27(6):1203-1212.

doi: 10.1046/j.1365-2958.1998.00763.x

150. Virji M, Makepeace K, Moxon ER. Distinct mechanisms of interactions of Opc-expressing meningococci at apical and basolateral surfaces of human endothelial cells; the role of integrins in apical interactions. *Mol Microbiol*. 1994;14(1):173-184.

doi: 10.1111/j.1365-2958.1994.tb01277.x

151. Mammarappallil JG, Elsinghorst EA. Epithelial cell adherence mediated by the enterotoxigenic *Escherichia coli* Tia protein. *Infect Immun*. 2000;68(12):6595-6601.

doi: 10.1128/iai.68.12.6595-6601.2000

152. Fleckenstein JM, Kopecko DJ, Warren RL, Elsinghorst EA. Molecular characterization of the tia invasion locus from enterotoxigenic *Escherichia coli*. *Infect Immun*. 1996;64(6):2256-2265.

doi: 10.1128/iai.64.6.2256-2265.1996

153. Gensberg K, Smith AW, Brinkman FS, Hancock RE. Identification of *oprG*, a gene encoding a major outer membrane protein of *Pseudomonas aeruginosa*. *J Antimicrob Chemother*. 1999;43(4):607-608.

doi: 10.1093/jac/43.4.607

154. Celia H, Noinaj N, Zakharov SD, *et al*. Structural insight into the role of the ton complex in energy transduction. *Nature*. 2016;538(7623):60-65.

doi: 10.1038/nature19757

ACCSCIENCE PUBLISHING

Microbes & Immunity

ORIGINAL RESEARCH ARTICLE

Isolation and identification of a highly pathogenic strain of porcine epidemic diarrhea virus

Yongbo Xia[1†], Xiaolu Li[1†], Xiaowei Wang[1], Xiaoyuan Diao[1], Wenjing Qiu[1], Yihong He[1], Yue Li[1], Yunfei Li[1], Chunyi Xue[1], Yongchang Cao[1], Hanqin Shen[2], and Zhichao Xu[1*]

[1]State Key Laboratory of Biocontrol, School of Life Science, Sun Yat-sen University, Guangzhou, Guangdong, China

[2]Guangdong Provincial Enterprise Key Laboratory of Healthy Animal Husbandry and Environment Control, Wen's Foodstuff Group Co. Ltd., Yunfu, Guangdong, China

Abstract

Porcine epidemic diarrhea virus (PEDV) causes acute watery diarrhea and high mortality in neonatal piglets, resulting in substantial economic losses to the global swine industry. Here, we successfully isolated a PEDV strain, designated CHN-CQ-2021, from PEDV-positive diarrheic samples collected from a pig farm in Chongqing, China. Electron microscopy observation revealed that the CHN-CQ-2021 strain exhibited typical coronavirus morphology and could be recognized by PEDV-specific antibodies. Phylogenetic analysis of its full-length genome and *S* gene further classified this isolate as a G2b variant strain. Importantly, 1-day-old newborn piglets were orally challenged with CHN-CQ-2021 at 2×10^6 50% tissue culture infectious dose/mL. Compared with the control group, the infected piglets developed severe diarrhea with 100% mortality. In addition, viral RNA was detected in rectal swabs and multiple tissues, including the intestinal tract and brain, with macroscopic/microscopic intestinal lesions and viral antigen distribution confirmed using histopathology and immunohistochemistry. These findings demonstrate the presence of a pathogenic PEDV strain in Chongqing, China, capable of causing severe neonatal piglets' enteric disease.

Keywords: Porcine epidemic diarrhea virus; Isolation and identification; Pathogenicity; Newborn piglets; China

[†]These authors contributed equally to this work.

***Corresponding author:**
Zhichao Xu
(xuzhich5@mail.sysu.edu.cn)

Citation: Xia Y, Li X, Wang X, *et al*. Isolation and identification of a highly pathogenic strain of porcine epidemic diarrhea virus. *Microbes & Immunity.* 2025;2(4):110-121. doi: 10.36922/MI025260059

Received: June 28, 2025

Revised: July 24, 2025

Accepted: September 05, 2025

Published online: October 3, 2025

1. Introduction

Porcine intestinal infectious diseases pose significant threats to the swine industry and have exhibited an increasing prevalence in multiple regions across global pig farming countries in recent years. Various pathogens, including viruses (such as norovirus, astrovirus, and rotavirus) and bacteria (such as *Salmonella*, *Campylobacter*, and *Escherichia coli*), can cause diarrhea in both humans and animals.[1-6] Among various pathogens, viral-induced enteric diseases are particularly severe,[7] resulting in substantial economic losses to the global swine sector. At present, clinically significant viral swine enteric pathogens include transmissible gastroenteritis virus, porcine rotavirus, porcine epidemic diarrhea

virus (PEDV), porcine deltacoronavirus, and swine acute diarrhoea syndrome coronavirus.[8-11] Despite the availability of vaccines for immunization control, frequent outbreaks of viral enteric diseases continue to occur, with more than 50% of cases attributed to PEDV infections.[12] Notably, PEDV exhibits a high mutation rate, enabling variant strains to evade immune protection conferred by existing vaccines derived from original strains.[13] This highlights the necessity for continuous monitoring and analysis of the biological characteristics of circulating PEDV strains to optimize prevention strategies.

PEDV is an enveloped, single-stranded positive-sense RNA virus belonging to the *Alphacoronavirus* genus, with a genome length of approximately 28 kb.[14] The 5' end of its genome contains a cap structure in the untranslated region, while the 3' end contains a polyadenylated tail.[15] The PEDV genome contains seven open reading frames (ORFs): ORF1a, ORF1b, and ORF2–6, encoding a total of four structural proteins (spike [S], envelope [E], membrane [M], and nucleocapsid [N]) and 16 non-structural proteins (nsp1–nsp16).[16] Porcine epidemic diarrhea (PED) was first reported in the United Kingdom in 1971, and the pathogen PEDV was first identified and isolated in Belgium in 1978, with the isolate named CV777.[17] Between 1970 and 1980, PEDV spread across Europe, causing significant mortality among piglets.[18] From 1980 to 2010, the disease occurred sporadically, with occasional reports from several countries, including the United Kingdom, Germany, and Italy.[18] In China, PED was first reported in 1973.[19] In October 2010, a large-scale PED outbreak emerged across pig farms nationwide, with mortality rates among neonatal piglets reaching 50–100% in affected farms, causing substantial economic losses to the Chinese swine industry.[19] Subsequent investigations revealed that variant PEDV strains had evolved to evade the immune protection conferred by CV777-derived vaccines,[20] indicating the importance of monitoring circulating PEDV strains and characterizing their biological properties to inform effective control strategies.

To investigate the biological characteristics of current circulating PEDV strains in Chinese pig farms, this study isolated viruses from diarrheic piglets obtained from a swine facility in Chongqing in 2021. The isolates underwent comprehensive genomic characterization and *in vivo* pathogenicity assessment. These findings enhance our understanding of PEDV pathogenesis and establish the foundation for vaccine development.

2. Materials and methods

2.1. Clinical samples collection

In early March 2021, an outbreak of PEDV was reported in swine herds in Chongqing, China, with mortality rates reaching up to 100%. Intestinal luminal contents were collected from PEDV-positive piglets exhibiting clinical signs of severe diarrhea and vomiting, cryopreserved at −80°C, and processed for viral isolation.

2.2. Virus isolation, plaque purification, and propagation in Vero cells

Before virus isolation, intestinal luminal contents were homogenized in an equal volume of sterile 1× phosphate-buffered saline (PBS, pH 7.4; Solarbio, China). Following homogenization, particulate debris was removed through centrifugation (11,000 *g*, 4°C, 10 min; 5804 R, Eppendorf, Germany), and supernatants were clarified through sterile 0.22-μm syringe filters (Millipore, United States of America). Vero cells (ATCC number: CCL-81; ATCC, USA) were utilized for PEDV isolation.

Virus isolation, plaque purification, and propagation were conducted as previously described with some modifications.[21] Briefly, Vero cells were cultured in a six-well plate until reaching 90% confluency. The cells were washed three times with sterilized 1× PBS buffer. Subsequently, 350 μL of Dulbecco's Modified Eagle Medium (DMEM; Solarbio, China) maintenance medium (serum-free DMEM medium supplemented with 7 μg/mL trypsin (Sigma, USA) and 200 μL of filtered sample were added to each well. Control wells received an equivalent volume of DMEM maintenance medium. The plates were incubated at 37□ in a 5% CO_2 atmosphere (Thermo, USA). Cells were observed daily for cytopathic effects (CPE). When CPE reached 80%, the plates were subjected to two freeze-thaw cycles. The supernatant was collected after centrifugation at 11,000 × *g* for 10 min at 4□, and stored at −80□, followed by further examination using quantitative real-time (RT)-polymerase chain reaction (PCR) as described below.

For virus plaque purification, supernatants from virus-infected Vero cells were serially diluted and inoculated onto fresh Vero cell monolayers. Cells were incubated with the diluted virus in maintenance medium for 1.5 h at 37°C under 5% CO_2. After incubation, the medium was aspirated, and cells were overlaid with 2 mL of maintenance medium containing 1.25% low-melting-point (LM), genetically quality-tested (GQT) agarose (Gibco, USA) to immobilize viral particles. Following a 24-h incubation, cells were stained with 2 mL of maintenance medium supplemented with 1.25% LM GQT Agarose and 0.01% Neutral Red solution (Sigma, USA). Plaques were isolated using sterile pipette tips and transferred into microcentrifuge tubes containing 0.5 mL of maintenance medium.

The purified plaques, named as CHN-CQ-2021, were propagated in Vero cells. Vero cells were cultured in T175 flasks until reaching 90% confluency, washed 3 times with

sterile 1× PBS (pH 7.4), and inoculated with 1 mL of PEDV CHN-CQ-2021 diluted in 50 mL of maintenance medium. Cells and supernatant were maintained at 37°C under 5% CO_2 and monitored for CPE. When CPE became evident (approximately 2 days post-infection), the cultures were subjected to two freeze-thaw cycles. The resulting cell lysates and supernatants were harvested for viral titer determination as described below.

2.3. Immunofluorescence assay (IFA)

The IFA experiment was performed as previously described with some modifications.[22] Briefly, Vero cells were seeded in 12-well plates and cultured overnight, followed by infection with PEDV (CHN-CQ-2021) at a multiplicity of infection (MOI) of 0.1. At 16–24 h post-PEDV infection, cells were fixed with 4% paraformaldehyde for 15 min, permeabilized with 0.5% Triton X-100 for 10 min at room temperature, and blocked with 3% bovine serum albumin (BSA). Subsequently, cells were sequentially incubated with PEDV-specific antiserum (M100048, Zoonogen, China) and Cy3-conjugated secondary antibody (A10521, Thermo, USA) in the dark at room temperature for 1 h. After three washes with 1× PBS, nuclei were counterstained with 4',6-diamidino-2-phenylindole (Solarbio, China) for 5 min. Fluorescence signals were visualized using an inverted fluorescence microscope (Leica, Germany).

2.4. Electron microscopic observation

Virus morphology was observed using transmission electron microscopy (TEM; JEM-1400, JEOL, Japan) as previously described, with some modifications.[22] Briefly, PEDV was propagated in Vero cells. Cell debris was removed through centrifugation at 11,000 × *g* (4□, 30 min). The clarified supernatant was mixed with 7% PEG6000 (Solarbio, China) and incubated overnight at 4□ with continuous agitation. The mixture was then centrifuged at 11,000 × *g* (4□, 1 h), and the pelleted virions were resuspended in 2 mL of 1× PBS and layered onto a discontinuous sucrose gradient (20–60%). After ultracentrifugation at 177,600 × *g* (4□, 2 h) using an ultracentrifuge (Himac CP 100WX, Hitachi Koki, Japan), distinct viral bands were carefully collected. Viral band was diluted in 1× PBS and subjected to additional ultracentrifugation (177,600 × *g*, 4□, 2 h) for sucrose removal. Purified virions were resuspended in minimal sterile 1× PBS and negatively stained with 3% (w/v) phosphotungstic acid (pH 6.8; Sigma, USA) for 2 min. Excess liquid was blotted using filter paper, and grids were air-dried before observation under TEM at 80 kV.

2.5. Infectious-virus titrations by a 50% tissue culture infectious dose ($TCID_{50}$) assay

Vero cells were seeded into 96-well plates and cultured overnight, followed by two washes with sterile 1× PBS. A 10-fold serially diluted PEDV (100 μL/well) was inoculated onto the cell monolayer, with eight replicates per dilution. Cells were maintained in a humidified incubator at 37°C with 5% CO_2 for 5–7 days. Viral titers were quantified by observing CPE and calculated using the Reed–Muench method, expressed as 50% tissue culture infectious dose ($TCID_{50}$)/mL.[23] Plaque-forming units (PFUs) were derived using Equation I as previously described,[24] and PFU values were used to determine the MOI.

$$PFU = 0.7 \times TCID_{50} \quad (I)$$

2.6. Measurement of PEDV (CHN-CQ-2021) growth

Vero cells were seeded into 35-mm cell culture dishes and infected with PEDV at an MOI of 0.1 when the cell density reached 90%. Cells cultured with DMEM maintenance medium without viral inoculation served as controls. Every 4 h post-inoculation (hpi), PEDV-infected cells and control cells were observed, and then, the cells were harvested and stored at −80□. After two freeze-thaw cycles, supernatants were harvested to determine viral titers as described above, and a growth curve of PEDV CHN-CQ-2021 was generated.

2.7. Genomic cloning and phylogenetic analysis of the whole genome and *S* genes

Viral RNA was extracted from PEDV cell lysates using an RNeasy kit (R4111-03, Magen, China) according to the manufacturer's instructions, followed by DNase I treatment to remove genomic DNA contamination. The specific primers (Sangon Company, China; Table 1) for amplification of the PEDV whole genome were designed with reference to the published sequence (GenBank: JX647847) and synthesized. The reaction mixture (50 μL total volume) contained 1 μL PrimeScript 1-Step Enzyme Mix, 25 μL 2× One-Step Buffer, 2.5 μM each of forward and reverse primers, 1 μg viral RNA, and RNase-free H_2O. The PCR reaction conditions were as follows: 50°C for 30 min; 94°C for 2 min; followed by 34 cycles of 94°C for 30 s, 55°C for 30 s, and 72°C for 2.5 min; with a final extension at 72°C for 10 min. Subsequently, the PCR products were subjected to 1% agarose gel electrophoresis, and target bands were excised and purified using a DNA gel extraction kit (UE-GX-50, US Everbright, China). Purified gene fragments were then sent for sequencing (Sangon Biotech, China). Viral genome sequences were assembled using DNAStar Lasergene 7.0 (Version 7.0, DNASTAR Inc., USA). The *S* gene and the whole genome of CHN-CQ-2021 were aligned with representative PEDV strains retrieved from the National Center for Biotechnology Information. Phylogenetic trees were constructed by the neighbor-joining method using MEGA 5 software available online (http://www.megasoftware.net/).

2.8. Experimental infection of conventional newborn piglets with PEDV CHN-CQ-2021 strain

The animal experiments were conducted in compliance with the ethical guidelines and regulations of the Institutional Animal Care and Use Committee of Sun Yat-sen University, and all procedures were approved by the committee. Ten 1-day-old healthy crossbred conventional piglets (Duroc × Landrace × Large White) were obtained from Wen's Foodstuffs Group Co., Ltd. (China). All piglets were confirmed negative for PEDV antigen by RT-PCR on rectal swabs and negative for PEDV antibodies (immunoglobulin [Ig]A/IgG) by enzyme-linked immunosorbent assay on serum samples.[25] All piglets were randomly divided into two groups ($n = 5$): one experimental group and one control group. Each group was housed in a separate isolation room. The experimental group was orally inoculated with 2 mL of the PEDV CHN-CQ-2021 strain containing 2×10^6 $TCID_{50}$, while the control group received 2 mL of DMEM maintenance medium. Rectal swabs of piglets were collected daily post-infection, and diarrhea was scored according to Chen *et al.*[26] Piglets that succumbed to infection were immediately necropsied, and fresh tissues (jejunum, ileum, cerebrum, cerebellum, and brainstem) were collected and fixed in 4% paraformaldehyde (Thermo, USA) for subsequent histopathological and immunohistochemical analysis. At the end of the experiment, piglets in the control group were euthanized and subjected to the same necropsy and tissue collection procedures.

2.9. RT-PCR analysis

The supernatants from rectal swabs or tissue homogenates were centrifuged at 6,010 × *g* for 5 min. Total RNA was extracted from the supernatants using an RNeasy kit (R4111-03, Magen, China) according to the manufacturer's instructions, followed by DNase I treatment. The specific primers (Table 2) and probe for the nucleocapsid (*N*) gene of PEDV were designed based on a previous publication[27] and synthesized by Sangon Company (China). RT-PCR was performed on a thermocycler (Applied Biosystems 7500 Fast instrument, Life Technologies, USA) in a 20 μL reaction volume containing 1 μg RNA, 10 μL 2 × Hifair V C58P2 MP Buffer, 0.8 μL of Hifair V C58P2 Enzyme Mix (Shanghai Yeasen Biotechnology Co., Ltd., China), 0.2 μmol/L probe, and 0.4 μmol/L of each primer. Thermal cycling conditions were as follows: 50□ for 20 min, 95°C for 5 min, followed by 40 cycles of 95°C for 15 s and 60°C for 30 s. A standard curve was generated using a plasmid construct. Briefly, the *N* gene was amplified from the PEDV CHN-CQ-2021 strain using specific primers (Table 2) designed based on the whole genome of PEDV CHN-CQ-2021. The PCR product was cloned into the pMD19-T vector (Takara, Japan). The plasmid was serially diluted 10-fold to generate a standard curve for each plate. Viral RNA quantities in test samples were calculated based on cycle threshold values relative to the standard curve.

Table 1. Primers of porcine epidemic diarrhea virus for whole-genome amplification

Primer name	Position	Primer sequences (5'→3')
PEDV-1F	190–209	GGCGTTCCGTCGCCTTCTAC
PEDV-1R	2751–2729	GCAAGTGCCTTCCAGATTCCTGT
PEDV-2F	2663–2684	GTATTATGCCACCAGTGTCCCA
PEDV-2R	4957–4938	CAGTTGCCAGCAGGCACTGT
PEDV-3F	4887–4906	ACCAGCGGTGCATTGCTTGA
PEDV-3R	7475–7453	CAATGTGCTCTTGCAATCCTGCA
PEDV-4F	7327–7350	CTGTTAAGTTAGTGGACTCAGCGT
PEDV-4R	9875–9856	ACTAGCGCCTTCAACTTGCA
PEDV-5F	9712–9731	GCGCTTGTGGTTCACCTGGT
PEDV-5R	12259–12240	GGATCCACAGCGAAAGCGCA
PEDV-6F	12182–12202	ACGCTTGCAGGCTGGTAAACA
PEDV-6R	14462–14442	TGGGCAGTGCTCTATCGCACT
PEDV-7F	14322–14341	ATACTAGGGGCGCTTCGGTT
PEDV-7R	16780–16760	GTCAGGGTGCACAGGAATGAA
PEDV-8F	16662–16684	GTATGTGTGCCCTTAAGCCTGAT
PEDV-8R	19002–18980	GTAAGTGGACGTTCGGCTTCATA
PEDV-9F	18874–18898	CGTAGCTTTTGAGTTGTATGCCA
PEDV-9R	21330–21309	GCAATTAGCTGTACAGGGTTCA
PEDV-10F	21080–21101	CCATTCCAGCTTATATGCGTGA
PEDV-10R	23487–23465	GTACATGTGAAGCTTCTCAGCGT
PEDV-11F	23272–23292	GTGTACGATCCTGCAAGTGGC
PEDV-11R	25715–25694	TCACCTCATCAACGGGAATAGA
PEDV-12F	25535–25557	TCGTCCAATTGGTTAATCTGTGC
PEDV-12R	27840–27820	TACCGTTGTGTGCAAGACCAA

Abbreviation: PEDV: Porcine epidemic diarrhea virus.

Table 2. Primers and probe for quantitative real-time polymerase chain reaction and full-length amplification of the porcine epidemic diarrhea virus nucleocapsid (*N*) gene

Primer name	Primer/probe sequences (5'→3')
PEDV-F	CGCAAAGACTGAACCCACTAATTT
PEDV-R	TTGCCTCTGTTGTTACTTGGAGAT
PEDV-probe	FAM-TGTTGCCATTGCCACGACTCCTGC-TAMRA
PEDV-N-CDS-F	ATGTCTGACGCAGAAGAGTG
PEDV-N-CDS-R	TTACATATACTTATACAGGCGAGC

Abbreviations: FAM: 6-carboxyfluorescein; TAMRA: Carboxytetramethylrhodamine; PEDV: Porcine epidemic diarrhea virus.

2.10. Histological and immunohistochemical analysis

Tissue samples collected from piglets were subjected to histopathological and immunohistochemical analyses as previously described, with some modifications.[22] Briefly, samples were fixed in 4% paraformaldehyde for over 36 h, dehydrated through a graded ethanol series, embedded in paraffin, sectioned, and mounted on glass slides. For histopathological examination, sections (5 μm) were dewaxed, rehydrated, and stained with hematoxylin and eosin for observation under a conventional light microscope. For immunohistochemical analysis, sections were blocked with 1% BSA and incubated with a diluted PEDV-specific mouse antiserum (1:100; M100048, Zoonogen, China) at 4□ for 12 h. After washing, the sections were incubated in a diluted peroxidase-labeled goat anti-mouse IgG secondary antibody (1:200; SA00001-1, Proteintech, USA) at room temperature for 50 min. Finally, the sections were treated with 3,3'-diaminobenzidine chromogen kit (K3468, Dako, Denmark) and counterstained with hematoxylin. Stained sections were visualized and documented under a microscope. Tissues from piglets in control groups were used as controls.

2.11. Statistical analysis

Statistical analyses were performed using GraphPad Prism software (version 8.4.3, GraphPad Software Inc., USA). Data were presented as mean ± standard deviation or mean ± standard error of the mean, as appropriate. The normality of data distribution was assessed using the Shapiro–Wilk test. Comparisons of PFU and RNA copy numbers between the treatment and control groups were analyzed for statistical significance. For normally distributed data, one-way analysis of variance followed by Tukey's *post hoc* multiple comparison test was applied. For non-parametric data, the Mann–Whitney *U*-test was used. $p<0.05$ was considered statistically significant.

3. Results

3.1. Isolation of a PEDV strain from the intestinal contents of a piglet with diarrhea

To analyze the biological characteristics of the currently prevalent PEDV strains in pig farms, the PEDV-positive piglet pathological materials collected from a pig farm in Chongqing were inoculated into Vero cells. Compared to the control, the Vero cells inoculated with the diseased material showed significant cell membrane fusion. Over time, the area of cytopathic changes expanded, accompanied by cell detachment Figure 1A and B, consistent with the typical CPE of PEDV. To further confirm that PEDV caused the cytopathic changes, IFA was performed using PEDV-specific antibody serum. As shown in Figure 1C and D, specific red fluorescence was observed in the cells inoculated with plaque-purified virion, whereas no fluorescence signal was observed in the control group. These results indicate the isolation of a PEDV strain from a diarrheic pig, named as CHN-CQ-2021.

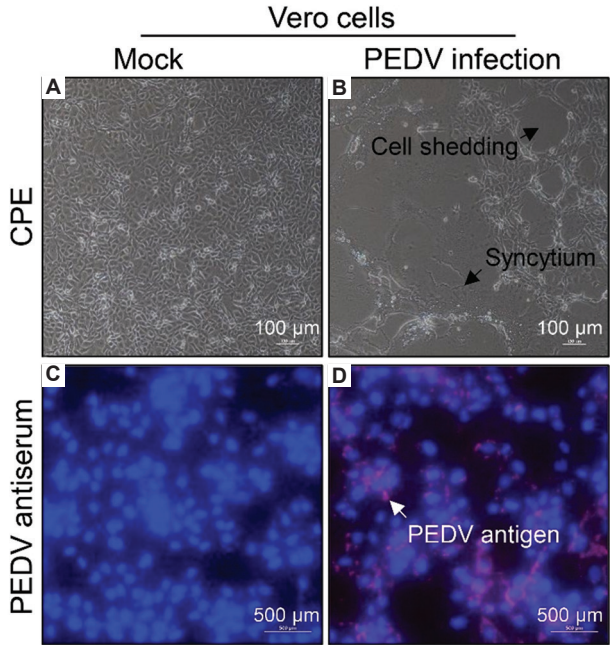

Figure 1. The cytopathic effect and immunofluorescence assay (IFA) analysis in porcine epidemic diarrhea virus (PEDV)-infected Vero cells. (A) Mock-inoculated Vero cells exhibited typical morphological integrity. Scale bar: 100 μm, magnification: 200×. (B) PEDV-infected Vero cells exhibited syncytia and cell shedding (indicated by arrows). Scale bar: 100 μm, magnification: 200×. (C) IFA performed at 24 h post-infection in mock-treated Vero cells. Scale bar: 500 μm, magnification: 40×. (D) IFA performed at 24 h post-infection in PEDV-infected cells, with arrows indicating specific PEDV antigen-positive signals. Scale bar: 500 μm, magnification: 40×.

To observe the morphology and size of the virus particles, the purified PEDV CHN-CQ-2021 strain was examined using TEM. Typical coronavirus morphology, with an envelope and spike proteins on its surface, was observed under the electron microscope (Figure 2). The diameter of the virus particles was approximately 80–120 nm. These observations further confirmed the isolation of a PEDV strain.

3.2. Stable proliferation of PEDV CHN-CQ-2021 strain in host cells

To analyze the proliferation kinetics of the PEDV CHN-CQ-2021 strain, the virus was inoculated into Vero cells. Samples were harvested at multiple time points, and viral titers were determined using the $TCID_{50}$ assay to generate the viral growth curve. Cell membrane fusion

was observed in Vero cells at 8 hpi. Prolonged incubation resulted in progressive expansion of the cytopathic area and the emergence of cell detachment (Figure 3A). Analysis of the virus proliferation curve further revealed that CHN-CQ-2021 reached its replication peak in Vero cells at 16 hpi (Figure 3B). These results demonstrate that the PEDV CHN-CQ-2021 strain can efficiently proliferate *in vitro*.

3.3. Phylogenetic analysis of whole-genome and *S* genes of PEDV CHN-CQ-2021

To investigate the genetic evolution of the strain, the complete genome of PEDV CHN-CQ-2021 was amplified using RT-PCR and compared with the full genome and *S* gene sequences of other reference strains retrieved from GenBank. Sequence alignment and phylogenetic analysis were performed using the neighbor-joining method to construct a phylogenetic tree, with bootstrap values applied to evaluate the reliability of the tree topology.[28] The PEDV CHN-CQ-2021 strain was classified within the G2b subgroup and displayed the closest genetic relationship to strain GD-1 (GenBank: JX647847). In contrast, it exhibited significant phylogenetic divergence from the G1-type classical strain branch represented by CV777 (Figure 4). These data suggested that the PEDV CHN-CQ-2021 strain was the most closely related to other PEDV strains from mainland China.

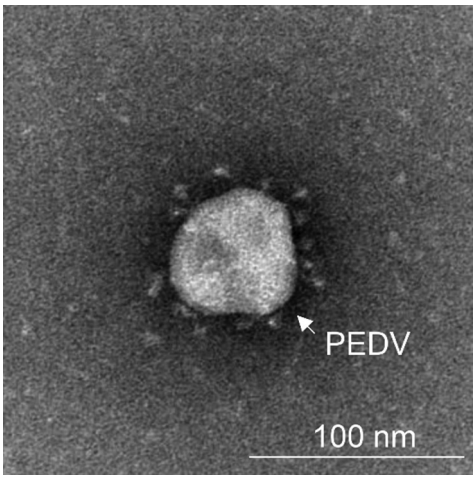

Figure 2. Electron micrograph of porcine epidemic diarrhea virus (PEDV) CHN-CQ-2021. The arrow indicates the crown-shaped spikes of PEDV CHN-CQ-2021. Scale bar: 100 nm, magnification: 30000×.

3.4. High pathogenicity of PEDV CHN-CQ-2021 strain in newborn piglets

To evaluate the pathogenicity of the PEDV CHN-CQ-2021 strain in piglets, newborn piglets were orally infected with the CHN-CQ-2021 strain. Compared to the control group, CHN-CQ-2021 strain-infected piglets exhibited typical clinical symptoms, including severe watery diarrhea and dehydration (Figure 5). Importantly, all CHN-CQ-2021 strain-infected newborn piglets died within 4 days post-inoculation (Figure 6). Further analysis of virus shedding and tissue tropism indicated that, compared to the control group, CHN-CQ-2021 strain-infected newborn piglets shed virus at varying levels during the 4-day observation period (Figure 7A), while viral nucleic acids were detected in both intestinal and brain tissues (Figure 7B). These results suggest that the PEDV CHN-CQ-2021 strain was highly pathogenic to newborn piglets.

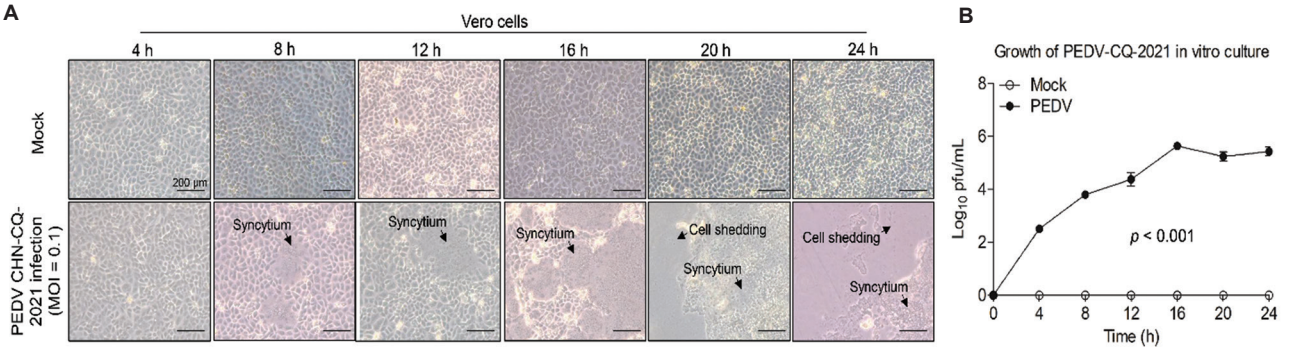

Figure 3. Measurement of PEDV CHN-CQ-2021 growth. Vero cells were seeded in 12-well plates and cultured until reaching 90% confluence. The cell monolayers were washed three times with sterile 1× phosphate-buffered saline (pH = 7.4), followed by infection with PEDV CHN-CQ-2021 (MOI = 0.1). The cell lysates and culture supernatants were collected at specified time points (0, 4, 8, 12, 16, 20, and 24 h post-inoculation) and stored at −80°C for subsequent viral titer quantification. (A) Microscopic images of Vero cells at specified time points (4, 8, 12, 16, 20, and 24 h post-inoculation) after mock or PEDV infection. The arrows indicate the CPE in PEDV-infected cells. Scale bar: 200 μm, magnification: 100×. (B) The growth of PEDV CHN-CQ-2021 in Vero cells. The data are presented as mean ± standard deviation (n = 3), based on three independent experiments.
Abbreviations: CPE: Cytopathic effect; MOI: Multiplicity of infection; PEDV: Porcine epidemic diarrhea virus.

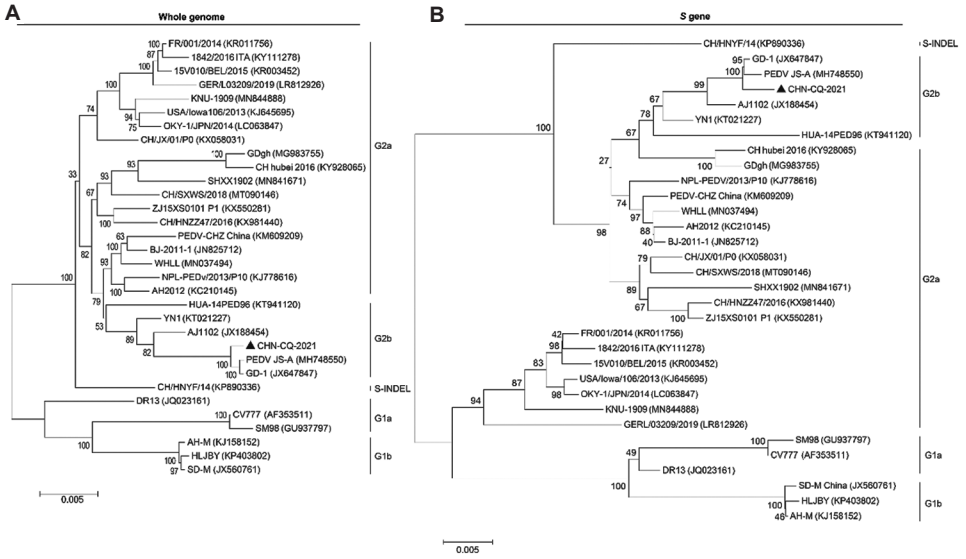

Figure 4. Phylogenetic trees of the whole genome and *S* gene of porcine epidemic diarrhea virus (PEDV) CHN-CQ-2021. (A) The genome-wide phylogenetic tree constructed using the neighbor-joining method in the MEGA software package (version 5, http://www.megasoftware.net/). (B) Phylogenetic tree of *S* genes of PEDV constructed using the neighbor-joining method in the MEGA software package (version 5, http://www.megasoftware.net/). Reference sequences, obtained from the GenBank database, are annotated with their respective strain names. The evolutionary distance scale bar corresponds to 0.005 nucleotide substitutions per site.

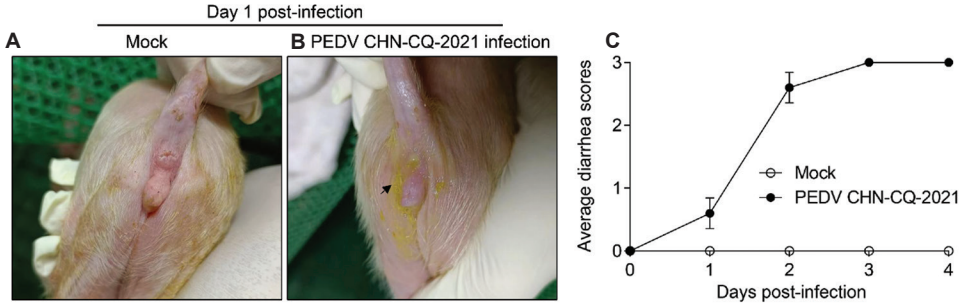

Figure 5. Investigation of watery diarrhea in piglets orally infected with porcine epidemic diarrhea virus (PEDV) CHN-CQ-2021. (A) Newborn piglets from the control group showed no clinical signs. (B) Watery diarrhea (indicated by the arrow) was observed on day 1 post-PEDV CHN-CQ-2021 infection. (C) Average diarrhea scores after PEDV infection.

3.5. Gross pathology, histopathology, and immunohistochemical in newborn piglets infected with PEDV CHN-CQ-2021

To further characterize the gross and histopathological changes of piglets after PEDV CHN-CQ-2021 infection, necropsy was performed on infected piglets, and the small intestine tissues were collected for histopathological and immunohistochemical analysis. The small intestines, which exhibited accumulation of yellow watery contents, displayed transparency, thinning of the intestinal wall, and gas distension (Figure 8B). No pathological changes were observed in other organs of PEDV-infected piglets or in the organs of the control group (Figure 8A), indicating that the small intestine is the primary target organ of PEDV infection. Microscopic lesions of the small intestine tissue were further analyzed. As shown in (Figure 8C-H), blunted intestinal villi were observed, whereas the intestinal structure in the control group remained normal. Immunohistochemical analysis confirmed the presence of PEDV antigen in the cytoplasm of villous enterocytes in PEDV-infected piglets (Figure 8L-N), consistent with the histopathological findings. In contrast, no PEDV antigen was detected in the control group (Figure 8I-K). Taken together, these results indicate that PEDV CHN-CQ-2021 infection causes diarrhea due to intestinal damage.

4. Discussion

PEDV was first reported in the United Kingdom in the last century; it has rapidly spread to numerous European and Asian countries,[17,18] posing a significant threat to the

sustainable development of the global swine industry. Notably, the emergence of a PEDV variant strain in China in 2010 resulted in substantial economic losses to pig farms nationwide,[29] primarily due to its ability to evade the immune protection conferred by existing vaccines.[30] Therefore, research on the biological characteristics of currently circulating PEDV strains is crucial for assessing the efficacy of existing vaccines and guiding vaccine development strategies. In this study, we isolated a highly pathogenic PEDV strain from the intestines of piglets with diarrhea. The genome of the isolated PEDV strain (CHN-CQ-2021) and pathogenicity were analyzed, which will help to understand the biological characteristics of prevalent PEDV strains in China.

The Vero cell line, derived from the kidney of an African green monkey in 1962,[31] has been widely used for the isolation of coronaviruses, such as PEDV and SARS-CoV-2.[21,27,32] In this study, we attempted to isolate PEDV from PEDV-positive clinical samples using Vero cells. Although multiple samples, including anal swabs and intestinal pathological tissues, were collected, successful viral isolation was exclusively achieved from fresh intestinal samples of diarrheic piglets. This finding suggests that intestinal pathological tissues with higher virus loads are easier to isolate viruses compared to anal swabs. Low viral titers resulting from suboptimal sample collection, transportation, or storage conditions may significantly hinder isolation efficiency. In addition, unfiltered samples, which were not sterilized by filtration, yielded higher isolation rates, likely because filtration removed a substantial number of viral particles. However, unfiltered samples required supplementation with high concentrations of antibiotics to suppress bacterial contamination and maintain cell viability. After three serial passages in Vero cells, the isolated virus induced significant CPE, which was subsequently confirmed as PEDV by indirect IFA and TEM observation. A viral growth curve generated by infecting Vero cells with CHN-CQ-2021 demonstrated robust viral proliferation, indicating its adaptability to this cell line and suitability for further mechanistic studies. Although we isolated the PEDV CHN-CQ-2021 strain, it is noteworthy that many clinical samples failed to yield viable virus. Our findings suggest that viral load in samples is a critical determinant for successful isolation. To improve isolation efficiency, pre-enrichment of viruses by passaging clinical materials through susceptible piglets before cell culture inoculation is strongly recommended.[26]

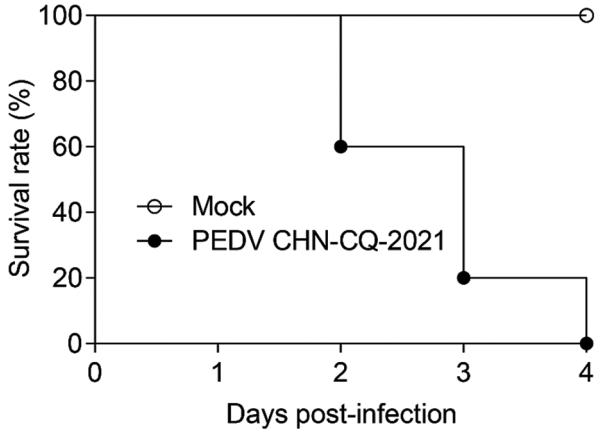

Figure 6. The survival rate of newborn piglets infected with porcine epidemic diarrhea virus (PEDV) CHN-CQ-2021. Mortality was monitored and recorded daily in each newborn piglet group from 1 to 4 days post-PEDV CHN-CQ-2021 infection.

To characterize the virus isolate, the whole genome of the CHN-CQ-2021 strain was sequenced and analyzed. Phylogenetic analysis revealed that the complete genomes of all PEDV strains retrieved from GenBank share high sequence similarity. Notably, the CHN-CQ-2021 strain isolated in Chongqing exhibited the closest genetic homology with PEDV strains AJ1102 and GD-1, which were previously isolated in Jiangsu and Guangdong, respectively. However, the mechanisms underlying their cross-regional transmission remain unclear and require further investigation. Many studies have confirmed that the

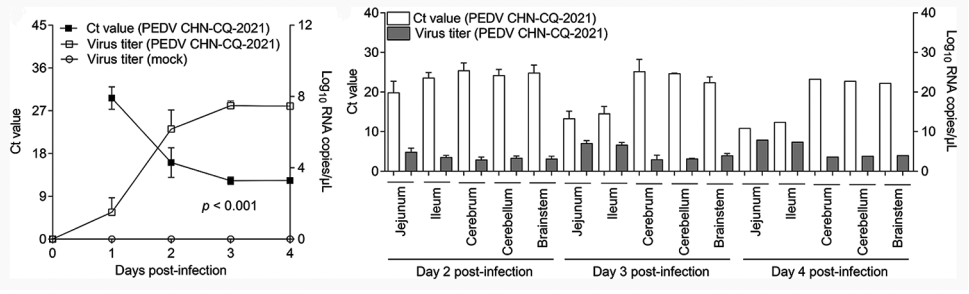

Figure 7. Viral shedding in rectal swabs and virus distribution in porcine epidemic diarrhea virus (PEDV)-inoculated piglets. (A) Cycle threshold (Ct) values from fecal swabs of PEDV-inoculated and mock piglets were measured to quantify viral RNA shedding. (B) Tissue tropism and viral distribution were assessed in newborn piglets at days 2, 3, and 4 post-PEDV CHN-CQ-2021 infection.

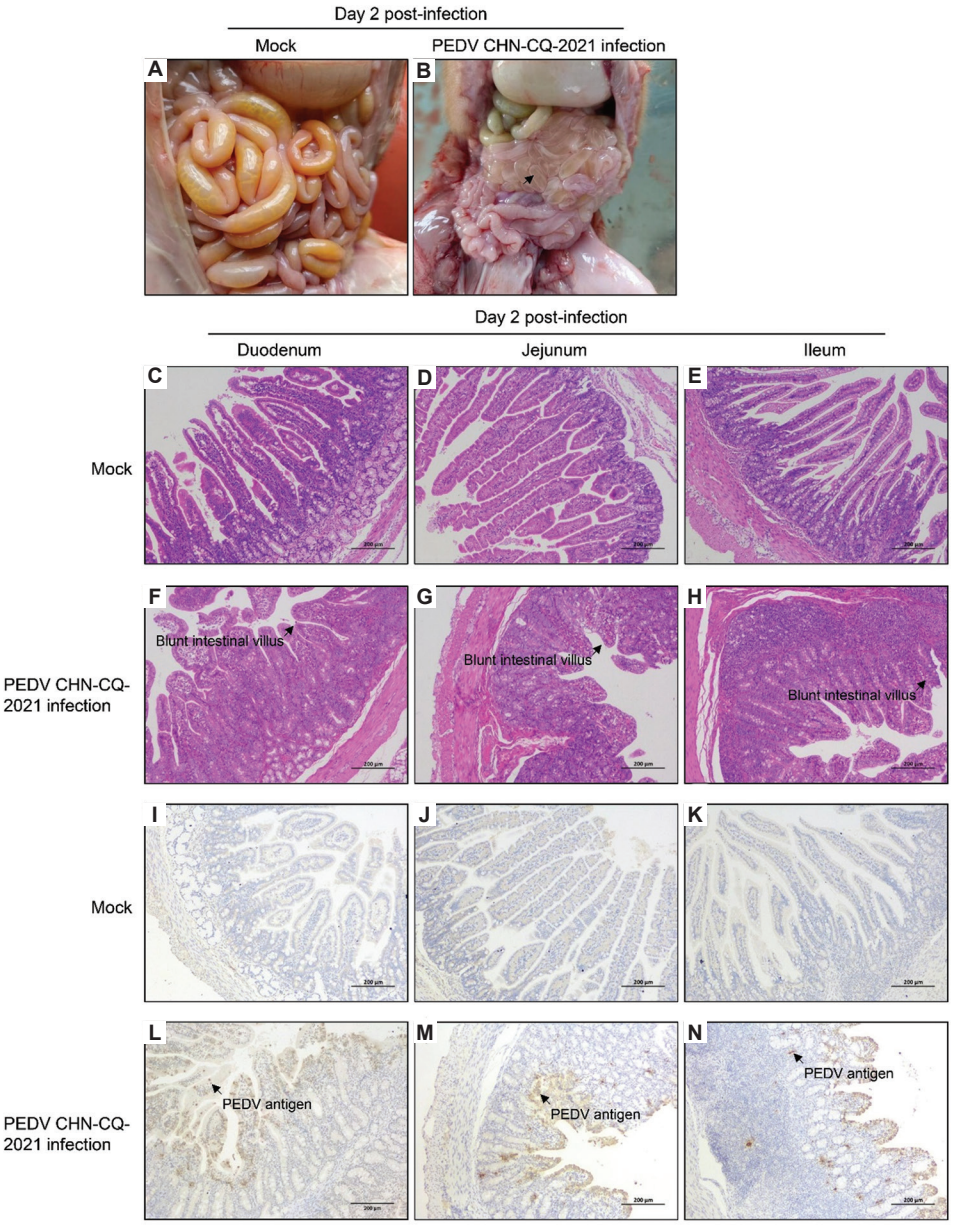

Figure 8. Intestinal pathological changes in newborn piglets inoculated with porcine epidemic diarrhea virus (PEDV) CHN-CQ-2021 strain. (A) Macroscopic examination of intestinal morphology in a control piglet at day 2 post-PEDV CHN-CQ-2021 infection (dpi). (B) Macroscopic observation of thin-walled intestinal tracts (arrow-indicated) in PEDV-challenged piglets at 2 dpi. (C-E) Histopathological analysis of hematoxylin and eosin (H&E)-stained intestinal tissue sections from a control piglet at 2 dpi. (F-H) H&E-stained intestinal tissue sections from a PEDV CHN-CQ-2021-challenged piglet at 2 dpi (The arrows indicate the blunt intestinal villi). (I-K) Immunohistochemical staining of intestinal tissue sections from a control piglet at 2 dpi. (L-N) Immunohistochemical staining of intestinal tissue sections from a PEDV CHN-CQ-2021-challenged piglet at 2 dpi (The arrows indicate the PEDV antigen).

S gene, which encodes the type I membrane glycoprotein, is the most genetically variable region in the coronavirus genome.[33] The S protein of coronavirus plays a critical role in receptor binding and virus entry.[33] Comparative analysis of the *S* gene sequence of the CHN-CQ-2021 strain revealed multiple nucleotide mutations compared to strains AJ1102 and GD-1. Whether these genetic variations contribute to the elevated virus replication efficacy and virulence requires further study.

It is noteworthy that numerous studies have already confirmed that PEDV is pathogenic to neonatal piglets, causing several symptoms, such as diarrhea, dehydration,

and death.[34,35] The PEDV GDS01 strain isolated in another study over a decade ago was initially highly pathogenic to newborn piglets.[36] However, its virulence has attenuated due to extensive *in vitro* passaging, which could affect vaccine evaluation and related studies. Orally inoculating 1-day-old newborn piglets with the CHN-CQ-2021 strain caused severe diarrhea and 100% mortality in piglets, indicating that this epidemic strain is highly pathogenic and poses a huge threat to pig farms. Viral nucleic acids could be detected in anal swabs, suggesting that fecal-oral transmission is a predominant route of PEDV dissemination. In addition, gross and histological examinations of intestinal tissues from infected piglets revealed extensive lesions. Microscopic observations showed severe cellular damage in the jejunum and ileum. Immunohistochemical analysis confirmed the predominant localization of PEDV antigens in the cytoplasm of enterocytes, consistent with previous studies.[36] These findings collectively demonstrate that PEDV CHN-CQ-2021 causes intestinal lesions, resulting in severe diarrhea. Interestingly, PEDV nucleic acids were also detected in the brains of virus-infected piglets. The mechanisms underlying PEDV entry into the brain and its potential neuropathogenicity remain to be elucidated. Importantly, we successfully isolated a highly pathogenic PEDV epidemic strain. However, several questions remain to be addressed in future research. For example, has the virulence of this strain increased compared to previously circulating strains? If so, what are the underlying mechanisms? Do current commercial vaccines confer protective immunity against this strain? If not, can this strain serve as a candidate for vaccine development? Clarifying these questions will aid in better controlling PEDV outbreaks.

5. Conclusion

A novel PEDV strain named CHN-CQ-2021 was isolated from the pathological samples of diarrheic piglets in this study. Phylogenetic analysis classified this strain as a G2b genotype variant, exhibiting the typical morphological features of coronavirus. Oral inoculation of newborn piglets with the CHN-CQ-2021 strain induced severe clinical symptoms, including watery diarrhea, dehydration, and high mortality, confirming its high pathogenicity. The isolation and characterization of the CHN-CQ-2021 strain provide a critical foundation for studying the pathogenic mechanisms of PEDV and developing prevention and control measures.

Acknowledgments

None.

Funding

This work was supported by the grant from the "Special Support Plan" of Guangdong Provincial Department of Agriculture and Rural-Youth top talent project (#NYQN2024001) and the Key-Area Research and Development Program of Guangdong Province (#2022B1111030001).

Conflict of interest

The authors declare that they have no competing interests.

Author contributions

Conceptualization: Zhichao Xu
Data curation: Yongbo Xia, Xiaolu Li
Formal analysis: Zhichao Xu
Funding acquisition: Zhichao Xu
Investigation: Yongbo Xia, Xiaolu Li
Methodology: Zhichao Xu
Project administration: Yongchang Cao, Zhichao Xu
Resources: Zhichao Xu, Chunyi Xue, Yongchang Cao
Software: Zhichao Xu
Supervision: Zhichao Xu, Chunyi Xue, Yongchang Cao
Validation: All authors
Visualization: Yongbo Xia, Xiaolu Li, Zhichao Xu
Writing–original draft: Xiaolu Li
Writing–review & editing: Zhichao Xu

Ethics approval and consent to participate

The animal study was supervised by the Institutional Animal Care and Use Committee of Sun Yat-sen University (IACUC-2023-B0404) and conducted in accordance with the regulations and guidelines of this committee.

Consent for publication

Not applicable.

Availability of data

The data that support the findings of this study are available from the corresponding author on reasonable request.

References

1. Chen J, Cheng Z, Chen J, Qian L, Wang H, Liu Y. Advances in human norovirus research: Vaccines, genotype distribution and antiviral strategies. *Virus Res*. 2024;350:199486.
   doi: 10.1016/j.virusres.2024.199486
2. Roach SN, Langlois RA. Intra- and cross-species transmission of astroviruses. *Viruses*. 2021;13(6):1127.
   doi: 10.3390/v13061127
3. Kotloff KL, Platts-Mills JA, Nasrin D, Roose A, Blackwelder WC, Levine MM. Global burden of diarrheal diseases among children in developing countries: Incidence, etiology, and insights from new molecular diagnostic techniques. *Vaccine*. 2017;35(49):6783-6789.

doi: 10.1016/j.vaccine.2017.07.036

4. Abebe E, Gugsa G, Ahmed M. Review on major food-borne zoonotic bacterial pathogens. *J Trop Med*. 2020;2020:4674235.

   doi: 10.1155/2020/4674235

5. Ghssein G, Barakat R, Nehme N, Awada R, Hassan HF. Fecal prevalence of *campylobacter* spp. In house dogs in lebanon: A pilot study. *Vet World*. 2023;16:2250-2255.

   doi: 10.14202/vetworld.2023.2250-2255

6. Awada R, Ghssein G, El Roz A, Farhat M, Nehme N, Hassan HF. Prevalence of *Campylobacter* spp. In broilers in north lebanon. *Vet World*. 2023;16:322-328.

   doi: 10.14202/vetworld.2023.322-328

7. Liu C, Dong X, Liu P, Lin X. Advances in porcine respiratory and intestinal organoids: Status and potential application for virus infections. *One Health Adv*. 2024;2(1):22.

   doi: 10.1186/s44280-024-00052-0

8. Zhou P, Fan H, Lan T, *et al*. Fatal swine acute diarrhoea syndrome caused by an hku2-related coronavirus of bat origin. *Nature*. 2018;556(7700):255-258.

   doi: 10.1038/s41586-018-0010-9

9. Jiao R, Ji Z, Zhu X, *et al*. Genome analysis of the g6p6 genotype of porcine group c rotavirus in China. *Animals (Basel)*. 2022;12(21):2951.

   doi: 10.3390/ani12212951

10. McCluskey BJ, Haley C, Rovira A, Main R, Zhang Y, Barder S. Retrospective testing and case series study of porcine delta coronavirus in u.S. Swine herds. *Prev Vet Med*. 2016;123:185-191.

    doi: 10.1016/j.prevetmed.2015.10.018

11. Liu Q, Wang HY. Porcine enteric coronaviruses: An updated overview of the pathogenesis, prevalence, and diagnosis. *Vet Res Commun*. 2021;45(2-3):75-86.

    doi: 10.1007/s11259-021-09808-0

12. Li C, Lu H, Geng C, *et al*. Epidemic and evolutionary characteristics of swine enteric viruses in south-central china from 2018 to 2021. *Viruses*. 2022;14(7):1420.

    doi: 10.3390/v14071420

13. Fragoso-Saavedra M, Liu Q. Towards developing multistrain pedv vaccines: Integrating basic concepts and sars-cov-2 pan-sarbecovirus strategies. *Virology*. 2025;604:110412.

    doi: 10.1016/j.virol.2025.110412

14. Lin F, Zhang H, Li L, *et al*. Pedv: Insights and advances into types, function, structure, and receptor recognition. *Viruses*. 2022;14(8):1744.

    doi: 10.3390/v14081744

15. Kocherhans RB, Bridgen A, Ackermann M, Tobler K. Completion of the porcine epidemic diarrhoea coronavirus (pedv) genome sequence. *Virus Genes*. 2001;23(2):137-144.

    doi: 10.1023/A:1012508705001

16. Li X, Wu Y, Yan Z, *et al*. A comprehensive view on the protein functions of porcine epidemic diarrhea virus. *Genes (Basel)*. 2024;15(2):165.

    doi: 10.3390/genes15020165

17. Pensaert MB, De Bouck P. A new coronavirus-like particle associated with diarrhea in swine. *Arch Virol*. 1978;58:243-247.

    doi: 10.1007/BF01317606

18. Song D, Park B. Porcine epidemic diarrhoea virus: A comprehensive review of molecular epidemiology, diagnosis, and vaccines. *Virus Genes*. 2012;44(2):167-175.

    doi: 10.1007/s11262-012-0713-1

19. Sun D, Wang X, Wei S, Chen J, Feng L. Epidemiology and vaccine of porcine epidemic diarrhea virus in china: A mini-review. *J Vet Med Sci*. 2016;78(3):355-363.

    doi: 10.1292/jvms.15-0446

20. Yao X, Qiao WT, Zhang YQ, *et al*. A new pedv strain ch/hljjs/2022 can challenge current detection methods and vaccines. *Virol J*. 2023;20(1):13.

    doi: 10.1186/s12985-023-01961-z

21. Xu Z, Zhang Y, Gong L, *et al*. Isolation and characterization of a highly pathogenic strain of porcine enteric alphacoronavirus causing watery diarrhoea and high mortality in newborn piglets. *Transbound Emerg Dis*. 2018;66(1):119-130.

    doi: 10.1111/tbed.12992

22. Xu Z, Zhong H, Zhou Q, *et al*. A highly pathogenic strain of porcine deltacoronavirus caused watery diarrhea in newborn piglets. *Virol Sin*. 2018;33(2):131-141.

    doi: 10.1007/s12250-018-0003-8

23. Reed LJ, Muench H. A simple method of estimating fifty per cent endpoint. *Am J Epidemiol.* 1938;27:493-497.

    doi: 10.1093/oxfordjournals.aje.a118408

24. Quinting BR, Robert B, Letellier C, *et al*. Development of a 1-step enzyme-linked immunosorbent assay for the rapid diagnosis of bovine respiratory syncytial virus in postmortem specimens. *J Vet Diagn Invest*. 2007;19:238-243.

    doi: 10.1177/104063870701900302

25. Bjustrom-Kraft J, Woodard K, Giménez-Lirola L, *et al*. Porcine epidemic diarrhea virus (pedv) detection and antibody response in commercial growing pigs. *BMC Vet Res*. 2016;12(1):99.

    doi: 10.1186/s12917-016-0725-5

26. Chen Q, Gauger P, Stafne M, *et al*. Pathogenicity and pathogenesis of a united states porcine deltacoronavirus

cell culture isolate in 5-day-old neonatal piglets. *Virology*. 2015;482:51-59.

doi: 10.1016/j.virol.2015.03.024

27. Madson DM, Magstadt DR, Arruda PHE, *et al*. Pathogenesis of porcine epidemic diarrhea virus isolate (us/iowa/18984/2013) in 3-week-old weaned pigs. *Vet Microbiol*. 2014;174(1-2):60-68.

doi: 10.1016/j.vetmic.2014.09.002

28. Huang YW, Dickerman AW, Piñeyro P, *et al*. Origin, evolution, and genotyping of emergent porcine epidemic diarrhea virus strains in the united states. *mBio*. 2013;4(5):e00737.

doi: 10.1128/mBio.00737-13

29. Zhang F, Luo S, Gu J, *et al*. Prevalence and phylogenetic analysis of porcine diarrhea associated viruses in Southern China from 2012 to 2018. *BMC Vet Res*. 2019;15(1):470.

doi: 10.1186/s12917-019-2212-2

30. Li W, Li H, Liu Y, *et al*. New variants of porcine epidemic diarrhea virus, china, 2011. *Emerg Infect Dis*. 2012;18(8):1350-1353.

doi: 10.3201/eid1808.120002

31. Kiesslich S, Kamen AA. Vero cell upstream bioprocess development for the production of viral vectors and vaccines. *Biotechnol Adv*. 2020;44:107608.

doi: 10.1016/j.biotechadv.2020.107608

32. Zhu N, Zhang D, Wang W, *et al*. A novel coronavirus from patients with pneumonia in china, 2019. *N Engl J Med*. 2020;382(8):727-733.

doi: 10.1056/NEJMoa2001017

33. Woo PCY, Huang Y, Lau SKP, Yuen KY. Coronavirus genomics and bioinformatics analysis. *Viruses*. 2010;2(8):1804-1820.

doi: 10.3390/v2081803

34. Yin L, Liu X, Hu D, Luo Y, Zhang G, Liu P. Swine enteric coronaviruses (PEDV, TGEV, and PDCoV) induce divergent interferon-stimulated gene responses and antigen presentation in porcine intestinal enteroids. *Front Immunol*. 2022;12:826882.

doi: 10.3389/fimmu.2021.826882

35. Yuan CZ, Zhang P, Liu P, *et al*. A novel pathway for porcine epidemic diarrhea virus transmission from sows to neonatal piglets mediated by colostrum. *J Virol*. 2022;96(14):e0047722.

doi: 10.1128/jvi.00477-22

36. Li Q, Xu Z, Wu T, *et al*. A flagellin-adjuvanted ped subunit vaccine improved protective efficiency against pedv variant challenge in pigs. *Vaccine*. 2018;36(29):4228-4235.

doi: 10.1016/j.vaccine.2018.05.124

ACCSCIENCE PUBLISHING

Microbes & Immunity

ORIGINAL RESEARCH ARTICLE

Assessment of oxidative toxicity and folate status in HIV patients on dolutegravir-based antiretroviral therapy

Onwuka Kalu Chima* and **Ejike Felix Chukwurah**

Department of Medical Laboratory Science/Haematology and Blood Transfusion, Faculty of Health Sciences and Technology, Ebonyi State University, Abakaliki, Ebonyi State, Nigeria

Abstract

Dolutegravir (DTG), a key component of antiretroviral therapy (ART), has demonstrated potent virologic suppression and superior efficacy compared to standard regimens in HIV management. However, concerns about its long-term safety persist, with emerging evidence suggesting potential adverse effects. Notably, studies have reported an increased risk of neural tube defects in infants born to women exposed to DTG during pregnancy, as well as associations with neuropsychiatric effects and sideroblastic anemia. This cross-sectional study investigated plasma folate and malondialdehyde (MDA) levels—markers of antioxidant status and oxidative stress, respectively—in HIV-positive patients receiving DTG-based ART at the University of Nigeria Teaching Hospital, Enugu. A total of 120 participants were recruited, comprising 40 treatment-naïve patients initiating DTG-based ART, 40 patients on DTG-based ART for 6 months, and 40 HIV-negative controls. Plasma folate was measured using chemiluminescence immunoassay, while MDA levels were determined spectrophotometrically. Results showed significantly elevated MDA levels in both treatment-naïve (5.72 ± 3.61 μmol/L) and 6-month DTG-treated patients (8.94 ± 5.03 μmol/L) compared to controls (1.19 ± 0.18 μmol/L). Conversely, folate concentrations were markedly lower in the DTG groups (2.23 ± 1.52 and 1.89 ± 0.54 ng/mL, respectively) than in controls (11.11 ± 1.31 ng/mL). These findings suggest that DTG-based ART may elevate oxidative stress while reducing antioxidant levels, underscoring the need for careful monitoring of its biochemical effects in HIV-positive individuals.

Keywords: Dolutegravir; Oxidative toxicity; Folate status; Antiretroviral therapy; HIV

***Corresponding author:**
Onwuka Kalu Chima
(chimaonwuka@unth.edu.ng)

Citation: Chima OK, Chukwurah EF. Assessment of oxidative toxicity and folate status in HIV patients on dolutegravir-based antiretroviral therapy. *Microbes & Immunity*. 2025;2(4):122-131. doi: 10.36922/MI025310074

Received: August 01, 2025

Revised: August 27, 2025

Accepted: September 10, 2025

Published online: October 10, 2025

1. Introduction

Dolutegravir (DTG), an integrase strand transfer inhibitor, has become a cornerstone of modern antiretroviral therapy (ART) owing to its potent virologic suppression, high genetic barrier to resistance, and favorable safety and efficacy profile across diverse populations. Its widespread adoption as part of first-line ART regimens has contributed significantly to global progress toward HIV epidemic control. Despite these clinical successes, concerns regarding the long-term safety of DTG have emerged, particularly in relation to neuropsychiatric adverse events (NPAEs), hematological alterations, teratogenicity through interference with folate metabolism, and potential contributions

to oxidative stress and metabolic dysregulation. These safety signals have sparked renewed scrutiny, especially in resource-limited settings where DTG is being rapidly scaled up as part of universal treatment strategies.

Real-world evidence has increasingly highlighted the neuropsychiatric burden associated with DTG. A cross-sectional study in Uganda reported that 41.7% of adult patients on DTG experienced at least one NPAE, with 9.1% experiencing severe or life-threatening outcomes requiring clinical intervention.[1] Comparable findings were reported in a multicenter study in Ethiopia, underscoring the importance of clinical vigilance in settings with limited access to psychiatric support.[2] Further evidence from the randomized DOBINeuro trial showed that patients switched from DTG/abacavir/lamivudine to bictegravir-based regimens experienced improvements in sleep disturbances, although other neuropsychiatric symptoms persisted, suggesting that DTG-associated tolerability challenges are nuanced and may not be completely reversible.[3]

In parallel, a growing body of experimental and clinical research has examined the relationship between DTG and folate metabolism. Preclinical evidence demonstrates that DTG disrupts the expression and function of critical folate transporters—including reduced folate carrier, proton-coupled folate transporter, and folate receptor-α—in human placental models and pregnant mice, thereby impairing cellular folate uptake under folate-deficient conditions.[4,5] In mice maintained on low-folate diets, DTG exposure induced neural tube defects (NTDs), such as exencephaly and cleft palates, whereas folic acid supplementation mitigated these abnormalities.[6]

Human evidence aligns with these findings: the ADVANCE trial in South Africa reported divergent folate responses depending on the ART regimen, with women on tenofovir alafenamide/emtricitabine (FTC) + DTG showing increased serum folate over 12 weeks, whereas those on tenofovir disoproxil fumarate (TDF)/FTC + DTG or TDF/FTC/Efavirenz experienced declines.[7] This variability suggests that DTG's impact on folate may depend on background regimen composition, baseline nutritional status, or host-related factors. The importance of adequate folate intake in mitigating DTG-associated teratogenic risks has been emphasized by several investigators. A 2024 review highlighted that supplementation or dietary fortification protects NTDs in pregnancies exposed to DTG, particularly in populations with poor baseline folate status.[8] Initial surveillance in Botswana suggested an elevated risk of NTDs in infants conceived on DTG,[9] and subsequent analyses reinforced this association in the context of low dietary folate intake.[10]

Mechanistic work further supports this biological interaction. Cabrera *et al.*[4] demonstrated that DTG acts as a non-competitive antagonist of folate receptor 1, inhibiting folate uptake despite adequate serum levels. Animal and cell-based studies confirmed that DTG-induced neurodevelopmental toxicity—including dopaminergic neuronal loss, reduced viability of stem cell-derived brain organoids, altered neurogenic gene expression such as *ngn1*, and impaired locomotor activity in zebrafish embryos—was largely attenuated by folic acid supplementation.[6,11-13]

Although the initial NTD safety signal has been attenuated by subsequent large-scale monitoring—with risk estimates declining as surveillance expanded[9] and pharmacovigilance studies have not confirmed a definitive link between DTG and NTDs,[14] clinical attention has shifted toward other emerging safety concerns, including weight gain, metabolic complications, and oxidative imbalance.[15]

A growing body of work suggests that DTG may induce oxidative stress and mitochondrial dysfunction, leading to systemic metabolic dysregulation. Elevated reactive oxygen species (ROS) production and perturbations in mitochondrial pathways have been observed, contributing to lipid accumulation, insulin resistance, and metabolic dysfunction in adipocytes. These effects appear to be mediated through impairment of fatty acid oxidation, dysregulation of lipoprotein lipase, and increased expression of pro-inflammatory cytokines such as tumor necrosis factor α and interleukin-6, mechanisms that mirror established pathways of oxidative stress-related metabolic disorders.[16,17] Such findings raise important concerns regarding long-term cardiometabolic outcomes in individuals on lifelong DTG therapy.

The central nervous system effects of DTG further compound its safety profile. Its penetrance across the blood-brain barrier has been associated with symptoms such as insomnia, depression, and anxiety, which in some cases necessitate treatment discontinuation. Systematic reviews estimate that up to 11.8% of patients discontinue DTG due to NPAEs, with older age, female sex, and ART-naïve status conferring increased risk.[14] Pharmacogenetic data suggest that individual susceptibility may be modified by genetic variation, with polymorphisms such as NR1I2 c.–22-7659C>T shown to reduce NPAE risk.[18] Preclinical evidence adds further mechanistic plausibility, indicating that DTG may exert neurotoxic effects through N-methyl-D-aspartate receptor activation, glutamate-mediated ROS production, and eryptosis, with recent work implicating endoplasmic reticulum stress at the blood-brain barrier as an additional pathway of DTG-induced central nervous system toxicity.[19]

Taken together, accumulating evidence underscores that, while DTG remains a highly efficacious antiretroviral agent with substantial public health benefits, its long-term safety profile requires continued vigilance. Concerns spanning neuropsychiatric events, folate metabolism, oxidative stress, and metabolic outcomes highlight the need for integrated pharmacovigilance, mechanistic research, and context-specific clinical guidance, particularly in regions with limited dietary folate intake and rising ART scale-up.

2. Materials and methods

2.1. Materials

2.1.1. Study design and setting

This was a quasi-experimental, prospective cohort study conducted at the University of Nigeria Teaching Hospital (UNTH), Ituku-Ozalla, Enugu State, Nigeria. The study was designed to evaluate the effects of DTG-based ART on hematological indices, micronutrient status, oxidative stress markers, and toxicity biomarkers among people living with HIV (PLWH).

2.1.2. Study population and group distribution

A total of 120 participants were recruited through purposive sampling and categorized into three groups of equal size (n = 40 per group):

(i) Group 1 - Treatment-naïve HIV-positive group: Newly diagnosed, ART-naïve HIV-positive individuals
(ii) Group 2 - DTG-experienced HIV-positive group: HIV-positive individuals who had received DTG-based ART for a minimum of 24 weeks
(iii) Group 3 - HIV-negative control group: Age- and sex-matched HIV-negative individuals without chronic illness or known hematological disorders.

Recruitment was conducted at the UNTH HIV clinic and the general outpatient department. HIV diagnosis was confirmed using the national HIV testing algorithm, while HIV-negative status was verified through serological screening.

2.2. Methods

2.2.1. Sample size determination

The minimum sample size was estimated using Fisher's formula for cross-sectional studies, based on the national HIV prevalence rate in Nigeria of 2.1%.[20] A minimum of 102 participants was required to achieve adequate statistical power at a 95% confidence level and a 5% margin of error. To compensate for possible attrition, 120 participants were enrolled, distributed equally across the three study groups (40 per group).

2.2.2. Eligibility criteria

Inclusion criteria were as follows:

(i) Aged 18–55 years
(ii) Confirmed HIV serostatus (positive or negative)
(iii) Written informed consent
(iv) For the DTG-experienced group: ≥24 weeks of continuous treatment with DTG-based ART.

Exclusion criteria included:

- Pregnancy
- Concurrent opportunistic infections (e.g., tuberculosis)
- Known metabolic, hematological, renal, or hepatic disorders
- Use of antioxidant supplements, cytotoxic drugs, or medications known to interfere with oxidative stress or folate metabolism.

2.2.3. Ethical considerations

Ethical approval for the study was obtained from the Health Research Ethics Committee of the UNTH (NHREC/05/01/2008B-FWA00002458-1RB00002323). All procedures were conducted in accordance with the principles of the Declaration of Helsinki. Written informed consent was obtained from all participants before enrolment. Confidentiality and data protection were maintained through data anonymization and restricted access to personal identifiers.

2.2.4. Sample collection and processing

Venous blood (5 mL) was collected aseptically from each participant into two tubes:

(i) Ethylenediaminetetraacetic acid tubes: For hematological profiling and plasma separation
(ii) Plain vacutainer tubes: For serum separation.

Samples in plain tubes were allowed to clot, then centrifuged at 3,000 rpm for 10 min, and serum aliquots were stored at −20°C until biochemical and immunological analyses were performed. Plasma and serum samples were thawed only once to minimize degradation of analytes.

2.2.5. Laboratory procedures

a. Determination of plasma folate levels

Plasma folate concentrations were quantified using the Maglumi 600 fully automated chemiluminescence immunoassay analyzer (Snibe Co., Ltd., China). The assay was based on a competitive chemiluminescent immunoassay in which folic acid was labeled with N-(4-aminobutyl)-N-ethylisoluminol and immobilized onto magnetic microbeads through folate-binding protein antibodies.

Test samples, calibrators, or controls were incubated with the labeled antigen, and the resulting complexes were magnetically separated from unbound fractions. Following a wash step, chemiluminescent starter reagents were added to initiate light emission. The relative light units generated were inversely proportional to the folate concentration in the test sample.[21]

b. Determination of malondialdehyde (MDA)

MDA concentrations were measured using the thiobarbituric acid reactive substances (TBARS) assay with a semi-automated chemistry analyzer (EMP Semi-Autochemistry Analyzer, Model: 168, Manufactured in China), following the method of Gutteridge and Wilkins.[22]

The assay is based on the reaction of MDA, a byproduct of lipid peroxidation, with thiobarbituric acid under acidic and high-temperature conditions to form a stable pink chromogen. Absorbance was measured spectrophotometrically at 532 nm. The concentration of MDA was calculated using the Beer-Lambert law:

$$\left[MDA\right](\mu M) = \frac{(A_{532} - A_{blank)} \times 10^6}{\varepsilon \times l} \quad \text{(I)}$$

Where ε is the molar extinction coefficient and l is the path length.

Alternatively, concentration was expressed as:[23]

$$[MDA](nmol/mL) = (A_{532}\text{-}A_{blank}) \times 6.41 \quad \text{(II)}$$

2.3. Statistical analysis

Data were analyzed using SPSS version 26.0 (IBM Corp., USA). Descriptive statistics (mean ± standard deviation for continuous variables and frequencies/percentages for categorical variables) were computed.

(i) Comparisons of means across the three groups were performed using independent sample *t*-tests and one-way analysis of variance, where appropriate
(ii) Chi-square tests were used for categorical variables
(iii) Effect sizes were calculated using Cohen's *d*, allowing interpretation of the magnitude of observed differences beyond statistical significance
(iv) A $p<0.05$ was considered statistically significant
(v) Results are presented in tables and figures to enhance clarity.

2.4. Confidentiality and data management

All participants' personal identifiers—including names, age, and contact details—were anonymized and coded before analysis. Laboratory samples were labeled with numeric codes rather than participant information. Data were stored on a password-protected computer with access limited to the research team. Individual laboratory results were communicated privately to each participant during counseling sessions at the HIV clinic.

3. Results

3.1. Baseline characteristics of the study population

Table 1 summarizes the sociodemographic characteristics of the study population. The distribution of participants by sex was fairly equitable, with males comprising 48–51% and females 49–52% across groups, showing no significant difference (p=0.816). The mean age of participants was 37.32 ± 8.63 years, spanning 19–53 years, representing mostly young- and middle-aged adults in their physiologically active stages.

However, age distribution differed significantly between groups (p<0.001). While the majority of HIV-negative

Table 1. Sociodemographic characteristics of study participants across treatment groups

Baseline characteristic	Subject	Control	x^2	*p*-value
Age group				
19–28	6 (16.2)	24 (64.9)	20.254	<0.001
29–38	13 (35.1)	8 (21.6)		
39–48	14 (37.8)	5 (13.5)		
49–58	4 (10.8)	0 (0.00)		
Sex				
Male	18 (48.6)	19 (51.4)	0.054	0.816
Female	19 (51.4)	18 (48.6)		
Educational status				
Primary	10 (27.0)	10 (27.0)	0.670	0.715
Secondary	16 (43.2)	13 (35.1)		
Tertiary	11 (29.7)	14 (37.8)		
Socioeconomic status				
Low	27 (73.0)	26 (70.3)	1.019	0.601
Middle	10 (27.0)	10 (27.0)		
High	0 (0.00)	1 (2.7)		
Occupation				
Artisan	7 (18.9)	0 (0.00)	20.567	0.001
Business/trader	21 (56.8)	14 (37.8)		
Civil servant	7 (18.9)	17 (45.9)		
Farmer	0 (0.00)	3 (8.1)		
Student	0 (0.00)	3 (8.1)		
Unemployed	2 (5.4)	0 (0.00)		
Marital status				
Single	14 (37.8)	18 (48.6)	0.881	0.348
Married	23 (62.2)	19 (51.4)		

Note: Data are expressed as *n* (%).

controls was younger adults aged 19–28 years (64.9%), the largest proportion of PLWH on DTG-based ART were in the 39–48 age category (37.8%), suggesting that HIV-positive individuals tended to be older.

Educational attainment was comparable between groups (p=0.715), with secondary education being the most frequent, followed by tertiary and primary education. Socioeconomic status was also similar (p=0.601), with over 70% of participants in both groups classified as low-income status, and only a minority reporting middle- or high-income status. In contrast, occupational status differed significantly (p=0.001): a majority of HIV-positive participants were traders (56.8%), while nearly half of the control groups were civil servants (45.9%). Marital status distribution showed no significant variation between groups (p=0.348), with both groups having a predominance of married individuals.

These findings suggest that, while educational and socioeconomic backgrounds were largely balanced across groups, the HIV-positive cohort was slightly older and more commonly engaged in trading, whereas controls were more likely to be in formal employment.

3.2. Biochemical outcomes

A significant increase in MDA levels was observed after 24 weeks of DTG-based ART (Table 2). Mean plasma MDA concentrations rose from 5.72 ± 3.61 μmol/L at baseline to 8.94 ± 5.03 μmol/L post-treatment (t = 2.767, p=0.009), reflecting a pronounced elevation in oxidative stress after therapy.

Comparison with HIV-negative controls further underscored the burden of oxidative imbalance. Mean MDA levels in the control group were markedly lower (1.19 ± 0.18 μmol/L), and both pre- and post-treatment values in the DTG group were significantly elevated relative to controls (p<0.001).

Folate levels did not show a statistically significant within-group change over 24 weeks of therapy (p=0.753). Mean plasma folate decreased from 2.23 ± 1.52 ng/mL at baseline to 1.86 ± 0.54 ng/mL post-treatment, suggesting only a minimal short-term effect of DTG initiation on folate status.

However, when compared with HIV-negative controls, who had substantially higher folate levels (11.11 ± 1.31 ng/mL), both pre- and post-treatment HIV-positive participants exhibited severe folate depletion (p<0.001). This pattern highlights that folate deficiency is a persistent feature of HIV infection, independent of immediate DTG exposure.

The effect size plot with dashed lines marking thresholds for small, medium, and large effects. It illustrates that folate shows an extremely large decrease, while MDA shows moderate-to-very large increases depending on the comparison.

To complement significance testing, Cohen's d effect sizes were calculated (Table 2 and Figure 1).

Within the groups (pre vs. post), the increase in MDA from baseline to post-treatment corresponded to a medium-to-large effect (d = 0.74). In contrast, the decline in folate corresponded to a small-to-medium effect (d = 0.32).

Between the groups (HIV vs. controls), very large to extremely large effects were observed for MDA, with values of d = 1.78 for pre versus control and d = 2.18 for post versus control. For folate, the differences were extremely large and negative, reflecting markedly lower levels in HIV patients compared to controls; specifically, d = −6.25 for pre versus control and d = −9.25 for post versus control.

These findings provide additional insight into the magnitude of observed biochemical alterations. The within-group effect of DTG on oxidative stress was moderate-to-large, suggesting that treatment contributed to further increases in lipid peroxidation beyond baseline HIV-associated levels. Conversely, the within-group decline in folate was small and not statistically significant, indicating that folate depletion is more strongly attributable to HIV infection itself rather than short-term DTG use. However, the between-group comparisons revealed extremely large differences in folate status, demonstrating the severity of micronutrient deficiency among PLWH relative to HIV-negative individuals.

Table 2. Mean values of malondialdehyde and folate among treatment-naïve, treatment-experienced, and control participants with Cohen's *d* effect sizes

Parameter	Control	Pre-DTG	Post-DTG	*p* (Pre vs. post)	*p* (Pre vs. control)	*p* (Post vs. control)	Cohen's *d* (pre vs. post)	Cohen's *d* (pre vs. control)	Cohen's *d* (post vs. control)
Malondialdehyde (μmol/L)	1.19±0.18	5.72±3.61	8.94±5.03	0.009	<0.001	<0.001	0.72 (moderate-large ↑)	1.66 (very large ↑)	1.94 (very large ↑)
Folate (ng/mL)	11.11±1.31	2.23±1.52	1.86±0.54	0.753	<0.001	<0.001	0.29 (small ↓)	6.8 (huge ↓)	8.2 (huge ↓)

Note: Data are expressed as means±standard deviations.
Abbreviation: DTG: Dolutegravir.

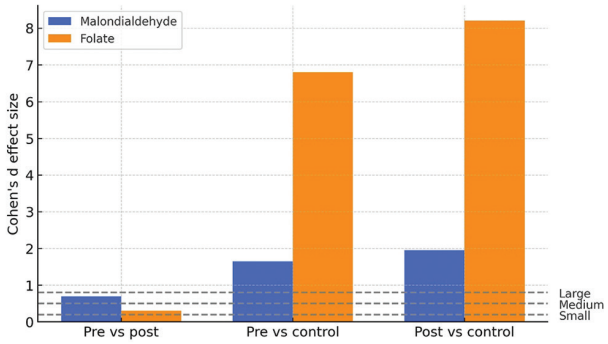

Figure 1. Effects of dolutegravir treatment on malondialdehyde and folate

4. Discussion

This study demonstrates that DTG-based ART is associated with significant biochemical alterations, most notably elevated oxidative stress and reduced folate availability. Taken together, these findings reveal two distinct but interconnected biochemical patterns.

First, DTG therapy was associated with a statistically significant and clinically meaningful increase in MDA, with effect size analysis confirming a moderate-to-large impact (d = 0.74). Both pre- and post-therapy MDA levels were substantially higher than in HIV-negative controls, indicating that oxidative imbalance is both a consequence of HIV infection and further exacerbated by ART. The moderate-to-large increase in MDA concentrations post-treatment is consistent with elevated lipid peroxidation and oxidative imbalance. Oxidative stress, reflected by biomarkers such as MDA, is a well-established driver of mitochondrial dysfunction, cellular senescence, and inflammatory activation in PLWH.[24,25] These mechanisms have been implicated in neurocognitive decline, cardiovascular disease, and accelerated aging, even among virally suppressed patients.[26] The persistence of high oxidative stress despite ART initiation suggests that integrase inhibitor therapy may not fully attenuate, and may even exacerbate, oxidative injury through ROS generation and impaired antioxidant defenses.

Second, folate levels remained markedly and consistently lower in HIV-positive participants compared with controls. The within-group change after DTG therapy was small and not statistically significant (Cohen's d = −0.33), but the between-group effect sizes were extremely large, with values such as d = −1.49 for pre versus control and d = −2.61 for post versus control. This suggests that while DTG initiation does not cause an acute decline, HIV infection itself is strongly associated with severe folate depletion. Folate is indispensable for one-carbon metabolism, DNA synthesis, and hematopoiesis, and its depletion predisposes patients to megaloblastic anemia and impaired immune recovery.[27] More importantly, maternal folate deficiency has been consistently linked to NTDs, raising major public health concerns for women of reproductive age receiving DTG-based ART. Our findings align with prior reports showing reduced folate levels among ART-experienced populations,[28,29] though they contrast with recent clinical trial data from Barlow-Mosha *et al.*,[30] which demonstrated more pronounced folate changes. Such discrepancies may reflect differences in baseline nutritional status, treatment duration, or population characteristics.

The oxidative and nutritional disturbances observed in this study are consistent with previous reports. Elevated MDA has been documented in both ART-naïve and ART-treated HIV populations, reflecting heightened lipid peroxidation and cytokine-driven inflammatory pathways.[31-33] Mechanistically, cytokine-mediated activation of lipoxygenase pathways may further potentiate ROS generation.[34] Similarly, folate depletion in HIV has been attributed to anorexia, increased metabolic turnover, and viral replication-driven nucleotide demand.[35,36] Given the estimated daily production of up to 10 billion virions in untreated HIV, such demands are likely to accelerate micronutrient depletion, compounding nutritional deficiencies.

Folate deficiency has dual consequences. It impairs DNA synthesis and causes defective S-phase progression, both of which are reversible upon repletion. In addition, it compromises immune function through reduced T-cell proliferation and blunted mitogen responses.[37] In the context of oxidative stress, these disturbances may act synergistically. ROS-mediated injury depletes antioxidant reserves, further lowering folate bioavailability, while folate deficiency compromises DNA repair capacity, thereby amplifying oxidative damage.[38] This bidirectional interplay could underlie the neuropsychiatric symptoms, hematologic toxicity, and heightened teratogenic risk reported in DTG-treated populations.[4] An additional layer of complexity may arise from genetic polymorphisms in folate metabolism (e.g., MTHFR variants), which could modulate individual susceptibility to drug-nutrient interactions and oxidative injury, further reinforcing the need for personalized monitoring strategies.

Clinically, these findings highlight that patients on DTG-based ART face a dual burden. They experience worsening oxidative stress after treatment initiation, coupled with profound pre-existing folate deficiency that remains uncorrected by therapy. This underscores the need for integrated management approaches that extend beyond viral suppression. Routine monitoring of oxidative

stress markers and serum folate should be considered, alongside adjunctive strategies such as targeted antioxidant support and folate supplementation. Such interventions may mitigate metabolic toxicity, improve hematological outcomes, and reduce neurodevelopmental risks in exposed infants. Although concerns about potential teratogenicity with DTG have been reported mainly from observational studies of exposure at conception, our study did not include pregnant women. Therefore, our findings do not provide direct evidence on this risk but rather suggest the need for further validation in pregnant populations. Further longitudinal and interventional studies are warranted to establish causality and evaluate the therapeutic efficacy of these strategies.

4.1. Perspectives on oxidative stress in HIV

The elevated oxidative stress observed in this study must be contextualized within the broader landscape of HIV management. Chronic HIV infection induces a pro-oxidant state, and while ART effectively reduces viral load, residual immune activation continues to sustain ROS generation. Mitochondria, as key regulators of cellular metabolism and apoptosis, are particularly vulnerable to oxidative injury. Persistent mitochondrial dysfunction has been linked to ART-related toxicities, including neuropathy, lipoatrophy, and lactic acidosis.[39] Although DTG is considered safer than thymidine analogues in this regard, the rise in MDA suggests that integrase inhibitors may not be metabolically inert.

Importantly, oxidative stress acts as a bridge between HIV and its non-AIDS comorbidities. Cardiovascular disease, osteoporosis, frailty, and neurocognitive impairment are all more prevalent in PLWH compared with the general population, even among those on suppressive ART. Our findings strengthen the hypothesis that oxidative stress contributes to this excess burden and may serve as a therapeutic target.

4.2. Comparative insights across ART classes

Previous studies have shown differential effects of ART classes on oxidative stress. Protease inhibitors, for instance, increase oxidative stress by inducing mitochondrial ROS production and promoting dyslipidemia. Nucleoside reverse transcriptase inhibitors, particularly stavudine and zidovudine, cause direct mitochondrial DNA depletion through inhibition of polymerase-γ.[40] By contrast, integrase inhibitors were initially thought to spare mitochondria, yet our findings suggest that the benefits may be relative rather than absolute. Understanding these nuances is critical as DTG becomes entrenched as the global first-line regimen.

4.3. Folate depletion: Clinical and public health significance

The extreme folate deficiency in our cohort highlights a major nutritional challenge. Folate insufficiency predisposes PLWH to anemia, impaired immune recovery, and teratogenic risk. While ART has transformed HIV into a chronic condition, quality of life and comorbidity prevention remain pressing concerns. Nutritional supplementation represents a low-cost intervention with the potential to improve outcomes.

Globally, the intersection between HIV and folate deficiency is particularly concerning in sub-Saharan Africa, where both HIV prevalence and baseline micronutrient deficiencies are high. Women of reproductive age are a critical population, as folate deficiency is directly linked to NTDs. The Botswana findings of increased NTDs among infants exposed to DTG at conception underscore the urgency of integrating micronutrient monitoring into HIV programs.[9]

4.4. Systematic interplay: Folate, one-carbon metabolism, and redox balance

Folate deficiency compromises one-carbon metabolism, leading to impaired DNA synthesis, methylation defects, and reduced production of nicotinamide adenine dinucleotide phosphate, which is essential for regenerating glutathione. Thus, folate deficiency and oxidative stress reinforce each other in a vicious cycle. This mechanistic insight provides a strong rationale for dual-target interventions: antioxidant therapy to counteract ROS and folate supplementation to restore one-carbon metabolism.

4.5. Clinical implications and future directions

The clinical implications of our findings are multifaceted. Monitoring oxidative stress markers (e.g., MDA, F2-isoprostanes) and serum folate in routine HIV care may help identify high-risk patients early. Nutritional counseling and supplementation should be prioritized, especially for women of childbearing age. Although antioxidant interventions are not yet standardized, they warrant further study in the context of DTG-based therapy.

Future research should move beyond observational findings to include randomized controlled trials evaluating the efficacy of folate and antioxidant supplementation in improving hematological, neurocognitive, and pregnancy outcomes. Moreover, integrating genetic screening for folate metabolism polymorphisms may allow for more personalized care.

5. Conclusion

This study provides preliminary evidence that DTG-based ART is associated with alterations in oxidative stress and

folate status among PLWH. While the findings are clinically significant, they must be interpreted with caution, given methodological limitations, including reliance on plasma folate alone, the use of the TBARS assay for MDA, and unmeasured confounding factors such as diet, lifestyle, and concomitant medications. Importantly, the observed changes likely reflect the combined influence of DTG, companion drugs (TDF/3TC), and underlying HIV-related inflammation rather than DTG alone. Nevertheless, the results highlight the need for routine monitoring of folate and oxidative stress biomarkers in patients on ART and suggest a potential role for targeted supplementation strategies. Future research incorporating longitudinal designs, functional folate markers, more specific assays, and cost-effectiveness analyses will be essential to validate and extend these findings, particularly in vulnerable groups such as pregnant women.

Acknowledgments

The authors would like to acknowledge laboratory directors of BIOQUEST and Praise Worth Laboratories, Enugu State, Nigeria, for providing the folate and malondialdehyde assays.

Funding

None.

Conflict of interest

The authors declare no conflicts of interest.

Author contributions

Conceptualization: All authors
Investigation: Onwuka Kalu Chima
Methodology: All authors
Writing–original draft: Onwuka Kalu Chima
Writing–review & editing: All authors

Ethics approval and consent to participate

Ethical approval for the study was obtained from the Health Research Ethics Committee of the University of Nigeria Teaching Hospital (NHREC/05/01/2008B-FWA00002458-1RB00002323). All procedures were conducted in accordance with the principles of the Declaration of Helsinki. Written informed consent was obtained from all participants before enrolment. Confidentiality and data protection were maintained through data anonymization and restricted access to personal identifiers.

Consent for publication

Specific consent for publication of participant data was not obtained because all data were anonymized and analyzed in aggregate. No identifiable information was included; therefore, additional consent was not required under the approved study protocol.

Availability of data

Data supporting the findings of this study are available from the corresponding author on reasonable request.

References

1. Mwebaza J, Meya D, Musiime V, Birungi C. Prevalence of neuropsychiatric adverse events and associated factors among adult patients on dolutegravir attending Mulago ISS clinic. *HIV Med.* 2023;24(4):491-501.

   doi: 10.1111/hiv.13428

2. Tesfaye E, Demelash K. Burden of care among caregivers of patients with mental illness in Ethiopia: A systematic review and meta-analysis. *BMC Public Health.* 2025;25:2414.

   doi: 10.1186/s12889-025-23461-1

3. Rossetti B, Ferrara M, Taramasso L, *et al.* Evolution of self-reported neuropsychiatric symptoms after switching from dolutegravir/abacavir/lamivudine to bictegravir/emtricitabine/tenofovir alafenamide: Results from the randomized DOBINeuro trial. *Infect Dis Ther.* 2025;14(1):293-304.

   doi: 10.1007/s40121-024-01083-1

4. Cabrera RM, Souder JP, Steele JW, *et al.* The antagonism of folate receptor by dolutegravir: Developmental toxicity reduction by supplemental folic acid. *AIDS.* 2019;33(11):1789-1798.

5. Gilmore JC, Hoque MT, Dai W, *et al.* Interaction between dolutegravir and folate transporters and receptor in human and rodent placenta. *EBioMedicine.* 2022;75:103771.

   doi: 10.1016/j.ebiom.2021.103771

6. Tukeman GL, Wei H, Lin YL, Wlodarczyk BJ, Finnell RH, Cabrera RM. Dolutegravir-induced neural tube defects in mice are folate responsive. *AIDS.* 2024;38(4):439-446.

   doi: 10.1097/QAD.0000000000003639

7. Chandiwana NC, Chersich M, Venter WDF, *et al.* Unexpected interactions between dolutegravir and folate: Randomized trial evidence from South Africa. *AIDS.* 2021;35(2):205-211.

   doi: 10.1097/QAD.0000000000002741

8. Zhou Q, Dong G, Wang Q, *et al.* Preconception folic acid supplementation for the prevention of birth defects: A prospective, population-based cohort study in mainland China. *BMC Pregnancy Childbirth.* 2024;24(1):114.

   doi: 10.1186/s12884-024-04319-9

9. Zash R, Holmes L, Diseko M, *et al.* Neural-tube defects and antiretroviral treatment regimens in Botswana. *N Engl J Med.* 2019;381(9):827-840.

doi: 10.1056/NEJMoa1805230

10. Assefa N, Abdullahi YY, Abraham A, *et al.* Consumption of dietary folate estimates and its implication for reproductive outcome among women of reproductive age in Kersa: Cross-sectional survey. *BMC Nutr.* 2021;7(1):69.

doi: 10.1186/s40795-021-00482-w

11. Jakimiuk A, Piechal A, Wiercińska-Drapało A, Nowaczyk A, Mirowska-Guzel D. Dolutegravir induces FOLR1 expression during brain organoid development. *Front Mol Neurosci.* 2024;17:1463159.

doi: 10.3389/fnmol.2024.1463159

12. Alcorn K. *Adequate Levels of Folate Protect Against Neural Tube Defects When Taking Dolutegravir*. *NAM aidsmap*; 2024. Available from: https://www.aidsmap.com [Last accessed on 2025 Sep 25].

13. Quirós Roldán M, Bresciani A, Savoldi A. Dolutegravir and folic acid interaction during neural system development: Zebrafish embryo model. *Int J Mol Sci.* 2024;25(9):4640.

doi: 10.3390/ijms25094640

14. Saint-Lary O, Martin C, Leclerc T. Post-marketing safety concerns with dolutegravir: A comprehensive pharmacovigilance review. *Front Pharmacol.* 2025;16:1399821.

doi: 10.3389/fphar.2025.1399821

15. Masenga SK, Kabwe LS, Chakulya M, Kirabo A. Mechanisms of oxidative stress in metabolic syndrome. *Int J Mol Sci.* 2023;24(9):7898.

doi: 10.3390/ijms24097898

16. Jain RG, Furfine ES, Pedneault L, White AJ, Lenhard JM. Metabolic complications associated with antiretroviral therapy. *Antiviral Res.* 2001;51:151-177.

doi: 10.1016/S0166-3542(01)00147-7

17. Alfadda AA, Sallam RM. Reactive oxygen species in health and disease. *J Biomed Biotechnol.* 2012;2012:936486.

doi: 10.1155/2012/936486

18. De Greef J, Yombi JC, Vincent A, *et al*. Dolutegravir and risk of neuropsychiatric adverse events: A pharmacogenetic study. *J Infect Dis.* 2025;231(6):1425-1429.

doi: 10.1093/infdis/jiaf098

19. Jakimiuk A, Piechal A, Wiercińska-Drapało A, Nowaczyk A, Mirowska-Guzel D. Central nervous system disorders after use of dolutegravir: Evidence from preclinical and clinical studies. *Pharmacol Rep.* 2023;75(6):1138-1151.

doi: 10.1007/s43440-023-00515-y

20. National Agency for the Control of AIDS (NACA). *National HIV/AIDS Indicator and Impact Survey (NAIIS) 2021: Technical Report*. Abuja, Nigeria: NACA; 2021.

21. Azim M, Hasan M, Ansari IH, Nasreen F. Chemiluminescence immunoassay: Basic mechanism and application. *Bangladesh J Nuclear Med.* 2018;18(2):171.

doi: 10.3329/bjnm.v18i2.35240

22. Gutteridge JM, Wilkins SC. Copper dependent hydroxyl radical damage to ascorbic acid; formation of thiobarbituric acid reactive products. *FEBS Lett.* 1982;137:327-330.

doi: 10.1016/0014-5793(82)81330-8

23. Buege JA, Aust SD. Microsomal lipid peroxidation. In: Fleischer S, Packer L, editors. *Methods in Enzymology.* Vol. 52. United States: Academic Press; 1978. p. 302-310.

24. Piantadosi CA, Suliman HB. Mitochondrial dysfunction in oxidative stress. *Free Radic Biol Med.* 2017;122:134-146.

doi: 10.1016/j.freeradbiomed.2018.01.003

25. Shytaj IL, Norelli S, Chirullo B, Palamara AT. Oxidative stress and HIV infection: Role in pathogenesis and therapeutic strategies. *Expert Rev Anti Infect Ther.* 2020;18(5):447-460.

doi: 10.1080/14787210.2020.1762438

26. Reust CE. Common adverse effects of antiretroviral therapy for HIV disease. *Am Fam Physician.* 2011;83(12):1443-1451.

27. Bailey LB, Gregory JF 3rd. Folate metabolism and requirements. *J Nutr.* 2015;145(3):593-596.

doi: 10.3945/jn.114.204009

28. Flax VL, Adair LS, Allen LH, *et al*. Plasma micronutrient concentrations are altered by antiretroviral therapy and lipid-based nutrient supplements in lactating HIV-infected Malawian women. *J Nutr.* 2015;145(8):1950-1957.

doi: 10.3945/jn.115.220109

29. Alani A, Vincent O, Adewumi A, *et al*. Plasma folate studies in HIV-positive patients at the Lagos University Teaching Hospital, Nigeria. *Indian J Sex Transm Dis AIDS.* 2010;31(2):99-103.

doi: 10.4103/0253-7184.74995

30. Barlow-Mosha LN, Ahimbisibwe GM, Chappell E, *et al*. Effect of dolutegravir on folate, vitamin B12 and mean corpuscular volume levels among children and adolescents with HIV: A sub-study of the ODYSSEY randomized controlled trial. *J Int AIDS Soc.* 2023;26(9):e26174.

doi: 10.1002/jia2.26174

31. Korencak M, Byrne M, Richter E, *et al.* Effect of HIV infection and antiretroviral therapy on immune cellular functions. *JCI Insight.* 2019;4(12):e126675.

doi: 10.1172/jci.insight.126675

32. Oyeyipo IP, Skosana BT, Everson FP, Strijdom H, du Plessis SS. Highly active antiretroviral therapy alters sperm parameters and testicular antioxidant status in diet-induced obese rats. *Toxicol Res.* 2018;34(1):41-48.

doi: 10.1039/c7tx00205h

33. Dhonju K, Gautam A, Dahal A, *et al.* Dolutegravir-induced acquired sideroblastic anemia in an HIV-positive patient: A challenging hematologic complication. *Clin Case Rep.* 2023;11(12):e8301.

doi: 10.1002/ccr3.8301

34. Kovacic P, Somanathan R. Broad overview of oxidative stress and its complications in human health. *Open J Prev Med.* 2013;3(1):32-41.

doi: 10.4236/ojpm.2013.31005

35. Rothenberg SP. Increasing the dietary intake of folate: Pros and cons. *Semin Hematol.* 1999;36(1):65-74.

36. Babafemi T. *General HIV Medicine*. Vol 1. Hyderabad: TFC Press; 2004. p. 10-11.

37. Dhur A, Galan P, Herberg S. Folate status and the immune system. *Prog Food Nutr Sci.* 1991;15(1-2):43-60.

38. Molloy AM, Scott JM. Folates and prevention of disease. *Public Health Nutr.* 2001;4(2B):601-609.

doi: 10.1079/PHN2000128

39. Lewis W, Dalakas M, Biesecker GM. Mitochondrial toxicity of antiviral drugs. *Nat Med.* 2003;6(3):249-255.

doi: 10.1038/nm0303-249

40. Savinelli S, Newman E, Mallon PWG. Metabolic complications associated with use of integrase strand transfer inhibitors (INSTI) for the treatment of HIV-1 infection: Focus on weight changes, lipids, glucose and bone metabolism. *Curr HIV/AIDS Rep.* 2024;21:567-580.

doi: 10.1007/s11904-024-00683-5

ACCSCIENCE PUBLISHING

Microbes & Immunity

MINI-REVIEW

Navigating glioblastoma therapy: A narrative review of emerging immunotherapeutics and small-molecule inhibitors

Matthew A. Abikenari[1]*, Iman Enayati[2], Daniel M. Fountain[1,3], and Maria Isabel Leite[1]

[1]Nuffield Department of Clinical Neurosciences, University of Oxford and Oxford University Hospitals, NHS Foundation Trust, Oxford, United Kingdom

[2]UCLA Department of Orthopaedic Surgery, University of California, Los Angeles, California, United States of America

[3]Department of Medicine, MRC Weatherall Institute of Molecular Medicine, John Radcliffe Hospital, Oxford, United Kingdom

Abstract

Glioblastoma multiforme (GBM) is the most common malignant primary tumor of the central nervous system (CNS), accounting for the majority of brain tissue tumors and CNS neoplasms. GBM has an incidence rate of 3.2/100,000 people in the United States, with an abysmal survival rate of 15 months with treatment and under 3 months for untreated patients. GBM remains incurable, with no disease-modifying treatment available. As a grade IV astrocytoma, GBM is highly aggressive, characterized by rapid proliferation, high metabolic demands, substantial angiogenesis, and diffuse infiltration of healthy parenchyma. The GBM genome is highly heterogeneous, with unpredictable amplification patterns, dysregulation, and mutational activation of *receptor tyrosine kinase* genes, tumor suppressor genes, and growth factor signaling. GBM's indistinct tumor margins, its highly adaptive interaction with the brain microenvironment, and the existence of the blood-brain barrier and the blood-brain tumor barrier further limit effective anti-GBM therapeutic strategies. Hence, anti-GBM drug discoveries and molecular techniques that aim for patient-specific treatment stratification are of profound clinical and therapeutic significance. The current paper aims to outline the fundamental pathophysiology, tumorigenicity, and immunosuppressive mechanism of GBMs, review current treatment options for GBMs, and examine the contemporary challenges and advances in anti-GBM drug discovery and delivery. Finally, the paper aims to shed light on the emergence of small-molecule inhibitors, immune checkpoint inhibitors, and vaccination therapy as potentially efficacious therapeutic strategies for treating GBM.

Keywords: Glioblastoma multiforme; Immunotherapy; Checkpoint inhibitors; Anti-GBM therapeutic strategies; Immunosuppressive mechanism; Small-molecule inhibitors

***Corresponding author:**
Matthew A. Abikenari
(mattabi@stanford.edu)

Citation: Abikenari MA, Enayati I, Fountain DM, Leite MI. Navigating glioblastoma therapy: A narrative review of emerging immunotherapeutics and small-molecule inhibitors. *Microbes & Immunity.* 2025;2(4):132-143. doi: 10.36922/mi.5075

Received: October 08, 2024

Revised: November 22, 2024

Accepted: December 9, 2024

Published online: December 30, 2024

1. Introduction

Glioblastoma multiforme (GBM) is the most common primary tumor of the central nervous system (CNS), accounting for roughly 50% of all brain tissue tumors and 16%

of all CNS neoplasms.[1,2] As the most malignant primary brain tumor, GBM has an incidence rate of 3.2/100,000 people in the United States, with a median age of 64.[3] The disease affects males 1.6-fold more frequently than females and Caucasians two-fold more frequently than African-Americans.[4] Glioblastoma remains one of the most deadly diagnoses of all cancer types that affect the human body,[5] with an abysmal median survival rate of 15 months after therapeutic interventions[6] and a 3-month survival rate in untreated patients.[7] Despite substantial advances in angiogenesis, chemotherapy, radiotherapy, immunotherapy, and gene therapy, GBM remains one of oncology's most challenging and treatment-resistant diagnoses.[8] The current paper aims to review the basic pathophysiology and tumorigenicity of GBM, the current challenges and advances in treatment and drug discovery, and the potential role of immunotherapy and small-molecule inhibitors (SMIs) as effective therapeutic strategies.

2. Histological grading: primary versus secondary GBM

Historically, glioblastoma was classified by the World Health Organization (WHO) based on macroscopic and microscopic histopathology, using a grading scale of I (most benign) to IV (most malignant) astrocytoma. GBM classification by the WHO now takes into account genetic mutations, molecular and cellular morphology, and historically well-known histological alterations characteristic of astrocytomas.[8,9] GBMs are bifurcated into primary and secondary GBMs. Primary GBMs feature the presence of *de novo*, wild-type isocitrate dehydrogenase (IDH) enzyme, accounting for 90% of all GBM cases, and tend to afflict older patient populations (mean age = 55 years). Furthermore, primary GBMs are characterized by extensive tissue necrosis, worse clinical outcomes, and substantially lower survival rates. Secondary GBMs encompass lower-grade astrocytomas such as grade II diffuse astrocytoma and grade III anaplastic astrocytoma, according to the WHO classification. Secondary GBMs feature the presence of mutant-type IDH enzyme, accounting for 10% of all GBMs and predominantly afflicting younger populations (mean age = 40 years). Furthermore, secondary GBMs are characterized by limited tissue necrosis, better clinical outcomes, and higher survival rates.[9-11] Out of the many genetic signatures characteristic of GBMs, *IDH1* mutation has shown substantial promise as a highly predictive biomarker for distinguishing secondary GBMs from primary GBMs.[11] Furthermore, patient IDH1 status presents a far more accurate overall survival prognosis than traditional histological grading and clinical classifications of high-grade astrocytomas.[12] Patients with *IDH1* mutation-linked gliomas tend to have substantially better clinical outcomes, longer survival, and more favorable response to treatment than those harboring wild-type *IDH1*.[13]

3. Pathogenesis

Most GBMs present supratentorially, affect the white matter of cerebral hemispheres, infiltrate the corpus callosum, and result in bilateral hemispheric involvement of the tumor.[14] The aggressive nature of GBMs is characterized by its rapid and diffuse infiltration of brain parenchyma, high metabolic demands, and substantial angiogenesis, coupled with uncontrolled proliferation and deregulation of a highly heterogeneous tumor genome.[15-18] As a high-grade astrocytic tumor, GBM exhibits microscopic features resembling those of the highly undifferentiated neoplastic astrocytes, comprises glial fibrillary acidic protein, and presents vascular proliferations and extensive interaction with the endothelium of the blood-brain barrier (BBB).[19,20] GBM cells infiltrate and invade healthy tissues using pre-existing routes such as the parenchymal tract, perivascular space, white-matter tracts, and the leptomeningeal space.[21,22] What makes GBM particularly pernicious is the tumor cell's tendency to extort existing cell types such as reactive astrocytes, glial and neural progenitors, stem cells, mitogens, and ligands in the brain microenvironment to induce further tumor proliferation and invasion of the parenchyma.[23] For instance, tumor cells require more oxygen during rapid proliferation and growth stages. A hypoxic microenvironment prevents rapid growth of the tumor and induces necrosis of surrounding tissue. To evade the adverse hypoxic microenvironment, tumor cells spread to healthy parenchyma, produce angiogenic factors that induce vascular proliferation, and eventually reclaim the high-oxygen microenvironment. Hence, the hypoxic environment induces tumor cell invasion.[24]

4. Treatment

Despite substantial advances in tumor resection surgeries, chemotherapy, radiotherapy, immunotherapy, and tumor-treating fields (TTFs), glioblastoma remains an incurable condition and poses a tremendous challenge to clinical oncology.[25] Neurosurgical tumor resection remains the first line of intervention for GBMs. The efficacy of total gross resection of the tumor through surgery largely depends on the size of invading tumor cell lines and the location of the lobes involved. Furthermore, the highly infiltrative nature of GBMs into the surrounding parenchyma presages the recurrence of the tumor within 2 – 4 cm of the initial resection site. Hence, even an ideal removal of 99% of

tumor volume by total gross resection holds extremely low efficacy as a treatment option. Furthermore, in many cases, surgical intervention into the neocortex, basal ganglia, and the brainstem is either unfeasible or comes at a significant cost to quality of life.[26,27]

Following safe surgical resection of the tumor, patients begin a radiotherapeutic intervention concomitant with temozolomide (TMZ) (Temodar®), an alkylating chemotherapeutic agent. Post-radiotherapy, patients are given adjuvant TMZ alone as a course of chemotherapy.[28] Other chemotherapeutic agents that have shown moderate efficacy are anti-angiogenic agents such as bevacizumab (an anti-vascular endothelial growth factor [VEGF] monoclonal antibody) and gefitinib and erlotinib (anti-epidermal growth factor receptor [EGFR] tyrosine kinase inhibitors [TKIs]).[29,30]

Alternating electric field therapy, also referred to as TTF, is an emergent FDA-approved therapy, serving as a concurrent treatment option for newly diagnosed GBM or recurrent GBM alongside TMZ. The TTF device, Optune®, works by a battery-powered device that delivers alternating electrical fields of low intensity to disrupt cell division and cause eventual apoptosis. TTF is a relatively safe mode of treatment as the induction frequency can be selectively adjusted to target GBM tumor cells, characterized by rapid cell divisions.[31,32] The major challenges in the treatment of glioblastoma are summarized in Table 1.

5. Immunotherapy

5.1. Mechanisms of immunosuppression in glioblastoma

Over the past decade, our understanding of immunosurveillance within the CNS has substantially shifted. The notion that the brain and spinal cord are immune-privileged has been radically discredited by the substantial literature demonstrating a robust immune response generated by B- and T-cell adaptive immunogens during inflammation-derived conditions such as common intracerebral infections, multiple sclerosis, and encephalitis.[33,34] This emerging shift in paradigm to view the brain as immunologically robust, with distinct and active lymphatic channels capable of priming B- and T-lymphocytes, presents a promising venture in developing novel immunotherapeutics for the treatment of GBM.[35] Unlike chemotherapy, immunotherapy carries non-existent cellular and genetic toxicity, low side effects, and a highly selective, patient-stratified therapeutic strategy that counteracts the highly heterogeneous genome of GBM cells.

Local and systemic immunosuppression is a consistent characteristic of GBM, recapitulated by immunosuppressive factors present in cervical lymph nodes, blood, bone marrow, and spleen. Common mechanisms of immunosuppression by the tumor cell include elimination of self-presenting

Table 1. Major challenges in the treatment of glioblastoma

Challenge	Mode of resistance
BBB	The BBB's highly selective endothelial tight junctions and P-glycoprotein efflux transporters prevent therapeutic agents from achieving effective concentrations in the central nervous system. This restricts the bioavailability of even highly potent drugs. Strategies such as nanoparticle-mediated delivery and focused ultrasound are being investigated to transiently disrupt the BBB for drug delivery.
Tumor infiltration and recurrence	Glioblastoma cells invade healthy brain parenchyma using white matter tracts, blood vessels, and the leptomeningeal space. This results in indistinct tumor margins and inevitable recurrence even after gross total resection. Novel intraoperative imaging techniques and localized drug delivery systems aim to address this challenge.
Genetic and molecular heterogeneity	GBM tumors exhibit patient-specific genomic landscapes, including mutations in EGFR, PTEN, and TP53, as well as IDH status. This heterogeneity renders one-size-fits-all therapies ineffective, necessitating personalized and stratified treatment approaches.
Immunosuppressive tumor microenvironment	The GBM microenvironment is characterized by hypoxia, upregulated VEGF, and infiltrating immunosuppressive cells such as TAMs, Tregs, and MDSCs. These factors collectively inhibit effector T-cell activity and promote tumor proliferation. Strategies targeting PD-L1, IDO, and TGF-β are being developed to modulate the tumor microenvironment.
Therapeutic resistance	Resistance mechanisms include MGMT-mediated repair of alkylating damage by TMZ, overexpression of efflux pumps, and activation of compensatory signaling pathways such as PI3K/AKT and MAPK. Combination therapies targeting these pathways are under investigation to overcome resistance.

Abbreviations: BBB: Blood-brain barrier; EGFR: Epidermal growth factor receptor; GBM: Glioblastoma multiforme; IDH: Isocitrate dehydrogenase; IDO: Indoleamine 2,3-dioxygenase; MAPK: mitogen-activated protein kinase; MDSCs: Myeloid-derived suppressor cells; MGMT: O6-Methylguanine-DNA methyltransferase; PD-L1: Programmed cell death ligand 1; PI3K/AKT: phosphatidylinositol 3-kinase/protein kinase B; PTEN: Phosphatase and tensin homolog; TAMs: Tumor-associated macrophages; TGF-β: Transforming growth factor beta; TMZ: Temozolomide; Tregs: Regulatory T-cells; VEGF: Vascular endothelial growth factor.

antigens through reduced regulation and expression of major histocompatibility complexes (MHCs) while simultaneously elevating immunosuppressive factors such as programmed cell death ligand 1 (PD-L1) and indoleamine 2,3-dioxygenase (IDO) cytosolic enzyme. PD-L1 ligand activates programmed cell death protein 1 (PD-1), which serves as an immune checkpoint receptor that inhibits the activity of CD8+ cytotoxic T-lymphocytes (CTLs).[36-38] IDO cytosolic enzyme is responsible for the catalysis of the rate-determining step of tryptophan-kynurenine metabolism, a major biochemical pathway in T-lymphocyte immune tolerance and immunosuppression. Further suppression of the immune system is mediated by transforming growth factor-beta (TGF-β), prostaglandins, as well as interleukin-10, which drives signal transducer and activator of transcription-3 expression in GBM cells.[39-42] The direct interplay between GBM and immune cells drives further immunosuppression by reducing the activity of natural killer cells, mediated by immunoregulatory molecules human leukocyte antigen (HLA)-A and HLA-G.[43-45]

Although the driving mechanisms of immunosuppression by GBM cells remain largely unknown, the most frequent mediators of such systemic and local immune escape appear to revolve around myeloid cells. In particular, CD45+/CD11b+ myeloid cells are the principal inflammatory cells responsible for the infiltration of GBM cells.[46] Hence, molecular strategies aimed at exploiting myeloid cells to induce an antitumor immune response and lower the biochemical dominance of immunosuppressive ligands present a promising approach in immunotherapies for glioblastoma. For instance, delivery of adjuvants such as toll-like receptor agonists and granulocyte-macrophage colony-stimulating factor and neutralization of TGF-β activity through myeloid cells has shown promise in counteracting the immunosuppressive effects of GBM.[47]

5.2. Immune checkpoint inhibitors (ICIs)

Out of all the contemporary advances in immunotherapy over the past decade, ICIs have substantially altered our conception of immunotherapy for various cancers in which conventional therapies have failed. ICIs induce an antineoplastic immune response by suppressing co-inhibitory receptors, ligands, and mechanistic pathways activated by GBM cells to deactivate the T-lymphocyte response against the tumor cells.[48-50] More importantly, the administration of ICIs, although not entirely deprived of treatment-related cytotoxicity, has prompted long-lasting and systemic remissions over several years.[51,52] For instance, inhibitors for immune checkpoints such as anti-PD-1/PD-L1 ICIs and anti-cytotoxic T-lymphocyte-associated antigen 4 (CTLA-4) have proven to be highly efficacious in the treatment of non-small-cell lung cancer (NSCLC) and advanced metastatic melanoma.[53-55]

FDA's approval of checkpoint inhibitors pembrolizumab and nivolumab in late 2014 for metastatic melanoma and the subsequent approval of nivolumab in 2015 for NSCLC initiated a cascade of growing literature into the potential therapeutics of checkpoint inhibitors for the treatment of GBMs.[56,57] A fundamental signature in prolonged immunosuppression of GBMs is the upregulation of PD-L1 on monocytes and tumor cells, which leads to the further inhibition of CD4+ and CD8+ T-lymphocytes.[58] Sustained T-cell activation, an essential characteristic of chronic inflammation in cancer, further upregulates PD-L1, leading to the recognition of PD-L1 on antigen-presenting cells and GBM tumor cells. This combined mechanistic pathway leads to exhaustion, lowered T-lymphocyte proliferation, and decreased survival.[59,60] Hence, the therapeutic target of ICI is to restore T-lymphocyte activation and proliferation of antitumor activity through the blockade of PD-L1 and CTLA-4 immune checkpoints.[61-63]

5.3. Vaccine therapy

Vaccine therapy is another area of promising immunotherapeutics in the treatment of GBMs. Predicated on the observation that GBM cells do not metastasize outside the brain, vaccine therapies aim to induce a strong antitumor immunogenic response by activating the adaptive immune system.[64,65] Vaccines, as "active" interventions, aim to precipitate a robust response from the patient's immune system and can either be cell-based, such as pulsing dendritic cells (DCs), or non-cell-based such as heat shock protein (HSP)-based vaccines. DC-based vaccines rely on the pulsation of glioblastoma antigens onto patient-derived DCs, allowing for the presentation of multiple antigens. DC-based vaccines offer a promising therapeutic approach, given that GBM tumor cells display substantial intra-tumoral heterogeneity.[66-68]

As intracellular chaperones, HSPs aid protein localization, folding, and stability. In commonly observed tumor microenvironments of GBM, hypoxia, hypothermia, inflammation, and substantial oxidative load lead to the activation of HSP. Hence, neoplastic cells rely on HSP for survival.[69] There is also evidence of transcriptional upregulation of HSPs during cancer, as observed in the increased translation of abnormal protein products.[70] In the context of GBM, HSP70 and HSP90 serve as critical molecular chaperones in the initiation and proliferation of tumor signaling pathways. Furthermore, HSP70 and HSP90 bind and display tumor-specific antigens. Hence, the therapeutic strategy of HSP vaccines relies on their

potential to express GBM tumor-specific antigens and to mediate an eventual antitumor immune response.[71,72]

Two other forms of vaccine that have demonstrated moderate efficacy in numerous clinical trials are autologous and peptide vaccines. Autologous vaccination involves the use of a patient's peripheral blood mononuclear cells (PBMC) to stimulate the cells with known glioma tumor antigens, and the subsequent infusion of the primed PBMC cells back into the patient.[73] Peptide vaccines are short protein sequences with active immunogenic mutations present in GBM introduced to patients to evoke an antitumor immune response against the neoplastic cells that shelter the known mutation.[74] For instance, EGFR variant III (EGFRvIII) is a known antigenic variant widely expressed in GBM and absent in normal tissue.[74] Moreover, EGFRvIII mutation also encodes an active tyrosine kinase known to amplify tumor growth and migration[75-77] and instigate tumor resistance against radiation and conventional chemotherapeutic agents.[16] Furthermore, expression levels of EGFRvIII mutation have served as an independent negative prognostic criterion of overall survival in GBM patients. Hence, multiple lines of evidence corroborate the EGFRvIII mutation sequence as a highly promising target for GBM peptide vaccine immunotherapy.[74,78] Summary of emerging vaccination therapy for glioblastoma is summarized in Table 2.

6. GBM drug delivery and medicinal chemistry: challenges and advances

6.1. Challenges

Despite decades of substantial progress in pharmacokinetics, medicinal chemistry, and nanomedicine, drug delivery in GBM remains a fundamental challenge for several reasons. A principal challenge is that of the BBB. Despite being a highly adaptive and neuroprotective property, the highly selective permeability of the tight junctions and endothelial cells forming the external lining of the CNS, preserved by astrocytes and pericytes, prevents the entry of drugs into the brain. Furthermore, the ample presence of P-glycoprotein and multidrug resistance proteins in the BBB anatomical structure prevents the build-up of the necessary amount of pharmacokinetically active drug in the CNS, preventing the activation of the drug's physiological cascade.[79,80]

Another major challenge in the drug delivery of GBMs is the lack of breadth the drugs carry to counteract the highly diffusive and infiltrative tumor cells that migrate far past the point of origin. Existing therapeutic drugs can only reach a few millimeters of the delivery site of interest surrounding the brain parenchyma. Furthermore, lack of diffusion during drug delivery can cause substantial local cytotoxicity at the delivery site.[81,82]

The third challenge arises from the intrinsic nature of GBM tumor cells: highly heterogeneous genome, with unpredictable patterns of amplification, dysregulation, and mutational activation of growth factor signaling; *receptor tyrosine kinase* genes; tumor suppressor genes; O6-methylguanine-DNA methyltransferase methylation; and various other molecular pathways of interconnected and interdependent influence that require patient-specific stratification to advance our understanding of pharmacokinetics in GBMs.[83-85] Drug delivery is further challenged by GBM's highly indistinct tumor margins, highly angiogenic properties that enhance vascular proliferation and hyperplasia, and rapidly adaptive and evasive interaction of the tumor with its surrounding microenvironment, such as overexpression of VEGF, acting as a hypoxia-induced promoter of tumor cell invasion and migration into healthy parenchyma.[86-88]

Table 2. Summary of emerging vaccination therapy for glioblastoma

Vaccine modality	Mechanism of action
Dendritic cell-based vaccines	Employing patient-derived dendritic cells pulsed with glioblastoma-specific antigens to prime CD8+ T-cell responses. This approach capitalizes on the innate ability of dendritic cells to present tumor antigens and stimulate a robust cytotoxic T-lymphocyte response against heterogeneous tumor cells. An example is the ICT-107 vaccine that targets antigens such as WT1, MAGE-1, and HER2.
Heat shock protein (HSP)-based vaccines	Leveraging HSP70 and HSP90 as molecular chaperones that bind and display tumor-specific antigens. These chaperones activate antigen-presenting cells, inducing a cytotoxic immune response. HSP vaccines exploit the reliance of tumor cells on HSPs for survival and metastasis in hypoxic microenvironments.
Autologous tumor-derived vaccines	Deriving patient-specific tumor lysates to pulse antigen-presenting cells or peripheral blood mononuclear cells, thereby creating a personalized vaccine that reflects the specific antigenic landscape of the patient's tumor. This approach directly addresses the challenge of intratumoral heterogeneity. An example is the HSPPC-96 derived from patient tumor lysates, demonstrating promise in clinical trials.
Peptide vaccines	Targeting neoantigens or mutated epitopes, such as EGFRvIII, to induce a focused immune response. These vaccines are designed to overcome tumor immune evasion mechanisms by presenting peptides highly specific to glioblastoma cells, thereby sparing normal tissues. An example is rindopepimut, an EGFRvIII-specific peptide vaccine.

In summary, the core challenge in drug discovery and therapeutic intervention for GBMs can be regarded as a paradox: physiological processes and anatomical structures that are highly adaptive and neuroprotective in a healthy brain microenvironment are transformed into the most vital source of supply and nourishment for the tumor cells, enhancing their survival and further perpetuating their aggressive and infiltrative nature.

6.2. Advances

Despite significant challenges to the effective drug delivery in GBM, there are substantial ongoing preclinical and clinical explorations into the therapeutic potential of SMIs, dual- and multi-targeting kinase inhibitors, EGFR, and fibroblast growth factor receptor inhibitors.[89] Historically, advances in the development of SMIs for treating GBM were limited by their low permeability across the BBB, despite their high selectivity and efficacy. However, contemporary advances in medicinal chemistry have allowed for the assembly of SMIs with diverse lipophilic structural components that can target small-molecular target mediators responsible for the regulation of known signaling pathways characteristic of GBM tumorigenicity.[90-92] Hence, there is a renewed emphasis on developing anti-GBM SMIs with optimal pharmacokinetic properties that effectively permeate the BBB/blood-brain tumor barrier (BBTB), along with minimal drug resistance and cytotoxicity.

For instance, dacomitinib, an irreversible EGFR TKI frequently used for the treatment of non-small-cell lung carcinoma, has shown substantial efficacy in inhibiting intracranial tumorigenicity, tumor cell proliferation, and increased tumor cell apoptosis in GBM xenografted mice.[93] Lapatinib, a dual- and multi-targeting kinase inhibitor, binds to the ATP pocket of EGFR/HER2 and prevents tyrosine kinase phosphorylation, leading to the inhibition of GBM cell growth signaling pathways: mitogen-activated protein kinase (MAPK) and phosphatidylinositol 3-kinase/protein kinase B (PI3K/AKT). Moreover, the inhibition of MAPK and PI3K/AKT, the major growth signaling pathways overexpressed in GBM cells, directly leads to the inhibition of GBM tumorigenicity and eventual GBM cell death.[94] Despite its efficacy, lapatinib treatment induces cytotoxic and genotoxic effects. To counteract lapatinib-induced cytotoxicity, patients receive a combination therapy of lapatinib and sorafenib: a selective multi-kinase inhibitor known to downregulate expression of myeloid cell leukemia 1, a known driver of lapatinib resistance.[94-96] The combination therapy stated above is of profound significance in the therapeutic potential of SMIs as anti-GBM drugs due to their high permeability across the BBB, substantial efficacy and selectivity, and low cellular and genetic toxicity.

An indispensable feature of effective SMI as an anti-GBM drug is the ability to permeate both the BBB and BBTB. The SMIs must have sufficient lipophilic properties in order for them to pass through the BBB/BBTB. Hence, the

Table 3. A detailed summary of small-molecule inhibitors in glioblastoma therapy

SMI	Mechanism of action
Dacomitinib	Dacomitinib is a second-generation, irreversible EGFR tyrosine kinase inhibitor. By covalently binding to the ATP-binding site of EGFR, dacomitinib inhibits downstream proliferative signaling, including MAPK and PI3K/AKT pathways, inducing tumor cell apoptosis. Preclinical studies have shown efficacy in crossing the BBB and targeting EGFR-mutant glioblastoma models.
Lapatinib	Lapatinib is a dual EGFR/HER2 tyrosine kinase inhibitor that binds to the ATP pocket of both receptors, thereby halting downstream oncogenic signaling. Lapatinib also modulates the PI3K/AKT and MAPK pathways, critical for glioblastoma cell proliferation and survival. Its combination with sorafenib has shown promise in overcoming resistance mediated by Mcl-1.
FGFR and multitarget inhibitors	Novel SMIs such as pemigatinib (FGFR inhibitor) and multitarget kinase inhibitors inhibit critical growth and survival pathways in GBM cells. These agents hold promise due to their ability to simultaneously target multiple oncogenic pathways, thereby reducing the risk of therapeutic resistance.
Sorafenib	Sorafenib is a multikinase inhibitor targeting VEGFR, PDGFR, and RAF kinases. It has been used in combination with other TKIs to counteract resistance mechanisms and inhibit angiogenesis, a hallmark of GBM progression. Sorafenib's ability to modulate both tumor cell proliferation and the tumor microenvironment underscores its potential as a dual-action therapy.
Nitrogen-enriched SMIs	Alkylamine-based SMIs, including piperazine and morpholine derivatives, exhibit enhanced BBB permeability due to their lipophilic properties. By modulating the oil-water partition coefficient, these compounds improve central nervous system bioavailability and selectively inhibit signaling pathways implicated in GBM progression.

Abbreviations: BBB: Blood-brain barrier; EGFR: Epidermal growth factor receptor; FGFR: Fibroblast growth factor receptor; GBM: Glioblastoma multiforme; HER2: Human epidermal growth factor receptor 2; MAPK: Mitogen-activated protein kinase; Mcl-1: Myeloid cell leukemia 1; PDGFR: Platelet-derived growth factor receptor; PI3K/AKT: Phosphatidylinositol 3-kinase/protein kinase B; RAF: Rapidly accelerated fibrosarcoma; SMIs: Small-molecule inhibitors; TKIs: Tyrosine kinase inhibitors; VEGFR: Vascular endothelial growth factor receptor.

drug must contain conjugated rings of varying saturation and aromaticity conducive to permeation across the GBM tumor microenvironment. An analysis of the American Chemical Society's recent review on all anti-GBM SMIs in active clinical trials reveals that nitrogen, particularly the oxygenated trialkylamine nitrogen, is a vital driver of active drug candidates with the potential for effective anti-GBM therapy.[89,97] The prominent role of alkylamines such as morpholine, piperazine, and dimethylamine as oxidative metabolites partly mediates this response. However, there is also increasing attention placed on the potential role of trialkylamines as elevators of the oil-water partition coefficient of SMIs, leading to enhanced antitumor activity.[98,99] Therefore, an effective strategy to uncover the therapeutics of novel SMIs as potential anti-GBM drugs is to examine the overlapping biochemical structures of pre-existing SMIs that have yielded pharmacokinetic efficacy in prior trials. A detailed summary of SMIs in glioblastoma therapy is shown in Table 3.

7. Conclusion

Although GBM remains an incurable condition, the future of neuro-oncology appears promising. Over the past decade, our understanding of angiogenesis, nanomedicine, medicinal chemistry, and immunotherapy has already led to an accumulation of highly effective therapeutic strategies for cancers that were previously deemed incurable. Undeniably, the GBM tumor microenvironment remains an immunologically distinct avenue, blocked by the BBB/BBTB and further complicated by a highly heterogeneous tumor genome. Nevertheless, current literature points to a promising, new treatment direction, which is contingent on the body's immunogenic responses and the delivery of novel drugs that demonstrate high safety profile, selective pharmacokinetics and low cytotoxicity. In particular, checkpoint inhibitors, immunotherapeutic vaccines, and SMIs provide a therapeutic potential that can allow for patient-specific treatment stratification, unlike conventional therapies such as TMZ and radiotherapy. Immunotherapeutic vaccines, ICIs, and SMIs offer highly personalized, precision-based molecular strategies that can counteract the highly heterogeneous GBM genome. Future studies must focus on delving into patient-specific immunotherapies and pharmacologically selective SMIs that can penetrate and survive the harsh microenvironment of GBM tumor cells.

Acknowledgments

None.

Funding

None.

Conflict of interest

The authors declare that they have no competing interest.

Author contributions

Conceptualization: Matthew A. Abikenari, Daniel M. Fountain, Maria Isabel Leite

Writing–original draft: Matthew A. Abikenari, Iman Enayati, Daniel M. Fountain

Writing–review & editing: Matthew A. Abikenari, Iman Enayati, Daniel M. Fountain

Ethics approval and consent to participate

Not applicable.

Consent for publication

Not applicable.

Availability of data

Not applicable.

References

1. Omuro A. Glioblastoma and other malignant gliomas: A clinical review. *JAMA*. 2013;310(17):1842.

   doi: 10.1001/jama.2013.280319

2. Thakkar JP, Dolecek TA, Horbinski C, *et al*. Epidemiologic and molecular prognostic review of glioblastoma. *Cancer Epidemiol Biomarkers Prev*. 2014;23(10):1985-1996.

   doi: 10.1158/1055-9965.epi-14-0275

3. Tamimi AF, Juweid M. Epidemiology and outcome of glioblastoma. In: *Glioblastoma*. Brisbane, AU: Codon Publications; 2017. p. 143-153.

   doi: 10.15586/codon.glioblastoma.2017.ch8

4. Ostrom QT, Gittleman H, Fulop J, *et al*. CBTRUS statistical report: Primary brain and central nervous system tumors diagnosed in the United States in 2008-2012. *Neuro Oncol*. 2015;17(suppl 4):iv1-iv62.

   doi: 10.1093/neuonc/nov189

5. Koshy M, Villano JL, Dolecek TA, *et al*. Improved survival time trends for glioblastoma using the seer 17 population-based registries. *J Neurooncol*. 2011;107(1):207-212.

   doi: 10.1007/s11060-011-0738-7

6. Malmström A, Grønberg BH, Marosi C, *et al*. Temozolomide versus standard 6-week radiotherapy versus hypofractionated radiotherapy in patients older than 60 years with glioblastoma: The nordic randomised, phase 3 trial. *Lancet Oncol*. 2012;13(9):916-926.

   doi: 10.1016/s1470-2045(12)70265-6

7. Zhang H, Wang R, Yu Y, Liu J, Luo T, Fan F. Glioblastoma

treatment modalities besides surgery. *J Cancer*. 2019;10(20):4793-4806.

doi: 10.7150/jca.32475

8. Louis DN, Perry A, Reifenberger G, *et al*. The 2016 World Health Organization classification of tumors of the central nervous system: A summary. *Acta Neuropathol*. 2016;131(6):803-820.

doi: 10.1007/s00401-016-1545-1

9. Ohgaki H, Kleihues P. The definition of primary and secondary glioblastoma. *Clin Cancer Res*. 2013;19(4):764-772.

doi: 10.1158/1078-0432.ccr-12-3002

10. Kleihues P, Ohgaki H. Primary and secondary glioblastomas: From concept to clinical diagnosis. *Neuro Oncol*. 1999;1(1):44-51.

doi: 10.1093/neuonc/1.1.44

11. Nobusawa S, Watanabe T, Kleihues P, Ohgaki H. IDH1 mutations as molecular signature and predictive factor of secondary glioblastomas. *Clin Cancer Res*. 2009;15(19): 6002-6007.

doi: 10.1158/1078-0432.ccr-09-0715

12. Amankulor NM, Kim Y, Arora S, *et al*. Mutant IDH1 regulates the tumor-associated immune system in gliomas. *Genes Dev*. 2017;31(8):774-786.

doi: 10.1101/gad.294991.116

13. Waitkus MS, Yan H. Targeting isocitrate dehydrogenase mutations in cancer: Emerging evidence and diverging strategies. *Clin Cancer Res*. 2021;27(2):383-388.

doi: 10.1158/1078-0432.ccr-20-1827

14. Nakada M, Kita D, Watanabe T, *et al*. Aberrant signaling pathways in glioma. *Cancers* (*Basel*). 2011;3(3):3242-3278.

doi: 10.3390/cancers3033242

15. McLendon R, Friedman A, Bigner D. Comprehensive genomic characterization defines human glioblastoma genes and core pathways. *Nature*. 2008;455(7216):1061-1068.

doi: 10.1038/nature07385

16. Nagane M. Neuro-oncology: Continuing multidisciplinary progress. *Lancet Neurol*. 2011;10(1):18-20.

doi: 10.1016/s1474-4422(10)70302-1

17. Stupp R, Weller M. 2010: Neuro-oncology is moving! *Curr Opin Neurol*. 2010;23(6):553-555.

doi: 10.1097/wco.0b013e3283407eed

18. Van Meir EG, Hadjipanayis CG, Norden AD, Shu HK, Wen PY, Olson JJ. Exciting new advances in neuro-oncology: The avenue to a cure for malignant glioma. *CA Cancer J Clin*. 2010;60(3):166-193.

doi: 10.3322/caac.20069

19. Brandao M, Simon T, Critchley G, Giamas G. Astrocytes, the rising stars of the glioblastoma microenvironment. *Glia*. 2018;67(5):779-790.

doi: 10.1002/glia.23520

20. Furnari FB, Fenton T, Bachoo RM, *et al*. Malignant astrocytic glioma: Genetics, biology, and paths to treatment. *Genes Dev*. 2007;21(21):2683-2710.

doi: 10.1101/gad.1596707

21. Farin A, Suzuki SO, Weiker M, Goldman JE, Bruce JN, Canoll P. Transplanted glioma cells migrate and proliferate on host brain vasculature: A dynamic analysis. *Glia*. 2006;53(8):799-808.

doi: 10.1002/glia.20334

22. De Gooijer MC, Guillén Navarro M, Bernards R, Wurdinger T, van Tellingen O. An experimenter's guide to glioblastoma invasion pathways. *Trends Mol Med*. 2018;24(9):763-780.

doi: 10.1016/j.molmed.2018.07.003

23. Coniglio SJ, Eugenin E, Dobrenis K, *et al*. Microglial stimulation of glioblastoma invasion involves epidermal growth factor receptor (EGFR) and colony stimulating factor 1 receptor (CSF-1R) signaling. *Mol Med*. 2012;18(3):519-527.

doi: 10.2119/molmed.2011.00217

24. Xie Q, Mittal S, Berens ME. Targeting adaptive glioblastoma: An overview of proliferation and invasion. *Neuro Oncol*. 2014;16(12):1575-1584.

doi: 10.1093/neuonc/nou147

25. Mrugala MM. Advances and challenges in the treatment of glioblastoma: A clinician's perspective. *Discov Med*. 2013;15(83):221-230.

26. Ohka F, Natsume A, Wakabayashi T. Current trends in targeted therapies for glioblastoma multiforme. *Neurol Res Int*. 2012;2012:878425.

doi: 10.1155/2012/878425

27. Scott J, Tsai YY, Chinnaiyan P, Yu HHM. Effectiveness of radiotherapy for elderly patients with glioblastoma. *Int J Radiat Oncol Biol Phys*. 2011;81(1):206-210.

doi: 10.1016/j.ijrobp.2010.04.033

28. Nabors LB, Portnow J, Ammirati M, *et al*. Central nervous system cancers, version 1.2015. *J Natl Compr Canc Netw*. 2015;13(10):1191-1202.

doi: 10.6004/jnccn.2015.0148

29. Bronte G, Rolfo C, Giovannetti E, *et al*. Are erlotinib and gefitinib interchangeable, opposite or complementary for non-small cell lung cancer treatment? Biological, pharmacological and clinical aspects. *Crit Rev Oncol Hematol*. 2014;89(2):300-313.

doi: 10.1016/j.critrevonc.2013.08.003

30. Iacob G, Dinca EB. Current data and strategy in glioblastoma

multiforme. *J Med Life*. 2009;2(4):386-393.

31. Fabian D, Guillermo Prieto Eibl MP, Alnahhas I, *et al*. Treatment of glioblastoma (GBM) with the addition of tumor-treating fields (TTF): A review. *Cancers* (*Basel*). 2019;11(2):174.

doi: 10.3390/cancers11020174

32. Stupp R, Taillibert S, Kanner AA, *et al*. Maintenance therapy with tumor-treating fields plus temozolomide vs temozolomide alone for glioblastoma: A randomized clinical trial. *JAMA*. 2015;314(23):2535.

doi: 10.1001/jama.2015.16669

33. Canessa A, Del Bono V, Miletich F, Pistoia V. Serum cytokines in toxoplasmosis: Increased levels of interferon-gamma in immunocompetent patients with lymphadenopathy but not in AIDS patients with encephalitis. *J Infect Dis*. 1992;165(6):1168-1170.

doi: 10.1093/infdis/165.6.1168

34. Waksman BH, Adams RD. Allergic neuritis: An experimental disease of rabbits induced by the injection of peripheral nervous tissue and adjuvants. *J Exp Med*. 1955;102(2):213-236.

doi: 10.1084/jem.102.2.213

35. Louveau A, Smirnov I, Keyes TJ, *et al*. Structural and functional features of central nervous system lymphatic vessels. *Nature*. 2015;523(7560):337-341.

doi: 10.1038/nature14432

36. Chae M, Peterson TE, Balgeman A, *et al*. Increasing glioma-associated monocytes leads to increased intratumoral and systemic myeloid-derived suppressor cells in a murine model. *Neuro Oncol*. 2014;17(7):978-991.

doi: 10.1093/neuonc/nou343

37. Nduom EK, Weller M, Heimberger AB. Immunosuppressive mechanisms in glioblastoma. *Neuro Oncol*. 2015;17(suppl 7): vii9-vii14.

doi: 10.1093/neuonc/nov151

38. Roszman T, Elliott L, Brooks W. Modulation of T-cell function by gliomas. *Immunol Today*. 1991;12(10):370-374.

doi: 10.1016/0167-5699(91)90068-5

39. Bodmer S, Strommer K, Frei K, *et al*. Immunosuppression and transforming growth factor-beta in glioblastoma. Preferential production of transforming growth factor-beta 2. *J Immunol*. 1989;143(10):3222-3229.

40. Huettner C, Czub S, Kerkau S, Roggendorf W, Tonn JC. Interleukin 10 is expressed in human gliomas *in vivo* and increases glioma cell proliferation and motility *in vitro*. *Anticancer Res*. 1997;17(5A):3217-3224.

41. Huettner C, Paulus W, Roggendorf W. Messenger RNA expression of the immunosuppressive cytokine IL-10 in human gliomas. *Am J Pathol*. 1995;146(2):317-322.

42. Jackson CM, Kochel CM, Nirschl CJ, *et al*. Systemic tolerance mediated by melanoma brain tumors is reversible by radiotherapy and vaccination. *Clin Cancer Res*. 2016;22(5):1161-1172.

doi: 10.1158/1078-0432.ccr-15-1516

43. Lauro GM, Di Lorenzo N, Grossi M, Maleci A, Guidetti B. Prostaglandin E2 as an immunomodulating factor released in vitro by human glioma cells. *Acta Neuropathol*. 1986;69(3-4): 278-282.

doi: 10.1007/bf00688305

44. Wiendl H, Mitsdoerffer M, Hofmeister V, *et al*. A functional role of HLA-G expression in human gliomas: An alternative strategy of immune escape. *J Immunol*. 2002;168(9):4772-4780.

doi: 10.4049/jimmunol.168.9.4772

45. Wischhusen J, Friese MA, Mittelbronn M, Meyermann R, Weller M. HLA-E protects glioma cells from NKG2D-mediated immune responses *in vitro*: Implications for immune escape *in vivo*. *J Neuropathol Exp Neurol*. 2005;64(6):523-528.

doi: 10.1093/jnen/64.6.523

46. Parney IF, Waldron JS, Parsa AT. Flow cytometry and *in vitro* analysis of human glioma-associated macrophages. Laboratory investigation. *J Neurosurg*. 2009;110(3):572-582.

doi: 10.3171/2008.7.jns08475

47. Preusser M, Lim M, Hafler DA, Reardon DA, Sampson JH. Prospects of immune checkpoint modulators in the treatment of glioblastoma. *Nat Rev Neurol*. 2015;11(9):504-514.

doi: 10.1038/nrneurol.2015.139

48. Hodi FS, O'Day SJ, McDermott DF, *et al*. Improved survival with ipilimumab in patients with metastatic melanoma. [published correction appears in *N Engl J Med*. 2010;363(13):1290]. *N Engl J Med*. 2010;363(8):711-723.

doi: 10.1056/NEJMoa1003466

49. O'Day SJ, Maio M, Chiarion-Sileni V, *et al*. Efficacy and safety of ipilimumab monotherapy in patients with pretreated advanced melanoma: A multicenter single-arm phase II study. *Ann Oncol*. 2010;21(8):1712-1717.

doi: 10.1093/annonc/mdq013

50. Topalian SL, Hodi FS, Brahmer JR, *et al*. Safety, activity, and immune correlates of anti-PD-1 antibody in cancer. *N Engl J Med*. 2012;366(26):2443-2454.

doi: 10.1056/NEJMoa1200690

51. Motzer RJ, Rini BI, McDermott DF, *et al*. Nivolumab for metastatic renal cell carcinoma: Results of a randomized phase II trial. *J Clin Oncol*. 2015;33(13):1430-1437.

doi: 10.1200/jco.2014.59.0703

52. Rizvi NA, Mazières J, Planchard D, *et al*. Activity and safety of nivolumab, an anti-PD-1 immune checkpoint inhibitor,

for patients with advanced, refractory squamous non-small-cell lung cancer (checkmate 063): A phase 2, single-arm trial. *Lancet Oncol*. 2015;16(3):257-265.

doi: 10.1016/s1470-2045(15)70054-9

53. Hellmann MD, Paz-Ares L, Bernabe Caro R, *et al*. Nivolumab plus Ipilimumab in advanced non-small-cell lung cancer. *N Engl J Med*. 2019;381(21):2020-2031.

doi: 10.1056/NEJMoa1910231

54. Larkin J, Chiarion-Sileni V, Gonzalez R, *et al*. Five-year survival with combined nivolumab and Ipilimumab in advanced melanoma. *New Engl J Med*. 2019;381(16):1535-1546.

doi: 10.1056/nejmoa1910836

55. Wolchok JD, Chiarion-Sileni V, Gonzalez R, *et al*. Overall survival with combined nivolumab and Ipilimumab in advanced melanoma. *New Engl J Med*. 2017;377(14): 1345-1356.

doi: 10.1056/nejmoa1709684

56. Omuro A, Reardon DA, Sampson JH, *et al*. Nivolumab plus radiotherapy with or without temozolomide in newly diagnosed glioblastoma: Results from exploratory phase I cohorts of checkmate 143. *Neurooncol Adv*. 2022;4(1):vdac025.

doi: 10.1093/noajnl/vdac025

57. Reardon DA, Kim TM, Frenel J, *et al*. Treatment with pembrolizumab in programmed death ligand 1-positive recurrent glioblastoma: Results from the multicohort phase 1 KEYNOTE-028 trial. *Cancer*. 2021;127(10):1620-1629.

doi: 10.1002/cncr.33378

58. Buchbinder EI, Desai A. CTLA-4 and PD-1 pathways: Similarities, differences, and implications of their inhibition. *Am J Clin Oncol*. 2016;39(1):98-106.

doi: 10.1097/coc.0000000000000239

59. Bloch O, Crane CA, Kaur R, Safaee M, Rutkowski MJ, Parsa AT. Gliomas promote immunosuppression through induction of B7-H1 expression in tumor-associated macrophages. *Clin Cancer Res*. 2013;19(12):3165-3175.

doi: 10.1158/1078-0432.ccr-12-3314

60. Moyes KW, Davis A, Hoglund V, *et al*. Effects of tumor grade and dexamethasone on myeloid cells in patients with glioma. *OncoImmunology*. 2018;7(11):e1507668.

doi: 10.1080/2162402x.2018.1507668

61. Abikenari M, Schonfeld E, Choi J, Kim LH, Lim M. Revisiting glioblastoma classification through an immunological lens: A narrative review. *Glioma*. 2024;7(2):3-9.

doi: 10.4103/glioma.glioma_4_24

62. Berghoff AS, Kiesel B, Widhalm G, *et al*. Programmed death ligand 1 expression and tumor-infiltrating lymphocytes in glioblastoma. *Neuro Oncol*. 2014;17(8):1064-1075.

doi: 10.1093/neuonc/nou307

63. Fecci PE, Mitchell DA, Whitesides JF, *et al*. Increased regulatory T-cell fraction amidst a diminished CD4 compartment explains cellular immune defects in patients with malignant glioma. *Cancer Res*. 2006;66(6):3294-3302.

doi: 10.1158/0008-5472.can-05-3773

64. Ampie L, Woolf EC, Dardis C. Immunotherapeutic advancements for glioblastoma. *Front Oncol*. 2015;5:12.

doi: 10.3389/fonc.2015.00012

65. Weller M, Kaulich K, Hentschel B, *et al*. Assessment and prognostic significance of the epidermal growth factor receptor vIII mutation in glioblastoma patients treated with concurrent and adjuvant temozolomide radiochemotherapy. [published correction appears in *Int J Cancer*. 2016 Aug 15;139(4):E9. doi: 10.1002/ijc.30155]. *Int J Cancer*. 2014;134(10):2437-2447.

doi: 10.1002/ijc.28576

66. Powers MV, Jones K, Barillari C, Westwood I, van Montfort RL, Workman P. Targeting HSP70: The second potentially druggable heat shock protein and molecular chaperone? *Cell Cycle*. 2010;9(8):1542-1550.

doi: 10.4161/cc.9.8.11204

67. Smaglo BG, Aldeghaither D, Weiner LM. The development of immunoconjugates for targeted cancer therapy. *Nat Rev Clin Oncol*. 2014;11(11):637-648.

doi: 10.1038/nrclinonc.2014.159

68. Young JC, Agashe VR, Siegers K, Hartl FU. Pathways of chaperone-mediated protein folding in the cytosol. *Nat Rev Mol Cell Biol*. 2004;5(10):781-791.

doi: 10.1038/nrm1492

69. Ampie L, Choy W, Lamano JB, Fakurnejad S, Bloch O, Parsa AT. Heat shock protein vaccines against glioblastoma: From bench to bedside. *J Neuro Oncol*. 2015;123(3):441-448.

doi: 10.1007/s11060-015-1837-7

70. Graner MW, Bigner DD. Chaperone proteins and brain tumors: Potential targets and possible therapeutics. *Neuro Oncol*. 2005;7(3):260-278.

doi: 10.1215/S1152851704001188

71. Srivastava PK, DeLeo AB, Old LJ. Tumor rejection antigens of chemically induced sarcomas of inbred mice. *Proc Natl Acad Sci U S A*. 1986;83(10):3407-3411.

doi: 10.1073/pnas.83.10.3407

72. Ullrich SJ, Robinson EA, Law LW, Willingham M, Appella E. A mouse tumor-specific transplantation antigen is a heat shock-related protein. *Proc Natl Acad Sci U S A*. 1986;83(10):3121-3125.

doi: 10.1073/pnas.83.10.3121

73. Schirrmacher V, Haas C, Bonifer R, Ahlert T, Gerhards R,

Ertel C. Human tumor cell modification by virus infection: An efficient and safe way to produce cancer vaccine with pleiotropic immune stimulatory properties when using Newcastle disease virus. *Gene Ther*. 1999;6(1):63-73.

doi: 10.1038/sj.gt.3300787

74. Sampson JH, Heimberger AB, Archer GE, *et al*. Immunologic escape after prolonged progression-free survival with epidermal growth factor receptor variant III peptide vaccination in patients with newly diagnosed glioblastoma. *J Clin Oncol*. 2010;28(31):4722-4729.

doi: 10.1200/JCO.2010.28.6963

75. Batra SK, Castelino-Prabhu S, Wikstrand CJ, *et al*. Epidermal growth factor ligand-independent, unregulated, cell-transforming potential of a naturally occurring human mutant EGFRvIII gene. *Cell Growth Differ*. 1995;6(10):1251-1259.

76. Boockvar JA, Kapitonov D, Kapoor G, *et al*. Constitutive EGFR signaling confers a motile phenotype to neural stem cells. *Mol Cell Neurosci*. 2003;24(4):1116-1130.

doi: 10.1016/j.mcn.2003.09.011

77. Chu CT, Everiss KD, Wikstrand CJ, Batra SK, Kung HJ, Bigner DD. Receptor dimerization is not a factor in the signalling activity of a transforming variant epidermal growth factor receptor (EGFRvIII). *Biochem J*. 1997;324(Pt 3): 855-861.

doi: 10.1042/bj3240855

78. Heimberger AB, Hlatky R, Suki D, *et al*. Prognostic effect of epidermal growth factor receptor and EGFRvIII in glioblastoma multiforme patients. *Clin Cancer Res*. 2005;11(4):1462-1466.

doi: 10.1158/1078-0432.CCR-04-1737

79. Hottinger AF, Stupp R, Homicsko K. Standards of care and novel approaches in the management of glioblastoma multiforme. *Chin J Cancer*. 2014;33(1):32-39.

doi: 10.5732/cjc.013.10207

80. Stupp R, Mason WP, van den Bent MJ, *et al*. Radiotherapy plus concomitant and adjuvant temozolomide for glioblastoma. *N Engl J Med*. 2005;352(10):987-996.

doi: 10.1056/NEJMoa043330

81. Giese A, Bjerkvig R, Berens ME, Westphal M. Cost of migration: Invasion of malignant gliomas and implications for treatment. *J Clin Oncol*. 2003;21(8):1624-1636.

doi: 10.1200/JCO.2003.05.063

82. Tzeng SY, Green JJ. Therapeutic nanomedicine for brain cancer. *Ther Deliv*. 2013;4(6):687-704.

doi: 10.4155/tde.13.38

83. Diehn M, Nardini C, Wang DS, *et al*. Identification of noninvasive imaging surrogates for brain tumor gene-expression modules. *Proc Natl Acad Sci U S A*. 2008;105(13):5213-5218.

doi: 10.1073/pnas.0801279105

84. Maher EA, Brennan C, Wen PY, *et al*. Marked genomic differences characterize primary and secondary glioblastoma subtypes and identify two distinct molecular and clinical secondary glioblastoma entities. *Cancer Res*. 2006;66(23):11502-11513.

doi: 10.1158/0008-5472.CAN-06-2072

85. Mischel PS, Nelson SF, Cloughesy TF. Molecular analysis of glioblastoma: Pathway profiling and its implications for patient therapy. *Cancer Biol Ther*. 2003;2(3):242-247.

doi: 10.4161/cbt.2.3.369

86. Dubois LG, Campanati L, Righy C, *et al*. Gliomas and the vascular fragility of the blood brain barrier. *Front Cell Neurosci*. 2014;8:418.

doi: 10.3389/fncel.2014.00418

87. Monteiro AR, Hill R, Pilkington GJ, Madureira PA. The role of hypoxia in glioblastoma invasion. *Cells*. 2017;6(4):45.

doi: 10.3390/cells6040045

88. Urbańska K, Sokołowska J, Szmidt M, Sysa P. Glioblastoma multiforme - an overview. *Contemp Oncol* (*Pozn*). 2014;18(5):307-312.

doi: 10.5114/wo.2014.40559

89. Thakur A, Faujdar C, Sharma R, *et al*. Glioblastoma: Current status, emerging targets, and recent advances. *J Med Chem*. 2022;65(13):8596-8685.

doi: 10.1021/acs.jmedchem.1c01946

90. Arévalo ÁST, Erices JI, Uribe DA, *et al*. Current therapeutic alternatives and new perspectives in glioblastoma multiforme. *Curr Med Chem*. 2017;24(25):2781-2795.

doi: 10.2174/0929867324666170303122241

91. Fernandes GFD, Fernandes BC, Valente V, Dos Santos JL. Recent advances in the discovery of small molecules targeting glioblastoma. *Eur J Med Chem*. 2019;164:8-26.

doi: 10.1016/j.ejmech.2018.12.033

92. Khaddour K, Johanns TM, Ansstas G. The landscape of novel therapeutics and challenges in glioblastoma multiforme: Contemporary state and future directions. *Pharmaceuticals* (*Basel*). 2020;13(11):389.

doi: 10.3390/ph13110389

93. Zahonero C, Aguilera P, Ramírez-Castillejo C, *et al*. Preclinical test of dacomitinib, an irreversible EGFR inhibitor, confirms its effectiveness for glioblastoma. *Mol Cancer Ther*. 2015;14(7):1548-1558.

doi: 10.1158/1535-7163.MCT-14-0736

94. Hamed HA, Tavallai S, Grant S, Poklepovic A, Dent P. Sorafenib/regorafenib and lapatinib interact to kill CNS

tumor cells. *J Cell Physiol*. 2015;230(1):131-139.

doi: 10.1002/jcp.24689

95. Haynik DM, Roma AA, Prayson RA. HER-2/neu expression in glioblastoma multiforme. *Appl Immunohistochem Mol Morphol*. 2007;15(1):56-58.

doi: 10.1097/01.pai.0000213133.09160.da

96. Lankheet NA, Hillebrand MJ, Rosing H, Schellens JH, Beijnen JH, Huitema AD. Method development and validation for the quantification of dasatinib, erlotinib, gefitinib, imatinib, lapatinib, nilotinib, sorafenib and sunitinib in human plasma by liquid chromatography coupled with tandem mass spectrometry. *Biomed Chromatogr*. 2013;27(4):466-476.

doi: 10.1002/bmc.2814

97. Sminia P, Westerman BA. Blood-brain barrier crossing and breakthroughs in glioblastoma therapy. *Br J Clin Pharmacol*. 2016;81(6):1018-1020.

doi: 10.1111/bcp.12881

98. Łazewska D, Wiecek M, Ligneau X, *et al*. Histamine H_3 and H_4 receptor affinity of branched 3-(1H-imidazol-4-yl)propyl N-alkylcarbamates. *Bioorg Med Chem Lett*. 2009;19(23):6682-6685.

doi: 10.1016/j.bmcl.2009.10.005

99. Wang D, Wang C, Wang L, Chen Y. A comprehensive review in improving delivery of small-molecule chemotherapeutic agents overcoming the blood-brain/brain tumor barriers for glioblastoma treatment. *Drug Deliv*. 2019;26(1):551-565.

doi: 10.1080/10717544.2019.1616235

ACCSCIENCE PUBLISHING

Microbes & Immunity

CASE REPORT

Primary cutaneous nocardiosis due to *Nocardia farcinica* in an immunocompetent patient: A case report

Maya Polashenski* and Olga Vasylyeva

Department of Infectious Disease, Rochester General Hospital, 1425 Portland Ave, Rochester, New York, United States of America

Abstract

Nocardia is an opportunistic pathogen that can present as pulmonary, central nervous system, or disseminated infection in immunocompromised host. However, primary cutaneous *Nocardia* infections have distinctive presentations in immunocompetent hosts. When infecting a host with an intact immune system, the infection tends to be more insidious, delaying accurate diagnosis and leading to inadequate treatment and persistent infection. Herein, we present a rare case of post-operative cutaneous nocardiosis in a 57-year-old immunocompetent patient with a delay in therapy resulting in a prolonged non-healing wound. Nineteen case reports were reviewed to identify trends in immune status, exposure, treatment regimens, and responses to therapy in both immunocompromised and immunocompetent patients with *Nocardia farcinica* cutaneous infection. This case report summarizes characteristics of patient populations where *N. farcinica* might be suspected and emphasizes the importance of a thorough environmental and occupational history in the case of immunocompetent patients. It also addresses challenges in the treatment of cutaneous *N. farcinica* as related to empiric therapy, antibiotic resistance, and duration of treatment, ultimately providing an algorithm to approach the management of primary cutaneous nocardiosis.

Keywords: Postoperative infection; Actinomycete; Nocardiosis; *Nocardia farcinica*; Primary cutaneous nocardiosis

***Corresponding author:**
Maya Polashenski
(maya.polashenski@rochesterregional.org)

Citation: Polashenski M, Vasylyeva O. Primary cutaneous nocardiosis due to Nocardia farcinica in an immunocompetent patient: A case report. *Microbes & Immunity*. 2025;2(4):144-149. doi: 10.36922/mi.5189

Received: October 17, 2024

Revised: November 30, 2024

Accepted: December 9, 2024

Published online: December 31, 2024

1. Introduction

Nocardia is a genus of bacteria that is an uncommon pathogen. It is better known as an opportunistic pathogen causing infection in lungs, central nervous system (CNS), or disseminated infection in an immunocompromised host. However, primary cutaneous *Nocardia* infections are unique in involving immunocompetent hosts. When infecting a host with an intact immune system, the infection tends to be more insidious, which risks impeding a timely diagnosis, leading to inadequate treatment and persistent infection. *Nocardia* species are able to survive in a host due to their ability to evade innate and cellular immune responses.[1] One way this is achieved is by resisting phagocytosis and even neutralizing destruction through oxidative killing mechanisms, which are accomplished by certain bacterial enzymes.[1] In addition, *Nocardia* species belongs to the optional intracellular organisms, with the ability to evade immune surveillance.[1]

Nocardia farcinica represents approximately 10% of nocardiosis cases.[2] *N. farcinica* is a culprit for primary cutaneous nocardiosis and resistant to several commonly used antibiotics. We present a rare case of post-operative cutaneous nocardiosis with delay in therapy resulting in prolonged non-healing wound. This report aims to emphasize the necessity to execute proper diagnosis, treatment, and monitoring for patients with *N. farcinica* infection limited to the skin/soft tissue.

2. Case presentation

A 57-year-old female with non-healing wound presented to the infectious disease clinic. The patient has a history of insulin-dependent type 2 diabetes with hemoglobin A1c (HbA1c) of 10.8% and tobacco dependence. The patient was diagnosed with trigger finger, suspected to be due to ganglion cysts and Dupuytren's disease for which she underwent elective outpatient cyst removal on the flexor tendon of her left third finger, as well as trigger finger release of the flexor tendon of the left thumb. Following the procedure, she had three surgical wounds, two of which (middle finger of the left arm and left third finger) healed well, but the left thumb wound persisted. She was prescribed two 10-day courses of cephalexin for presumed postoperative infection at 2 and 5 weeks postoperatively. Despite this, the patient presented to the emergency room at post-operative week 5 for pain, swelling and purulent drainage at the base of her left thumb. She was admitted for observation, underwent incision and drainage in the operating room, with operative note describing small amount of purulent drainage, and the wound was loosely closed with two sutures. During the admission, she was afebrile, did not have leukocytosis, but did have mildly elevated sedimentation rate (60 mm/h, reference range 0 – 30 mm/h) and C-reactive protein (1.3 mg/dL, reference range 0.0 – 1.0 mg/dL). She was treated with 6 days of ceftriaxone and discharged with instructions to complete 4 more days of cefuroxime. Gram staining of the purulent fluid revealed few white blood cells and no organisms, and the growth of *N. farcinica* was detected in culture.

Over the next 2 months, the wound persisted to drain, and cultures of drainage sent on post-operative week 9, 10, and 13 all grew *N. farcinica*. The patient underwent another operative debridement during post-operative week 10. In this time frame, she completed an additional 10 days of cefuroxime and two 2-week courses of ciprofloxacin, prescribed by her hand surgeon. She was referred to the infectious disease clinic on post-operative week 15 for a non-healing, painful wound with black eschar and joint swelling in the setting of cutaneous nocardiosis despite multiple short courses of antibiotics and debridement (Figure 1). The source of persistent nocardiosis was hypothesized to

Figure 1. Palmar surface of the patient's left hand

be related to a camping trip shortly after the trigger finger release, as the patient used well water at the campsite to wash her hands. She did not engage in gardening work nor had exposure to soil in other settings. Laboratory data, imaging findings, past medical history, and medication list were reviewed for signs of immunodeficiency. She had a normal complete blood count and differential, normal kidney and liver function, and elevated blood sugar with high HbA1c of 10.8%. Her medication list included: Insulin lispro correctional scale with meals, lisinopril 20 mg daily, gabapentin 600 mg 3 times daily as needed, venlafaxine 75 mg daily, pantoprazole 40 mg daily, and zolpidem 10 mg at bedtime. She was prescribed extended antibiotic therapy with trimethoprim-sulfamethoxazole (TMP-SMX) twice daily based on susceptibilities in Table 1. The duration of treatment was up to 3 – 6 months, depending on the response to therapy. Unfortunately, she did not follow up in the infectious disease clinic after the initial appointment; however, there is documentation from a routine endocrinologist visit 4 months later indicating no wounds were seen on examination.

3. Discussion

Nocardia is a Gram-positive, catalase-positive, weakly acid-fast, aerobic actinomycete notable for its branching filamentous form.[3] It is an environmental pathogen, most frequently found in soil, but also in fresh and salt water. There are many species of *Nocardia* that are clinically relevant. Nocardiosis manifests in different organ systems depending on the subspecies and host. Lung involvement is the most common and usually occurs in immunocompromised patients as a result of *Nocardia asteroides* infection. Also common among immunocompromised patients is CNS involvement or dissemination of disease to multiple organs, often from a

Table 1. Isolate's antimicrobial susceptibility

	AM K	AM C	CRO	CIP	DOX	LZD	MIN	MFX	TOB	TMP- SMX
MIC (μg/mL)	1 (S)	16 (I)	64 (R)	0.25 (S)	4 (I)	2 (S)	4 (I)	0.06 (S)	64 (R)	1 (S)

Note: These results are derived from post-operative week 12.
Abbreviations: MIC: Minimum inhibitory concentration; AMC: Amoxicillin- clavulanate; AMK: Amikacin; CIP: Ciprofloxacin; CRO: Ceftriaxone; DOX: Doxycycline; I: Intermediate; LZD: Linezolid; MFX: Moxifloxacin; MIN: Minocycline; R: Resistant; S: Susceptible; TOB: Tobramycin; TMP-SMX: Trimethoprim/sulfamethoxazole.

pulmonary source.[1] Alternatively, patients can have direct exposure by inoculation from the environment, which is most likely caused by *N. farcinica.* First described in 1888 by Edward Nocard in his discovery of bovine farcy, this pathogen was initially named *Streptothrix farcinica.* One year later, it was re-characterized by Trevisan who named it "*Nocardia farcinica*."[1]

Primary cutaneous nocardiosis due to *N. farcinica* in particular is known for preferentially infecting immunocompetent individuals. The presentation differs between immunocompromised and immunocompetent patients. The criteria to be considered immunocompromised for the purpose of this discussion includes primary immunodeficiency, untreated or advanced HIV, active malignancy receiving chemotherapy, status post-solid organ transplant (SOT), or hematopoietic stem cell transplant (HCT) with concurrent immunosuppressive medications, chronic use of corticosteroids, and treatment with immunomodulating therapy such as biologics.[4] Immunocompromised patients have greater morbidity and mortality with *Nocardia* infections due to higher rates of dissemination. In a retrospective chart review, *Nocardia* infection-related mortality was 71% and 32% in HCT and SOT patients, respectively.[5] The article did not specify which of these patients were infected with *N. farcinica* over other subspecies of *Nocardia*, but *N. farcinica* was listed as one of the top three isolated subspecies. *N. farcinica* has been isolated in brain abscess pathology, which is also more common in immunocompromised patients.[1] *Nocardia* brain abscesses are considered the most severe form of dissemination and mortality rates among patients with disseminated disease are 20% for immunocompetent patients and 55% for immunocompromised patients.[1] Immunocompetent patients with nocardiosis tend to have indolent courses and the infection is more likely to be limited to the skin.[4] The lesions caused by cutaneous nocardial infection vary and can present as ulcerations, papules, nodules, and abscesses. The spectrum of presentations and indolent course could lead to underdiagnosis in immunocompetent patients, especially if the empiric antibiotics were in the class that *N. farcinica* is susceptible to. Among the 15 case reports reviewed and one retrospective review of transplant patients of cutaneous *N. farcinica*, 19 patients were immunosuppressed (Table 2). It is relatively rare to detect infected individuals with intact immune systems; more details are discussed in Table 3.

All three immunocompetent cases we reviewed had documented culture data about *N. farcinica* growth as well as obvious environmental exposures to this pathogenic organism. The treatment regimens varied based on extent of subcutaneous infection as well as tolerance to the chosen antibiotics, but the gold standard of treatment, TMP-SMX was attempted in each of the cases. There was resolution of infection documented in each case as demonstrated in Table 3. Our case presents a woman with several risk factors, including uncontrolled diabetes, smoking, and recent surgery, who had a persistent abscess growing *N. farcinica*. This patient was not a gardener and denied contact with soil or decomposing organic matter. On detailed history, it was discovered that she went for camping soon after a surgical procedure, she had and washed her hands with well water. This was hypothesized to be an environmental exposure to *N. farcinica.* The proposed treatment was 3 – 6 months of TMP- SMX while evaluating for resolution of the cutaneous lesion. There was consideration of her other risk factors as mentioned above playing a role in delayed wound healing; however, the lack of involvement of post-operative wound healing in two of three cases reviewed in literature argue against that. Nevertheless, more investigations regarding diabetes, smoking, and surgical site infection as risk factors for non- healing wounds implicated in *Nocardia* species-related infections are warranted, as they were not the primary inclusion criteria for immunosuppressed states based on the literature review for this paper.

There are several challenges in treating *N. farcinica*, one of which is choosing the proper antibiotics. Treatment is based on susceptibility of the organism; however, empiric therapy is often required as receiving antimicrobial susceptibility results takes time.[20] Historically, TMP-SMX has been used as monotherapy of choice,[21] but there are no official guidelines in place. Linezolid (LZD) is another option.[3] Treatment depends on whether a patient is immunocompetent or immunocompromised, as well as the location of infection. A review done in 2021 aimed to create a potential algorithm for treatment of nocardiosis based on these criteria.[22] Using this algorithm, an

immunocompetent patient with only skin involvement can be managed with empiric monotherapy (TMP-SMX versus LZD) while awaiting antibiotic susceptibility and then transitioned to the targeted oral regimen based on sensitivities. Based on common susceptibilities, 3 – 6 months of TMP-SMX remains the gold-standard course of treatment. Other options include minocycline or amoxicillin-clavulanate (AMC) depending on sensitivities. As noted in Table 1, there is susceptibility to fluoroquinolones (moxifloxacin and ciprofloxacin) and the patient received two 2-week courses of ciprofloxacin prior to the initiation of TMP-SMX. A literature review from 2017 of *Nocardia* species susceptibilities comments on historical fluoroquinolone resistance especially in *N. farcinica* being as high as 50%.[21] The patient may have benefited from those additional weeks of therapy with an effective antibiotic based on lab data; however, based on evidence from many other cases, fluoroquinolones are not considered first-line therapy. Surveillance for up to a year is recommended for recurrence evaluation.[4] Secondary prophylaxis is generally not considered necessary for immunocompetent patients. The treatment algorithm for lung disease or disseminated infection with or without CNS involvement recommends using multidrug regimen for initial treatment and once sensitivities resume, therapy can be narrowed accordingly. Secondary prophylaxis is reserved for severely immunocompromised patients or in conjunction with removal of implants or devices for patients with bacteremia or endocarditis.[4] According to these criteria, the patient in this case received inappropriate management more than 2 months after the initial diagnosis, after she had already had several debridement procedures and four cultures growing *N. farcinica*.

Part of the inappropriate management could be due to the slow growing nature of *Nocardia* as well as resistance patterns that are not commonly known outside of the infectious disease specialty. In the case described, the first aerobic wound culture was collected, requiring re- incubation due to insufficient growth, and was ultimately identified as *N. farcinica* 6 days later. The patient had been discharged on empiric cephalosporins by then. No sensitivities were listed with the initial cultures. Repeat cultures a month later similarly identified *N. farcinica* within 6 days and sensitivities came back 1 month after that. *N. farcinica* has inherent resistance to

Table 2. Distribution of immunocompromised patients with different immunodeficiency types

Type of immunodeficiency	Treatment with corticosteroids	Number of patients	Ref.
Various autoimmune disorders*	Yes	4	Merinopoulos *et al.*[6] Auzary *et al.*[7] Yokota *et al.*[8] Granier *et al.*[9]
Hematopoietic cell transplant	Yes	1	Hemmersbach-Miller *et al.*[5]
Leprosy	Yes	1	De Nardo *et al.*[10]
Lymphoma	No	2	Malani *et al.*[11] Torres *et al.*[12]
Multiple myeloma	No	1	Angeles *et al.*[13]
Nephrotic syndrome	Yes	2	Gao *et al.*[2] Zhu *et al.*[14]
Solid organ transplant	Yes	8	Hemmersbach-Miller *et al.*[5] Rees *et al.*[15] Ghandour *et al.*[16]

*Cogan's syndrome, aplastic anemia, systemic sclerosis/polymyositis and bullous pemphigoid.

Table 3. Immunocompetent cases of cutaneous nocardiosis caused by *N. farcinica*

Case report	Patient description	Type of wound	Mode of transmission	Treatment	Outcome
Schiff *et al.*[17]	54-year- old, male	Non- healing lesion of right face	Infected after being struck with a shovel	I.V. AMK for 2 weeks followed by I.M. amikacin for 6 weeks (intolerant to TMP-SMX)	Complete resolution of lesion including long-term follow-up for 2 years
Bosamiya *et al.*[18]	37-year- old, male	Left leg lesion with lymphatic spread to right elbow	Accidentally infected due to occupation as a farmer	TMP-SMX for 6 – 12 months	Complete resolution of cutaneous lesions of left leg and right elbow within 7 days of initiating treatment
Acuner *et al.*[19]	37-year- old, male	Non- healing skin lesions and recurrent muscle abscesses of right forearm	Infected due to arm laceration from grease canister	Incision and drainage of abscesses for 5 times with concomitant TMP-SMX over 5 months, followed by 10 days of I.V. AMK and I.V. IMI, followed by 1 month of TMP- SMX	Resolution of clinical symptoms after 1 month of second course of TMP- SMX; negative ultrasound findings for abscesses; only revealing scar tissue

Abbreviations: AMK, Amikacin; I.M.: Intramuscular; IMI: Imipenem; I.V.: Intravenous; TMP-SMX: Trimethoprim/sulfamethoxazole.

several antibiotics, including most beta-lactam antibiotics (notably ampicillin and third-generation cephalosporins), clarithromycin and most aminoglycosides.[23,24] Research on the genomic sequence of *N. farcinica* demonstrated a chromosome containing plasmids and genes responsible for this intrinsic multidrug resistance.[24] Cephalosporins are the first-line empiric therapy for many skin and soft tissue infections, which can cause challenges in choosing empiric antibiotics for patients who have primary cutaneous nocardiosis. This is especially true in immunocompetent patients when more common bacterial causes will often be the leading differential diagnosis. In the case described above, the patient was prescribed four courses of cephalosporins despite identification of *N. farcinica* on aerobic culture early on. This was compounded by the slow growing nature of the pathogen, since sensitivities were not released for 2 months after the initial culture grew. This highlights the importance of early consultation for antibiotic recommendations from infectious disease specialists in cases of *Nocardia* infections.

The limitations of this case report include lack of dedicated infectious disease follow-up, and no photo-based evidence of cure since the patient was noted to have resolution of her wound at another specialist's appointment. In addition, there is limited documentation available regarding the patient's procedure for trigger finger release and cyst removal on flexor tendon, as well as the outpatient incision and drainage itself, as it was completed at a facility where our electronic health record is not synchronized.

4. Conclusion

We presented a case of an immunocompetent patient who had a non-healing surgical wound after a camping trip where she used well water, despite multiple surgical interventions and months of empiric antibiotic treatment using cephalosporins. Her wound cultures grew *N. farcinica* repeatedly. Literature review shows that *N. farcinica* in immunocompetent patients is often preceded by environmental exposure and requires prolonged treatment with specific antibiotics, with first-line therapy being TMP-SMX to resolve the infection. It is important to involve infectious disease specialists as early as possible when primary cutaneous nocardiosis is diagnosed to expedite treatment with proper antibiotics and shorten the duration of therapy.

Acknowledgments

None.

Funding

None.

Conflict of interest

The authors declare that they have no competing interests.

Author contributions

Conceptualization: Maya Polashenski
Investigation: Maya Polashenski
Writing – original draft: Maya Polashenski
Writing – review & editing: Olga Vasylyeva

Ethics approval and consent to participate

Informed consent was verbally obtained to write up the patient's case and use the photograph of her hand.

Consent for publication

Verbal informed consent was obtained prior to submitting this manuscript for publication.

Availability of data

Data are available from the corresponding author on reasonable request.

References

1. Fatahi-Bafghi M. Nocardiosis from 1888 to 2017. *Microb Pathog*. 2018;114:369-384.

   doi: 10.1016/j.micpath.2017.11.012

2. Gao S, Liu Q, Zhou X, Dai X, He H. Primary cutaneous nocardiosis due to *Nocardia farcinica*: A case report of an often overlooked infection. *Infect Drug Resist*. 2021;14:1435-1440.

   doi: 10.2147/IDR.S306161

3. Wilson JW. Nocardiosis: Updates and clinical overview. *Mayo Clin Proc*. 2012;87(4):403-407.

   doi: 10.1016/j.mayocp.2011.11.016

4. Rawat D, Rajasurya V, Chakraborty RK, Sharma S. Nocardiosis. In: *StatPearls*. Treasure Island, FL: StatPearls Publishing; 2023.

5. Hemmersbach-Miller M, Stout JE, Woodworth MH, Cox GM, Saullo JL. *Nocardia* infections in the transplanted host. *Transpl Infect Dis*. 2018;20(4):e12902.

   doi: 10.1111/tid.12902

6. Merinopoulos D, Khan H, Ginwalla S, Lane S, Watts R. *Nocardia farcinica* complicating Cogan's syndrome. *Oxf Med Case Reports*. 2014;2014(2):36-38.

   doi: 10.1093/omcr/omu016

7. Auzary C, Mouthon L, Soilleux M, Cohen P, Boiron P, Guillevin L. Localized subcutaneous *Nocardia farcinica* abscess in a woman with overlap syndrome between systemic scleroderma and polymyositis. *Ann Med Interne* (*Paris*). 1999;150(7):582-584.

8. Yokota S, Kawabe K, Yamada H, Nunomura M. Case of subcutaneous abscess caused by *Nocardia farcinica* in an aplastic anemia patient. *Nihon Ishinkin Gakkai Zasshi*. 2010;51(2):93-97.

doi: 10.3314/jjmm.51.93

9. Granier F, Kahla-Clémenceau N, Richardin F, *et al*. *Nocardia farcinica* infection. Cutaneous form in an immunodepressed patient. *Presse Med*. 1994;23(7):329-331.

10. De Nardo P, Giancola ML, Noto S, *et al.* Left thigh phlegmon caused by *Nocardia farcinica* identified by 16S rRNA sequencing in a patient with leprosy: A case report. *BMC Infect Dis*. 2013;13:162.

doi: 10.1186/1471-2334-13-162

11. Malani AK, Gupta C, Weigand RT, Gupta V, Rangineni S. Thigh abscess due to *Nocardia farcinica*. *J Natl Med Assoc*. 2006;98(6):977-979.

12. Torres OH, Domingo P, Pericas R, Boiron P, Montiel JA, Vázquez G. Infection caused by *Nocardia farcinica*: Case report and review. *Eur J Clin Microbiol Infect Dis*. 2000;19(3):205-212.

doi: 10.1007/s100960050460

13. Angeles RM, Lasala RP, Fanning CV. Disseminated subcutaneous nocardiosis caused by *Nocardia farcinica* diagnosed by FNA biopsy and 16S ribosomal gene sequencing. *Diagn Cytopathol*. 2008;36(4):266-269.

doi: 10.1002/dc.20804

14. Zhu N, Zhu Y, Wang Y, Dong S. Pulmonary and cutaneous infection caused by *Nocardia farcinica* in a patient with nephrotic syndrome: A case report. *Medicine* (*Baltimore*). 2017;96(24):e7211.

doi: 10.1097/MD.0000000000007211

15. Rees W, Schüler S, Hummel M, Hetzer R. Primär kutane *Nocardia-farcinica*-infektion nach herztransplantation. [Primary cutaneous *Nocardia farcinica* infection following heart transplantation]. [Published correction appears in *Dtsch Med Wochenschr*. 1994;119(45):1568]. *Dtsch Med Wochenschr*. 1994;119(38):1276-1280.

doi: 10.1055/s-2008-1058833

16. Ghandour M, Shereef H, Homida H, Revankar S, Zachariah MS. Disseminated nocardiosis in a renal transplant recipient. *Cureus*. 2021;13(1):e12497.

doi: 10.7759/cureus.12497

17. Schiff TA, McNeil MM, Brown JM. Cutaneous *Nocardia farcinica* infection in a nonimmunocompromised patient: Case report and review. *Clin Infect Dis*. 1993;16(6):756-760.

doi: 10.1093/clind/16.6.756

18. Bosamiya SS, Vaishnani JB, Momin AM. Sporotrichoid nocardiosis with cutaneous dissemination. *Indian J Dermatol Venereol Leprol*. 2011;77(4):535.

doi: 10.4103/0378-6323.82409

19. Acuner B, Cömert F. Recurrent subcutaneous abscess due to *Nocardia farcinica* in an immunocompetent patient: A case report. *Wound Manag Prev*. 2021;67(5):33-39.

20. McTaggart LR, Doucet J, Witkowska M, Richardson SE. Antimicrobial susceptibility among clinical *Nocardia* species identified by multilocus sequence analysis. *Antimicrob Agents Chemother*. 2015;59(1):269-275.

doi: 10.1128/AAC.02770-14

21. Zhao P, Zhang X, Du, P, Li G, Li L, Li Z. Susceptibility profiles of *Nocardia* spp. to antimicrobial and antituberculotic agents detected by a microplate Alamar Blue assay. *Sci Rep.* 2017;7:43660.

doi: 10.1038/srep43660

22. Margalit I, Lebeaux D, Tishler O, *et al*. How do I manage nocardiosis? *Clin Microbiol Infect*. 2021;27(4):550-558.

doi: 10.1016/j.cmi.2020.12.019

23. Lao CK, Tseng MC, Chiu CH, *et al*. Clinical manifestations and antimicrobial susceptibility of *Nocardia* species at a tertiary hospital in Taiwan, 2011-2020. *J Formos Med Assoc*. 2022;121(10):2109-2122.

doi: 10.1016/j.jfma.2022.06.011

24. Brown-Elliott BA, Brown JM, Conville PS, Wallace RJ Jr. Clinical and Laboratory features of the *Nocardia* spp. based on current molecular taxonomy. *Clin Microbiol Rev*. 2006;19(2):259-282.

doi: 10.1128/cmr.19.2.259-282.2006

ACCSCIENCE PUBLISHING

Microbes & Immunity

COMMUNICATION

Ea_8Mab-9: A novel monoclonal antibody against erythropoietin-producing hepatocellular receptor A8 for flow cytometry

Tomohiro Tanaka, Haruto Yamamoto, Yu Kaneko, Keisuke Shinoda, Takuya Nakamura, Guanjie Li, Shiori Fujisawa, Hiroyuki Satofuka, Mika K. Kaneko, Hiroyuki Suzuki*, and Yukinari Kato*

Department of Antibody Drug Development, Tohoku University Graduate School of Medicine, Sendai, Miyagi, Japan

Abstract

Erythropoietin-producing hepatocellular receptor A8 (EphA8) is a type I transmembrane protein that belongs to the largest erythropoietin-producing hepatocellular (Eph) family among receptor tyrosine kinases. By binding to its membrane-bound ephrin-A or ephrin-B ligands on adjacent cells, Eph receptors form complexes and mediate bidirectional signaling activities, triggering cell-cell adhesion and repulsion. Increased expression of EphA8 correlates with poor prognosis in some types of cancer. Therefore, developing sensitive monoclonal antibodies (mAbs) for EphA8 has been desired for treatment, diagnosis, and further basic research. In particular, there are no anti-EphA8 mAbs that can be used for flow cytometry. A novel, specific, and sensitive anti-human EphA8 mAb, which applies to flow cytometry, clone Ea_8Mab-9 (mouse immunoglobulin G_1, kappa), was established using the Cell-Based Immunization and Screening method. Ea_8Mab-9 reacted with EphA8-overexpressed Chinese hamster ovary-K1 cells (CHO/EphA8) and EphA8-overexpressed LN229 glioblastoma cells (LN229/EphA8) in flow cytometry. Notably, Ea_8Mab-9 did not recognize other members of the Eph receptor family. Furthermore, Ea_8Mab-9 demonstrated a high binding affinity for CHO/EphA8 and LN229/EphA8, with dissociation constants of 1.3×10^{-9} M and 1.6×10^{-9} M, respectively. The reaction of Ea_8Mab-9 with CHO/EphA8 was completely blocked by a recombinant EphA8 protein. Ea_8Mab-9 could be useful for analyzing the EphA8-related biological responses using flow cytometry, owing to its high affinity and specificity.

Keywords: EphA8; Cell-Based Immunization and Screening method; Monoclonal antibody; Flow cytometry

***Corresponding authors:**
Hiroyuki Suzuki (hiroyuki.suzuki.b4@tohoku.ac.jp)
Yukinari Kato (yukinari.kato.e6@tohoku.ac.jp)

Citation: Tanaka T, Yamamoto H, Kaneko Y, *et al*. Ea_8Mab-9: A novel monoclonal antibody against erythropoietin-producing hepatocellular receptor A8 for flow cytometry. *Microbes & Immunity.* 2025;2(4):150-160. doi: 10.36922/MI025060010

Received: February 3, 2025

1st revised: March 28, 2025

2nd revised: May 20, 2025

Accepted: May 28, 2025

Published online: June 18, 2025

1. Introduction

Erythropoietin-producing hepatocellular (Eph) receptors are the most prominent family of receptor tyrosine kinases (RTKs) and regulate tissue homeostasis, including cell proliferation and migration, tissue remodeling, angiogenesis, axon guidance, and synaptic plasticity in the nervous system.[1-3] Eph receptors are classified into EphA and EphB subfamilies according to the sequence homology and binding mode to membrane-bound ephrin ligands. The EphA subfamily includes nine members, such as EphA1

to EphA8 and EphA10. The EphB subfamily consists of five members, such as EphB1 to EphB4 and EphB6. Eight ephrin ligands have been identified, including glycosylphosphatidylinositol-anchored ephrin A1 to A5 and transmembrane ephrin B1 to B3. Following the binding to receptors, forward signaling is activated on the receptor side, and reverse signaling is generated on the ligand side, controlling various biological homeostasis.[3] Eph receptors play critical roles in the nervous system (EphA3, EphA4, EphA5, EphB1, EphB2, and EphB3),[4,5] cardiovascular system (EphB4),[6] immune system (EphA1, EphA2, EphA3, EphA4, EphA7, EphA10, EphB1, EphB2, EphB4, and EphB6),[7] and gastrointestinal system (EphB2 and EphB3).[8]

EphA8 complementary DNA (cDNA) was first isolated from a rat brain cDNA library and named eek (eph- and elk-related kinase, EEK) in 1991.[9] Another group cloned the mouse EphA8 molecule in 1997.[10] EphA8 is one of the members of the RTK family, and its regulatory mechanism is thought to be based on tyrosine kinase (TK) activity. Phosphorylation of Tyr-615 in the EphA8 juxtamembrane domain mediates a strong association with the SH2 domain of Fyn, a member of the Src TKs.[11] Phosphorylation of Tyr-838 in the EphA8 kinase domain modulates Fyn binding to Tyr-615, resulting in attenuation of cell adhesion through cellular cytoskeletal modifications.[11] Interestingly, TK activity-independent functions of EphA8 are also emerging. Ephrin A5-induced EphA8-integrin interaction is promoted by phosphatidylinositol 3-kinase in a TK-independent manner.[12] Similar to representative growth factor receptors such as epidermal growth factor receptor, Eph receptors play a role in cell proliferation primarily through forward signaling.[13,14] In addition to regulating cell-cell attachment and cell motility, EphA8 is involved in organ development and axon growth.[15,16] EphA8 induces caspase-dependent apoptotic cell death of ephrin A5-expressing neural epithelial cells during early brain development.[15] Loss of EphA8 disrupts axon guidance during mammalian nervous system development.[16] Furthermore, EphA8 facilitates neurite outgrowth by sustaining mitogen-activated protein kinase activity in neuronal cells.[17]

EphA8 expression has also been reported to be associated with cancer.[2,18-21] EphA8 upregulation is observed in various cancers, including oral tongue squamous cell carcinoma (OTSCC),[22] ovarian cancer,[23] gastric cancer,[24] and breast cancer.[25] EphA8 and ephrin A5 contribute to the invasiveness of stem cells isolated from MDA-MB-231, a triple-negative invasive breast cancer cell line.[26] In contrast, tumor suppressor functions of EphA8 have also been proposed. Reducing expression of miR-10a, a promoter of cancer invasion, leads to increased EphA8 expression and suppression of cancer progression in colorectal cancer and glioma.[27,28] Further research is necessary to clarify the role of EphA8 in either promoting or suppressing cancer-related functions.

Various monoclonal antibodies (mAbs) against human Eph receptors, including EphA2,[29] EphB2,[30] and EphB4,[31] have previously been developed by the Cell-Based Immunization and Screening (CBIS) method. This method preserves the native structure of membrane proteins during immunization and enables the efficient generation of antibodies that recognize modifications and/or three-dimensional structures of the extracellular domains of membrane proteins. Since flow cytometry is used for high-throughput screening in the CBIS method, mAbs suitable for this application are prioritized. However, anti-EphA8 mAbs suitable for flow cytometry are not yet available. Therefore, the establishment of anti-EphA8 mAbs is essential to support basic research and preclinical studies related to cancer therapy.

In this study, an anti-human EphA8 mAb (clone Ea_8Mab-9) suitable for flow cytometry was successfully established using the CBIS method.

2. Materials and methods

2.1. Cell lines and stable transfectants

LN229, Chinese hamster ovary (CHO)-K1, and P3X63Ag8U.1 (P3U1) cells were obtained from the American Type Culture Collection (USA). The cDNA encoding human EphA8 (Accession No. NM_020526; Catalog No.: RC220352) was purchased from OriGene Technologies Inc. (USA). The open reading frame of EphA8, excluding the signal sequence, was subcloned into the pCAG-Ble vector (FUJIFILM Wako Pure Chemical Corporation, Japan) with either an interleukin 2-signal sequence and PA16 tag or a MAP16 tag at the N-terminus, using the in-fusion HD Cloning Kit (Takara Bio Inc., Japan). The resulting plasmid was transfected into the cell lines using the Neon Transfection System (Thermo Fisher Scientific Inc., USA). Subsequently, LN229 and CHO-K1 cells stably overexpressing EphA8 with a deletion of amino acids 1 – 27 and an N-terminal MAP16 tag (hereafter described as LN229/EphA8 and CHO/EphA8, respectively), as well as LN229 cells stably overexpressing EphA8 with the same deletion and an N-terminal PA16 tag (hereafter described as LN229/PA16-EphA8), were established using a cell sorter (SH800, Sony Corp., Japan).

cDNAs for various Eph receptors were obtained, including EphA1 (Catalog No.: RC213689, Accession No.: NM_005232), EphA4 (Catalog No.: RC211230,

Accession No.: NM_004438), EphA5 (Catalog No.: RC213206, Accession No.: NM_004439), EphA6 (Catalog No.: RC223510, Accession No.: NM_001080448), EphA7 (Catalog No.: RC226293, Accession No.: NM_004440), EphA10 (Catalog No.: RC218374, Accession No.: NM_001099439) EphB1 (Catalog No.: RC214301, Accession No.: NM_004441), EphB2 (Catalog No.: RC223882, Accession No.: NM_004442), EphB6 (Catalog No.: RC229404, Accession No.: NM_004445), were purchased from OriGene Technologies Inc. (USA). EphA2 (Catalog No.: HGY095959, Accession No.: NM_004431), EphA3 (Catalog No.: HGY053437, Accession No.: NM_005233), and EphB3 (Catalog No.: HGX039581, Accession No.: NM_004443) cDNAs were purchased from RIKEN DNA Bank (Japan).

EphA2 and EphB3 cDNAs were cloned into a pCAGzeo vector (FUJIFILM Wako Pure Chemical Corporation, Japan). EphB6 cDNA was cloned into a pCMV6 vector. EphA1 cDNA was cloned into a pCAGzeo-ssnPA vector. EphA3, EphA4, EphA5, EphA6, EphA7, EphA8, EphA10, and EphB1 cDNAs were cloned into a pCAGzeo_ssnPA16 vector.

The plasmids were also transfected into CHO-K1 cells, and stable transfectants were established by staining with specific antibodies: an anti-EphA2 mAb (clone SHM16; BioLegend, USA), an anti-EphB3 mAb (clone 647354; R & D Systems Inc., USA), an anti-EphB6 mAb (clone T49-25; BioLegend), and an anti-PA16 tag mAb (clone NZ-1 for EphA2, EphA3, EphA4, EphA5, EphA6, EphA7, EphA10, and EphB1), followed by sorting using the SH800 cell sorter. After sorting, cells were cultivated in a medium containing 0.5 mg/mL of Zeocin (InvivoGen, USA) or 0.5 mg/mL of G418. Eph receptors-overexpressed CHO-K1 (e.g., CHO/EphA1) clones were finally established. CHO/PA16-EphB4 cells were described previously.[31]

CHO-K1, P3U1, and CHO-K1 cells overexpressing each Eph receptor were cultured in Roswell Park Memorial Institute (RPMI)-1640 medium (Nacalai Tesque Inc., Japan) supplemented with 10% heat-inactivated fetal bovine serum (FBS; Thermo Fisher Scientific Inc., USA), 100 units/mL penicillin, 100 μg/mL streptomycin, and 0.25 μg/mL amphotericin B (Nacalai Tesque Inc., Japan). LN229 and LN229/EphA8 cells were cultured in Dulbecco's Modified Eagle Medium (Nacalai Tesque Inc., Japan) supplemented with 10% heat-inactivated FBS (Thermo Fisher Scientific Inc., USA), 100 units/mL penicillin, 100 μg/mL streptomycin, and 0.25 μg/mL amphotericin B (Nacalai Tesque Inc., Japan). All cells were cultured in a humidified incubator at 37°C with 5% CO_2 and 95% air.

2.2. Antibodies

The Alexa Fluor 488-conjugated anti-mouse immunoglobulin g (IgG) secondary antibody was purchased from Cell Signaling Technology Inc. (USA).

2.3. Development of hybridomas

To develop anti-EphA8 mAbs, two 6-week-old female BALB/cAJcl mice purchased from CLEA Japan (Japan) were immunized intraperitoneally with 1×10^8 LN229/PA16-EphA8 cells. The immunogen was harvested after a brief exposure to 1 mM ethylenediaminetetraacetic acid (EDTA; Nacalai Tesque Inc., Japan). For the initial immunization, Alhydrogel adjuvant 2% (InvivoGen, USA) was added. Three additional injections of 1×10^8 LN229/PA16-EphA8 cells were performed without an adjuvant addition every week. A final booster immunization was performed with 1×10^8 LN229/PA16-EphA8 cells intraperitoneally 2 days before harvesting splenocytes. Splenocytes from the immunized mice were fused with P3U1 myeloma cells using polyethylene glycol 1,500 (PEG1,500; Roche Diagnostics, USA) under warmed conditions.

Hybridomas were cultured in RPMI-1640 medium supplemented as shown above, with additional supplementation of hypoxanthine, aminopterin, and thymidine (HAT) (HAT; Thermo Fisher Scientific Inc., USA), 5% BriClone (NICB, Ireland), and 5 μg/mL of plasmocin (InvivoGen, USA). The hybridoma supernatants were screened by flow cytometry using CHO/EphA8 and parental CHO-K1 cells. The culture supernatant from Ea_8Mab-9-producing hybridomas was filtrated and purified using Ab-Capcher Extra (ProteNova, Japan).

2.4. Flow cytometric analysis

CHO-K1, CHO/EphA1, CHO/EphA2, CHO/EphA4, CHO/EphA6, CHO/EphA7, CHO/EphA8, CHO/EphB1, CHO/EphB6, LN229, and LN229/EphA8 cells were harvested after brief exposure to 1 mM EDTA (Nacalai Tesque Inc., Japan). CHO/EphA3, CHO/EphA5, CHO/EphA10, CHO/EphB2, CHO/EphB3, and CHO/EphB4 cells were harvested after brief exposure to 0.25% trypsin and 1 mM EDTA (Nacalai Tesque Inc., Japan). All cells were then washed with 0.1% bovine serum albumin (BSA) in phosphate-buffered saline (PBS), treated with the primary mAb for 30 min at 4°C, and subsequently treated with Alexa Fluor 488-conjugated anti-mouse IgG (1:1000). Fluorescence data were collected using the SA3800 Cell Analyzer (Sony Corp., Japan).

2.5. Determination of K_D by flow cytometry

CHO/EphA8 and LN229/EphA8 were suspended in 100 µL of serially diluted Ea_8Mab-9 (10 µg/mL to 0.0006 µg/mL), followed by treatment with Alexa Fluor 488-conjugated anti-mouse IgG (1:200). Fluorescence data were subsequently collected using the BD FACSLyric system (BD Biosciences, USA). The dissociation constant (K_D) was calculated by fitting the binding isotherms into the built-in one-site binding model in GraphPad PRISM 6 (GraphPad Software Inc., USA).

2.6. Determination of K_D by enzyme-linked immunosorbent assay (ELISA)

The recombinant EphA8-Fc (recEphA8) (Sino Biological Inc., China) was immobilized on Nunc Maxisorp 96-well immunoplates (Thermo Fisher Scientific Inc., USA) at 10 µg/mL for 30 min at 37°C. After washing with PBS containing 0.05% Tween20 (PBST; Nacalai Tesque Inc., Japan), wells were blocked with 1% BSA in PBST for 30 min at 37°C. The plates were then incubated at serially diluted Ea_8Mab-9 (10 µg/mL to 0.0006 µg/mL), followed by treatment with peroxidase-conjugated anti-mouse IgG_1 (1:2000; SouthernBiotech, USA). Finally, enzymatic reactions were conducted using the ELISA POD substrate TMB kit (Nacalai Tesque Inc., Japan). The K_D value was determined as described above.

3. Results

3.1. Development of anti-EphA8 mAbs using the CBIS method

Currently, polyclonal antibodies against EphA8 for flow cytometry are commercially available. However, they are insufficient for therapeutic applications. Therefore, the establishment of mAbs targeting EphA8 is essential to develop various mAb-based therapeutic modalities. To develop anti-EphA8 mAbs for flow cytometry, the CBIS method was employed using EphA8-overexpressed cells. Hybridoma that produced anti-EphA8 mAbs were screened by flow cytometry (Figure 1). Two female BALB/cAJcl mice were intraperitoneally immunized with LN229/PA16-EphA8 cells once weekly for 5 weeks. Subsequently, hybridomas were seeded into 96-well plates, and the culture supernatants were screened to identify those that specifically reacted with CHO/EphA8 cells but not with parental CHO-K1 cells. Several highly CHO/EphA8-reactive supernatants of hybridomas were obtained. The most sensitive clone, Ea_8Mab-9 (mouse IgG_1, kappa), was ultimately established through limiting dilution and additional analysis.

3.2. Flow cytometric analysis

Flow cytometric analysis was conducted using Ea_8Mab-9 against CHO-K1, CHO/EphA8, LN229, and LN229/EphA8 cells. Results indicated that Ea_8Mab-9 bound to CHO/EphA8 (Figure 2A, upper) and LN229/EphA8 (Figure 2B, upper) in a dose-dependent manner. In contrast, no binding was observed to parental CHO-K1 (Figure 2A, lower) or LN229 (Figure 2B, lower) cells, even at the highest tested concentration of 10 µg/mL. These findings indicate that Ea_8Mab-9 specifically reacts to EphA8 in flow cytometric applications.

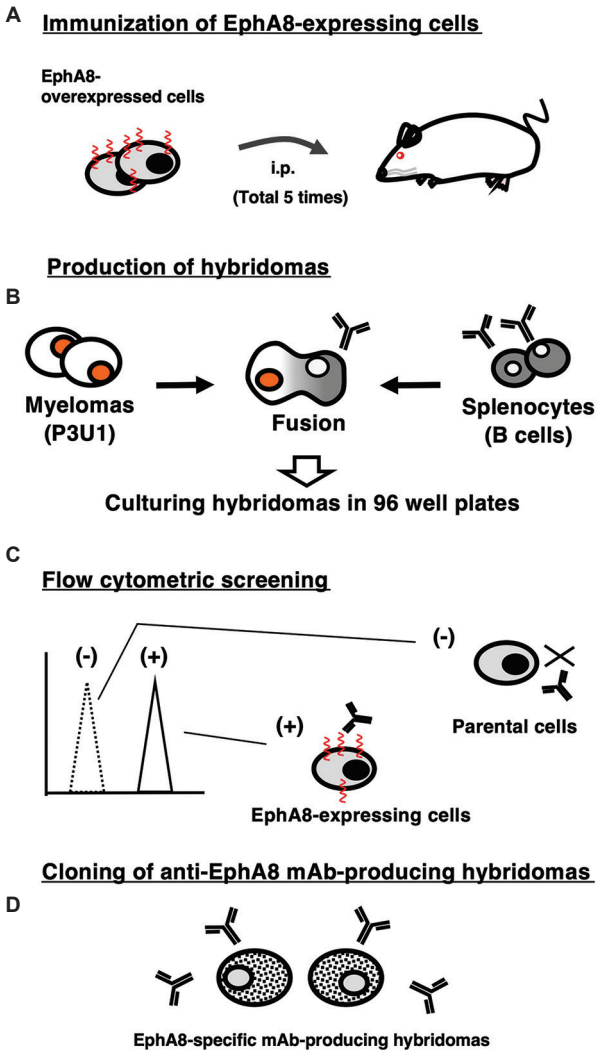

Figure 1. A schematic diagram of anti-EphA8 mAb development using the CBIS method. (A) LN229/PA16-EphA8 cells were immunized into two mice by intraperitoneal injection. (B) The spleen cells from immunized mice were fused with P3U1 myeloma cells using PEG1,500. (C) The culture supernatants of hybridoma were screened by flow cytometry using CHO-K1 and CHO/EphA8 cells to select EphA8-specific mAb-producing hybridomas. (D) After limiting the dilution of hybridomas to obtain the single clone and additional screening, the mAb clone Ea_8Mab-9 (mouse IgG_1, kappa) was finally established. Abbreviations: CBIS: Cell-Based Immunization and Screening; CHO: Chinese hamster ovary; i.p.: Intraperitoneal; mAb: Monoclonal antibody; EphA8: Erythropoietin-producing hepatocellular receptor A8; IgG: immunoglobulin g; PEG1,500: Polyethylene glycol 1,500.

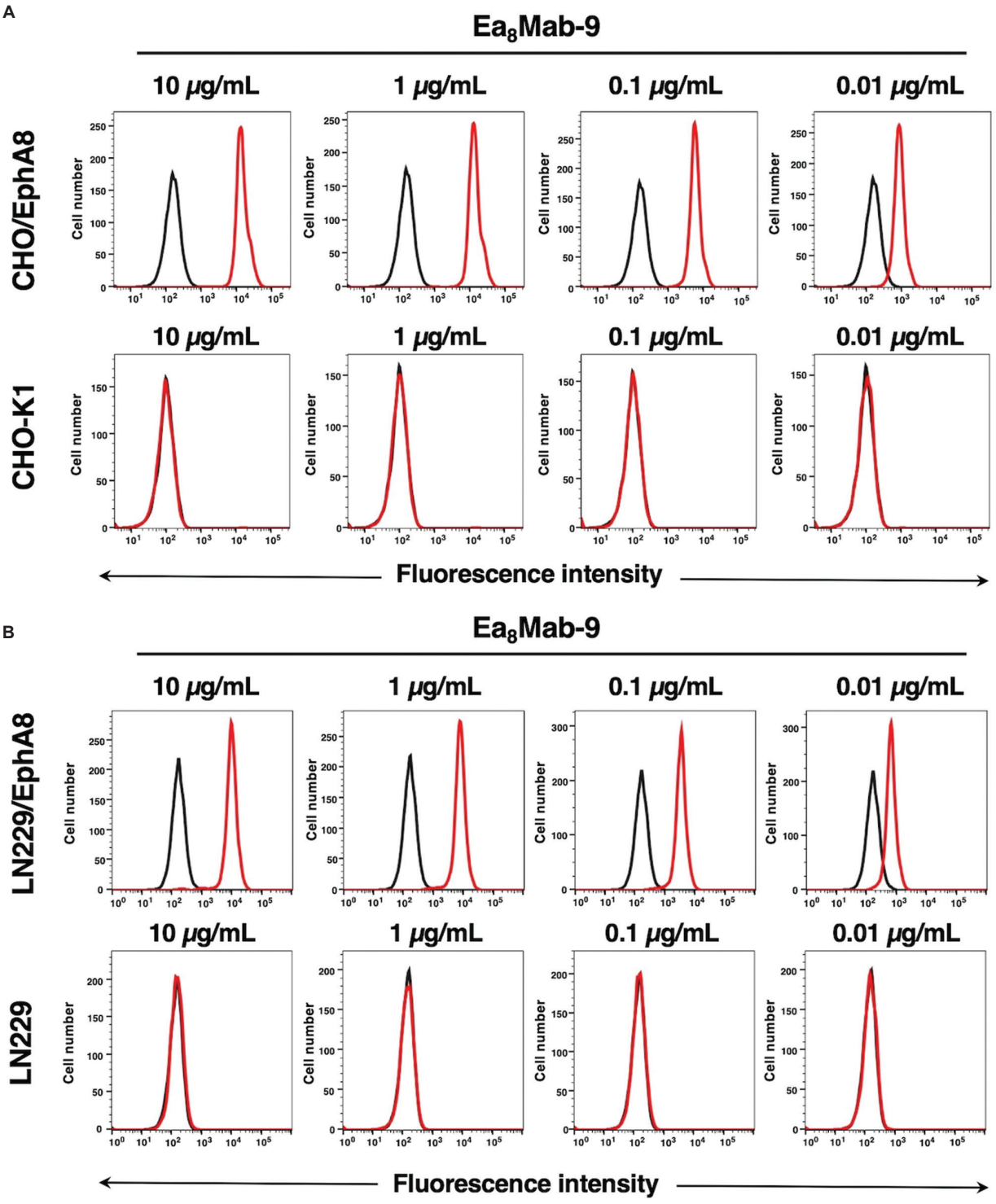

Figure 2. Flow cytometric analysis of Ea_8Mab-9 in EphA8 receptor-expressed CHO-K1 and LN229 cells. (A) CHO/EphA8 (upper panels) and CHO-K1 (lower panels) cells were treated with 0.01 – 10 μg/mL of Ea_8Mab-9 (red line), followed by treatment with Alexa Fluor 488-conjugated anti-mouse IgG. Fluorescence data were collected using the SA3800 Cell Analyzer. The black line represents the negative control (no primary antibody treatment). (B) LN229/EphA8 (upper panels) and LN229 (lower panels) cells were treated with 0.01 – 10 μg/mL of Ea_8Mab-9 (red line), followed by treatment with Alexa Fluor 488-conjugated anti-mouse IgG. Fluorescence data were collected using the SA3800 Cell Analyzer. The black line indicates the negative control (no primary antibody treatment).
Abbreviations: CHO: Chinese hamster ovary; EphA8: Erythropoietin-producing hepatocellular receptor A8; IgG: immunoglobulin g.

3.3. Specificity of Ea_8Mab-9 to Eph receptor-expressed CHO-K1 cells

CHO-K1 cells overexpressing all Eph receptors, including EphA1 to A8, EphA10, EphB1 to B4, and EphB6, were established. Using these fourteen cell lines, the specificity of Ea_8Mab-9 was evaluated. As shown in Figure 3, Ea_8Mab-9 recognized CHO/EphA8 cells but did not bind to any other Eph receptor-expressed CHO-K1 cells. These results confirm the high specificity of Ea_8Mab-9 for EphA8 among the Eph receptor family.

3.4. Determination of the binding affinity of Ea_8Mab-9 by flow cytometry

The binding affinity of Ea_8Mab-9 was assessed with exogenously EphA8-expressed CHO/EphA8 and LN229/EphA8 cells using flow cytometry. Results showed that the K_D values of Ea_8Mab-9 were 1.3×10^{-9} M for CHO/EphA8 cells and 1.6×10^{-9} M for LN229/EphA8 cells (Figure 4). The reproducibility of the binding data was confirmed (Figure A1). These results demonstrate that Ea_8Mab-9 possesses a high affinity for EphA8.

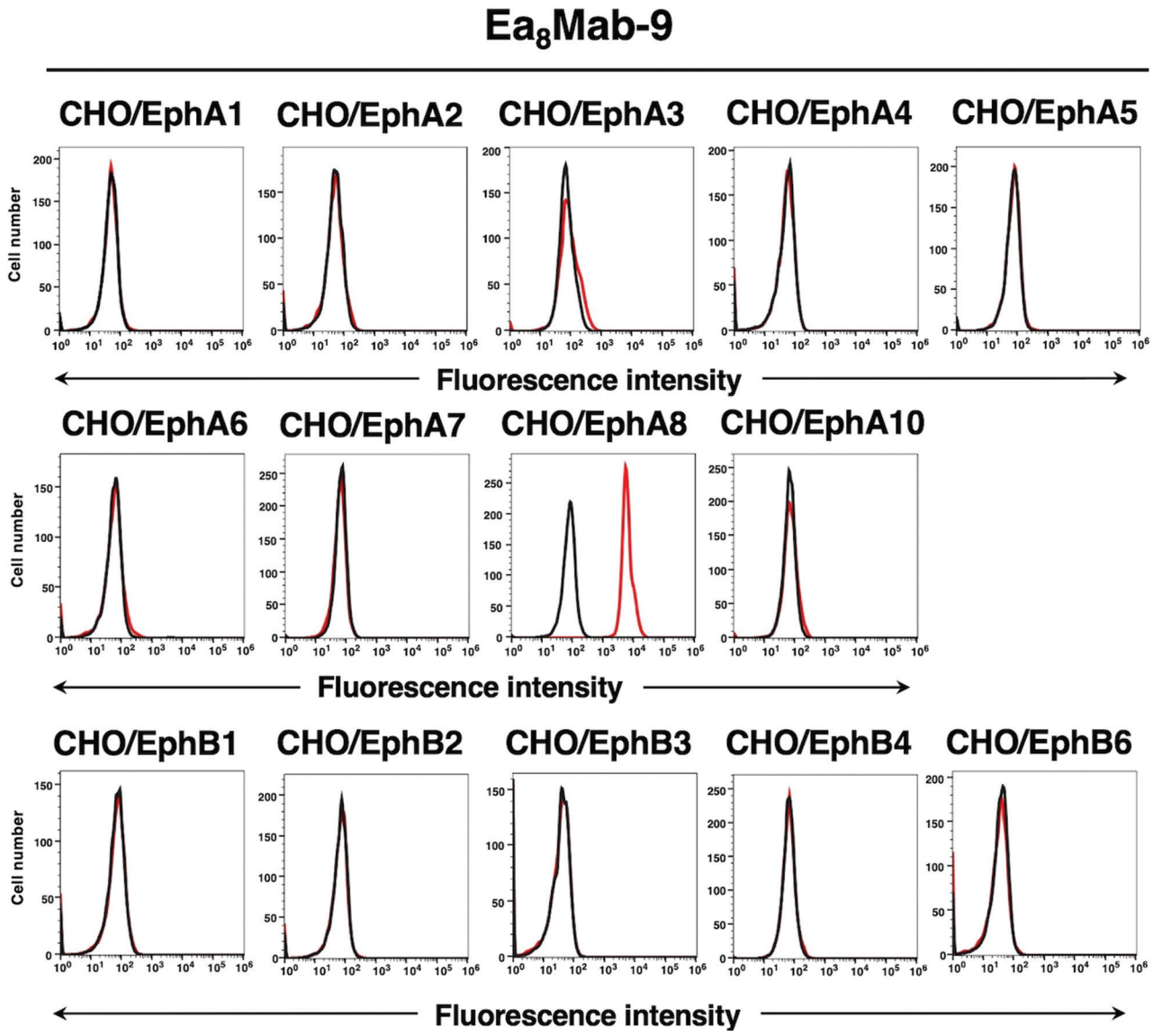

Figure 3. Flow cytometry of Ea_8Mab-9 in Eph receptor-expressed CHO-K1 cells. CHO-K1 cells transfected to express each of the fourteen Eph receptors were treated with 10 μg/mL of Ea_8Mab-9 (red line) or control blocking buffer (black line), followed by the treatment with Alexa Fluor 488-conjugated anti-mouse IgG.
Abbreviations: CHO: Chinese hamster ovary; EphA8: Erythropoietin-producing hepatocellular receptor A8; IgG: immunoglobulin g.

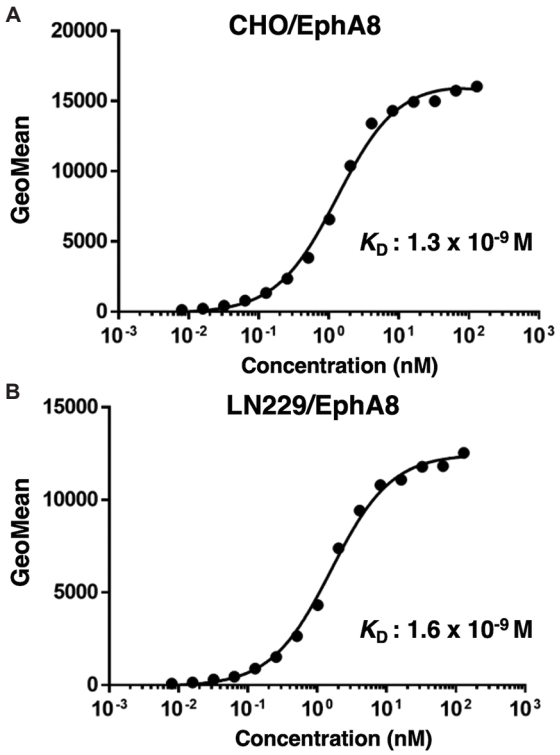

Figure 4. Determination of the binding affinity of Ea_8Mab-9 by flow cytometry. (A) CHO/EphA8 and (B) LN229/EphA8 cells were incubated in 100 µL of serially diluted Ea_8Mab-9 (10 µg/mL to 0.0006 µg/mL). Cells were then treated with Alexa Fluor 488-conjugated anti-mouse IgG. Fluorescence data were collected using the BD FACSLyric system, and K_D was calculated using GraphPad PRISM 6 software.
Abbreviations: CHO: Chinese hamster ovary; GeoMean: Geometric mean; K_D: Dissociation constant; EphA8: Erythropoietin-producing hepatocellular receptor A8.

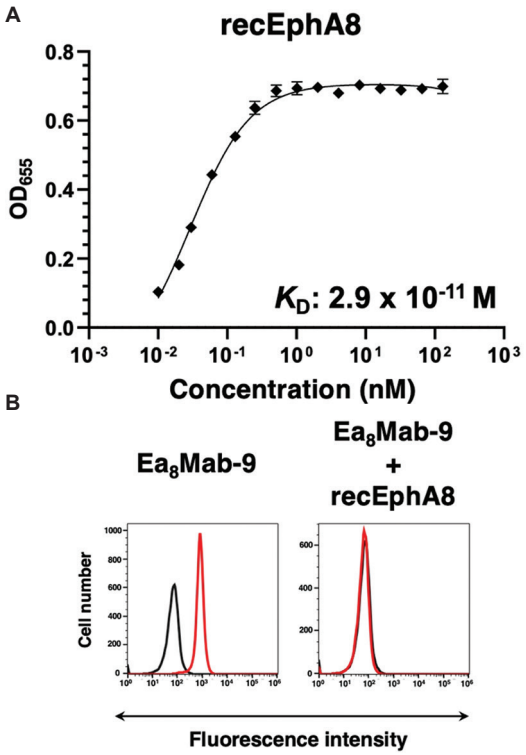

Figure 5. Determination of the binding affinity of Ea_8Mab-9 by ELISA and blocking assay. (A) Recombinant EphA8 (recEphA8) was immobilized on immunoplates and incubated with the serially diluted Ea_8Mab-9, followed by detection with peroxidase-conjugated anti-mouse immunoglobulins (n = 3). Enzymatic reactions were conducted, and the optical density at 655 nm (OD_{655}) was measured. Data are presented as mean ± SD. The K_D value was determined as described above. (B) Blocking assay using recEphA8. CHO/EphA8 cells were treated with control blocking buffer, Ea_8Mab-9 (0.01 µg/mL), or Ea_8Mab-9 (0.01 µg/mL) preincubated with recEphA8 (3 µg/mL) for 30 min at 4°C, followed by treatment with Alexa Fluor 488-conjugated anti-mouse IgG. The black line represents the negative control (blocking buffer).
Abbreviations: CHO: Chinese hamster ovary; ELISA: Enzyme-linked immunosorbent assay; K_D: Dissociation constant; OD: Optical density; SD: Standard deviation; EphA8: Erythropoietin-producing hepatocellular receptor A8.

3.5. Determination of the binding affinity of Ea_8Mab-9 using ELISA

The binding affinity of Ea_8Mab-9 against recEphA8 was evaluated using ELISA. As shown in Figure 5A, the K_D value of Ea_8Mab-9 was 2.9 × 10^{-11} M. Furthermore, the recEphA8 competitively inhibited the binding of Ea_8Mab-9 in flow cytometry (Figure 5B). These results also confirmed the high affinity and specificity of Ea_8Mab-9 for EphA8.

4. Discussion

In this study, an anti-EphA8 mAb, Ea_8Mab-9, was first developed and showed high affinity and specificity in flow cytometry (Figures 2-4) and ELISA (Figure 5). Additional anti-EphA8 mAb clones for flow cytometry were also established (http://www.med-tohoku-antibody.com/topics/001_paper_antibody_PDIS.htm#EphA8). Ea_8Mab-9 and these clones are expected to facilitate the elucidation of EphA8 functions in various research fields. In particular, no commercially available anti-EphA8 antibodies are suitable for flow cytometry. Ea_8Mab-9 is expected to lead to a more detailed elucidation of the role of EphA8 in cancer, including the tumor microenvironment and neuronal research. Furthermore, previous efforts have enhanced antibody-dependent cellular cytotoxicity (ADCC) and complement-dependent cytotoxicity activities by switching isotypes and eliminating fucosylation in mAbs.[32] Since Ea_8Mab-9 is a mouse IgG_1 subclass, which lacks ADCC activity, a mouse IgG_{2a} version will be generated to examine antitumor efficacy in tumor xenograft models in future studies.

EphA8 regulates brain development and neural outgrowth in normal tissues,[15,17] and its overexpression

has been reported in cancers.[22,23,25] EphA8 TK-dependent activation appears to be essential for its function. For example, Tyr-phosphorylated EphA8 regulates cell-cell adhesion by interacting with Fyn.[11] In breast cancer, EphA8 suppresses cell apoptosis via Akt activation and correlates with poor prognosis.[25] In addition, EphA8 expression may mediate the resistance to paclitaxel treatment.[25] In gastric cancer, EphA8 promotes malignancy through Akt signaling and interaction with a disintegrin and metalloproteinase domain-containing protein 10.[24] In OTSCC patients, EphA8 expression significantly correlates with tumor, node, metastasis stage, but not with other risk factors such as age, gender, drinking, and smoking history.[22] Since EphA8 has been reported to cooperate with stem cells,[26] further evaluation of its relationship with other membrane protein markers such as CD44 and CD133 may be valuable.[33,34] To analyze the population of EphA8-expressing cancer cells, detecting naïve EphA8 on these cells is necessary. Because Ea_8Mab-9 recognizes EphA8 with high affinity, it will be helpful for diagnosis and experiments using flow cytometry. However, the suitability of Ea_8Mab-9 for immunofluorescence or immunohistochemistry has not yet been investigated. If unsuitable for these applications, identifying EphA8-expressing cells in tissue samples may be challenging.

Eph receptors have been widely studied in the context of cancer and are gaining attention as therapeutic targets.[2,35] Clinical trials have been conducted for various modalities, including compounds, antibody drugs, and chimeric antigen receptor (CAR)-T cells targeting Eph receptors and ephrin ligands such as EphA2, EphA3, EphA5, EphB4, ephrin A4, and ephrin B2.[2,21] However, there are currently no drugs approved specifically for Eph receptors or ephrin ligands. Given that mAbs against HER2,[36] podoplanin,[37] and podocalyxin[38] established using the CBIS method have revealed applicability in CAR-T therapy, it is worthwhile to investigate the potential application of Ea_8Mab-9 for CAR-T therapy targeting EphA8-positive tumors.

5. Conclusion

Ea_8Mab-9, established using the CBIS method, may serve as a valuable tool for analyzing EphA8-related biological responses by flow cytometry, owing to its high affinity and specificity.

Acknowledgments

None.

Funding

This research was supported in part by the Japan Agency for Medical Research and Development under grant numbers: JP24am0521010 (to Y. Kato), JP24ama121008 (to Y. Kato), JP24ama221339 (to Y. Kato), JP24bm1123027 (to Y. Kato), and JP24ck0106730 (to Y. Kato), and by the Japan Society for the Promotion of Science Grants-in-Aid for Scientific Research (KAKENHI) under grant numbers: 22K06995 (to H. Suzuki), 24K18268 (to T. T.), 24K11652 (to H. Satofuka), and 25K10553 (to Y. Kato).

Conflict of interest

The authors declare that they have no conflict of interest

Author contributions

Conceptualization: Mika K. Kaneko, Yukinari Kato
Formal analysis: Tomohiro Tanaka
Funding acquisition: Tomohiro Tanaka, Hiroyuki Satofuka, Hiroyuki Suzuki, Yukinari Kato
Investigation: Tomohiro Tanaka, Haruto Yamamoto, Yu Kaneko, Keisuke Shinoda, Takuya Nakamura, Guanjie Li, Shiori Fujisawa, Hiroyuki Satofuka
Methodology: Mika K. Kaneko
Writing – original draft: Tomohiro Tanaka
Writing – review & editing: Hiroyuki Suzuki, Yukinari Kato

Ethics approval and consent to participate

All animal experiments were approved by the Animal Care and Use Committee of Tohoku University (Permit number: 2022MdA-001).

Consent for publication

Not applicable.

Availability of data

The data of this study are available in the article.

Further disclosure

The paper has been uploaded to a preprint server (DOI: 10.20944/preprints202412.1044.v1).

References

1. Tuzi NL, Gullick WJ. Eph, the largest known family of putative growth factor receptors. *Br J Cancer*. 1994;69(3):417-421.
   doi: 10.1038/bjc.1994.77
2. Pasquale EB. Eph receptors and Ephrins in cancer progression. *Nat Rev Cancer*. 2024;24(1):5-27.
   doi: 10.1038/s41568-023-00634-x
3. Pasquale EB. Eph-ephrin bidirectional signaling in physiology and disease. *Cell*. 2008;133(1):38-52.
   doi: 10.1016/j.cell.2008.03.011
4. Hruska M, Dalva MB. Ephrin regulation of synapse

formation, function and plasticity. *Mol Cell Neurosci*. 2012;50(1):35-44.

doi: 10.1016/j.mcn.2012.03.004

5. Drescher U. The Eph family in the patterning of neural development. *Curr Biol*. 1997;7(12):R799-R807.

doi: 10.1016/s0960-9822(06)00409-x

6. Yang D, Jin C, Ma H, *et al*. EphrinB2/EphB4 pathway in postnatal angiogenesis: A potential therapeutic target for ischemic cardiovascular disease. *Angiogenesis*. 2016;19(3):297-309.

doi: 10.1007/s10456-016-9514-9

7. Darling TK, Lamb TJ. Emerging roles for Eph receptors and ephrin ligands in immunity. *Front Immunol*. 2019;10:1473.

doi: 10.3389/fimmu.2019.01473

8. Herath NI, Boyd AW. The role of Eph receptors and ephrin ligands in colorectal cancer. *Int J Cancer*. 2010;126(9):2003-2011.

doi: 10.1002/ijc.25147

9. Chan J, Watt VM. eek and erk, new members of the Eph subclass of receptor protein-tyrosine kinases. *Oncogene*. 1991;6(6):1057-1061.

10. Park S, Sánchez MP. The eek receptor, a member of the Eph family of tyrosine protein kinases, can be activated by three different Eph family ligands. *Oncogene*. 1997;14(5):533-542.

doi: 10.1038/sj.onc.1200857

11. Choi S, Park S. Phosphorylation at Tyr-838 in the kinase domain of EphA8 modulates Fyn binding to the Tyr-615 site by enhancing tyrosine kinase activity. *Oncogene*. 1999;18(39):5413-5422.

doi: 10.1038/sj.onc.1202917

12. Gu C, Park S. The EphA8 receptor regulates integrin activity through p110gamma phosphatidylinositol-3 kinase in a tyrosine kinase activity-independent manner. *Mol Cell Biol*. 2001;21(14):4579-4597.

doi: 10.1128/mcb.21.14.4579-4597.2001

13. Wang SD, Rath P, Lal B, *et al*. EphB2 receptor controls proliferation/migration dichotomy of glioblastoma by interacting with focal adhesion kinase. *Oncogene*. 2012;31(50):5132-5143.

doi: 10.1038/onc.2012.16

14. Bhatia S, Bukkapatnam S, Van Court B, *et al*. The effects of ephrinB2 signaling on proliferation and invasion in glioblastoma multiforme. *Mol Carcinog*. 2020;59(9):1064-1075.

doi: 10.1002/mc.23237

15. Kim Y, Park E, Noh H, Park S. Expression of EphA8-Fc in transgenic mouse embryos induces apoptosis of neural epithelial cells during brain development. *Dev Neurobiol*. 2013;73(9):702-712.

doi: 10.1002/dneu.22092

16. Park S, Frisén J, Barbacid M. Aberrant axonal projections in mice lacking EphA8 (Eek) tyrosine protein kinase receptors. *EMBO J*. 1997;16(11):3106-3114.

doi: 10.1093/emboj/16.11.3106

17. Gu C, Shim S, Shin J, *et al*. The EphA8 receptor induces sustained MAP kinase activation to promote neurite outgrowth in neuronal cells. *Oncogene*. 2005;24(26):4243-4256.

doi: 10.1038/sj.onc.1208584

18. Cui Z, Liu C, Wang X, Xiang Y. A pan-cancer analysis of EphA family gene expression and its association with prognosis, tumor microenvironment, and therapeutic targets. *Front Oncol*. 2024;14:1378087.

doi: 10.3389/fonc.2024.1378087

19. Sahoo AR, Buck M. Structural and functional insights into the transmembrane domain association of Eph receptors. *Int J Mol Sci*. 2021;22(16):8593.

doi: 10.3390/ijms22168593

20. Pergaris A, Danas E, Goutas D, Sykaras AG, Soranidis A, Theocharis S. The clinical impact of the EPH/ephrin system in cancer: Unwinding the thread. *Int J Mol Sci*. 2021;22(16):8412.

doi: 10.3390/ijms22168412

21. Janes PW, Vail ME, Gan HK, Scott AM. Antibody targeting of Eph receptors in cancer. *Pharmaceuticals (Basel)*. 2020;13(5):88.

doi: 10.3390/ph13050088

22. Liu L, Wang X, Ge W. EphA8 is a prognostic factor for oral tongue squamous cell carcinoma. *Med Sci Monit*. 2018;24:7213-7222.

doi: 10.12659/msm.910909

23. Liu X, Xu Y, Jin Q, *et al*. EphA8 is a prognostic marker for epithelial ovarian cancer. *Oncotarget*. 2016;7(15):20801-20809.

doi: 10.18632/oncotarget.8018

24. Wang Y, Zhou N, Li P, *et al*. EphA8 acts as an oncogene and contributes to poor prognosis in gastric cancer via regulation of ADAM10. *J Cell Physiol*. 2019;234(11):20408-20419.

doi: 10.1002/jcp.28642

25. Wang GH, Ni K, Gu C, *et al*. EphA8 inhibits cell apoptosis via AKT signaling and is associated with poor prognosis in breast cancer. *Oncol Rep*. 2021;46(2):183.

doi: 10.3892/or.2021.8134

26. Lucero M, Thind J, Sandoval J, Senaati S, Jimenez B, Kandpal RP. Stem-like cells from invasive breast carcinoma cell line MDA-MB-231 express a distinct set of Eph receptors and ephrin ligands. *Cancer Genomics Proteomics*. 2020;17(6):729-738.

doi: 10.21873/cgp.20227

27. Ren W, Chen S, Liu G, Wang X, Ye H, Xi Y. TUSC7 acts as a tumor suppressor in colorectal cancer. *Am J Transl Res*. 2017;9(9):4026-4035.

28. Yan Y, Wang Q, Yan XL, *et al*. miR-10a controls glioma migration and invasion through regulating epithelial-mesenchymal transition via EphA8. *FEBS Lett*. 2015;589(6):756-765.

doi: 10.1016/j.febslet.2015.02.005

29. Satofuka H, Suzuki H, Tanaka T, Li G, Kaneko MK, Kato Y. Development of an anti-human EphA2 monoclonal antibody Ea2Mab-7 for multiple applications. *Biochem Biophys Rep*. 2025;42:101998.

doi: 10.1016/j.bbrep.2025.101998

30. Ubukata R, Suzuki H, Hirose M, *et al*. Establishment of a highly sensitive and specific anti-EphB2 monoclonal antibody (Eb2Mab-12) for flow cytometry. *MI*. 2025:5728.

doi: 10.36922/mi.5728

31. Nanamiya R, Suzuki H, Kaneko MK, Kato Y. Development of an anti-EphB4 monoclonal antibody for multiple applications against breast cancers. *Monoclon Antib Immunodiagn Immunother*. 2023;42(5):166-177.

doi: 10.1089/mab.2023.0015

32. Suzuki H, Ohishi T, Tanaka T, Kaneko MK, Kato Y. A cancer-specific monoclonal antibody against podocalyxin exerted antitumor activities in pancreatic cancer xenografts. *Int J Mol Sci*. 2023;25(1):161.

doi: 10.3390/ijms25010161

33. Paya L, Rafat A, Talebi M, *et al*. The effect of tumor resection and radiotherapy on the expression of stem cell markers (CD44 and CD133) in patients with squamous cell carcinoma. *Int J Hematol Oncol Stem Cell Res*. 2024;18(1):92-99.

doi: 10.18502/ijhoscr.v18i1.14748

34. Da Silva DD, Araldi RP, Belizario MR, Rocha WG, Maciel RMB, Cerutti JM. DLK1 is associated with stemness phenotype in medullary thyroid carcinoma cell lines. *Int J Mol Sci*. 2024;25(22):11924.

doi: 10.3390/ijms252211924

35. Zhou Y, Sakurai H. Emerging and diverse functions of the EphA2 noncanonical pathway in cancer progression. *Biol Pharm Bull*. 2017;40(10):1616-1624.

doi: 10.1248/bpb.b17-00446

36. Hosking M, Shirinbak S, Omilusik K, *et al*. 268 development of FT825/ONO-8250: An off-the-shelf CAR-T cell with preferential HER2 targeting and engineered to enable multi-antigen targeting, improve trafficking, and overcome immunosuppression. *J Immunother Cancer*. 2023;11(Suppl 1):A307-A307.

doi: 10.1136/jitc-2023-SITC2023.0268

37. Chalise L, Kato A, Ohno M, *et al*. Efficacy of cancer-specific anti-podoplanin CAR-T cells and oncolytic herpes virus G47Δ combination therapy against glioblastoma. *Mol Ther Oncolytics*. 2022;26:265-274.

doi: 10.1016/j.omto.2022.07.006

38. Mishima Y, Okada S, Ishikawa A, *et al*. Development of chimeric antigen receptor T cells targeting cancer-expressing podocalyxin. *Regen Ther*. 2025;28:292-300.

doi: 10.1016/j.reth.2024.12.010

Appendix

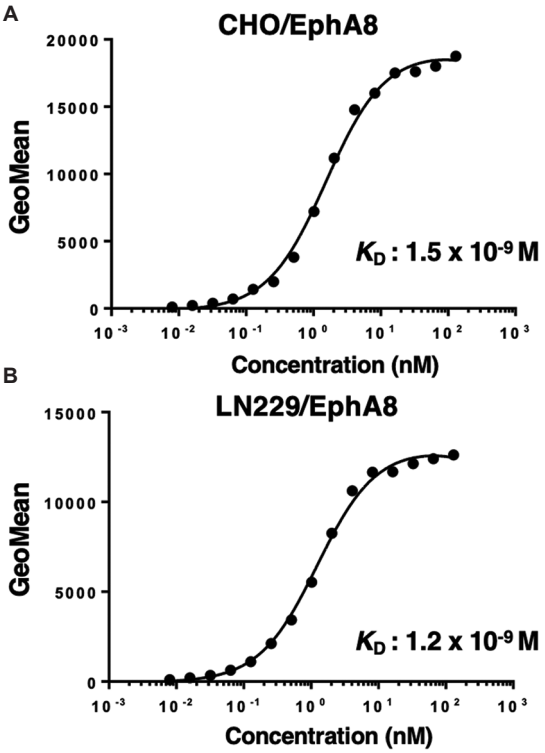

Figure A1. Reproducibility of the binding affinity of Ea_8Mab-9 against EphA8-expressed cells. (A) CHO/EphA8 and (B) LN229/EphA8 cells were incubated in 100 μL of serially diluted Ea_8Mab-9 (10 μg/mL to 0.0006 μg/mL). Cells were then treated with Alexa Fluor 488-conjugated anti-mouse IgG. Fluorescence data were collected using the BD FACSLyric system, and K_D was calculated using GraphPad PRISM 6 software.
Abbreviations: CHO: Chinese hamster ovary; GeoMean: Geometric mean; K_D: Dissociation constant; EphA8: Erythropoietin-producing hepatocellular receptor A8

Our Journals

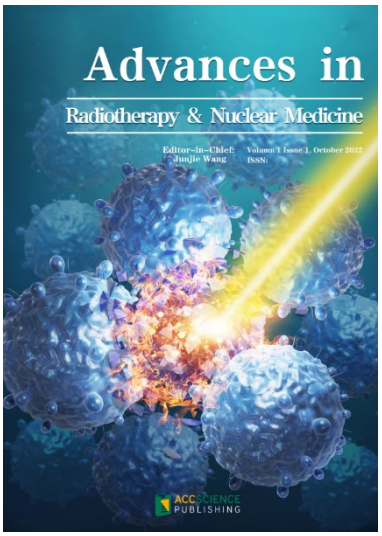

Advances in Radiotherapy & Nuclear Medicine (ARNM) is a peer-reviewed and open-access journal that aims to publish and disseminate novel research in the breadth of neurology and neuroscience. *ARNM* covers subject areas, including but not limited to the following:

- Conventional Radiotherapy (CR)
- Stereotactic Body Radiation Therapy (SBRT)
- Brachytherapy (BT)
- Boron Neutron Capture Therapy (BNCT)
- Particle Therapy (proton and heavy ions) (PT)
- Targeted and Immunotherapy (TI)
- Combined Modality Therapy (Heat therapy, electric field therapy, nursing, technology) (CMT)
- Radiation Biology (RB)
- Radiation Physics (RP)
- Innovative Radiation Technology (IRT)
- Positron Emission Tomography (PET)
- Radiopharmaceuticals and Radio-tracer (RR)
- Molecular Imaging and Radionuclide Therapy (MI & RT)
- Single-photon Emission Computed Tomography (SPETCT)

Artificial Intelligence in Health is an online open-access, multidisciplinary journal dedicated to publishing high-quality peer-reviewed research in all areas of Artificial Intelligence in health and medicine science. By publishing high-quality research papers, reviews, and case studies, the journal seeks to contribute to the scientific community's understanding of the potential, challenges, and impact of AI and its applications on health delivery, patient outcomes, and population health. *Artificial Intelligence in Health* covers topics, including but not limited to the following: AI-based medical diagnosis and prognosis, AI clinical decision support systems, AI-driven drug discovery and development, AI-enabled healthcare operations and management, and the research and application in telemedicine, AI-assisted electronic health records and clinical informatics, AI-based research and application of wearable devices for diagnosis and treatment and social implications of AI in health.

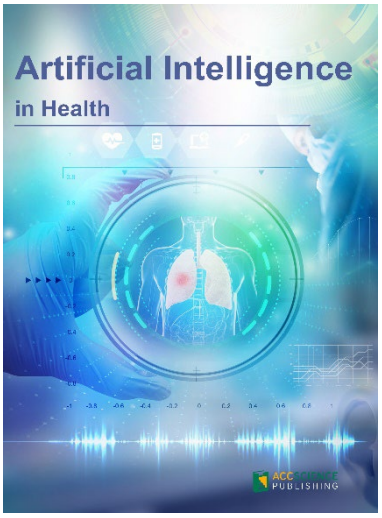

Start a new journal

Write to us via email if you are interested to start a new journal with AccScience Publishing. Please attach your CV, professional profile page and a brief pitch proposal in your email. We shall inform you of our decision whether we are interested to collaborate in starting a new journal.

Contact: info@accscience.com

https://accscience.com/journal/MI

Contact
www.accscience.com
9 Raffles Place, Republic Plaza 1 #06-00 Singapore 048619
Email: editorial@accscience.com
Phone: +65 8182 1586